LEABHARLANN CHOLÁISTE NA TRÍONÓIDE, BAILE ÁTHA CLIATH | TRINITY COLLEGE LIBRARY DUBLIN
Ollscoil Átha Cliath | The University of Dublin

Terms and Conditions of Use of Digitised Theses from Trinity College Library Dublin

Copyright statement

All material supplied by Trinity College Library is protected by copyright (under the Copyright and Related Rights Act, 2000 as amended) and other relevant Intellectual Property Rights. By accessing and using a Digitised Thesis from Trinity College Library you acknowledge that all Intellectual Property Rights in any Works supplied are the sole and exclusive property of the copyright and/or other IPR holder. Specific copyright holders may not be explicitly identified. Use of materials from other sources within a thesis should not be construed as a claim over them.

A non-exclusive, non-transferable licence is hereby granted to those using or reproducing, in whole or in part, the material for valid purposes, providing the copyright owners are acknowledged using the normal conventions. Where specific permission to use material is required, this is identified and such permission must be sought from the copyright holder or agency cited.

Liability statement

By using a Digitised Thesis, I accept that Trinity College Dublin bears no legal responsibility for the accuracy, legality or comprehensiveness of materials contained within the thesis, and that Trinity College Dublin accepts no liability for indirect, consequential, or incidental, damages or losses arising from use of the thesis for whatever reason. Information located in a thesis may be subject to specific use constraints, details of which may not be explicitly described. It is the responsibility of potential and actual users to be aware of such constraints and to abide by them. By making use of material from a digitised thesis, you accept these copyright and disclaimer provisions. Where it is brought to the attention of Trinity College Library that there may be a breach of copyright or other restraint, it is the policy to withdraw or take down access to a thesis while the issue is being resolved.

Access Agreement

By using a Digitised Thesis from Trinity College Library you are bound by the following Terms & Conditions. Please read them carefully.

I have read and I understand the following statement: All material supplied via a Digitised Thesis from Trinity College Library is protected by copyright and other intellectual property rights, and duplication or sale of all or part of any of a thesis is not permitted, except that material may be duplicated by you for your research use or for educational purposes in electronic or print form providing the copyright owners are acknowledged using the normal conventions. You must obtain permission for any other use. Electronic or print copies may not be offered, whether for sale or otherwise to anyone. This copy has been supplied on the understanding that it is copyright material and that no quotation from the thesis may be published without proper acknowledgement.

IN VITRO AND *IN VIVO* STUDIES ON THE NEUROPEPTIDE THYROTROPIN-RELEASING HORMONE (TRH)

BY

AOIFE CULLEN

A DISSERTATION SUBMITTED TO THE UNIVERSITY OF DUBLIN FOR THE DEGREE OF DOCTOR OF PHILOSOPHY.

SCHOOL OF BIOCHEMISTRY AND IMMUNOLOGY

AND

TRINITY COLLEGE INSTITUTE OF NEUROSCIENCE

TRINITY COLLEGE

DUBLIN

TRINITY COLLEGE
10 AUG 2009
LIBRARY DUBLIN
THESIS
8717

Declaration

I hereby certify that none of the work presented in this thesis has been submitted for any degree, at this, or any other University. I declare that the work presented in this thesis is entirely my own, with the exception of microdialysis amino acid and amine content analyses, which were completed by the laboratory group of Prof. Laura Della Corte of the Dipartimento di Farmacologia Preclinica, Università degli Studi di Firenze, Viale G. Pieraccini 6, Firenze, Italy. I agree that the library may lend or copy this thesis upon request.

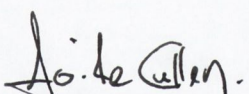

Aoife Cullen

Acknowledgements

Firstly, I would like to express my sincere thanks to my supervisor, Prof. Keith F. Tipton for his constant support and guidance. Prof. Tipton has provided help, advice and assistance throughout my time in Lab 1 and his patience and good humour are limitless. Many, many pints of Guinness are owed to him. I am also enormously grateful to my supervisors, Dr. Gavin Davey and Dr. Julie Kelly, for giving me their help, time and the opportunity to undertake this research. I want to express my gratitude to Prof. Laura Dell Corte for arranging my trip to Florence, helping me find funding and accommodation and most of all for the opportunity to work in her lab.

A huge thank you to all the friends I have made here in Trinity, who have helped, listened and in the past few months supported and consoled. Many thanks in particular to Eamon, Ed, Joe, Jayne, Laura, Orla, Seán, Stephen and Susan and especially to Sinead.To Dr. John Rochford of the Biology Teaching Centre, an enormous thanks for the opportunity to work there, for the experience and a steady income. Thanks also to all the staff of Biochemistry, in particular to Mary-Pat, Miriam, Liam, Kyran, Noel and Liam.

Particular thanks must go to all in Prof. Laura Della Corte's group, who welcomed me to their lab, taught me some Italian, and most importantly did the experiments with me. I am grateful to Dr. Andrew Harkin and Dr. Julie Kelly for the use of their HPLCs in my hour of need and when I'd finally given up on the method.

The financial support provided by the HRB, TCIN, Erasmus and COST is gratefully acknowledged.

Table of Contents

		Page Number
DECLARATION		i
ACKNOWLEDGEMENTS		ii
SUMMARY		iv
ABBREVIATIONS		vi
DETAILED LIST OF CONTENTS		vii
CHAPTER 1	GENERAL INTRODUCTION	1
CHAPTER 2	GENERAL METHODS	51
CHAPTER 3	INHIBITION OF THYROTROPIN-RELEASING HORMONE DEGRADING ENZYME	72
CHAPTER 4	ASSESSMENT OF NEUROTOXICITY AND NEUROPROTECTION OF *IN VITRO* MODELS	107
CHAPTER 5	STUDIES ON THE PROTECTIVE EFFECT OF TRH AGAINST CELLULAR INSULTS	156
CHAPTER 6	ASSESSMENT OF NEUROTOXICITY AND NEUROPROTECTION IN *IN VIVO* MODELS	225
CHAPTER 7	GENERAL DISCUSSION	271
BIBLIOGRAPHY		282
APPENDIX A		317
APPENDIX B		318
PUBLICATIONS		320

Summary

Thyrotropin-releasing hormone (pyroglutamyl–histidyl–prolineamide; TRH), a tripeptide, a hypothalamic–pituitary–thyroid axis hormone, has neuromodulatory properties and is found in the brain in locations where it has no pituitary or thyroid functions. It is released from nerve terminals in response to depolarisation and has both stimulatory and inhibitory effects on post-synaptic neurones. TRH co-localises with several neurotransmitters including acetylcholine, serotonin and glutamate. The interaction that TRH has with these neurotransmitters and the dual role it plays in either stimulation or inhibition of the neurones it acts on suggest TRH may be a key homeostatic modulator. Furthermore, it may protect against pathological changes or insults to the central nervous system (CNS).

The potential therapeutic uses of TRH in CNS disorders are limited by its rapid degradation by TRH-degrading enzyme (TRH-DE), which shows highest activity levels in the brain. Inhibition of this enzyme should lead to increased levels of TRH in the CNS and protect peripherally administered TRH against degradation. Developing inhibitors of TRH-DE is however hampered by the absence of a crystal structure of the enzyme. Potential inhibitors of TRH-DE were designed by structural modifications of TRH and testing their inhibitory potency using the purified enzyme. A lead structure, pyroglutamyl–asparaginyl–prolineamide, had previously been identified and further modifications and substitutions of this compound were studied. It was found that the asparagine and proline residues provided key interactions with the enzyme, although the enzyme–ligand interaction tolerated modification with aromatic groups and extension of the *C*-terminus yielded potent inhibition of TRH-DE.

Systems in which *in vitro* analysis of the effects of TRH were established, using rat-hippocampal slice incubation and superfusion models. Kainic acid, an excitotoxic glutamate glutamate analogue, was used to induce general neuronal and glial-specific death, confirmed by the loss of lactate dehydrogenase and glutamine synthase from the tissue. TRH protected against this cell death and also against apoptosis, as measured by prevention of caspase activation.

Decreases of dopamine and serotonin levels due to kainate toxicity were measured by HPLC with electrochemical detection. TRH was found to protect against this amine depletion but induced the release of noradrenaline from the slices. Glutamine, measured fluorometrically, following HPLC was substantially depleted from the slices. TRH protected against this glutamine loss, in addition it protected against the kainate-induced loss of the excitatory amino acids aspartate and glutamate and against taurine depletion, but had no effect on GABA loss. The protective effect of TRH was also measured using a cell-culture system in which the neuron-like cell line, SH-SY5Y cells were exposed to (a) kainate, to induce excitotoxicity, (b) 1-methyl-4-phenylpyridinium, to induce mitochondrial malfunction and (c) staurosporine, to induce apoptosis. It was found that TRH protected against cell death induced by each of these toxins, although to a varying extent, being most effective against the excitotoxic route. TRH protection was both concentration and time dependent.

Neuroprotection by TRH was also studied *in vivo* by microdialysis. Kainate was infused to the striatum of rats and the effects of pre-treatment with TRH, injected intraperitoneally, on the neurotransmitter release and were measured. TRH prevented a kainate-induced increase in aspartate release and attenuated the decreases in the release of the dopamine metabolite 3,4-dihydroxyphenylacetic acid and the serotonin metabolite 5-hydroxyindole acetic acid due to kainate infusion. Anaesthesia was necessary prior to kainate, and this caused significant alteration in neurotransmitter release, particularly noradrenaline, glutamate and GABA, and thus the effects of kainate, and of TRH, on neurotransmitter release from the striatum were difficult to interpret. Following the microdialysis studies the animals underwent a social-learning memory recall test and it was found that kainate induced a significant impairment in the memory, but pre-treatment with TRH protected against this. In a second study kainate was used to cause memory and learning defects, measured by performance in the Morris water-maze spatial test. TRH again showed protection against kainate impairment with significantly improved escape latencies and swim distances.

Abbreviations

5-HIAA	5-Hydroxy indole acetic acid
5HT	5-Hydroxytryptamine (serotonin)
ACh	Acetylcholine
AMC	7-Amino-4-methyl-coumarin
ANOVA	analysis of variance
APA	Aminopeptidase A
APN	Aminopeptidase N
Asn	Asparagine
Asp	Aspartate
ATP	Adenosine-5'-triphosphate
BSA	Bovine serum albumin
$[Ca^{2+}]_i$	Intracellular calcium concentration
CaM-K	Calmodulin-dependent protein kinase
CNS	Central nervous system
DA	Dopamine
DAG	Diacylglycerol
DMEM	Dulbecco's Modified Eagle's Medium
DMSO	Dimethyl sulfoxide
DPP IV	Dipeptidyl peptidase IV
FCS	Fetal calf serum
GABA	γ-aminobutyric acid
Gln	Glutamine
Glu	Glutamate
GS	Glutamine synthase
His	Histidine
HPLC	High-performance liquid chromatography
HPT	Hypothalamic–pituitary–thyroid axis
HVA	Homovanillic acid
i.p.	Intraperitoneal
IP_3	Inositol triphosphate
KA	Kainate
LDH	Lactate dehydrogenase

MCA	Middle cerebral artery
Me	Methyl
mol	Mole
MPP^+	1-Methyl-4-phenylpyridinum ion
NA	Noradrenaline
NAD^+	B-nicotinamide adenine dinucleotide
NADH	B-nicotinamide adenine dinucleotide (reduced form)
NMDA	*N*-Methyl-D-aspartate
OPA	*o*-Phthalaldehyde
PAP I	Pyroglutamyl peptidase I
PAP II	Pyroglutamyl peptidase II (TRH-DE)
PBS	Phosphate buffered saline
PE	Prolyl endopeptidase
pGlu	Pyroglutamate
PIP_2	Phosphatidylinositol (4,5)-bisphosphate
PKC	Protein kinase C
PLC	Phospholipase C
Pro	Proline
ROS	Reactive oxygen species
RP	Reverse phase
rpm	Revolutions per minute
s	Seconds
S.E.M.	Standard error of the mean
SAR	Structure–activity relationship
TRH	Thyrotropin-releasing hormone (TRH)
TRH-DE	Thyrotropin-releasing hormone-degrading enzyme
TRHR1	TRH receptor 1
TRHR2	TRH receptor 2
TSH	Thyroid-stimulating hormone (thyrotropin)

DETAILED LIST OF CONTENTS

CHAPTER 1 GENERAL INTRODUCTION 1

1.1 THYROTROPIN-RELEASING HORMONE (TRH) 2

1.2 THE FUNCTION OF TRH AS A HORMONE 2

1.2.1 Regulation of the hypothalamic–pituitary–thyroid axis 2

1.3 THE FUNCTION OF TRH AS A NEUROTRANSMITTER 4

1.3.1 Distribution of TRH 4
1.3.2 Evolution of TRH 7
1.3.3 Neuronal release of TRH 7
1.3.4 Co-localisation of TRH 8

1.4 THE BIOSYNTHESIS OF TRH 9

1.4.1 Mechanisms of TRH synthesis 9
1.4.2 The regulation of TRH synthesis 10

1.5 THE TRH SIGNALLING PROCESS 11

1.5.1 TRH binds to specific receptors 11
1.5.2 TRH receptor signalling mechanism 12
1.5.3 TRH functions through K^+ channel blockade 13
1.5.4 The distribution of TRH receptors 14
1.5.5 TRH receptor internalisation 18

1.6 DEGRADATION OF TRH 18

1.6.1 TRH-degrading Enzyme 19
1.6.2 Structure of TRH-DE 20

1.7 THE CENTRAL EFFECTS OF TRH 23

1.7.1 The effect of TRH or TRHR deletion 23
1.7.2 The effect of TRH on arousal and sleep time 25
1.7.3 The effect of TRH on appetite 26
1.7.4 The effect of TRH on mood disorders 27
1.7.5 TRH regulates body temperature 28
1.7.6 The effect of TRH on locomotion 28
1.7.7 TRH and pain perception 29

1.8 THE INTERACTION OF TRH WITH NEUROTRANSMITTERS 29

1.8.1 The interaction of TRH and GABA 30
1.8.2 The interaction of TRH and serotonin 31
1.8.3 The interaction of TRH and acetylcholine 31
1.8.4 The interaction of TRH and dopamine 32
1.8.5 TRH and glutamate 32

1.9 GLUTAMATE NEUROTRANSMISSION 33

1.9.1 NMDA receptors 34
1.9.2 AMPA receptors 34

1.9.3 Kainate receptors 34
1.9.4 Metabotropic glutamate receptors 35
1.9.5 The role of glial cells in glutamate signalling 36
1.9.6 The effect of TRH on glutamate signalling 37
1.10 EXCITOTOXICITY 38
1.10.1 Free radicals and excitotoxicity 39
1.10.2 Failure of the small glutamate compartment 39
1.11 THE ROLE OF TRH IN DISEASE STATES 40
1.11.1 The potential of TRH therapy in Alzheimer's disease 41
1.11.2 The potential of TRH therapy in ALS 42
1.11.3 Parkinson's disease and the potential of TRH therapy 43
1.11.4 Epilepsy 45
1.11.5 TRH improves memory and learning deficits 46
1.11.6 TRH treatment for spinocerebellar degeneration 46
1.11.7 The effect of TRH on alcoholism 47
1.11.8 TRH and head injury and spinal trauma 48
1.11.9 Ischaemia and brain injury 49
1.12 OVERVIEW OF PROJECT AIMS 50

CHAPTER 2 GENERAL METHODS 51

2.1 SOURCES OF REAGENTS 52
2.2 PREPARATION OF SOLUTIONS 52
2.3 PIPETTING 52
2.4 PH DETERMINATION 52
2.5 CENTRIFUGATION 53
2.6 SPECTROPHOTOMETRY 53
2.7 PROTEIN DETERMINATION 54
2.7.1 Bio-Rad assay for protein determination 54
2.7.2 Markwell assay for protein determination 54
2.8 TISSUE SLICE SUPERFUSION SYSTEM 57
2.9 ENZYME ASSAYS
2.9.1 Assay of lactate dehydrogenase activity 58
2.9.2 Assay of glutamine synthetase activity 58
2.9.3 Assay of apoptosis activation 61
2.9.3.1 Lysis Buffer 61
2.9.3.2 Reaction Buffer 61
2.10 ASSAY OF BIOGENIC AMINES AND THEIR METABOLITES 64
2.11 ASSAY OF NEUROACTIVE AMINO ACIDS 68
2.12 STATISTICAL ANALYSIS AND CURVE FITTING 71

CHAPTER 3 INHIBITION OF THYROTROPIN-RELEASING HORMONE DEGRADING ENZYME 72

3.1 INTRODUCTION 73

3.2 METHODS 75

3.2.1 Composition of buffer 75
3.2.2 HPLC mobile phase 75
3.2.3 Enzyme Purification 75
3.2.3.1 Purification of Thyrotropin-releasing hormone- degrading enzyme 75
3.2.3.2 Purification of dipetidyl peptidase IV 76
3.2.4 Standard Curve of Pyroglutamate 76
3.2.5 Standard curve of 7-amino-4-methylcoumarin 77
3.2.6 Screening of novel inhibitor compounds 80
3.2.6.1 Hydrolysis of Peptides 83
3.2.6.2 Continuous coupled fluorometric assay 83
3.2.6.3 Discontinuous fluorometric assay 84
3.2.6.4 Kinetic analysis of inhibition by non-linear regression 85

3.3 RESULTS 86

3.3.1 HPLC screening of peptides 86
3.3.1.1 Degradation profile of TRH 86
3.3.1.2 Glp-Asn(*N*-Bzl)-ProNH_2 is hydrolysed by TRH-DE 86
3.3.2 The kinetic parameters of TRH-AMC 89
3.3.3 Kinetic properties of peptides resistant to TRH-DE hydrolysis 89
3.3.4 Kinetic properties of peptides hydrolysed by TRH-DE 90
3.3.5 Kinetic analysis of Inhibition by non-linear regression 95
3.3.5.1 Kinetic parameters of Glp-Asn-Pro-Tyr-TrpAMC 95
3.3.5.2 Kinetic parameters of Gl-Asn-Pro-Tyr-Trp-TrpAMC 100

3.4 DISCUSSION 104

3.4.1 Structure–activity relationships 104
3.4.2 Effects of modifications to the Asn side-chain 104
3.4.3 The effects of replacing or modifying the proline residue 104
3.4.4 Carboxy terminus extension 105

CHAPTER 4 ASSESSMENT OF NEUROTOXICITY AND NEUROPROTECTION OF *IN VITRO* MODELS 107

4.1 INTRODUCTION 108

4.2 METHODS 110

4.2.1 The effects of a range of kainate doses on the lactate dehydrogenase (LDH) content of hippocampal slices 110
4.2.2 The effect of TRH on viability as determined by LDH activity 110

4.2.3 The effect of TRH on kainate induced apoptosis as determined by measurement of caspase activation 111
4.2.4 Effects of TRH on Kainate toxicity: Amino Acid Release 111
4.2.5 Effects of TRH on Kainate toxicity: Amino Acid Content 112
4.2.6 Effect of TRH on kainate induced loss of glial-cell viability, as determined by assay of glutamine synthase (GS) activity 112
4.2.7 Effect of TRH on kainate toxicity: Catecholamines, their metabolites and serotonin 112
4.3 RESULTS 113
4.3.1 The superfusion system: Basal levels 113
4.3.2 *In vitro* effects of a range of kainate doses on hippocampal slices 115
4.3.3 The effect of TRH on viability, as determined by assay of lactate dehydrogenase activity 117
4.3.4 The effect of kainate on apoptosis as determined by measurement of caspase activation 126
4.3.5 The effect of TRH on kainate induced apoptosis 126
4.3.6 TRH prevents an increase in the release of glutamine from hippocampal slices 129
4.3.7 Effect of TRH on KA toxicity: alterations in the level of amino acids 132
4.3.8 The effect of TRH and kainate on glial-cell viability 138
4.3.9 Effects of TRH on kainatate toxicity: Biogenic amine levels 140
4.4 DISCUSSION 148

CHAPTER 5 STUDIES ON THE PROTECTIVE EFFECT OF TRH AGAINST CELLULAR INSULTS 156
5.1 INTRODUCTION 157
5.2 METHODS 160
5.2.1 Culturing 160
5.2.2 Cell Counting 160
5.2.3 Cell Plating 160
5.2.4 Cell toxicity studies 161
5.2.5 Cell Viability 161
5.2.5.1 The MTT viability assay 161
5.2.5.2 Propidium iodide exclusion 162
5.2.5.3 Lactate dehydrogenase release 162
5.2.5.4 Caspase activity 163
5.3 RESULTS 164
5.3.1 Dose-dependant and time-dependant effects of toxins on SH-SY5Y death 164
5.3.2 The effect of TRH on staurosporine toxicity 168
5.3.2.1 MTT viability studies 168
5.3.2.2 Propidium Iodide studies 172
5.3.2.3 Effect of TRH and staurosporine on LDH release 177
5.3.2.4 Caspase activity following staurosporine treatment 177
5.3.2.5 Comparison of the different detection procedures 182
5.3.3 The effect of TRH on kainate induced toxicity 186

5.3.3.1 Viability studies with MTT assay 186
5.3.3.2 Propidium iodide studies 189
5.3.3.3 Effect of TRH and kainate on LDH release 193
5.3.3.4 Caspase activity following kainate treatment 196
5.3.3.5 Comparison of the different detection procedures 199
5.3.4 The effect of TRH on MPP^+-induced toxicity 202
5.3.4.1 Studies with the MTT assay 202
5.3.4.2 Propidium iodide studies 205
5.3.4.3 Effect of TRH and MPP^+ on LDH release 209
5.3.4.4 Caspase activity following MPP^+ treatment 212
5.3.4.5 Comparison of the different detection procedures 215
5.4 DISCUSSION 218

CHAPTER 6 ASSESSMENT OF NEUROTOXICITY AND NEUROPROTECTION IN *IN VIVO* MODELS 225
6.1 INTRODUCTION 226
6.1.1 Kainate toxicity *in vivo* 226
6.1.1.1 Free radical toxicity 227
6.1.2 TRH effects *in vivo* 228
6.1.3 Microdialysis 228
6.1.4 Short-term working memory 228
6.1.5 Water Maze spatial task 229
6.2 METHODS 230
6.2.1 Microdialysis Animal Studies 230
6.2.1.1 Surgery and microdialysis procedure 230
6.2.1.2 Measurement of amino acid release 232
6.2.1.3 Measurement of biogenic amine release 232
6.2.1.4 Measurement of free radicals 233
6.2.2 Social recognition study 233
6.2.3 Water Maze Task 233
6.2.3.1 Experimental treatment of animals 234
6.3 RESULTS 237
6.3.1 The effect of TRH on kainate challenge to the striatum 237
6.3.1.1 *In vivo* monitoring of amino acid release during kainate challenge 237
6.3.1.2 *In vivo* monitoring of amine release during kainate challenge with TRH treatment 245
6.3.1.3 *In vivo* monitoring of the release of hydroxy radicals following kainate challenge with TRH treatment 254
6.3.2 Social Recognition studies 258
6.3.3 Water-maze studies with kainate and TRH 261
6.3.3.1 Escape latency 261
6.3.3.2 Distance swam 261
6.3.3.3 Probe Test 264
6.4 DISCUSSION 266

CHAPTER 7 GENERAL DISCUSSION 271

7.1 THE CLINICAL POTENTIAL OF TRH 272
7.2 THE INHIBITION OF TRH-DE 272
7.3 *IN VITRO* MODELS OF NEUROTOXICITY 274
7.4 *IN VITRO* ATTENUATION OF NEUROTOXICITY BY TRH 276
7.5 *IN VIVO* ATTENUATION OF NEUROTOXICITY BY TRH 279
7.6 FURTHER STUDIES 281

BIBLIOGRAPHY 282

APPENDIX A 317
APPENDIX B 318
PUBLICATIONS 320

CHAPTER 1

GENERAL INTRODUCTION

1.1 Thyrotropin-releasing hormone (TRH)

Thyrotropin-releasing hormone was originally isolated from porcine and ovine hypothalami as a thyroid-stimulating hormone (TSH, thyrotropin) releasing factor (Bowers et al. 1968; Schally et al. 1969). In 1969, Boler et al., followed by Burgus et al. announced that TRH is a tri-peptide, consisting of L-pyroglutamyl-L-histidyl-prolineamide (L-pGlu-L-His-L-ProNH_2) (Boler et al. 1969; Burgus et al. 1970). This tripeptide is now called thyrotropin-releasing hormone (TRH) and is depicted in Fig. 1.1.

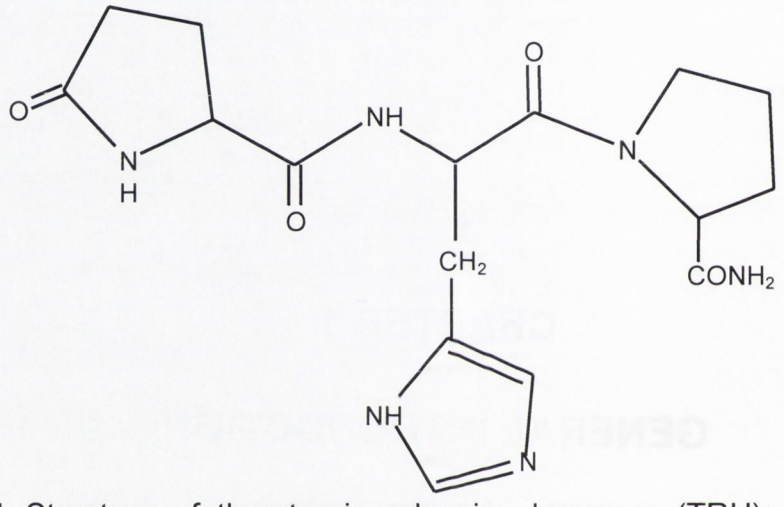

Figure 1.1 Structure of thyrotropin releasing hormone (TRH): TRH is a tri-peptide consisting of L-pyroglutamyl-Lhistidyl-prolineamide (L-pGlu-L-His-L-ProNH_2).

1.2 The function of TRH as a hormone

1.2.1 Regulation of the hypothalamic–pituitary–thyroid axis

The hypothalamic–pituitary–thyroid axis (HPT axis) is a highly regulated system in which TRH plays a role in regulating hormone release (see Fig. 1.2). TRH is secreted from neurons in the hypothalamic paraventricular nucleus and stimulates the synthesis and release of TSH from thyrotroph cells of the anterior pituitary gland. In turn, TSH stimulates the synthesis and release of thyroxine (T_4). When T_4 reaches target cells, it is converted to triiodothyronine (T_3). When

T_4 reaches a critical level, it inhibits TRH and TSH release. Thyroid hormones negatively regulate TRH release and hypothalamic pre-TRH mRNA content (Scanlon and Toft 2000).

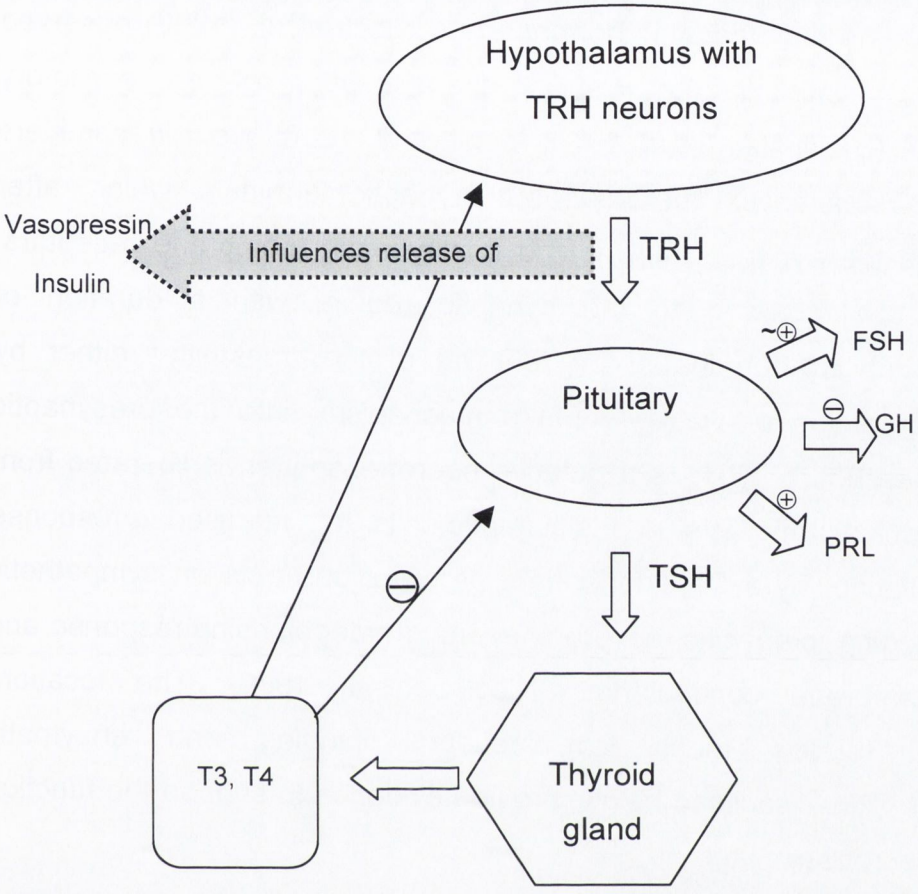

Figure 1.2 Physiological regulation of the hypothalamus–pituitary–thyroid (HPT) axis. ⊖=negative regulation, ⊕=stimulatory effect, ~⊕=mildly stimulatory effect. Neurons in the hypothalamic paraventricular nucleus secrete TRH, triggering the pituitary to make thyroid-stimulating hormone (TSH). TSH stimulates the synthesis and release of thyroxine (T_4). When T_4 reaches target cells, it is converted to triiodothyronine (T_3). When T_4 reaches threshold levels it inhibits TRH and TSH release. TRH also plays a role in stimulating the release of prolactin (PRL) and follicle stimulating hormone (FSH) and inhibiting growth hormone (GH) release from the pituitary, it also influences the release of vasopressin and insulin.

In addition to TSH, TRH stimulates the release of other hormones, including prolactin (PRL) and growth hormone (GH), it has a weak stimulatory effect on follicle-stimulating hormone (FSH) secretion and also indirectly influences the release of vasopressin and insulin (Leong et al. 1983; Scanlon 1991; Lechan and Kakucska 1992; Mason et al. 1995; Hermann et al. 2002; Nillni et al. 2002). Thus, as summarised in Fig. 1.2, TRH is central to HPT axis regulation (2008).

1.3 The function of TRH as a neurotransmitter

TRH, similar to many other brain peptides, has been classified as a neuromodulator. Brownstein et al. (1975) first suggested that TRH may not function simply as a hypothalamic hormone and Nicoll et al. (1980) observed that TRH has some of the classic characteristics of an excitatory neurotransmitter (Brownstein et al. 1975; Nicoll et al. 1980). Neurotransmitters are defined as substances liberated at presynaptic terminals, which, after diffusing across the synaptic gap, act on postsynaptic membrane receptors. Their actions are localised to the synaptic region, with a duration of milliseconds, and are terminated by removal of the transmitter either by enzymatic degradation or via a reuptake mechanism, into the presynaptic terminal (Krieger 1983). TRH, as a putative neurotransmitter, is liberated from presynaptic terminals and acts on postsynaptic cells. It is released in response to nerve stimulation, by a Ca^{2+}-dependent process, and acts on sympathetic neurons, by binding to specific receptors, exerting a depolarising response and increasing membrane conductance (Nicoll et al. 1980). The location, phylogenetics, release mechanism, receptor binding and enzymatic degradation of TRH, discussed below, provide evidence to support the function of TRH as a neurotransmitter.

1.3.1 Distribution of TRH

More than two-thirds of TRH in the rat-brain is found outside of the traditional "thyrotrophic zone" of the hypothalamus (Winokur and Utiger 1974). TRH is found throughout the nervous system of vertebrate and invertebrate species in locations where it has no pituitary–thyroid function. It is found mainly in neural tissue, although it has also been shown to be located outside the nervous system. In addition to the hypothalamus, TRH is found in many brain regions, including the diencephalon, telencephalon, mesencephalon, myelencephalon and spinal cord (Hokfelt et al. 1975; Nilsson et al. 1975). The expression level of the TRH precursor peptide, preproTRH is graphed in Fig. 1.3. The highest mean concentration of TRH in the rat is found in the hypothalamus (126 pg/mg tissue in rat), extra-neural tissues express mean levels of TRH ranging from

0.6–4.8 pg/mg tissue, and serum concentrations of 12.4 pg/ml (Fuse et al. 1990). A table based on published literature, indicating the current knowledge on the distribution of TRH and its predecessor prepro-TRH or its alternative splice products (see section 1.4) in tissues is out lined in Table 1.1.

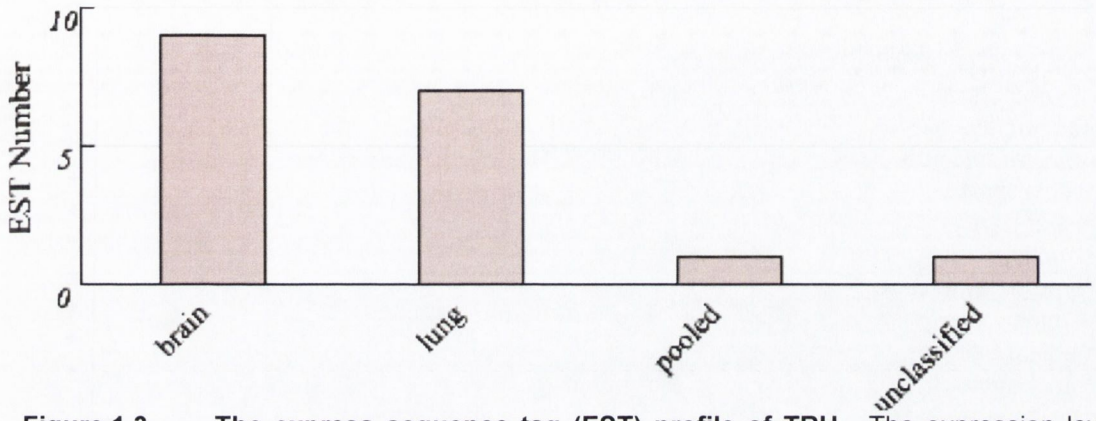

Figure 1.3 The express sequence tag (EST) profile of TRH. The expression level of pre-prothyrotropin, the precursor of TRH in humans (from SynDB, the synapse database (taken fromhttp://syndb.cbi.pku.edu.cn/sdb_pro.php?query=trh&id=TRH_HUMAN&seq_filter=1) (24/10/2008).

Table 1.1 The distribution of prepro-TRH, the splice product TRH and alternative peptides cleaved from prepro-TRH (Nillni and Sevarino 1999).

Tissue	prepro-TRH-derived peptides	TRH	
		Perikarye	Fibers
Olfactory bulb	Partial processing prepro-TRH154–169 prepro-TRH172–199		
Accessory			+
External plexiform layer		+	
Internal plexiform layer		+	
Glomerular layer		+	+
Anterior olfactory nucleus		+	
Hippocampus:			
CA2		+	
CA3		+	
Stratum oriens			+
Dentate gyrus:			
Molecular Layer		+	
Granular Layer		+	
Nucleus accumbens			+
Caudate-putamen		+	+
Medial nucleus		+	+
Central nucleus		+	+
Septum			+
Bed nucleus, anterior commissure		+	
Bed nucleus, stria terminalis		+	+

Tissue	prepro-TRH-derived peptides	TRH	
		Perikarye	Fibers
Diagonal band of Broca		+	+
Entorhinal cortex		+	
Pyriform cortex			+
Paraventricular nucleus			+
Paratenial nucleus			+
Reticular nucleus	Some intermediates, no TRH		+
Ventromedial nucleus			+
Lateral			+
Hypothalamus:			
Anterior hypothalamus		+	+
Supraoptic nucleus		+	
Paraventricular nucleus	prepro-TRH is fully processed		
Magnocellular part		+	+
Parvocellular part		+	+
Arcuate nucleus		+	+
Lateral hypothalamic area		+	+
Median eminence	TRH+ non-TRH peptides		+
Ventromedial nucleus			+
Dorsomedial nucleus		+	+
Perifornical region		+	
Premammillary nucleus			+
Preoptic area	prepro-TRH is fully processed	+	+
Subfornical organ			+
Mesencephalon and metencephalon:			
Locus coeruleus			+
Motor nucleus V			+
Oculomotor nucleus			+
Parabrachial nucleus			+
Periaqueductal gray	prepro-TRH is fully processed	+	+
Red nucleus			+
Substantia nigra, pars lateralis		+	
Trochlear nucleus			+
Myelencephalon:			
Cochlear nucleus		+	
Dorsal motor nucleus, vagus		+	+
External cuneate nucleus		+	
Facial nucleus			+
Hypoglossal nucleus			+
Inferior olive			+
Lateral reticular nucleus		+	
Nucleus ambigus			+
Nucleus tractus solitarius:			
Medial			+
Pontine nuclei		+	
Raphe nuclei:			
Dorsal		+	+
Median		+	+
Reticular formation			+
Spinal Cord	pST10 detected		
Anterior funiculus			+
Central canal			+
Dorsal horn (laminae II and III)		+	+
Intermediolateral column			+
Lateral funiculus			+
Ventral horn (lamina IX)			+

1.3.2 Evolution of TRH

The genomic structure of the preproTRH gene and the three-dimensional structures of preproTRH are highly conserved during the course of evolution in vertebrates. All known preproTRH genes (e.g. human, rat, mouse, frog, medaka and chicken) consist of three exons (Aoki et al. 2007). Within this preproTRH gene, the progenitor sequences for TRH are always located in exon 3 (Aoki et al. 2007). The behavioural role of TRH appears to have been conserved during the evolution of simple species to complex ones, whilst its role in controlling TSH secretion appears to occur only in mammals and birds and has no influence on the reptilian pituitary–thyroid axis (Sawin et al. 1981; Jackson 1986; Mason et al. 1995). This suggests that the primary function of TRH may be as a neurotransmitter and its behavioural role may be older phylogenetically than its role as a regulator of thyroid function (Jackson 1978, 1986; Mason et al. 1995).

1.3.3 Neuronal release of TRH

TRH is stored as a regulated pool within secretory granules in synaptic terminals of neurons. These terminals make both asymmetric and symmetric contacts, primarily with dendrites. The symmetric synaptic contact-dendrites are somewhat smaller than those receiving asymmetric synaptic contact from TRH terminals. The morphological differences between these asymmetric and symmetric synapses is due to the variation in the thickness of the postsynaptic densities, which implies differences in the distribution of receptors, glycoproteins and/or ion channels in the postsynaptic membrane (Rinaman and Miselis 1990). TRH is released from these terminals in a Ca^{2+}-dependent process in response to a depolarising concentration of potassium and may have either excitatory or inhibitory effects on post-synaptic neurons. These opposite effects may be explained by the possible correlation between synaptic structure and function, asymmetric synapses are excitatory while symmetric synapses are inhibitory (Rinaman and Miselis 1990). The receptor binding process is discussed in Section 1.5.

1.3.4 Co-localisation of TRH

TRH has been found by immunohistochemical and immunocytochemical studies to co-localise with other neurotransmitters and/or neuromodulators in several areas of the brain. These include serotonin (5-HT) and Substance P (SP) in medullary bulbospinal neurons (Hokfelt et al. 1989; Poulat et al. 1992a), dopamine (DA) in the olfactory bulb, and histamine, enkephalins (ENK) and neuropeptide Y (NPY) in various loci of the hypothalamus (Hokfelt et al. 1989). TRH also influences release of the neurotransmitters noradrenaline (NA) and adrenaline (Lechan and Kakucska 1992). Table 1.2 outlines the intraneural co-localisation of TRH with neurotransmitters in various sites of the CNS. Since serotonin co-localises with γ-aminobutyric acid (GABA) (Kachidian et al. 1991), cholecystokinin (Mantyh and Hunt 1984) and proctolin (Hokfelt et al. 1989), this suggests that TRH may also coexist with these in some neuronal populations. The effects of this co-localisation are considered further in Section 1.8.

Table 1.2 Intraneuronal co-localisation of TRH with neurotransmitters

Neuroactive substance	Site of co-localisation with TRH	References
Serotonin	Medullary raphe	(Hokfelt et al. 1989). (Arvidsson et al. 1994)
	Spinal cord (ventral horn)	(Hokfelt et al. 1989; Poulat et al. 1992b)
Substance P	Medullary raphe	(Hokfelt et al. 1989) (Arvidsson et al. 1994)
	Spinal cord (ventral horn)	(Hokfelt et al. 1989; Poulat et al. 1992b)
Neuropeptide Y	Hypothalamus (periacqueductal gray)	(Hokfelt et al. 1989)
Enkephalin	Hypothalamus (perifornical area)	(Hokfelt et al. 1989; Merchenthaler 1991)
Dopamine	Olfactory bulb (periglomerular layer)	(Hokfelt et al. 1989)
Histamine	Hypothalamus (tuberomammillary neurons)	(Airaksinen et al. 1992)
Human growth hormone-like peptide	Hypothalamus medullary raphe	(Lechan et al. 1983; Hokfelt et al. 1989)

The evidence thus indicates TRH is a neurotransmitter/neuromodulator and it fulfils many of the criteria for neurotransmitter status:

- It is present in secretory granules and exocytosis is responsive to membrane depolarisation
- It is released in a Ca^{2+}-dependent process after depolarisation
- It acts through specific postsynaptic receptors that are widely distributed throughout the CNS (see Section 1.5)
- It is rapidly cleared through a specific mode of inactivation (i.e. proteolysis) (Section 1.6.1)

1.4 The biosynthesis of TRH

1.4.1 Mechanisms of TRH synthesis

Like most neuropeptides, TRH is derived from a larger precursor protein, prepro-TRH. This is then processed by carboxypeptidases, the prohormone convertases, PC1 and PC2, cleave prepro-TRH to TRH and various other peptides, referred to as cryptic peptides. This cleavage takes place during axonal transport after removal of the signal peptide (Friedman et al. 1995b; Nillni et al. 1995; Nillni et al. 1996). Multiple copies of TRH are found on the prepro-TRH peptide, with six copies on human and five copies on rat and four TRH copies on chicken prepro-TRH, with seven additional peptides on the rat prepro-TRH (Lechan et al. 1986; Jackson 1989; Yamada et al. 1990; Croissandeau et al. 1992). The cryptic peptides derived from pro-TRH processing include pFT22, pEH24 and pST10, and these may have behavioural or physiological activity (Bulant et al. 1988).

Processing of TRH from the precursor is followed by amidation of the proline residue by peptidyl glycine alpha-amidating monoxygenase, the amide moiety being donated by the C-terminal glycine, finishing with cyclization of the *N*-terminal glutamine by glutaminyl cyclase (EC2.3.2.5; Jackson, 1982). Post-translational processing of TRH appears to be restricted to the neuronal perikarya, as there is no immunoreactivity to pro-TRH peptide in axons or terminals of the median eminence or spinal cord (Jackson 1989). The mechanism of TRH synthesis and processing is represented diagrammatically in Figure 1.4.

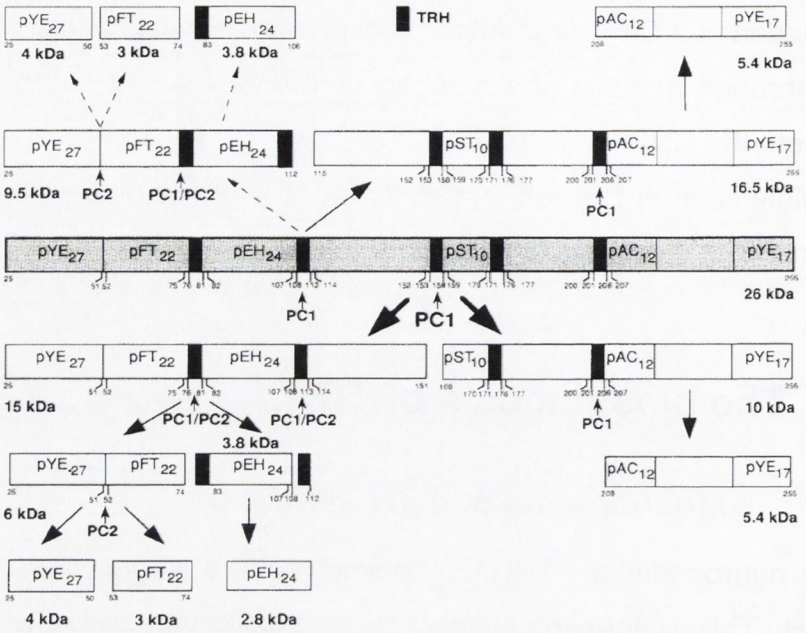

Figure 1.4 Diagrammatic representation of rat pro-TRH processing. The pro-TRH peptide contains multiple copies (5 in rats) of the TRH peptide (black rectangles), in addition to various other peptides (shaded portions). Alternative cleavage of this pro-TRH by prohormone convertase enzymes PC1 and PC2 regulates TRH biosynthesis from Nillni et al., 1996).

1.4.1 The regulation of TRH synthesis

The rate of TRH biosynthesis varies across brain areas and may also vary by cell type, probably as a result of specific neuronal stimuli (Bulant et al. 1988; Lechan and Segerson 1989). It appears that thyroid hormones regulate TRH mRNA levels in the hypothalamus, via an inverse relationship, in order to maintain TRH levels at concentrations that are sufficient to ensure functional integrity of the HPT axis (Lechan and Segerson 1989). TRH levels in extrahypothalamic areas are not regulated by thyroid hormones, but are probably controlled by other behavioural and physiological demands (Mason et al. 1995). Regulation of post-translational processing has also been indicated as a possible rate-limiting step for TRH biosynthesis and may be the principal factor controlling non HPT axis TRH levels (Fuse et al. 1990).

1.5 The TRH signalling process

1.5.1 TRH binds to specific receptors

The effects of TRH are mediated by activation of specific cell surface receptors containing saturable, non-interacting, high-affinity binding sites that exhibit strict structural specificity for TRH at all three amino-acid positions, with a binding constant for TRH of roughly 10nM (Urayama et al. 1999; Sun et al. 2003). The rate of TRH and receptor association and dissociation are highly temperature-dependent, with receptor–TRH binding at a lower affinity and dissociating more rapidly at higher temperatures (Hinkle 1989). These receptors are G-protein-coupled receptors (GPCRs) with seven transmembrane-spanning domains and an extracellular *N*-terminal region containing *N*-glycosylation sites (Straub et al. 1990).

Receptors for TRH have been identified in many species, including fish, lower vertebrates, frogs, rats, mice, cows and humans. To date, three TRH receptor subtypes have been identified, TRH receptor type 1 (TRHR1) was originally cloned from mouse, TRH receptor type 2 (TRHR2) from rat and TRH receptor type 3 (TRHR3) from *Xenopus laevis* (Straub et al. 1990; Itadani et al. 1998; O'Dowd et al. 2000; Bidaud et al. 2002). However, TRHR3 has, as yet, only been found in the frog and it is possible that it is in fact a receptor for a different ligand as it binds TRH only weakly (Lu et al. 2003).

To date, only a single receptor for TRH has been identified in humans, and this receptor has a greater homology with TRHR1 than TRHR2. TRHR2 has been found, thus far, in rat, mouse and *Catostomus commersoni*, but not in humans (O'Dowd et al. 2000; Harder et al. 2001b; Harder et al. 2001a; Colson and Gershengorn 2006). Rat TRHR2 is 51% identical to TRHR1 and important functional differences between the two receptors are implied by variations in agonist-induced internalisation and desensitisation. There are differences in anatomic distribution of TRHR2, with TRHR2 exhibiting higher basal signalling, and TRHR1 considered the “endocrine receptor” (O'Dowd et al. 2000; Harder et al. 2001b; Harder et al. 2001a; Colson and Gershengorn 2006). However, all

six residues that interact directly with TRH within the binding site of TRHR1 are conserved in TRHR2 (Perlman et al. 1997). It is possible in some models to distinguish between the receptors as ligands have been designed that distinguish between mouse TRH receptors, being selective for TRHR2 (Jiang et al. 2005).

1.5.2 TRH receptor signalling mechanism

The properties of TRHR1 and TRHR2 have been characterised in detail and shown to be similar in structure and binding characteristics. Both bind TRH and analogues with indistinguishable affinities and signal with similar potencies and mechanisms of signal transduction (Hinkle 1989; Sharif 1989; O'Dowd et al. 2000). TRHR1 and TRHR2 both use a $G_{q/11}$ protein for transducing a Ca^{2+} signal during the initial response to TRH (Miranda et al. 2005) and function by activating the phospholipase C–protein kinase C signal-transduction pathway (O'Dowd et al. 2000; Lei et al. 2001), which is outlined in Figure. 1.5.

Activation of the phosphoinositide-specific phospholipase-C (PLC) pathway stimulates turnover of inositol phospholipid (IP_3), as membrane phosphatidylinositol 4,5-bisphosphate (PIP_2) is hydrolysed to IP_3 and 1,2-diacylglycerol (DAG). These second messengers stimulate increases in intracellular free calcium-ion concentration ($[Ca^{2+}]_i$), extracellular Ca^{2+} uptake and activation of protein kinase C (PKC) (Kiley et al. 1991; Hsieh and Martin 1992). TRHR activation stimulates calcium/calmodulin-dependent protein kinase (Jefferson et al. 1991, Cui et al. 1994) and mitogen-activated protein kinase (MAPK) (Kanda et al. 1994, Ohmichi et al. 1994). K^+-channel conductances are modulated and cGMP levels also increase (Nakayama et al. 1996; Lei et al. 2001; Kubek and Garg 2002; Miranda et al. 2005).

Although TRHR1 and R2 signal via the same pathways, the receptors have been reported to show marked differences in basal signalling activities. Nevertheless, the maximum levels of PIP_2 hydrolysis due to TRH binding to TRHR1 or TRHR2 appear to be indistinguishable (O'Dowd et al. 2000; Sun et al. 2003).

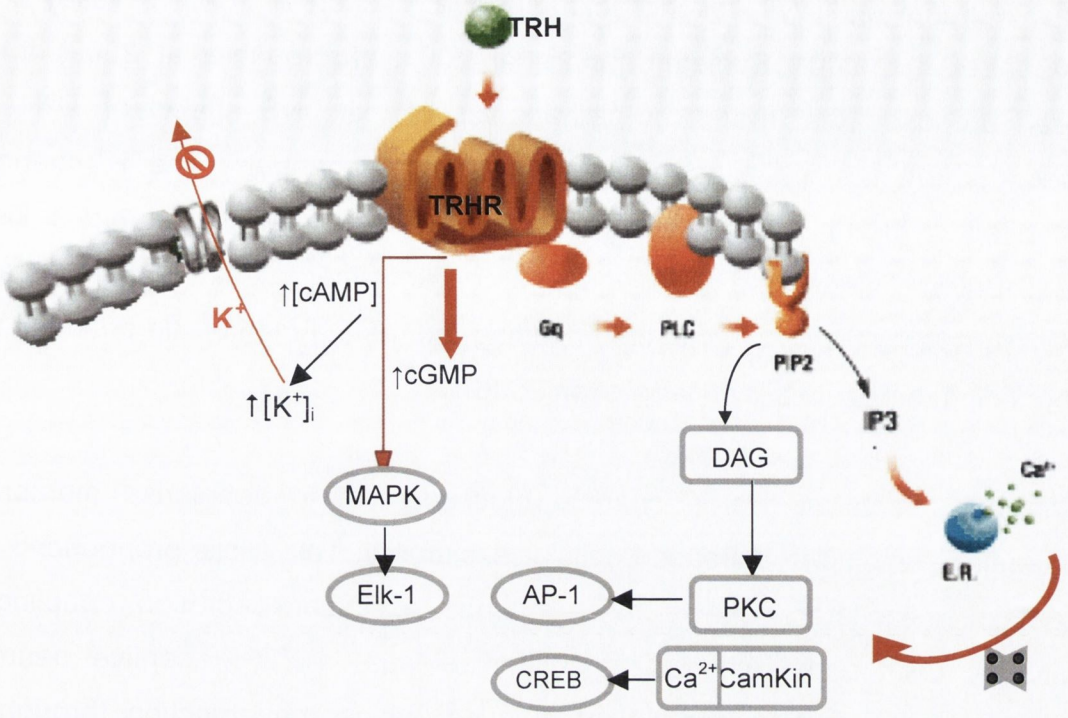

Figure 1.5 TRH signalling mechanism. TRH binds to the TRHR, which operates in conjunction with a $G_{q/11}$ protein, stimulating the PLC pathway and resulting in increased $[Ca^{2+}]_i$ resulting in activation of calcium/calmodulin-dependent protein kinase (Ca^{2+}/CamKin), PKC and MAPK. It also induces gene transcription via transcription factors CREB, AP-1 and Elk-1. The Ca^{2+} inward current results in K^+ channel inhibition, depolarises the cell membrane and results in excitation of the cell. This in turn may cause neurotransmitter release, or motoneuron excitation. PLC: phospolipase C; PIP_2: phosphatidylinositol 4,5-bisphosphate; IP_3: inositol 1,4,5-trisphosphate; DAG: diacylglycerol.

1.5.3 TRH functions through K^+ channel blockade

The actions of TRH are numerous and varied, but a common mechanism appears to underlie these activities (Gary et al. 2003). TRH exerts a depolarising effect through a sustained Ca^{2+}-sensitive inward current that is accompanied by a blockade of K^+ metabotrophic receptors in neurons that are receptive to TRH modulation (Nistri 1990; Nistri et al. 1990).

There are three major classes of K^+-channels: voltage gated channels (K_V), inwardly rectifying channels (K_{IR}) and two pore domain channels (K_{2P}). TRH has been shown to interact with sub-species of each class. TRH blocks K^+-currents from the pituitary K_V human ether-à-go-go-related gene (HERG) channels, neuronal K_{IR} G protein-coupled inwardly-rectifying (GIRK) channels

and neuronal K_{2P} TWIK-related acid-sensitive K^+-channel (TASK) (Talley et al. 2000; Lei et al. 2001; Schledermann et al. 2001; Yarbrough et al. 2007). It has been proposed that many, or perhaps all, of the CNS effects of TRH are mediated by the inhibition of these potassium channels. The K^+-channels inhibited by TRH in CA1 interneurons are most likely to be K_{2P} channels (Deng et al. 2006). This class of K^+-channel has background or leak K^+-channels and, therefore, may play a crucial role in setting the resting membrane potential and regulating cell excitability (Deng et al. 2006).

The net effects of this K^+-channel blockade are to depolarise membrane potentials, leading to increased cellular excitability. This elicits pronounced and sustained excitatory effects that enhance excitation–secretion coupling in pituitary cells and excitation-transmitter release in TRH-receptive neurons, motoneuron excitation and spinal reflexes, which may function through an increase in cyclic AMP (Richerson 2004; Yarbrough et al. 2007). This TRH inhibition may then be negated by activation of $GABA_B$ (γ-aminobutyric acid type b) receptors (Richerson 2004).

The K^+ channels are recognised as potential therapeutic targets in the treatment of multiple sclerosis, Alzheimer's disease, Parkinson's disease, epilepsy, stroke, brain tumours, brain/spinal cord ischaemia, pain, schizophrenia and migraine (Judge et al. 2007). The etiologies of these diseases may be due in part to the dysfunction of these channels and, thus, TRH, as an inhibitor of K^+-channels could play a role in channel regulation.

1.5.4 The distribution of TRH receptors

Despite the similarities between the TRHR1 and TRHR2 subtypes in structure, binding characteristics and mechanisms of signal transduction, the receptors exhibit different tissue distributions.

TRH receptors are distributed heterogeneously throughout the CNS, with TRHR binding sites or their mRNA having been found throughout the

extrahypothalamic nervous system, nucleus accumbens septi, various cranial nerve motor nuclei, the medulla oblongata, ventral spinal cord, cerebellum, cortex, the thalamus and the basal ganglia, where they probably serve neurotransmitter or neuromodulatory functions (Table 1.3).

TRHR1 is highly expressed in limbic structures, with highest expression found in the anterior pituitary, neuroendocrine brain regions, the autonomic nervous system and visceral brain stem regions, whereas TRHR2 is expressed primarily in the thalamus, cerebral and cerebellar cortex, medial habenulae, medial geniculate nucleus, pontine nuclei and throughout the reticular formation (Sharif 1989; Heuer et al. 2000; O'Dowd et al. 2000; Lu et al. 2003). Table 1.3, from Heuer et al. (2000), outlines the mRNA expression levels of TRHR1 and TRHR2 in the CNS as well as the distribution of the mRNA encoding prepro-TRH and the principal enzyme that degrades TRH, TRH-degrading enzyme (TRH-DE).

This specific pattern of distribution suggests that the two receptors may serve different and highly specific functions for the transmission of TRH signals. The physiological functions of TRH mediated by each of these receptor subtypes may be separated into control of the vegetative and autonomic system as well as on the somatomotor system by TRHR1, which is considered the “endocrine receptor”, whereas TRHR2 receptors regulate sensory processing regions and areas controlling higher cognitive functions, providing a basis for the effects of TRH on arousal, locomotor activity and pain perception (O'Dowd et al. 2000; Harder et al. 2001b; Harder et al. 2001a; Colson and Gershengorn 2006).

Table 1.3 The mRNA expression levels of TRH-R1, TRH-R2, TRH-DE and TRH in the rat brain and spinal cord. The relative densities of the hybridisation are ranked as follows: +++++, maximum density; ++++, very dense; +++, dense; ++, moderate; +, low; -, below detection; *, single scattered neurons, (Heuer et al. 2000).

Location	TRHR2	TRHR1	TRH-DE	TRH
Olfactory bulb				
Glomerular cell layer	+	-	++	+++++
External plexiform layer	+	-	++++	+++
Mitral cell layer	+	-	+++	+
Internal plexiform layer	-	-	++++	-
Anterior olfactory nucleus	++	+	++++	+++
Accessory olfactory bulb	-	+++++	+++	++
Cerebral cortex				
Layer 1	-	-	-	-
Layer 2	++	++	+	-
Layer 3	++	+	++++	-
Layer 4	-	+	++++	-
Layer 5	++++	+	++	-
Layer 6a	+++	+	+++++	-
Layer 6b	-	+	+++++	-
Perirhinal cortex	-	++++	++	-
Enterorthinal cortex	-	+++	++	-
Piriform cortex	-	+++	+++++	-
Dorsal endopiriform cortex	-	+++	+++	-
Ncl. of lateral olfactory tract	-	+	+++++	-
Taenia tecta	+++	+	+++++	++
Indusium griseum	-	-	++++	+
Nucleus accumbens, shell	-	++	+	+
Septum, lateral septum	-	-	++++	-
Medial septum	+++	++	+	-
Diagonal band of Broca horizontal limb	++	++++	+	-
Vertical limb	+	+++	++	-
Caudate-putamen	±	-	+	+++++
Globus pallidus	++	-	+	+
Subthalamic nucleus	++	-	+	-
Ventral pallidum	++	+	++	+
Amygdala				
Lateral amygdala	-	+++	++	-
Amygdalohippocampal area		+	-	+*
Medial amygdaloid nucleus	++	+++	+++	-
Central amygdaloid nucleus	++	+	+++	-
Basomedial amygdaloid nucleus	-	+++	±	-
Basolateral amygdaloid nucleus	++	-	-	++
Posterolateral cortical nucleus	-	++	+	-
Posteromedial cortical nucleus	-	+++	+	+++
Hippocampus				
CA1	-	+*	+++	-
CA2	-	+*	+++++	-
CA3	-	+*	++++	-
Dentatus gyrus	-	++	+	++
Subiculum	+++++	-	++++	++*
Diencephalon				
Habenulae medial	+++++	-	++++	-
Thalamus				
Ventral posterior thalamic nucleus	+++++	-	++	-
Centromedial	+++++	-	+*	-
Anterodorsal	+++++	-	++	-
Anteroventral	++++	-	+	-

Location	TRHR2	TRHR1	TRH-DE	TRH
Reticular thalamic nucleus	-	-	-	+++++
Paraventricular thalamic nucleus	+++++	+++++	-	-
Xiphoid thalamic nucleus	++++	-	++	-
Bed nucleus of stria terminalis	++++	+++	+++	++++
Hypothalamus				
Anterior hypothalamic area	+++	+++++	+++	++++
Medial preoptic area	-	++	++++	+++++
Suprachiasmatic nucleus	-	+++	+++	-
Paraventricular hypothalamic nucleus	-	++	+++	+*
Medial parvocellular part	-	+	++	+++++
Zona incerta	+++	+++	++	-
Arcuate ncl.	-	+++	+++	++++
3rd ventricle, ventral part	--	-	+++++	-
Ventromedial hypothalamic nucleus	VL-/D+	+	+	-
Dorsomedial hypothalamic nucleus	-	++	+	+++++
Lateral hypothalamic nucleus	++	+++	+++	+++++
Mesencephalon				
Superior colliculi				
Superficial gray	++	+++	++	-
Inferior gray	++	-	+	-
Inferior colliculi	++++	-	+	-
Medial geniculate nucleus	++++	-	++	-
Substantia nigra	++	±	++	-
Pars compacta				
Pars reticulata	-	++	+++	-
Periaqueductal gray	-	+++	++	-
Pontine nucleus	+++++	-	-	+++
Interpeduncular nucleus	++++	-	+	-
Facial nucleus	-	++++	±	-
Motor nucleus of trigeminus	-	++++	±	-
Reticulotegmental nucleus	+++++	-	-	++
Cerebellum				
Granular layer	+++*	-	+++++*	++++*
Molecular layer	++++*	-	-	-
Purkinje cell layer	-	-	-	-
Brainstem				
Reticular formation	+++++	+*	+++	-
Parabrachial nucleus	+ (medial)	++ (lateral)	++	-
Dorsal tegmental nucleus	+++	-	-	-
Noradrenergic A5	++	-	-	-
Barrington nucleus	-	++	-	-
Raphe obscurus/magnus	-	-	-	+++++
Ncl. tractus solitarii	-	+++	++	-
Area postrema	-	-	+++++	++
Hypoglossal nucleus	-	+++++	+	-
Dorsal motor nucleus of vagus	++	++++	++++	++
Nucleus ambiguous	-	++++	+	-
Ncl. cuneatus	++	+	++	-
Spinal trigeminal nucleus	+++	++(external)	++	+++++
Medullary reticular nucleus	+++	+	++	-
Spinal cord				
Superficial dorsal horn	+	+++	+++	+++
Deep dorsal horn	+++++	+	++	-
Ventral horn	+++++	++++	++	-
Motoneurons	-	+++++	++++	-

1.5.5 *TRH receptor internalisation*

TRH binding is followed by TRHR phosphorylation, β-arrestin binding and rapid clatharin-dependent internalisation of the receptor, with TRHR2 being internalised faster than TRHR1 ($t_{1/2}$ = 0.20 min for TRHR2 and $t_{1/2}$ = 1.6 min for TRHR1 upon Methyl-TRH stimulation(O'Dowd et al. 2000). The carboxyl terminus of the receptor plays an important role and coated pits are involved in the endocytosis (Ashworth et al. 1995; Heuer et al. 2000; Cook and Hinkle 2004). These internalised receptors are either targeted to lysosomes, where they undergo degradation, or are recycled back to the plasma membrane (Ashworth et al. 1995; Cook and Hinkle 2004).

1.6 Degradation of TRH

TRH is rapidly metabolised by endopeptidases, having a biological half-life in the order of only 5 minutes in humans (Faden et al. 2005). The levels of TRH are regulated by enzymatic inactivation both intra- and extracellularly. Several enzymes that degrade TRH have been identified, as detailed in Table 1.4, and the method of degradation is presented in Fig. 1.6. These include post proline cleaving enzyme, also known as prolylendopeptidase (PE), and pyroglutamyl aminopeptidase I (PAP I), both of which are cytosolic enzymes, and by the membrane-bound thyrotropin-releasing hormone-degrading enzyme (TRH-DE), also called pyroglutamyl aminopeptidase II (PAP II), and the serum peptidase thyroliberinase, which exhibits identical chemical characteristics to TRH-DE and is thought to result from an alternative cleavage of TRH-DE (Friedman and Wilk 1985; Lin and Wilk 1998). It is generally acknowledged that thyroliberinase and TRH-DE are primarily responsible for removal of TRH *in vivo* (O'Cuinn et al. 1990).

Table 1.4 **Enzymes that degrade TRH.** TRH has a short half-life (~5 min) following its release from cells. Three enzymes are responsible for its degradation, with TRH-DE considered the most critical to TRH metabolism.

Enzyme	Abbreviation	EC Number	Properties
Pyroglutamyl aminopeptidase I	PAP I	3.4.19.3	A soluble cysteine protease
Prolyl endopeptidase	PE	3.4.21.26	A soluble serine protease
Pyroglutamyl aminopeptidase II	PAP II, TRH-DE	3.4.19.6	Membrane bound and located primarily in the CNS
Thyroliberinase		3.4.19.6	Similar to PAP II but missing the transmembrane anchor

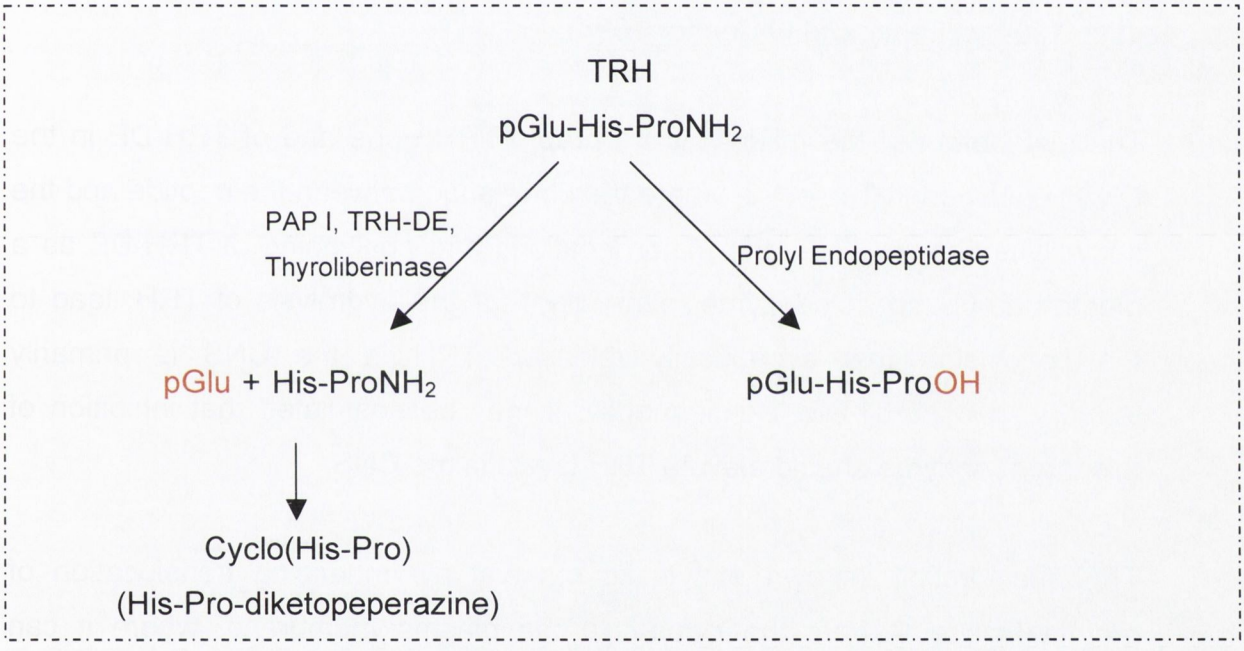

Figure 1.6 **Enzymatic pathways of TRH degradation.** TRH-DE, a membrane bound enzyme is highly specific for TRH and is considered to be the most critical enzyme in TRH degradation, due to its concentration in the CNS. Both PAP I and PE are cytosolic enzymes. Thyroliberinase is found in serum and is thought to result from an alternative cleavage of TRH-DE, with loss of the membrane anchor (Friedman and Wilk 1985). The source of this serum enzyme may be the liver (Lin and Wilk 1998).

1.6.1 TRH-degrading Enzyme

TRH-DE is considered the first 'neuropeptide specific peptidase' (Wilk 1986) due to its unprecedented degree of specificity for the particular peptide conformation of TRH (O'Cuinn et al. 1990; Bauer et al. 1997b). TRH-DE is

primarily an enzyme of the CNS, exhibiting highest levels of activity in the brain, where it has a heterogeneous distribution, but with highest activity in the hippocampus and cerebral cortex (Friedman et al. 1995a). TRH-DE in the CNS is localised on synaptosomal and adenohypophyseal plasma membranes (Bauer et al. 1990; O'Leary and O'Connor 1995). It is also present at lower levels in the lung, retina and liver (Vargas et al. 1992).

The cDNA sequence of TRH-DE indicates that it is a membrane-bound enzyme. It also provides evidence that it is an ectoenzyme, i.e., an integral membrane protein with an extracellularly localised active site (Bauer et al. 1981; Friedman and Wilk 1986; Bauer et al. 1990; Cruz et al. 1991; Schauder et al. 1994; O'Leary and O'Connor 1995).

The distribution of the mRNA of the prepro-TRH gene and of TRH-DE in the CNS is outlined in Table 1.3, where the correlation between the peptide and the enzyme is shown. Thus, the major locations and positioning of TRH-DE as a membrane-bound ectoenzyme, convenient for the hydrolysis of TRH, lead to the conclusion that synaptically released TRH in the CNS is primarily terminated by TRH-DE. Consequently, it may be postulated that inhibition of this target enzyme should elevate TRH levels in the CNS.

TRH may inhibit its own enzymatic removal by enhancing translocation of protein kinase C from the cytosol to the plasma membrane, where it can inactivate TRH-DE by phosphorylation of the enzyme (Mason et al. 1995).

1.6.2 Structure of TRH-DE

TRH-DE is a homodimeric glycoprotein composed of two identical 116 kDa subunits, which are associated non-covalently (Bauer et al. 1990; Papadopoulos et al. 2000). It is a member of the metallopeptidase family (see MEROPS: The peptidase database, http://merops.sanger.ac.uk/) and shares significant homology with two M1 aminopeptidases, aminopeptidase A (APA) (32% homology) and aminopeptidase N (APN) (34% homology), with homology occurring most notably in the extracellular domain (Bauer 1994; Papadopoulos

et al. 2001; Chavez-Gutierrez et al. 2006). TRH-DE is a zinc peptidase that contains the conserved HEXXH + E sequence in the extracellular domain, which is characteristic of zinc-enzymes. Glutamate residues in this motif coordinate the Zn^{2+} atom (Czekay and Bauer 1993; Bauer 1994; Schauder et al. 1994). The structure of TRH-DE is not yet known, but theoretical modelling and mutational analyses have been used to elucidate details of the enzyme's active site and overall structure (see Figures 1.7–1.9; (Kelly et al. 2005; Chavez-Gutierrez et al. 2006). These homology studies have been performed by multiple alignment of the M1 family members (APA, APN and leukotriene A_4 hydrolase) to create three-dimensional models of TRH-DE. Docking studies have been used to investigate the interaction between the enzyme and TRH.

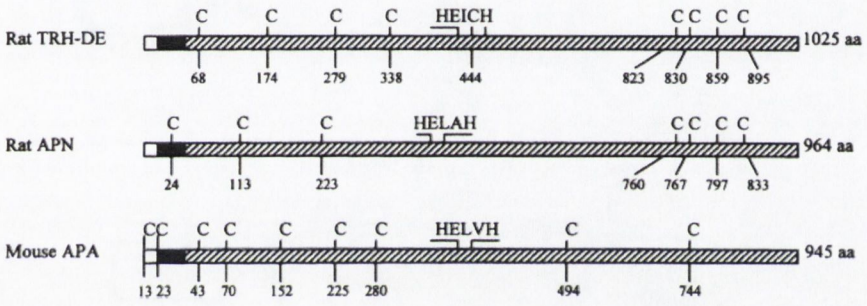

Figure 1.7 Schematic representation of the primary structure of rat TRH-DE, rat APN and mouse APA. TRH-DE is a zinc metallopeptidase that contains the conserved HEXXH sequence in its extracellular domain. It shares significant homology with two M1 aminopeptidases, A and N, creating a basis for homology modelling and docking studies of TRH-DE (Papadopoulos et al. 2000).

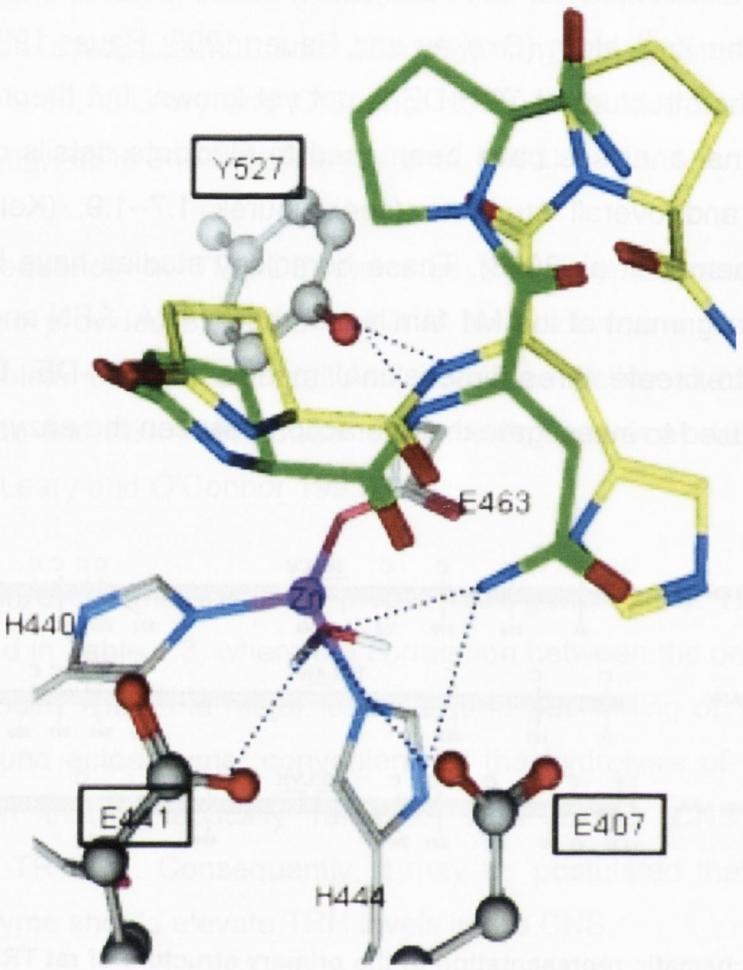

Figure 1.8 Modelling the TRH-DE active site. The interaction between key active-site residues of human TRH-DE (labeled in black) and TRH (yellow) or the inhibitor Glp-Asn-Pro (green) are illustrated using the crystal structure of leukotriene A_4 hydrolase (LTA_4H) as a template for homology modelling by MOE (Molecular Operating Environment; Chemical Computing Group). The zinc residue is labeled pink and broken lines indicate possible hydrogen-bond interactions between the P_1' asparagine residue of Glp-Asn-Pro and the enzyme (Kelly et al. 2005).

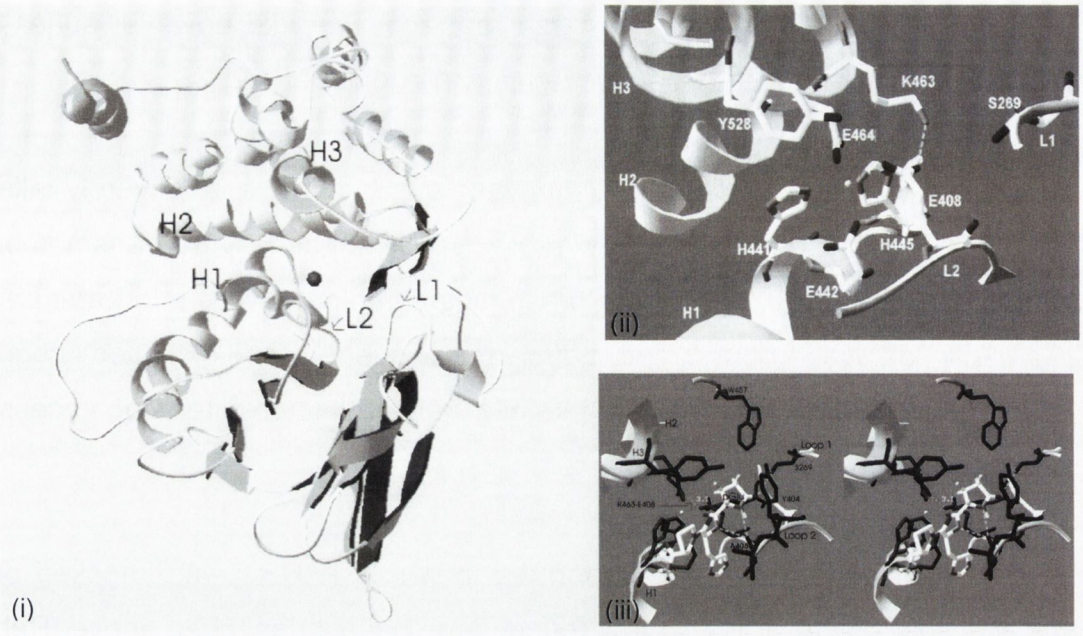

Figure 1.9 Model of Rat TRH-DE. (i) A three-dimensional model of the catalytic region of TRH-DE was generated by Chavez-Gutierrez et al. (2006) using Insight II (Accelrys Software Inc., San Diego, CA) with the human LTA_4H x-ray crystal structure as a template for homology modelling. (ii) A close up of the catalytic site, with helices 1 and 2 (*H1*, *H2*) containing the HEXXH motif residues. (iii) TRH-DE with TRH docked. The Zn^{2+} residue in i, ii and iii is shown as a grey sphere (Chavez-Gutierrez et al. 2006).

1.7 The central effects of TRH

TRH appears to function as a modulator of CNS actions, normalising the intensity and quality of CNS activity by affecting brain chemistry, behaviour and physiology. These centrally induced effects are not mediated by the endocrine effects of TRH, since most of the CNS effects of TRH can be achieved even when the endocrine targets of the tripeptide have been removed, but they may work in conjunction with, and are dependent upon, the behavioural/physiologic state of the organism (Nemeroff et al. 1984; Mason et al. 1995).

1.7.1 The effect of TRH or TRHR deletion

Knockout mice, targeting the prepro-TRH gene have been generated. These $TRH^{-/-}$ mice had no apparent abnormality in the central nervous system, gastrointestinal tract, reproductive system or visual system. Although no

behavioural characterisation has been reported, they did however suffer from hypothyroidism and mild hyperglycaemia (Yamada et al. 1997).

A patient exhibiting hypothyroidism was found to have a severely altered, inactive, TRH receptor, with the protein missing all seven transmembrane domains (Collu et al. 1997). The presenting symptoms were short stature with markedly delayed bone maturation; the patient also exhibited cognitive deficiencies, although this was a family trait and, therefore, not necessarily associated with the receptor mutation.

Two studies have also been performed in which TRHR1 was knocked out in mice, giving results similar to that found in the patient described above (Rabeler et al. 2004; Zeng et al. 2007). While both studies found $TRHR1^{-/-}$ mice to have hypothyroidism, there were differences in some of their findings. Rabeler et al. (2004) found the $TRHR1^{-/-}$ mice to be clearly growth retarded, but Zeng et al. (2007) reported that they were normal in both body length and weight. Both studies concluded that the mice had no overt developmental abnormalities, and neither reproduction nor lactation was severely impaired. Behavioural evaluation performed on the $TRHR1^{-/-}$ mice revealed elevated anxiety and depression levels, suggesting that TRH is involved in mood regulation (Zeng et al. 2007).

It has been proposed that TRH maintains the balance between ergotropism and trophotropism, having a homeostatic role as it acts to normalise the intensity and quality of CNS activity (Mason et al. 1995; Gary et al. 2003). It may be that TRH functions only under certain physiological conditions, such as stress or healing (Gary et al. 2003). When TRH is infused into animals it acts as an excitatory agent with organism-wide effects on arousal, sleep, cognition, locomotion and mood. Gary's concept of TRH acting as a homeostatic modulator of the CNS is depicted in Fig. 1.11, with the effect of TRH activation being dependent on the particular state of the organism (Gary et al. 2003). It has been suggested that one of the roles for TRH in the brain is as an intrinsic regulator of thalamocortical network activity, which would provide a potential

mechanism for TRH's wake-promoting and anti-epileptic effects (Broberger and McCormick 2005).

TRH enhances motor neuron firing in response to excitatory amino acids, increases motoneuron recruitment by antidromic stimulation and depolarises ventral roots (Nillni and Sevarino 1999). TRH increases cholinergic transmission and augments the excitatory input of acetylcholine (ACh). It is thought that many effects of TRH are mediated by cholinergic mechanisms (Yarbrough 1983; Nillni and Sevarino 1999; Gary et al. 2003). TRH modulates the activity of several other neurotransmitters, including dopamine, serotonin and opiates, so it may affect the actions of the many drugs that affect these and other neurotransmitters (Nemeroff et al. 1984; Griffiths 1985).

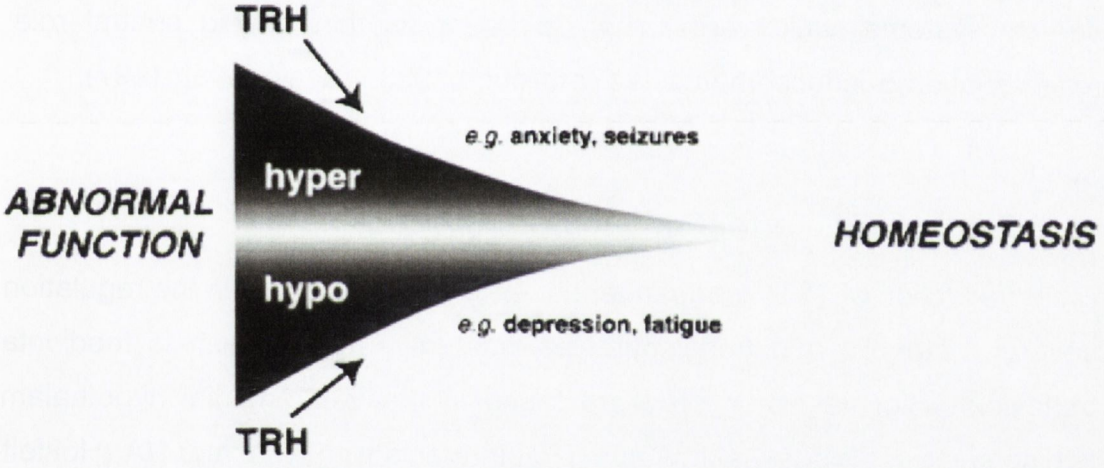

Figure 1.10 Conceptualisation of the homeostatic modulatory role of TRH. Significant alterations in CNS neuronal activity, resulting from either hyper- or hypo-function, can clinically manifest as anxiety and seizures or as depression and fatigue, respectively. TRH neuronal systems are activated by the perturbed CNS function and respond by returning the system back to homeostasis (Gary et al. 2003).

1.7.2 The effect of TRH on arousal and sleep time

The first noted ergotropic effect of TRH was on arousal and sleep time (Metcalf and Dettmar, 1981). TRH has analeptic properties, with administration resulting in reversal of sedation and increased wake time and/or decreased sleep time in several species, whether caused by drugs such as barbiturates, trauma or by natural physiological conditions such as hibernation (Metcalf and Dettmar 1981;

Nillni and Sevarino 1999). TRH has the ability to arouse animals from drug narcosis induced by alcohol and other CNS depressants, including opiates, phenothiazines and benzodiazepines and it has been demonstrated that TRH levels rise in the medial septum as rats recover from ethanol-induced sedation (Morzorati and Kubek 1993). When microinjected into the dorsal hippocampus of the ground squirrel, TRH produced physiological and behavioural arousal from hibernation (Stanton et al. 1981).

This effect of TRH appears to operate through cholinergic pathways, and it has been shown to prevent the post-concussive elevation of cortical ACh and reduction of cortical NA (Tanaka et al. 1997). The medial septal area of the brain has the greatest degree of sensitivity to TRH administration, where cholinergic activity is enhanced in the septohippocampal and nucleus basalis-cortical systems, which are known to be areas that play a central role in reversal of drug-induced narcosis (Yarbrough 1983; Tanaka et al. 1997).

1.7.3 The effect of TRH on appetite

A central action of TRH, independent of endocrine activity, is in the regulation of several metabolic and behavioural parameters, one of which is food intake behaviour. High levels of TRH are found in the ventromedial hypothalamus (which serves to signal satiety) and TRH interacts with NPY and NA (Hokfelt et al. 1989). However, it has also been suggested that this effect is independent of catecholamine pathways, and that TRH thereby decreases appetite (Appenzeller and Oribe 1997). Enkephalin, NPY and NA are all important to intake behaviour, which suggests that TRH plays a role in appetite regulation. This is consistent with findings that TRH suppresses food and water intake and causes an increase in gastrointestinal motility as well as an increase in the volume and acidity of gastric secretion (Steward et al. 2003; Ao et al. 2006; Lechan and Fekete 2006; Schuhler et al. 2007). This indicates that TRH possesses anorexigenic capacity.

1.7.4 The effect of TRH on mood disorders

TRH appears to be involved in the pathophysiology of mood disorders, since its synthesis and TRHR levels undergo a prolonged increase in the brain (hippocampus, amygdala, entorhinal cortex and pyriform cortex — regions known to be involved in depression) following treatment with mood stabilisers such as valproate and lithium chloride, and during electroconvulsive therapy (ECT), a treatment for major depression (Sattin et al. 1987; Knoblach and Kubek 1994; Pekary et al. 2000; Sattin et al. 2002; Pekary et al. 2004).

TRH administration enhances the pharmacological action of antidepressant drugs. It has therefore been suggested that the beneficial effects of antidepressants may be mediated by TRH (Gary et al. 2003). The intravenous or intrathecal administration of TRH induces rapid (within hours) remission of major depression in humans and has a sustained antidepressant effect in patients with bipolar disorders of type I and II (Callahan et al. 1997; Marangell et al. 1997; Szuba et al. 2005; Zeng et al. 2007).

The anxiolytic effects of TRH have also been demonstrated, administration to healthy pre-menopausal women resulted in improvement in ratings of tension and anxiety, with no difference to the behavioural effects of TRH in normal subjects (Winokur et al. 1982). This gives further evidence for TRH functioning as a homeostatic regulator, where its effects may be influenced by the state of activity of the CNS.

Behavioural experiments on TRHR1$^{-/-}$ mice (Section 1.7.1) and senescence-accelerated mice (mice showing age-related emotional changes as well as learning and memory impairments) demonstrated that TRH has a key role in regulating anxiety and depression-elevated anxiety as well as depression, providing further evidence that TRH is involved in mood regulation (Miyamoto et al. 1994; Zeng et al. 2007).

1.7.5 TRH regulates body temperature

Thermoregulation is controlled from the brainstem and spinal cord. TRH has a prominent role in integrating a number of thermogenic responses, at least in some species. The effect of TRH on core body temperature is variable and species-dependent. In man, intravenous injection of TRH causes cutaneous vasodilation, sweating and thus a drop in core body temperature (Sugenoya et al. 1988). It can cause hypothermia (when given into the ventricles) by serving to reduce body temperature through lowering the reference temperature for heat dissipation (Nillni and Sevarino 1999). TRH produces hypothermia in cats, whilst inducing hyperthermia in other species (e.g. mouse, rabbit, Siberian hamster) (Metcalf and Myers 1975; Boschi et al. 1983a; Sugenoya et al. 1988; Schuhler et al. 2007).

The effect of TRH on body temperature is coordinated principally in the anterior preoptic area of the hypothalamus, and the effect has been shown to be unrelated to the endocrine function of TRH (Metcalf and Myers 1975; Nillni and Sevarino 1999; Lechan and Fekete 2006). In species where TRH causes hyperthermia, the increase in body temperature is not simply a result of the induction of locomotor activity, since experiments with the Siberian hamster showed that the body temperature increased through peripheral vasoconstriction, increased metabolic heat production and shivering, suggesting that endogenous TRH is important in arousal from hypothermic states (Schuhler et al. 2007). TRH has been shown to antagonise hypothermia produced by ethanol, morphine, barbiturates, chlorpromazine and endogenous neuropeptides, including neurotensin, bombesin and β-endorphin (Nemeroff et al. 1984; Horita et al. 1986). This indicates that TRH plays an important role in temperature homeostasis.

1.7.6 The effect of TRH on locomotion

Investigators have documented pronounced and long-lasting excitatory effects of TRH on amphibian and mammalian spinal motoneurons and spinal reflexes (Yarbrough 2003). The systemic administration of TRH to rats elicits locomotor

activation, including frequent rearing, sniffing, grooming, preening, wet-dog shakes, jaw movements, paw licking and tail rattle (Miyamoto and Nagawa 1977). TRH has been shown to antagonise motor impairment and convulsions caused by ethanol, volatile general anaesthetics, sedative–hypnotic drugs and by other CNS depressants (Nemeroff et al. 1984).

TRH elicits distinct effects on the CNS that can be either dependent or independent of the dopamine system of the mesolimbic area and nucleus accumbens, which indicates that there are overlapping, but distinct, TRH mechanisms that induce locomotion (Miyamoto and Nagawa 1977; Funk et al. 1997).

1.7.7 TRH and pain perception

TRH has an analgesic effect. Peripheral or central injection with TRH of mice has shown TRH to have antinociceptive properties that are equal to or greater than those of morphine, although the duration of pain relief is short (Boschi et al. 1983b; Tanabe et al. 2007). This is most likely due to the short biological half-life of TRH (in the order of ~5 minutes) (Morley 1979; Moss and Bundgaard 1990).

1.8 The interaction of TRH with neurotransmitters

The homeostatic role of TRH described in the previous section, and the beneficial effects of endogenous and administered TRH, lead to the assumption that it may be of benefit in a number of disease states. The involvement of TRH with several neurotransmitter systems, particularly ACh, serotonin and noradrenalin, is thought to be implicated in its beneficial effects (see Table 1.2 for co-localisation of TRH with neurotransmitters and Figure 1.11 for an example of the convergence of multiple inputs on the *Xenopus* melanotrope cell).

The interaction of TRH with these neurotransmitter systems will be considered in the following sections, with particular emphasis on the glutamatergic system,

in particular disease states resulting from excitotoxicity, which was the main focus of the present work.

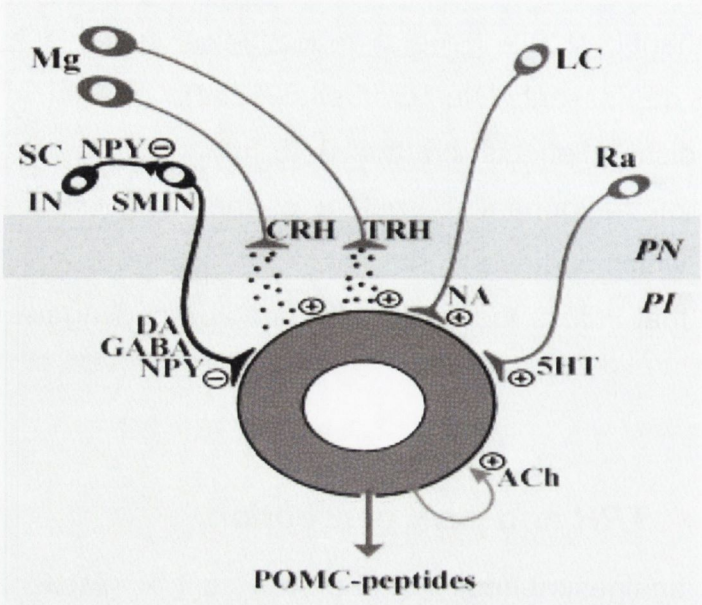

Figure 1.11 The converging neurochemical input on a melanotrope cell. CRH, corticotropin-releasing hormone; DA, dopamine; GABA, γ-aminobutyric acid; IN, interneurons; LC, locus coeruleus; Mg, magnocellular nucleus; NA, noradrenaline; NPY, neuropeptide Y; PI, pars intermedia; PN, pars nervosa; POMC, pro-opiomelanocortin; Ra, raphe nucleus; SC, suprachiasmatic nucleus; SMIN, suprachiasmatic melanotrope-inhibiting neuron; TRH, thyrotropin-releasing hormone; 5HT, serotonin (from Kolk et al. 2002).

1.8.1 The interaction of TRH and GABA

Many of the physiological functions of TRH, including arousal, sleep, cognition, locomotion and mood, are also physiological functions in which GABAergic transmission has an underlying role (Deng et al. 2006). GABA is the primary inhibitory neurotransmitter of the CNS and functions in inhibiting the activity of signal-receiving neurons (Mihic and Harris 1997).

TRH and GABA coexist in the caudal raphe nuclei, and hippocampal cells expressing receptors to TRH are found in the stratum radiatum of the CA1 and CA3 regions suggesting that they are GABAergic interneurons and that TRH may regulate the function of GABA in the hippocampus (Kachidian et al. 1991; Heuer et al. 2000; Deng et al. 2006).

It has been demonstrated that administration of TRH increased GABA release in each region of the hippocampus and it has been suggested that TRH facilitates this GABA release by inhibiting resting K^+ conductances (Deng et al. 2006). TRH has been shown to block the K_{2P} channel, resulting in membrane depolarization and an increase in action potential firing of the GABAergic interneurons, facilitating the release of GABA (Deng et al. 2006).

1.8.2 The interaction of TRH and serotonin

TRH and serotonin are both neurotransmitters of the descending bulbo-spinal tract. It is well established that serotonin coexists with TRH in caudal raphe neurons of the midline and ventral medulla, which project into the dorsal vagal complex (DVC). Both TRH and serotonin operate by the same mechanism — convergence on and inhibition of TASK1 potassium channels (Section 1.5.3) (Richerson 2004). The increased motor neuron excitability produced after systemic administration of a TRH analogue in rats is potentiated by co-administration of a 5-HT agonist, resulting in an increase in amplitude and duration of response, thus, the effects of 5-HT and TRH on downstream targets might be complementary and supra-additive (Richerson 2004).

1.8.3 The interaction of TRH and acetylcholine

Unlike the effect of a combination of TRH and serotonin, no synergistic interaction has been detected between acetylcholine (ACh) and TRH; the action is probably mediated by the blockade of K^+ channels by TRH, which would be expected to augment responses to excitatory inputs such as ACh (Yarbrough 2003). TRH has been demonstrated to activate the cholinergic neurons of the cortex and the hippocampus in a selective manner, with a marked and long-lasting increase in the release of endogenous ACh (Giovannini et al. 1991; Nguyen et al. 2007).

TRH has been shown to use cholinergic mechanisms in the behavioural effects it mediates. The analeptic effects of TRH indicate this. In addition a TRH analogue can reverse the learning deficits and the hippocampal decrease in

choline uptake induced by lesioning of the medial septal cholinergic neurons (Horita et al. 1989; Giovannini et al. 1991).

The behavioural effects observed in rats following systemic administration of TRH, such as wet-dog shaking, sniffing, forepaw licking, tail elevation, face washing and hyperactivity, do not coincide with the release of ACh and are of a shorter duration, indicating that cognitive rather than motor behaviour is more susceptible to the interaction between ACh and TRH (Giovannini et al., 1991). Thus, not all of the effects of TRH are mediated by ACh, with other neurotransmitter systems, including the dopaminergic system, playing a role.

1.8.4 The interaction of TRH and dopamine

The dopaminergic system is involved in at least some of the effects of TRH since both TRH and its analogues have been shown to modulate the central actions of dopamine (Bennett et al. 1989). Some of the tic-like behaviours elicited by TRH in rodents, such as head-shakes and wet-dog shakes, may be mediated by the D_1 dopamine receptor, as Mushiroi et al (1996) have shown that the D_1 dopamine receptor antagonist, SCH23390, blocks the analeptic effect of a TRH analogue and it has also been reported to attenuate the TRH-induced forepaw licking tic behaviour of mice (Mushiroi et al. 1996; McCreary and Handley 1999).

Injection of TRH into the nucleus accumbens of the rat has been shown to cause an increase in DA metabolism in both the nucleus accumbens and in the striatum (Kalivas et al. 1987). The TRH analogue, TA-0910, stimulates locomotor action, mediated primarily via dopaminergic neurons, especially in the nucleus accumbens of the mesolimbic DA system (Yamamura et al. 1991).

1.8.5 TRH and glutamate

Glutamate is an endogenous excitatory amino acid that plays a major role in synaptic transmission; it is the most abundant excitatory neurotransmitter in the

mammalian CNS. TRH and glutamate show co-localisation throughout the neuroaxis (Sattin et al. 2003).

It is possible that TRH is involved in the vesicular release of glutamate because TRH neurons in the hypothalamic paraventricular nucleus and in the non-hypophysiotropic lateral hypothalamic area co-express mRNA for a glutamate vesicular transporter (VGLUT-2, a brain-specific Na^+-dependent inorganic phosphate cotransporter) (Nie et al. 2005; Wittmann et al. 2005).

It has been shown that glutamatergic neurons of the hypothalamic attack area (HAA), a region of the hypothalamus that controls attacking behaviour, co-express TRH signals in a large subpopulation of neurons (Hrabovszky et al. 2005b). These glutamatergic neurons co-expressing TRH possibly fulfill specific roles that, due to their localisation, are specifically involved in the control of behaviour, particularly the control of aggression (Hrabovszky et al. 2005b).

Another of the functions of the glutamate releasing hypophysiotropic TRH neurosecretory system has been proposed to be the regulation of important glial functions at the sites of release (Hrabovszky et al. 2005a).

The role of glutamate signalling and its modification by TRH is of significant importance in this study and, therefore, the method of glutamate neurotransmission is described in further detail below.

1.9 Glutamate neurotransmission

The interaction of TRH with the glutamatergic system is a major theme of this thesis and thus further study of the method of glutamate neurotransmission is considered here. Glutamate functions by activating three families of receptors, the *N*-methyl-D-aspartate (NMDA) receptors, the α-amino-3-hydroxy-5-methyl-4-isoxazole propionic acid (AMPA)/kainate receptors and the metabotropic receptors. Each family differs in subunit composition, ligand-recognition properties, transduction mechanisms and in the biophysical properties of the

ion conductances stimulated by their activation. Within each receptor family there are a number of different subtypes that may serve different physiological roles (Doble 1995).

Activation of the ionotropic glutamate receptor (iGluR) members (NMDA, kainate and AMPA receptors) is essential in memory and learning, and dysfunctions of this system are found in several CNS diseases (Meldrum and Garthwaite 1990). iGluR mediated glutamate excitatory synaptic transmission occurs through ligand-gated ion channels.

1.9.1 NMDA receptors

Glutamate receptors that preferentially recognise NMDA as a ligand are termed NMDA receptors. These receptors are blocked at resting membrane potentials by magnesium ions and they cannot be activated by glutamate. This magnesium block is voltage-dependent and, once the cell has been depolarised by another excitatory mechanism, the receptor can be activated by glutamate, permitting the entry of sodium and calcium ions and the efflux of potassium ions (Doble 1995).

1.9.2 AMPA receptors

AMPA receptors were first identified for preferentially recognising quisqualic acid and were later termed AMPA receptors. The activation of the AMPA receptors allows the entry of sodium and the efflux of potassium ions from the cell and, unlike the NMDA receptors, will only permit the passage of calcium ions under particular circumstances. AMPA receptors mediate rapid glutamate excitatory transmission and are responsible for the principal excitatory circuits of the hippocampus and the cerebellum (Doble 1995).

1.9.3 Kainate receptors

On many neurons, both AMPA and kainate receptors can be activated by both ligands and, thus, both subtypes are usually referred to as AMP/kainate

receptors. Like AMPA receptors, kainate receptors allow the entry of sodium and the efflux of potassium ions from the cell. There is a high density of kainate receptors in the CNS, particularly in the CA3 region of the hippocampus (Doble 1995).

1.9.4 Metabotropic glutamate receptors

The metabotropic glutamate receptors (mGluRs) are a family of G-protein-coupled receptors, of which, eight subtypes have been cloned to date. These have been classified into three major groups (Macek et al. 1998). Activation of these receptors modulates cell excitability and fast synaptic transmission. One of the most prominent roles of mGluRs in the CNS is to serve as presynaptic receptors that inhibit transmission at glutamatergic synapses (Macek et al. 1998). mGluRs play an important role in processes requiring synaptic plasticity, such as learning and memory, neuronal development and neurodegeneration (Dhami and Ferguson 2006). Excessive activation of mGluRs has been shown to induce seizures and appears to contribute to excitotoxicity and cell death, demonstrating a role for mGluRs in the pathological states of convulsion and neurodegeneration (Schoepp et al. 1995).

Activation of the glutamate metabotropic receptor increases the formation of two second-messengers, IP_3 and DAG, and activates calcium-stimulated PLC. IP_3 causes an elevation of free intracellular calcium from intracellular non-mitochondrial calcium stores. Calcium regulates a number of cellular signal-transduction processes, including the activation of PKC and calcium/calmodulin-dependent protein kinase, whilst DAG stimulates the activation of the PKC pathway (Naarala et al. 1993).

Similar to the TRHR, mGluRs are also known to internalise upon agonist binding, and are desensitised in a G-protein-coupled receptor kinase (GRK)- and PKC-dependent manner (Naarala et al. 1993). Activators of PKC can inhibit the presynaptic effect of mGluRs at corticostriatal synapses (Macek et al. 1998). Since TRH is an activator of PKC (O'Dowd et al. 2000; Lei et al. 2001), it is possible that TRH could inhibit mGluRs.

1.9.5 *The role of glial cells in glutamate signalling*

The correct functioning of the glutamatergic neurotransmission system is aided by glial cells (astrocytes in particular) playing a key role in maintaining extracellular concentrations of glutamate at a low level. Glutamate is removed from the extracellular space by specific transporter proteins, e.g. EAAT-1 and EAAT-2, and is transformed into non-toxic glutamine within the astrocyte by the cytoplasmic enzyme glutamine synthase (GS).

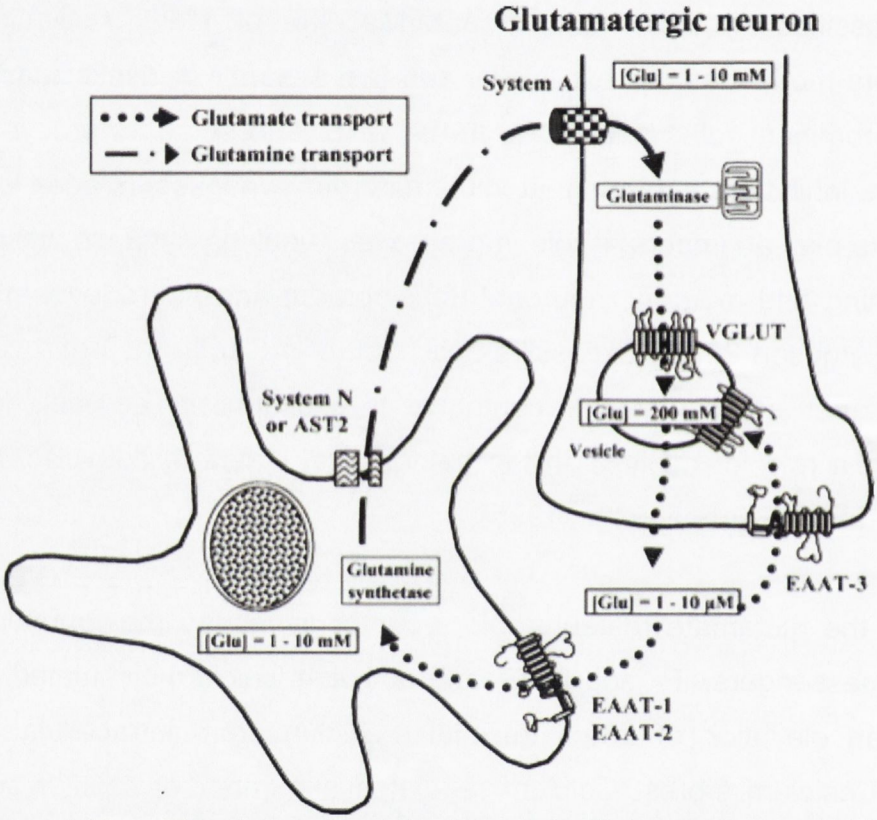

Figure 1.12 **The glutamate–glutamine cycle**. Glutamate is secreted from vesicles within glutamatergic neurons upon depolarisation. This extracellular glutamate is taken up into cells by specific transporter proteins, e.g. EAAT-1 and EAAT-2 (expressed uniquely in glial cells). A glial-specific cytoplasmic enzyme, glutamine synthase (GS), transforms the glutamate into non-toxic glutamine within the cell. Glutamine may then be released by the glial cells back into the extracellular space, where it has no effect, as it does not activate excitatory amino-acid receptors. Glutamine can then be taken up into glutamatergic neurons and reconverted into glutamate by glutaminase. This cycle prevents accumulation of glutamate in amounts that are toxic to postsynaptic neurons. GS levels have been shown to be depleted following injury, ischaemia or disease, resulting in an increase in glutamate to neurotoxic levels (Gras et al. 2006).

GS is glial-specific and is a key enzyme in the 'small glutamate compartment', which functions in the recycling of glutamate and prevention of its accumulation in amounts that are toxic to postsynaptic neurons. The glutamine produced may be released by the glial cells back into the extracellular space, where it has no effect, as it does not activate excitatory amino acid receptors, it can be taken up into nerve terminals and reconverted into glutamate by glutaminase, to be released in a new round of synaptic transmission (Doble 1999; Kruchkova et al. 2001). This glutamate–glutamine cycle is depicted in Fig. 1.12. In this way, the neurotransmitter pool is replenished and glutamate neurotoxicity is prevented.

1.9.6 The effect of TRH on glutamate signalling

Excessive glutamate stimulation of neurons has been implicated in many disease states and causes excitotoxicity (Section 1.10). It is thought that TRH may be an efficacious neuroprotectant against excessive glutamate excitation. Many models have been established in which glutamate or one of its receptor ligands have been used, both *in vivo* and *in vitro* to induce excitotoxicicty and in which the protective capacity of TRH has been measured. It has been shown that TRH reduces glutamate-stimulated increases in $[Ca]_i$ *in vitro* (Koenig et al. 1996). It has also been shown that pretreatment with TRH reduces glutamate-, NMDA- and KA-induced cell damage in rat hippocampal slices and primary cortical neurons (Pizzi et al. 1999; Jaworska-Feil et al. 2001; Veronesi et al. 2007a).

A pathophysiology of major depression has been proposed to involve the hyperactivation of pre-frontal to limbic glutamate circuits because of the loss of glutamate regulation by TRH (Sattin 1999). Treatment with ECT induces TRH synthesis (see Section 1.7.4) within glutamate-signalling circuits, reducing glutamate activation of NMDA, AMPA and voltage-regulated postsynaptic effects (Sattin 1999; Koenig et al. 2001).

1.10 Excitotoxicity

Excitotoxicity has been implicated in a number of chronic neurodegenerative diseases, such as Alzheimer's disease, Huntington's disease, Parkinson's disease and amyotrophic lateral sclerosis. It has also been implicated in the brain damage resulting from insults such as Rasmussen's encephalitis, schizophrenia, hypoglycaemia, trauma epilepsy and stroke [though reactive oxygen species (ROS), following reperfusion, are also a contributor to damage] (Choi 1988; Meldrum and Garthwaite 1990; Meldrum 2002).

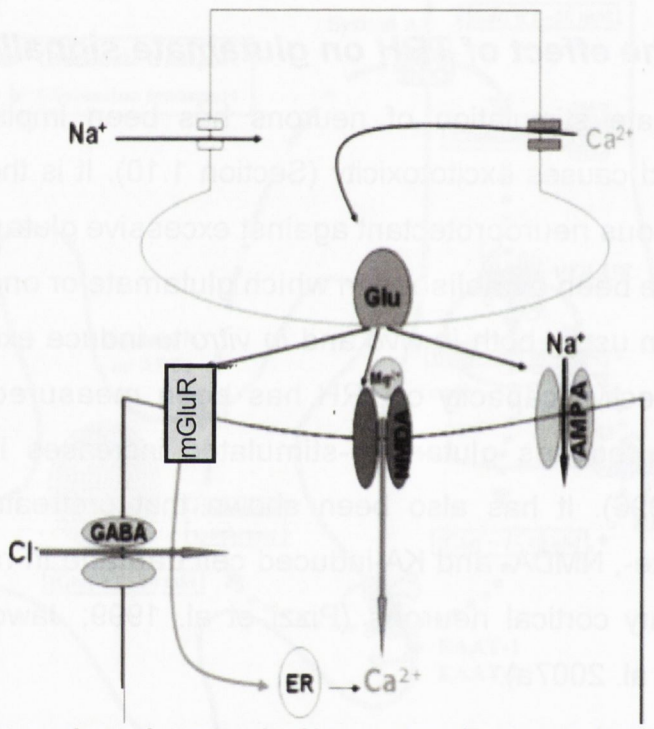

Figure 1.13 The excitotoxic cascade. Neuronal excitation can lead to chronic depolarization and the release of glutamate (Glu), causing an influx of Ca^{2+} into dendrites via the NMDA receptor. This Ca^{2+} influx can result in a subsequent loss of neuronal Ca^{2+} homeostasis, a defining factor of glutamate-mediated toxicity (Sullivan 2005).

Excitotoxic cell death involves prolonged depolarisation of neurons, changes in intracellular calcium concentrations, and the activation of enzymatic and nuclear mechanisms of cell death (Doble 1999). This excitotoxic cascade is outlined in Figure 1.13. In classical excitotoxicity, elevated levels of extracellular glutamate cause persistent depolarisation of the neuron, triggering a cascade of cellular events, including sodium and calcium influx and the exocytosis of

glutamate that eventually leads to cell death (Doble 1999). Glutamate toxicity acts via two distinct pathways: an excitotoxic one, in which glutamate receptors are hyperactivated, and an oxidative one, resulting in glutathione depletion, oxidative stress and cell degeneration (Gras et al. 2006).

1.10.1 Free radicals and excitotoxicity

Excitotoxicity is mediated by calcium, as activation of the mGlu and NMDA receptors results in an increase in intracellular calcium levels (Figure 1.13). Calcium ions regulate a number of cellular signal transduction processes, including the activation of protein kinase C and calcium/calmodulin-dependent protein kinase and thus play a critical role in toxic cell killing and programmed cell death (Naarala et al. 1993). Calcium ions lead to activation of calcium-dependent enzymes, such as NADPH oxidase, cytosolic phospholipase A2, nitric oxide synthase (NOS) and xanthine oxidase. These enzymes produce reactive oxygen and nitrogen species (ROS/RNS), which oxidatively modify nucleic acids, lipids, sugars and proteins, leading to nuclear damage, mitochondrial damage, proteasome inhibition and endoplasmic-reticulum stress (Doble 1999).

Free radicals play an important role in the excitotoxic process with production of these being a major contributor to cell death due to damage to intracellular organelles as membrane damage and ultimately cell lysis results from lipid peroxidation and the activity of the calcium-dependent lipases (Doble 1999). Free radicals are also contribute to cell death following cerebral ischemia. There is an overproduction of ROS following reperfusion consumption of endogenous antioxidants, neurons are particularly vulnerable to free radicals due to their relatively low levels of endogenous antioxidants (McCulloch and Dewar 2001).

1.10.2 Failure of the small glutamate compartment

The conversion of glutamate to glutamine by glutamine sythase can fail to prevent glutamate neurotoxicity under pathological conditions, such as in the

diseases described above. There is reportedly also a decline in GS expression and/or activity in the process of neuronal degeneration that follows injury or focal ischaemia and in the pathophysiology of a variety of neurological disorders and GS activity is also inhibited in HIV infection, probably as a result of the effects of inflammatory mediators and viral proteins (Kruchkova et al. 2001; Gras et al. 2006). Patients with Alzheimer's disease show a diminished and changed distribution of GS in the cerebral cortex, possible causes of which are the increased ammonia levels and the toxic agents derived from senile plaques (Häberle et al. 2006). GS deficiency has been suggested as a possible molecular basis for mesial temporal lobe epilepsy, since these patients express 40% less GS in the hippocampus than the normal population (Häberle et al. 2006). Should this glutamate conversion pathway fail due to disease conditions, as shown in Fig 1.13, glutamate levels would build up, resulting in further secondary damage caused by the excitotoxicity instigated by the excessive glutamate levels.

1.11 The role of TRH in disease states

Neurodegenerative diseases are a major cause of morbidity in the elderly and are therfore an important issue in public health. A major hypothesis to explain the pathogenesis of such diseases is excitotoxicity. In addition to excitotoxicity, changes in cholinergic, dopaminergic and serotonin levels may be manifested in neurodegenerative diseases.

The interaction of TRH with a number of neurotransmitters (Section 1.8) and its apparent regulatory role as a homeostatic modulator indicates that TRH may have an important role to play in neurological protection following various disease conditions. Pathological changes, chemical insults or the side effects of therapeutic drug (e.g. tranquillizers, anaesthesia, alcohol or narcotics) perturb homeostasis. The TRH regulatory system may be activated in response to these perturbations of homeostasis. As previously described in Section 1.5.3, the fundamental molecular event of TRH receptor activation is the blockade of potassium channels. This blockade results in increased excitabilities of

neuronal and pituitary circuitry. This event may be responsible for the restoration of homeostasis and alleviation of the damage due to disease or trauma. This may explain why TRH appears to be useful to varying degrees in multiple and unrelated clinical disorders (Yarbrough et al. 2007).

Because of its location and action within the CNS, this potential therapeutic property of TRH has resulted in various trials to determine its beneficial effects in neurological and psychiatric disorders. However, potential therapeutic uses of TRH are limited by its rapid degradation after its release from cells and the poor penetration of TRH into the brain following systemic administration. With peripheral administration, high doses of TRH are required to produce CNS effects because of poor penetration into brain and rapid peripheral inactivation. This has prompted an interest in synthesising more stable analogues of TRH, preferably with a higher CNS rather than endocrine receptor affinity, thus having only behavioural, not hormonal-effects.

1.11.1 The potential of TRH therapy in Alzheimer's disease

Alzheimer's is the most common neurodegenerative disorder in the aging population and is characterised by the progressive and irreversible deafferentation of the limbic system, neocortex and basal forebrain.

In Alzheimer's disease, a transformation in the cleavage of the amyloid precursor protein occurs, resulting in misfolded proteolytic products, i.e. the insoluble amyloid-β peptides 1–42 ($A\beta_{1-42}$). These peptides aggregate and then accumulate in the neuronal endoplasmic reticulum and extracellularly (Ewbank 1999; Walsh et al. 2000). This leads to the formation of lesions called senile plaques (Glenner 1988; Selkoe 2001). In addition to the formation of lesions, the microtubule-associated protein Tau is hyperphosphorylated and accumulates in the neurons, resulting in the formation of neurofibrillary tangles (Alonso et al. 1996). TRH plays a role in the regulation of Tau phosphorylation, through phosphokinase A and C pathways, suggesting treatment with TRH

could provide a treatment against the formation of neurofibrillary tangles (Luo and Stopa 2004). Premature apoptosis and/or an aberration in apoptosis regulation has also been implicated in the pathogenesis of Alzheimer's, with increased activation of neuronal caspases demonstrated in brains from Alzheimer's patients (Fadeel et al. 1999). These lesions, tangles and apoptosis of neuronal cells leads to a loss of synapses and neurodegeneration, which in turn leads to dementia. The role of excitotoxicity has also been implicated as β-amyloid peptides appear to sensitise neurons to excitotoxic cell death, thereby aggravating neurodegeneration (Doble 1999).

A further route to neurodegeneration may be caused by mutations in the gene encoding voltage gated potassium channels. Alterations in the expression of a K^+ channel (Kv3.4, a channel in neurons producing currents that spike at high rates), resulting in its up-regulation to high levels in diseased brains, has been reported (Angulo et al. 2004; Waters et al. 2006). Interestingly, it has also been demonstrated that the amount of TRH found in the hippocampus of Alzheimer's-disease patients is significantly lower than that of age-matched controls (Luo et al. 2002). Since TRH functions by the inhibition of potassium channels, it is possible that using TRH therapy may endow some form of protection.

TRH has been used in trials as a therapy for Alzheimer's disease. It has resulted in significant improvement in arousal and a modest improvement in semantic memory (Mellow et al. 1989). This is probably as a result of enhancement of ACh transmission by TRH, but the improvement observed is short-lived.

1.11.2 The potential of TRH therapy in ALS

Amyotrophic lateral sclerosis (ALS), also known as Lou Gehrig's disease, is a progressive, fatal neurodegenerative disease that is caused by gradual degeneration of motor neurons in the cortex, brainstem and spinal cord, leading to loss of voluntary muscle movement. This disease is characterised by

progressive muscular weakness, leading to paralysis and eventually death, usually due to respiratory failure (Brown 1997; Doble 1999; Boillee et al. 2006) There is stark evidence that excitotoxicity caused by a glutamatergic defect contributes to ALS (Doble 1999). In post-mortem spinal cord analysis, it has been reported that there is a loss of EAAT-2 (Doble 1999), a glial specific glutamate transporter (see Figure 1.12). This loss would prevent the conversion of glutamate into glutamine, leading to an excessive build up of excitatory extracellular glutamate. There is substantial evidence to indicate that oxidative toxicity is associated with ALS neuronal death (Bogdanov et al. 2000). In ALS a mutation of the gene encoding superoxide dismutase (SOD) results in the generation of hydroxyl radicals in cells more readily, making cells pro-apoptotic because of increased free radical damage (Fadeel et al. 1999; Bogdanov et al. 2000). Additionally, it is known that the EAAT-2 transporter is very sensitive to free-radical damage (Doble 1999).

TRH has been studied as a treatment for ALS because TRH excites anterior motor horn cells, which undergo a loss of innervation in ALS. The studies showed a transient, statistically significant, effect in at least some muscles, leading to the conclusion that the effect of TRH in ALS is a definite, acute and transient response (Brooks 1989). TRH may be functioning to protect against the excess levels of glutamate resulting from the loss of the small glutamate compartment regulation.

1.11.3 Parkinson's disease and the potential of TRH therapy

Parkinson's disease (PD) is the second most common neurodegenerative disorder following Alzheimer's disease. It is the result of neurodegeneration occurring in the nigro-striatal dopaminergic neurons and of dopamine depletion. It is clinically characterized by bradykinesia, postural instability, gait difficulty and tremor. Depigmentation, neuronal loss, and gliosis of the substantia nigra are typical brain abnormalities found in PD (Gibb and Lees 1991).

The mechanisms of cell death have not yet been fully elucidated, but increased oxidative stress, abnormal mitochondrial function and excitotoxicity have all been suggested to be initiators or mediators of neuronal damage (Mariani et al. 2005). Large amounts of oxidative stress are produced by the catabolism of dopamine, and high levels of lipid peroxidation are observed in the substantia nigra of PD patients (Doble 1999). The hallmark of the disease is the loss of brain cells producing dopamine. There is general consensus that the number of cortical neuronal nicotinic receptors is decreased. Loss of the nicotinic receptors may precede degeneration of cholinergic and dopaminergic neurons in affected regions (Dworakowska and Dolowy 2000). It has been demonstrated that TRH activates cholinergic neurons (Giovannini et al. 1991; Nguyen et al. 2007), suggesting that it may act as a protective agent. Dysfunctions of various K^+ channels (e.g., Kv, K(ATP) and Kir2) may also be involved in the pathogenesis of PD (Wang et al. 2008), again giving rise to the possible efficacy of TRH treatment.

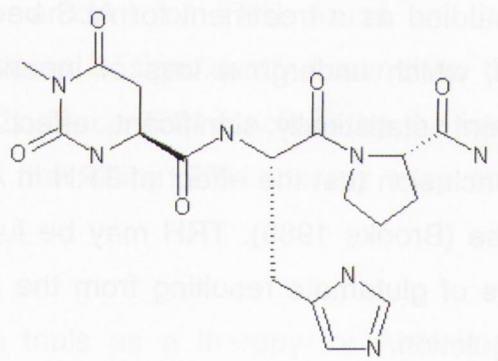

Figure 1.14 The structure of Taltirelin. A structural analogue of TRH, (-)-*N*-[(S)-hexahydro-1-methyl-2,6-dioxo-4-pyrimidinylcarbonyl]-L-histidyl- L-prolinamide tetrahydrate. It is more potent than TRH in ameliorating cerebellar functional disorders and also has neuroprotective effects in mouse transient brain ischemia (Urayama et al. 2002) and, as demonstrated by its anti-ataxic effects in rats, may be mediated by NMDA receptors and stimulates locomotor activity via the dopaminergic system (Yamamura et al. 1991; Kinoshita et al. 1998a).

As mentioned in Section 1.8.4, TRH may act on the D1 dopamine receptor. The TRH analogue, Taltirelin (Figure 1.14), can stimulate locomotor action via dopaminergic neurons, demonstrated in the nucleus accumbens of the rat mesolimbic DA system (Yamamura et al. 1991), which may be of use as a

treatment in PD. TRH has been demonstrated to increase dopamine levels in the striatum of Japanese encephalitis virus-induced post-encephalitic parkinsonism rats (Ogata et al. 1998). Although these diseases are different, it suggests that TRH could be of therapeutic value. TRH may increase dopamine levels by activating tyrosine hydroxylase (Togari et al. 1988), the rate-limiting enzyme in the conversion of tyrosine to L-dopa in catecholamine synthesis.

1.11.4 Epilepsy

There is direct evidence that at least one form of epilepsy, Rasmussen's encephalitis, is due to excitotoxicity caused by abnormal activation of AMPA receptors (Doble 1999). It has been reported that epileptic seizures can be associated with neuronal tissue damage and cell loss in the central nervous system, which is most likely due to sustained excitation and subsequent excitatory amino acid-mediated excitotoxicity (Sullivan 2005).

It appears that TRH is involved in seizure modulation (Kubek et al. 1989; Pekary et al. 2000; Jaworska-Feil et al. 2001; Koenig et al. 2001). TRH induction has consistently been found in the hippocampus after chronic electroconvulsive seizure (ECS), a seizure paradigm that is commonly used to test the efficacy of anticonvulsant drugs (Knoblach and Kubek 1994). Furthermore, TRH and TRH-analogues have been shown to have anticonvulsant properties in several animal and human models of seizures (Jaworska-Feil et al. 2001; Koenig et al. 2001; Kubek and Garg 2002). As TRH increases cholinergic transmission in the hippocampus and cortex (Yarbrough 1976; Okada 1991), it is possible that TRH could be used to reverse ECS-induced neurochemical and behavioural deficits.

The anticonvulsant effects of TRH are effected, at least in part, by the enhanced release of GABA from inhibitory hippocampal interneurons. This is due to blockade of K_{2P} channels by removal of extracellular Mg^{2+}, resulting in a block of the NMDA glutamate channel (Deng et al. 2006).

1.11.5 TRH improves memory and learning deficits

TRH and/or its analogues improve performance in learning-impaired mice, and restores learning or memory deficits in rats made cognitively deficient by anticholinergic treatment, electrochemical shock treatment (ECT), or by surgical lesions (Ballard et al. 1996; Ogasawara et al. 1996; Katsumata et al. 2001; Faden et al. 2003b). These effects appear to be largely mediated by enhanced cortical ACh (TRH selectively activates cholinergic neurons, Section 1.8.3). Human trials have demonstrated modest cognitive improvements in patients with alcoholic dementia, in the ECT postictal state and in Alzheimer's disease (Gary et al. 2003).

1.11.6 TRH treatment for spinocerebellar degeneration

There is considerable interest in TRH as a spinal neuromodulator and in its analogues as potential therapeutic agents in spinal-cord injury and in motoneuron disorders. A number of reports confirm the ameliorative effects of TRH and its analogues in experimentally induced spinal cord and other neurological injuries. TRH has been reported to improve electrophysiological recovery of damaged spinal-cord tissue (Faden et al. 1989). Improvement may result from the trophic effects of TRH on spinal motoneurons, from the ability of TRH to increase spinal-cord blood flow, or from the ability to reduce oedema at the site of spinal cord injury. An interesting feature is that studies have shown no difference in the histopathology of TRH-treated animals despite there being a functional improvement (Faden, et al 1984). Although Behrmann et al. (1993) observed significant sparing of the white matter of the spinal cord in TRH-analogue treated animals (Behrmann et al. 1993).

It is thought that TRH and its analogues exert direct excitatory effects on spinal neurons rather than acting via release of other neurotransmitters (Horita 1998). However, it is possible that the therapeutic property of TRH is unrelated to its excitatory effect on motoneurons (as demonstrated by the ineffectiveness of some TRH analogues, despite their excitatory properties) (Deshpande and Warnick 1994). Taltirelin (Figure 1.14), with the trade-name Ceredist®, is

marketed by Tanabe Seiyaku Pharmaceuticals Ltd. in Japan as a drug for patients with spino-cerebellar degenerative diseases (Kinoshita et al. 1998b). Ceredist® has a reduced affinity for brain- and, particularly, pituitary TRH-receptors, compared with TRH. Compared to TRH, it has an enhanced half-life and bioavailability in humans, providing greater and longer-lasting CNS action. In patients undergoing treatment with this TRH analogue, improvements were recorded in gait, speech and coordination (Kinoshita et al. 1998b).

1.11.7 The effect of TRH on alcoholism

Because alcohol intoxication is accompanied by incoordination and sedation indicative of neuronal inhibition, researchers have investigated alcohol's effects on GABA and its receptors (Mihic and Harris 1997). Alcohol is a drug of abuse that has facilitatory influences on dopaminergic and serotonergic systems in the brain. Alcohol has been shown to casuse the release of DA in the mesolimbic system, and alcohol-preferring rats have 10–15% lower DA content in the nucleus accumbens, which may be one neurochemical mechanism involved in the positive reinforcing properties of ethanol (Rezvani et al. 1992).

TRH antagonises the sedation, motor impairment and hypothermia produced by ethanol (Rezvani et al. 1992). Pre-treatment with TRH has been shown to reduce the error-producing effect of ethanol and to increase reaction times in humans without interfering with the blood ethanol concentration *versus* time curve (Knutsen et al. 1989). The TRH analogue Taltirelin (see Fig. 1.14) dose-dependently reduced ethanol intake in alcohol-preferring rats and commensurately increased their water consumption (Rezvani et al. 1992).

Thus, the evidence suggests that brain TRH systems are involved in the modulation of ethanol-mediated behaviour and, possibly, alcohol preference. TRH has modulatory effects on central dopaminergic/serotonergic systems, which may provide a hypothesis on the mechanism of ethanol-interaction. The TRH-mediated DA release may substitute for ethanol-mediated DA release, thus removing the motivation to consume alcohol. It has also been demonstrated that drugs that facilitate serotonergic transmission by inhibiting 5-

HT re-uptake can suppress a preference for alcohol in humans and animal models (Rezvani et al. 1992). As TRH modulates central serotonergic systems, and TRH and 5-HT coexist in neurons in certain brain areas (see Section 1.3.4), the enhancement of serotonergic activity may explain the effect of TRH on alcohol consumption.

1.11.8 TRH and head injury and spinal trauma

There is significant interest in TRH as a treatment for human traumatic brain injury and spinal cord injury, either to prevent damage progression or to speed-up neuronal recovery. TRH and its analogues have been shown to be capable of promoting recovery in animal models of head injury (Tanaka et al. 1997; Faden et al. 1999). Cats with brain-stem compression injury show improved neurological and EEG parameters, and mice with head-impact injuries demonstrated less behavioural disturbance after TRH treatment (Nillni and Sevarino 1999). The TRH analogue, Montirelin (Figure 1.15), has been shown to have beneficial effects in spinal trauma (Grünenthal, 1997) possibly acting through the cholinergic and noradrenergic systems, which it has been reported to enhance (Itoh et al. 1994a; Ogasawara et al., 1996). Montirelin has been shown to stimulate dopamine release from the rat striatum and causes a marked enhancement of NA turnover in the mouse brain (Itoh et al. 1994; Ogasawara et al. 1996).

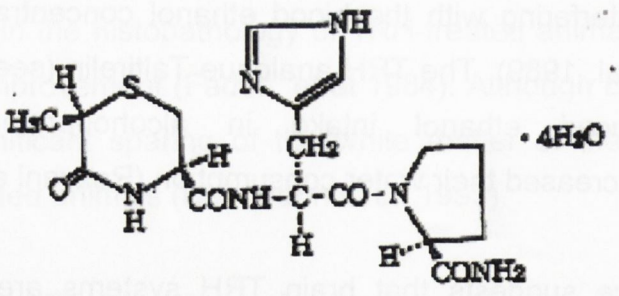

Figure 1.15 The structure of Montirelin. Montirelin,, (3R,6R)-6-methyl-5-oxo-3-thiomorpholinyl carbonyl-L-histidiyl-L-prolineaminde tetrahydrate, is a structural analogue of TRH. In addition to its use following spinal trauma, it has been patented as a drug for the treatment of ALS, for inhibiting sleep apnoea and for treating senile dementia and posttraumatic nervous injuries (US Patent Numbers 4788179, 5968932, 4956364, 4906614, respectively).

1.11.9 Ischaemia and brain injury

Ischemia, a diminished blood supply to the brain, results in neuronal death. This death results from multifactorial processes that may be interrelated, such as excessive glutamatergic transmission and inadequate energy supply. The reperfusion of blood stimulates ROS production, leading to increased levels of hydroxyl radicals (see Section 1.10.1). It has been demonstrated that inhibition of glutamate-mediated synaptic transmission may be neuroprotective (Obrenovitch et al. 2000).

Animal models of stroke have provided a test-model for the potential therapeutic application of TRH and its analogues, which have demonstrated improved recovery and reduced neurological deficits following cerebral damage induced by experimental hematoma and ischemia (Nillni and Sevarino 1999; Urayama et al. 2002).

Katsumata et al. (2001) modelled stroke in rats by middle cerebral artery (MCA) occlusion-induced infarcts, and administered a TRH-analogue, JTP-2942 (Figure 1.16), post-surgery, which significantly improved survival, protected against ischaemic damage and reduced infarct size (Katsumata et al. 2001).

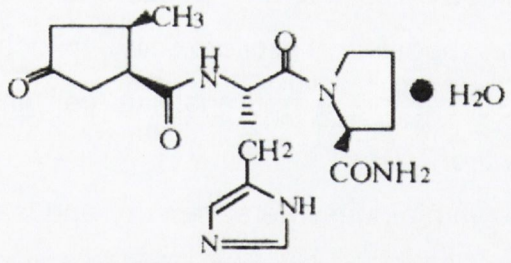

Figure 1.16 Structure of JTP-2942. A structural analogue of TRH, (*N*-[(1S, 2R)-2-methyl-4-oxocyclopentylcarbonyl]-L-histidyl- L-prolinamide monohydrate). JTP-2942 improves local cerebral blood flow and local glucose utilization in rats with cerebral ischemia in acute and chronic phase models (Ikeda et al. 1998).

This analogue exhibits strongly enhanced acetylcholine release in the rat hippocampus and frontal cortex and following MCA occlusion, it caused activation of damaged neuronal networks and also structural changes (Toide et al. 1993; Yonemori et al. 2000). In addition to cholinergic activation, JTP-2942

directly activates dopaminergic, noradrenergic and serotonergic neurons (Yonemori et al. 2000). The drug Montirelin has also been shown to have beneficial effects following cerebral ischaemia (Grünenthal, 1997).

1.12 Overview of project aims

Thyrotropin-releasing hormone (TRH) is a tri-peptide that has a wide range of effects on the central nervous system (CNS) and has potential therapeutic value in the treatment of CNS disorders. This potential is limited by the short biological half-life of TRH, primarily due to the actions of TRH-degrading enzyme (TRH-DE). Excitotoxicity, which causes the prolonged depolarisation of neurones, has been implicated in a number of chronic neurodegenerative diseases, such as Alzheimer's disease, Huntington's disease, Parkinson's disease and amyotrophic lateral sclerosis. The primary focus of this thesis was to examine the biological effects of TRH during excitotoxic conditions. The aims of this thesis were to:

- Determine the kinetic parameters of new TRH-like compounds, measured with purified TRH-DE and use these for structure–activity relationshop (SAR) analysis.
- Construct an *in vitro* system for the study of the effects of TRH following excitotoxicity induced by kainate on hippocampal slices.
- Construct *in vitro* models of excitotoxicity, mitochondrial toxicity and apoptotic cell death using a neuronal-like cell line to determine the protective potential of TRH.
- To establish an *in vivo* model where memory and learning were impaired by kainate toxicity and to measure the effect of TRH against this effect.
- To measure the effects of TRH on striatal release of neurotransmitters and the formation of reactive oxygen species following kainate application.

CHAPTER 2

GENERAL METHODS

2.1 Sources of Reagents

A detailed list of sources of all compounds and reagents is presented in Appendix A. Reagents are listed in each category in alphabetical order. The source of each reagent is indicated by the supplier's name.

2.2 Preparation of Solutions

All aqueous solutions were prepared using distilled, deionized water with a conductivity of less than 2 mOhm. The water had been deionised by passing through a Millipore Milli-U10 model water purification system. Reagents were weighed out using a Mettler College Toledo B2002-S top-loading balance, for weights of greater than 2 g, and a Mettler College 150 Analytical balance for weights less than 2 g.

2.3 Pipetting

All volumes in the range 5 µl–5 mL were dispensed with Gilson automatic pipettes. All pipettes were checked regularly for accuracy according to manufacturer's recommendations. Larger volumes were measured using volumetric flasks and calibrated volumetric cylinders.

2.4 pH Determination

All pH measurements were made using a Corning pH meter, model 240 equipped with a Corning general-purpose combination electrode. The pH meter was calibrated before use using BDH standard solutions at pH values of pH 4, pH 7 and pH 10.01. The pH of solutions was adjusted when necessary using solutions of NaOH, HCl, KOH as appropriate.

2.5 Centrifugation

All large volumes of material were centrifuged using a Sorvall RC–50 centrifuge using the following rotors;

GSA 6 x 250 mL g max. = 27 600 g

SS-34 8 x 50 mL g max. = 48 700 g

Small volumes were centrifuged using a Beckman bench-top Microfuge™, operating at a fixed speed corresponding to 15,000 g, or using a refrigerated variable speed Eppendorf 5415-R bench-top centrifuge with a g max of 16,100 g. All centrifugation was carried out at 4°C, unless otherwise stated. Rotors were pre-cooled to this temperature before use. All g forces quoted refer to the relative centrifugal force at the bottom of the centrifugal tube. Centrifugal time does not include acceleration or deceleration time.

2.6 Spectrophotometry

All enzyme kinetic rates were measured using a Perkin–Elmer LS50B luminescence spectrophotometer, a Varian Cary 300 UV–Visible dual beam spectrophotometer, an Agilent 8453 spectrophotometer and multi-well plate reader fluorescence and absorption spectrophotometers from Molecular devices (Spectra Max 340 PC). All simple absorbance readings were measured using a Unicam Helios spectrophotometer. The cuvettes in the spectrophotometers were maintained at a constant temperature by a circulating water bath throughout the multi-cell holders and allowed to equilibrate to that temperature before use and the plate readers used an integrated heating block. All buffers were brought to the temperature of the spectrophotometer in a separate water bath before use. Disposable plastic cuvettes and 96 well plates were used for all spectrophotometric determinations.

2.7 Protein Determination

Protein determinations were carried out using the Bio-Rad micro assay procedure or the Markwell method during this work. Choice of protein assay method was based on sample type, presence of interfering substances in addition to the protein concentration.

2.7.1 Bio-Rad assay for protein determination

The Bio-Rad protein assay is based on the method of Bradford, in which the absorbance maximum for an acidic solution of Coomassie® Brilliant Blue G-250 dye shifts from 465 nm to 595 nm when binding to protein occurs. The Coomassie blue dye binds to primarily basic and aromatic amino acid residues, especially arginine. Concentration determinations were carried out in triplicate by combining 800 µL of each sample, or sample dilution with 200 µL of dye reagent concentrate vortexing and for cells on microplates by combining 80 µL of cell suspension with 20 µL dye reagent. Samples were incubated for ~5 min and absorbance was measured at 595 nm with a spectrophotometer or microplate reader. Comparison to a standard curve of a concentration range of bovine serine albumin (BSA) standards provides a relative measurement of protein concentration. Five concentrations of BSA standards, were prepared with a linear range of 1 to 10 µg/mL, for those read using a spectrophotometer and 8.0 µg/mL to approximately 80 µg/mL for 96-well plates.

2.7.2 Markwell assay for protein determination

Protein concentration was determined by the method of Markwell *et al.* (1978). Stock solutions were prepared as follows:

A: 2% sodium carbonate in 0.4% (w/v) sodium hydroxide
0.16% (w/v) sodium potassium tartrate
1% (w/v) sodium dodecyl sulphate (SDS)

B: 4% (w/v) copper sulphate ($CuSO_4.5H_2O$)

C: This solution was prepared fresh each day, prior to use, and comprised of 100 volumes solution A:1 volume solution B.

D: 1:1 dilution of Folin Ciocalteau's reagent in H_2O

Samples (homogenate) were diluted to a volume of 1 mL with distilled H_2O to a protein concentration of 50–350 mg/mL. To this, 3 mL of solution C was added, mixed thoroughly and allowed stand at room temperature for 10 min. A 0.3 mL volume of solution D was then added, mixed, and allowed stand for 45 min at room temperature for colour development. The absorbance was read at 660 nm against 1 mL H_2O, taken through the above procedure, as a blank reading. All assays were carried out in triplicate. Protein concentration was calculated from a standard curve, prepared from BSA (bovine serum albumin, 0.05 mg/mL to 0.35 mg/mL) taken through the same procedure (Figure 2.1).

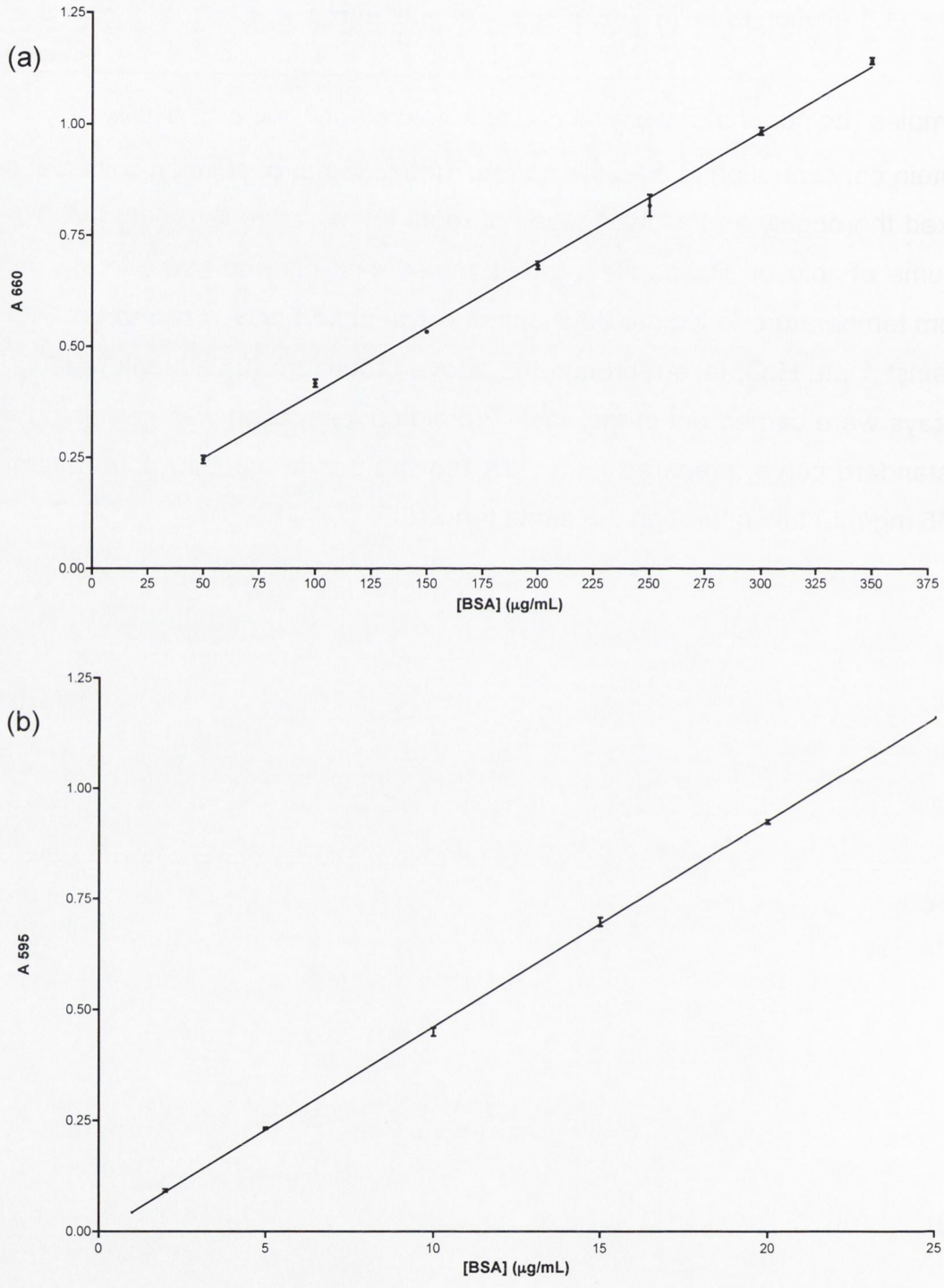

Figure 2.1 Standard Curves for Protein Determination

Standard curves for protein determination using the method of (a) Markwell et al. (1978), and the (b) Bio-Rad method. Absorbencies were corrected for the absorbance of a reagent blank. Each point represents the mean of triplicate determinations from a single experiment ± S.E.M.

2.8 Tissue slice superfusion system

Male Wistar rats (200–250 g) were used in these experiments. Animals were killed by cervical dislocation and the brains were immediately removed and placed in ice-cold Krebs buffer, which contained a final concentration of 112.5 mM NaCl; 4.7 mM KCl; 1.2 mM KH_2PO_4; 1.2 mM $MgSO_4$; 11.5 mM glucose; 25.0 mM $NaHCO_3$ and 2.5 mM $CaCl_2$ at pH 7.4. Hippocampal slices of 400 µm thickness were taken using a Campden Vibroslice.

Slices undergoing superfusion were placed in a number of open chambers measuring 2 cm in diameter with a volume of 3 mL. Each slice was subjected to superfusion with Krebs buffer at 37°C. Following a pre-incubation of 30 min in Krebs buffer, slices were then incubated for a further 30–60 min or treated with toxins following which they were incubated for another 30 min. Following incubation periods, slices were homogenised in the appropriate solutions depending on assay requirements and either assayed directly or stored at −80°C, in the case of lactate dehydrogenase assays at 4°C.

Slices that underwent incubation experiments were placed in organ dishes containing 2 mL of Krebs buffer and directly oxygenated with 95% O_2, 5% CO_2 and given a pre-incubation period of 30 min prior to further treatment and maintained at 37°C. After the incubation, the slices were removed and the incubation medium was stored at 4°C for LDH assays or at −80°C for amino acid analysis.

2.9 Enzyme assays

Assays of enzymatic activity were carried out using spectrophotometric and fluorescence methods.

2.9.1 Assay of lactate dehydrogenase activity

Lactate dehydrogenase activity was assayed by monitoring the conversion of NADH to NAD^+ at 340 nm at 37°C, coupled with the reduction of pyruvate to lactate. Solutions required are as follows:

200 mM Potassium phosphate buffer (KPO_4) adjusted to pH 7.2 with KH_2PO_4

1.3 mM NADH prepared fresh and stored on ice

7 mM Sodium pyruvate

KPO_4 buffer was used as a blank. 100 µL of sodium pyruvate and 100 µL of (diluted) sample homogenate was added to 700 µL buffer. The blank rate was observed for ~2 min. 100 µL NADH was then added and the rate of reaction was determined over ~5 min. The rate of change of absorption per minute was then calculated and used to determine the units of enzyme per mg of protein in each sample.

2.9.2 Assay of glutamine synthase activity

Toxic effects on glial cells were studied by assaying slices for glutamine synthase (GS) activity. Assays were carried out according to the method of Wellner and Meister (1966).

Stock solutions were prepared as follows:

A: 0.01 M NaH_2PO_4

0.15 mM L-Glutamine

0.1 M Sodium acetate

Added daily: 100 µL ATP (5 mg/mL):10 mL A.

Adjust to pH 5.5

B: To 10 mL A add:

0.066 g $MnCl_2$

0.139 g Hydroxylamine

C: Terminating solution:

10% $FeCl_3$ in 0.2 M HCl

50% TCA

25% HCl

Tissue was homogenised in 0.1 M sodium acetate buffer, pH 7.4 (10%, w/v). 0.2 mL of sample was pre-incubated with 0.5 mL solution A at 37°C for 10 min. 0.15 mL solution B was added and the incubation continued for 20 min. The reaction was stopped by the addition of 0.75 mL of solution C. Precipitated protein was removed by centrifugation at 1,800 g for 10 min. The resulting colour development was measured spectrophotometrically at 500 nm. L-glutamic acid γ-mono-hydroxamate (GHA) standards (0 to 0.2 mg/mL) were used to prepare a standard curve (see Figure 2.2) from which GHA formed was calculated. GS activity was calculated and expressed as nmol GHA formed/mg protein/min. Protein concentration was determined by the Markwell assay (Section 2.3.2), which is particularly suited to membrane-containing samples, was used.

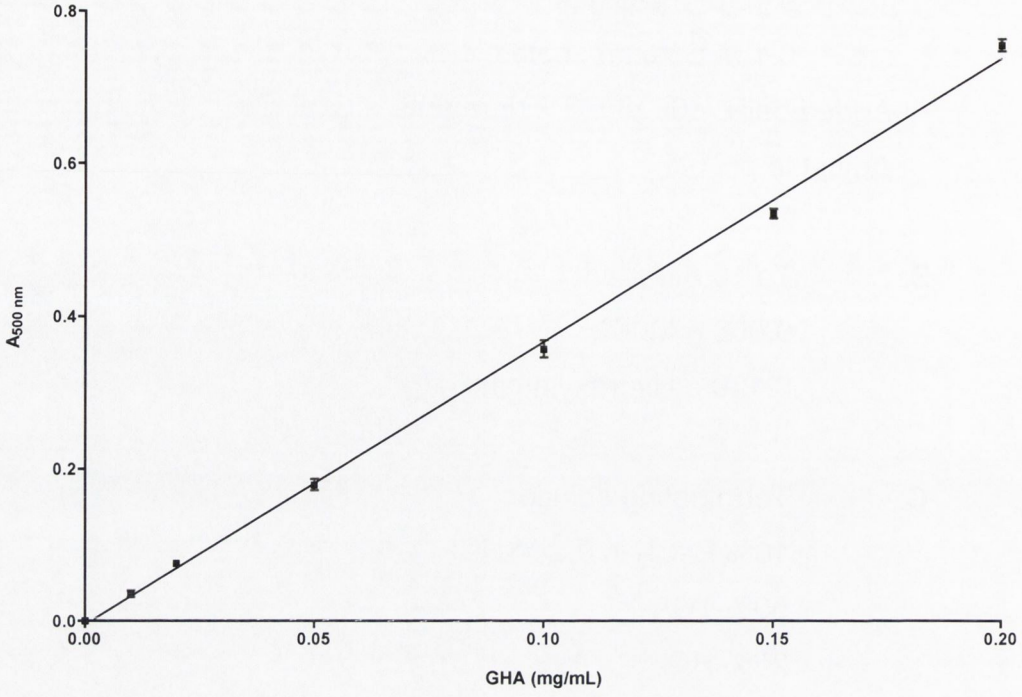

Figure 2.2 Determination of glutamine synthase activity

Glutamine synthase (GS) activity was expressed as mmol GHA (γ-monohydroxamate) formed per min per mg of protein. A standard curve of absorbance at 500 nm versus GHA concentration of prepared standards was constructed. GHA formed was then determined from this graph. The above figure represents a typical standard curve. Data points represent the mean ± S.E.M. (n=4).

2.9.3 Assay of apoptosis activation

Toxic effects instigating apoptosis of slices and cell cultures were studied by assaying for caspase activity. The cleavage of AMC from the fluorogenic caspase-3 substrate, Acetyl-Asp-Glu-Val-Asp-AMC (Ac-DEVD-AMC) was assayed using lysed hippocampal and cell culture slices. Solutions required were made up as follows:

2.9.3.1 Lysis Buffer

A stock solution of 50 mL of lysis buffer was made up and stored at −80°C in 5mL aliquots.

10 mM HEPES
2 mM EDTA
0.1% CHAPS / NP40
5 mM DTT
1 mM PMSF
10 µg/mL pepstatin A
20 µg/mL leupeptin
10 µg/mL aprotinin

2.9.3.2 Reaction Buffer

100 mM HEPES
20% v/v glycerol
0.5 mM EDTA
5 mM DTT *added fresh*

This assay is a general measure of caspase activation as Ac-DEVD-AMC also acts as a substrate of caspase-6, caspase-7, caspase-8 and caspase-10. Cleavage of this substrate by caspase-3 shows Michaelis-Menten kinetics (K_m = 9.7±1.0 µM).

Homogenised hippocampal slices were diluted 1:10 (v/v) and centrifuged at 5000 g at 4°C for 5 min and the supernatant removed. The pellets were then resuspended in 200 µl of the lysis buffer described above (Section 2.5.3.1). Cells cultured on 96-well plates were pelleted by centrifugation at 600 g for 5 min and the supernatant was removed by aspiration. The cells were washed with phosphate buffered saline (PBS), centrifuged and the supernatant removed. The cell pellets were then resuspended in 100 µL of lysis buffer. The samples were then sonicated in a sonication bath and then left on ice for 60 min for cell lysis to occur. The lysed tissue was centrifuged at 3,000 rpm for 10 minutes. 10 µL of the supernatant was transferred to a well of a black 96 multi-well plate. Reaction buffer was used as a negative control. The Ac-DEVD-AMC substrate was added to the reaction buffer to produce a 1.65 µM final concentration of substrate and 100 µL of this was added to each sample and the controls. Production of fluorescent free-AMC, released by caspase activity, was monitored over 60 min at 37°C using a microplate fluorimeter (Spectra Max Gemini, Molecular Devices) at excitation and emission wavelengths of 360 and 460 nm, respectively. A standard curve of the product (AMC) was prepared by dilution of the appropriate amount of a 5 mM AMC stock solution into the reaction buffer to yield AMC solutions ranging in concentration from 0–1 µM (Figure 2.3). The standard curve was used to calculate caspase activity and expressed as AMC formed/mg protein/min. The protein concentration was determined by the BioRad method (Section 2.3.1).

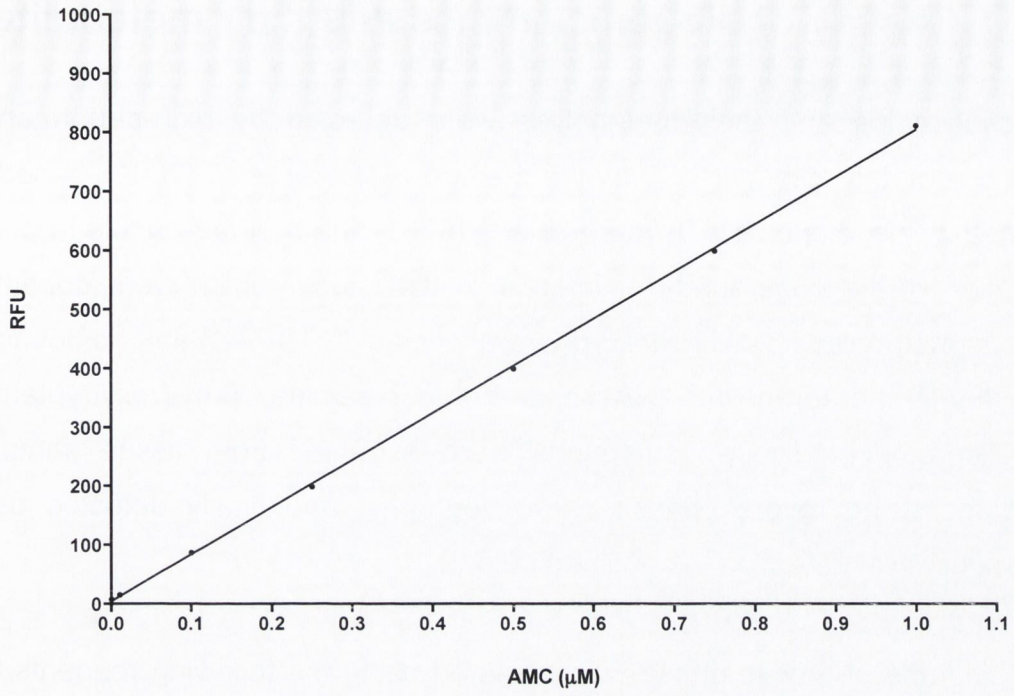

Figure 2.3 Standard curve of 7-amino 4-methylcoumarin

A standard curve of 7-amino 4-methylcoumarin (AMC) was prepared in order to determine caspase-3 activity. AMC is the cleavage product of the caspase-3 substrate, Ac-DEVD-AMC. A range of AMC concentrations from 0–1 μM were prepared and 100 μL of each standard was pipetted into microplate wells of a black multi-well plate, in triplicate and read at excitation and emission wavelengths of 360 and 460 nm, respectively on a microplate fluorimeter (Spectra Max Gemini, Molecular Devices). Data points represent mean values ± S.E.M. (n=3). In all cases error bars were smaller than the point sizes.

2.10 Assay of biogenic amines and their metabolites

Catecholamines and their metabolites were detected by high-performance-liquid-chromatography (HPLC), by the method of Harkin *et al.* (2001), based on the method developed by Seyfried *et al.* (1986). The method enabled optimal resolution of the compounds of interest to this study, which were dopamine (DA), its metabolites 3,4-dihydroxyphenylacetic acid (DOPAC) and homovanillic acid (HVA), noradrenaline (NA) and the indoleamine, 5-hydroxytryptamine (5HT; serotonin). These compounds were extracted from tissue samples, separated using reverse phase chromatography, and finally detected using electrochemical detection, as outlined below.

A 1 L volume of mobile phase was prepared using the following reagents that were dissolved in distilled, refiltered water:

0.1 M citric acid.H_2O

0.1 M sodium dihydrogen phosphate

1.4 mM octane-1-sulfonic acid

0.1 M ethylenediaminetetraacetic acid disodium (EDTA)

Once dissolved, the solution was vacuum filtered and 100 mL of methanol was added under constant stirring. The pH of the resulting solution was then adjusted to 2.8 by the addition of 4 M NaOH. Use of a low pH is necessary to ensure retardation of acidic compounds and provide an optimal concentration of the ion-pairing reagent (octane-1-sulfonic acid) in order to manipulate the retention times of the amines on the HPLC column. A typical trace for the separation of a number of standards is shown in Figure 2.4.

Electrochemical detection (ECD) was performed using a Shimadzu electrochemical detector with the oxidation potential of the working electrode set at +0.8 V. ECD is a highly sensitive method for detection of catecholamines based on their ability to be oxidized at positive potentials. By applying such a

positive potential at an electrode surface, catecholamines can be oxidised at the ring hydroxyl groups to produce an orthoquinone derivative with the release of two electrons. The number of electrons released is directly proportional to the number of molecules oxidised.

Hippocampal slices were prepared for amine extraction by homogenisation in a 500 µL volume of ice cold mobile phase that contained 100 ng/mL of the internal standard *N*-Methyl-serotonin. The samples were sonicated and the volume brought to 1 mL with mobile phase containing the standard and were filtered through Microcon® centrifugal filter devices at 14000 g for 15 min at 4°C. A 20 µl sample of the resultant supernatant was injected onto a guard chromatographic column (Luna RP-18, 3 cm × 4.6 mm internal diameter, particle size 5 µm from Phenomenex, UK) prior to separation on the main HPLC column (LI Chrosorb RP-18, 25 cm × 4 mm internal diameter, particle size 5 µm from Phenomenex, UK) for separation of the neurotransmitters (flow rate 1 mL/min at approximately 200 bar). The signal from the electrochemical detector was integrated and chromatograms were generated using a Merck-Hitachi D-2000 integrator, which calculated the retention times of the peak-height and –area of the amines and metabolites detected.

The amines and metabolites were identified based on the retention time using the retention times of standards and by the presence of the internal standard, which also allowed correction of processing losses in the sample preparation process.

Standard curves of the amines of interest were prepared from fresh solutions of standards (Sigma) prepared in mobile phase (Figure 2.5). A plot relating concentration of compound to peak-area over a range of 0–500 ng/mL following 20 µL injections was shown to be linear. These standard curves were then used to relate the peak area of the amines detected in samples to the concentration of that amine. Results were expressed as ng/µg protein.

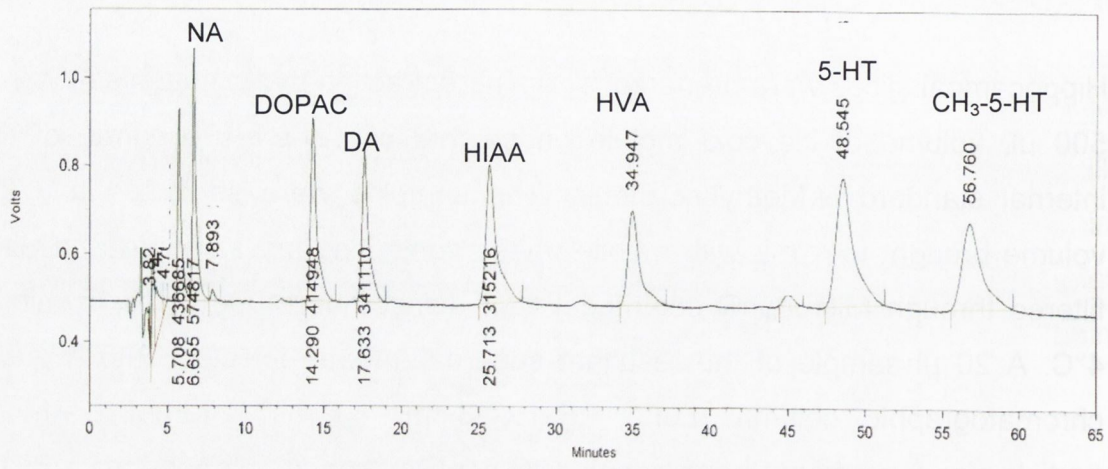

Figure 2.4 Sample HPLC trace of biogenic amine standards

A sample trace of the separation of standards (obtained under the conditions outlined in Section 2.6.) The separation of noradrenaline (NA; retention time (RT) = 6.6 min); DOPAC (RT = 14.3 min); dopamine (DA, RT = 17.6 min); 5-hydroxyindole acetic acid (HIAA, RT = 25.7) homovanillic acid (HVA, RT = 34.9 min), serotonin (5-HT, RT = 48.55 min) and the internal standard 5-methyl serotonin (CH_3-5-HT, RT = 56.76 min) over a 65 min elution period is demonstrated. Standards were prepared in mobile phase at a concentration of 250 ng/mL. Injections of 20 µl were made onto the HPLC column.

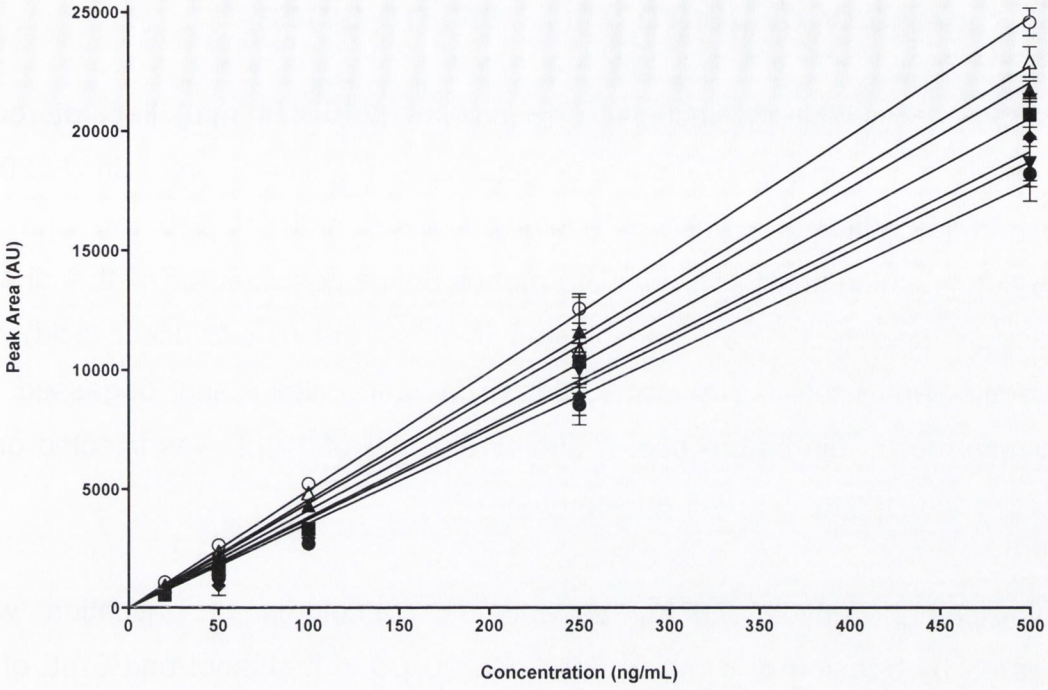

Figure 2.5 Standard curve of amines and metabolites

The above standard curve is representatative of that obtained following injection of 20 µL of prepared standards (20–500 ng/mL). A linear relationship was observed between measured peak area and the standard concentration. ■ = NA (noradrenaline), ▲= DA (Dopamine), △ = DOPAC (3,4-dihydroxyphenylacetic acid), ○=5HIAA (5-hydroxy indole acetic acid) ▼=HVA (homovanillic acid), ●= 5HT (5-hydroxytryptamine; serotonin) and ◆=CH_3-5-HT (methyl-serotonin – internal standard). Data points represent mean values ± S.E.M. (n=3).

2.11 Assay of neuroactive amino acids

A reverse phase 5 µm Nucleosil C18 column (250 × 4 mm) kept at room temperature was used. Column effluent was monitored with an FL2000 fluorescence detector using an excitation wavelength of 340 nm and an emission wavelength of 455 nm. The mobile phase consisted of methanol and potassium acetate (0.1 M, pH adjusted to 5.52 with glacial acetic acid). All solvents were filtered through 0.22 µm Millipore filters and degassed by sonication for 5 min before use. A sample volume of 40 µL was injected onto the column using an AS3000 autosampler.

The *o*-phthalaldehyde (OPA) reagent for pre-column derivatisation was prepared by addition of 5 mg of OPA and 20 µL of methanol and 5 µL of 2-mercaptoethanol to 5 mL of $NaHCO_3$, pH 9.5, to give a final concentration of 1 mg/mL (7.5 mM). This was incubated with the samples for one minute at a ratio of 2:1 prior to injection to the column.

Hippocampal slices were prepared for amino acid detection by homogenisation in a 500 µL volume of ice cold mobile phase that contained 10 µM of the internal standard cysteic acid. The samples were sonicated and the volume brought to 1 mL with mobile phase containing the standard and were filtered through Microcon® centrifugal filter devices at 14000 g for 15 min at 4°C.

Amino acids were separated using the mobile phase with an increasing gradient of methanol and decreasing potassium acetate, at a flow rate of 1 mL/min. The concentration of methanol was increased from 25 to 90% over 25 min, with a corresponding decrease in potassium acetate.

Calibration curves were prepared by adding medium containing a range of concentrations (20–250 µM) of the complete set of the amino acids being analysed in 0.05 mM HCl.

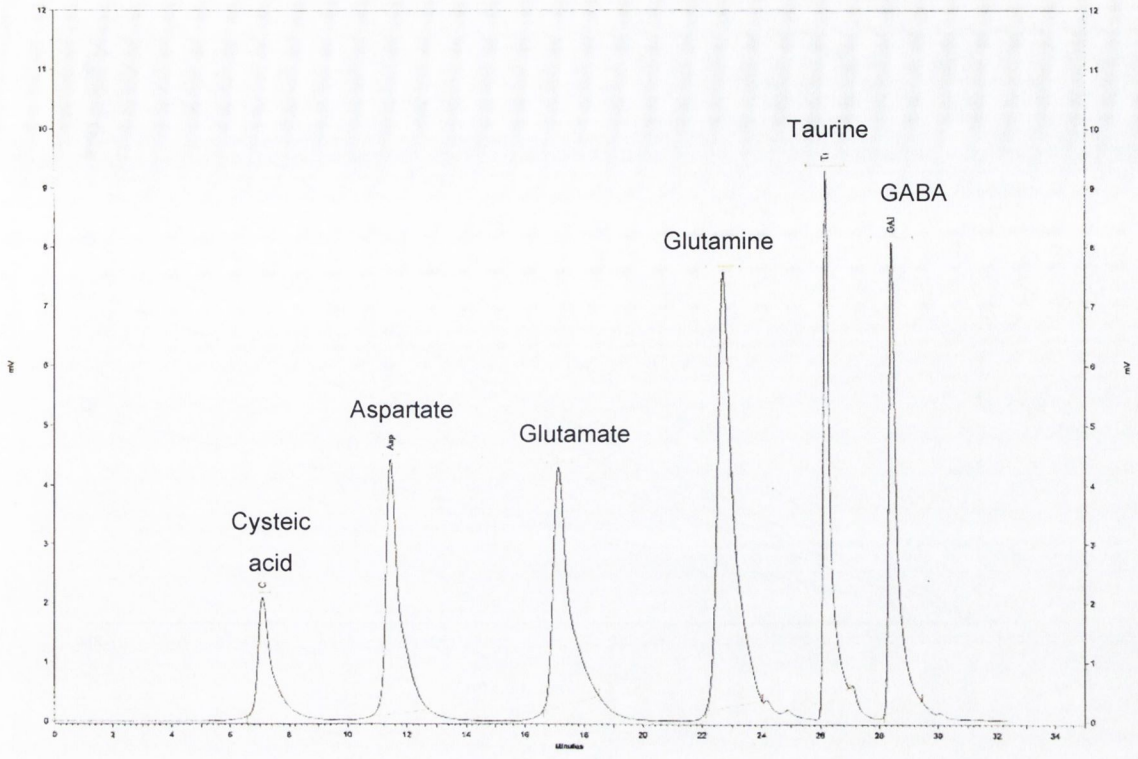

Figure 2.6 HPLC elution of derivatised amino acid standards

A sample trace of the separation of amino acid standards (30 µM) obtained under the conditions outlined in Section 2.7. The separation of the internal standard, cysteic acid (retention time (RT) = 7.097 min); aspartate (RT =11.438 min); glutamate (RT =17.145 min); glutamine (RT = 22.705 min), taurine (RT =26.170 min) and GABA (RT =28.412 min) over a 35 min elution period. Standards were prepared in mobile phase at a concentration of 30 µM. Injections of 40 µl were made onto the HPLC column.

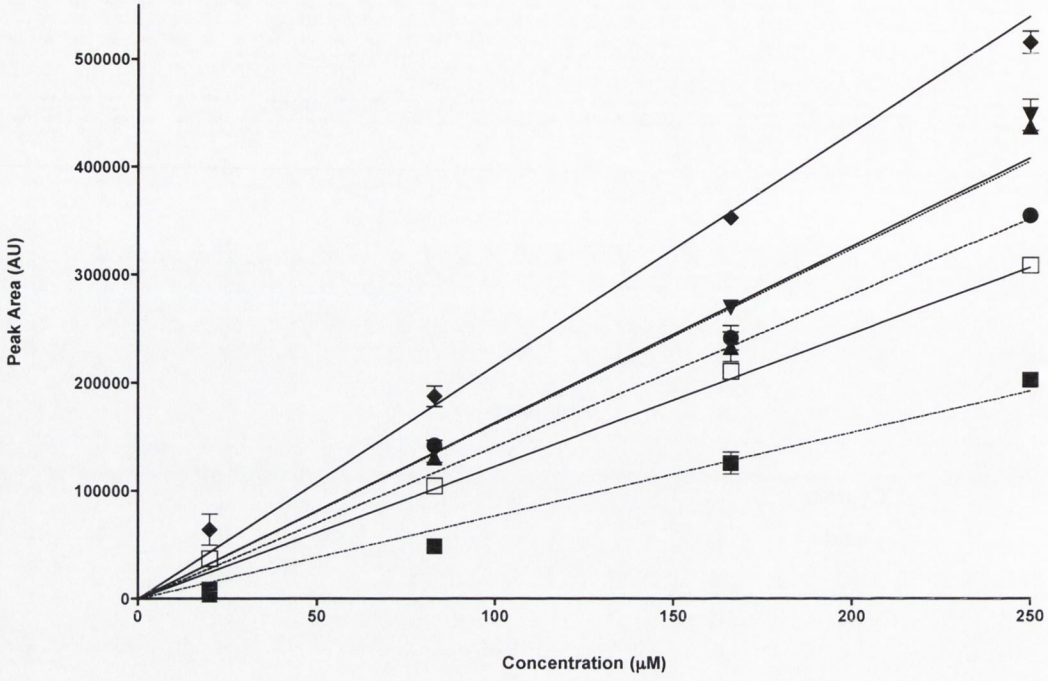

Figure 2.7 Standard curves of amino acids following HPLC elution

Standards of 20–250 µM concentrations of OPA derivatised amino acids were eluted from a C18 reverse phase and the fluorescence of each amino acid was detected using an FL2000 fluorescence detector and the area of the resulting fluorescence peak was measured and plotted against the corresponding amino acid concentration to produce a standard curve. ■=Cysteic acid (internal standard), ▲=aspartate, ▼=glutamate, ◆=glutamine, ●= taurine and □=GABA. Linear regression was performed on the data (n=3) and the equation of the line was used to determine the concentration of amino acids detected in samples.

2.12 Statistical analysis and curve fitting

Statistical analysis of data sets was performed using Prism (Version 4.0c, 2005) computer program (GraphPad Software Inc.). P values quoted were obtained by comparison of sets of data using one- and two-way analysis of variance (ANOVA) with post-hoc testing and paired or unpaired Students' t-test, as appropriate.

All K_m and V_{max} values and their errors were determined using the commercial computer program Prism from GraphPad software. The program fits sets of experiments data to the Michaelis-Menten equation that describes the behaviour of enzymes in the presence of increasing concentrations of substrate (Michaelis and Menten, 1913)

$$v = \frac{V_{max}[S]}{K_m + [S]}$$

Where v is the velocity of the enzyme reaction, [S] is the substrate concentration, V_{max} is the maximum enzyme velocity and K_m is the Michaelis constant. Double-reciprocal plots are used for illustrative purposes.

CHAPTER 3

INHIBITION OF THYROTROPIN-RELEASING HORMONE-DEGRADING ENZYME

3.1 Introduction

The therapeutic potential of Thyrotropin-releasing hormone (TRH) is impeded by its rapid degradation. Research strongly indicates that the key enzyme responsible for the degradation of extracellular TRH is TRH-degrading enzyme (TRH-DE) (Wilk 1986; Charli et al. 1988; O'Cuinn et al. 1990; Bauer et al. 1997a). It follows that inhibitors of TRH-DE should, in principle, protect TRH from degradation and thus enhance its potential therapeutic benefits.

Knowledge of the structure of TRH-DE could be exploited for the design of novel and selective inhibitors, however, to date the crystal structure for TRH-DE has not been elucidated. In the absence of any crystal-structure data, modelling and docking studies may predict how well potential inhibitors can fit into and bind to enzyme sites and the value of using this strategy for inhibitor design increases as the accuracy of modelling improves (Bohacek et al. 1996).

Homology modelling is a method of estimating the three-dimensional structure of a protein on its sequence similarities with related proteins whose structures are known. TRH-DE shares most homology (~30%) with the zinc metallopeptidases, aminopeptidases A and N, but the crystal structures for these enzymes have not yet been resolved. However, the crystal structure of another member of the zinc metallopeptidase family, leukotriene A_4 hydrolase (LTA_4H) (EC 3.3.2.6), has been resolved and a putative model for TRH-DE has been developed based on this, see Introduction, Fig.s 1.8 and 1.9 (Kelly et al. 2005; Chavez-Gutierrez et al. 2006).

Without a definitive three-dimensional TRH-DE structure, the use of structure–activity relationships (SAR) can provide critical information for the design of inhibitors. Initially, modifications to the structure of the natural substrate can be made and studies of the inhibitory properties of substrate analogues can be used to feed back into the design process of inhibitors.

Using this approach a lead inhibitor was discovered by Kelly *et al.,* 2000 through substituting the histidine residue with asparagine, which resulted in a tripeptide that binds to TRH-DE with a greater affinity than TRH, with a K_i of 17.5 μM (Kelly et al. 2000). This peptide was then further modified to Glp-Asn-ProAMC, to produce the most potent inhibitor of TRH-DE known to date, with a K_i of 0.5 μM, TRH has a K_m of 35 μM (Kelly et al. 2000). The increased affinity produced by the addition of coumarin to the C-terminus of Glp-Asn-ProNH_2 suggested that the substrate-binding area of TRH-DE contained a hydrophobic pocket with which the C-terminus of the peptide interacts.

The purpose of the studies described in this chapter was to analyse the kinetic properties of modified analogues of Glp-Asn-ProNH_2. Initially, analogues were screened for their ability to resist hydrolysis by TRH-DE and subsequently fluorometric assays were used to determine the kinetic parameters of the analogues. The K_i values for potent inhibitors were then examined in more detail by non-linear regression analysis of the initial-rate data.

3.2 Methods

3.2.1 Composition of buffer

Potassium phosphate buffer, 20 mM, pH 7.5 was prepared for assays. 20 mM potassium dihydrogen phosphate was added to 20 mM dipotassium hydrogen phosphate until the appropriate pH was reached. The buffer was stored at 4°C.

3.2.2 HPLC mobile phase

An elution gradient composed of two mobile phases was used for HPLC separation of novel peptides and degradation produces. Mobile phase 1 composed of water and 0.08% (v/v) trifluoroacetic acid (TFA) and mobile phase 2 of 40% acetonitrile with 0.08% (v/v) TFA. A linear gradient of 0–70% acetonitrile was used, outlined in Table 3.1, with a P4000 Quaternary Pump (Spectrasystem P1000 from TSP).

Table 3.1 Linear gradient of mobile phase

The gradient used to elute TRH and novel peptides and their degradation products. Phase 1 consisted of water and 0.08% (v/v) TFA and phase 2 of 40% acetonitrile and 0.08% (v/v) TFA.

Time (min)	Phase 1	Phase 2
0	100	0
10	50	50
15	30	70
25	50	50
27	100	0
30	100	0

3.2.3 Enzyme Purification

3.2.3.1 Purification of Thyrotropin-releasing hormone-degrading enzyme

TRH-DE used was purified almost 20,000-fold from porcine brain by Kelly and Bauer at the MMPI, Hanover, Germany by the procedure described by Kelly *et al.* (1999). The purified enzyme was subjected to SDS-polyacrylamide gel

electrophoresis and, after Coomassie-staining, showed one major band, with a relative molecular mass of 116,000, consistent with previously reported size for TRH-DE (Bauer 1994). The preparation was assayed and found to be devoid of peptidase activities other than TRH-DE, including the other TRH-degrading enzymes, pyroglutamate aminopeptidase I (PAP I) and prolyl endopeptidase (PE).

The TRH-DE used was found to have a protein concentration of 0.8 mg ml^{-1} and a specific activity with TRH-AMC as a substrate of 2.8×10^{-3} μkatal/mg (Kelly et al. 1999).

3.2.3.2 Purification of dipetidyl peptidase IV

Dipetidyl peptidase IV (DPP-IV) (EC 3.4.14.5) was obtained from Dr Carvell Williams (Queen's University Belfast) and had been purified 370-fold from bovine kidney (Brownlees et al. 1992). The enzyme had a protein concentration of 7.7 mg ml^{-1} and specific activity of 0.29 μkatal/mg with Gly-Pro-AMC (100 μM) as substrate (Kelly et al. 1999). As with TRH-DE, no other peptidase activities were found to be present in the preparation.

3.2.4 Standard Curve of Pyroglutamate

A 1 mM stock solution of pyroglutamate (pGlu) was prepared in potassium phosphate buffer, pH 7.5. Dilutions were made to 5 concentrations (0.18–0.9 μM) in triplicate containing 0.15% (v/v) TFA.

The peak height measured by UV absorption at 206 nm for each concentration following elution from the HPLC using a reverse phase C-18 column (Waters) was used to generate a standard curve for determining the concentration of pGlu produced by TRH-DE action on the novel peptides was plotted (Figure 3.1).

The quantitative detection limit for a 40 μL injection volume was calculated to be 0.1 mM, employing a signal to noise ratio of 10. This standard curve was plotted

using PC1000 system software from TSP and used to calculate the amount of pGlu released from novel peptides that were substrates of TRH-DE.

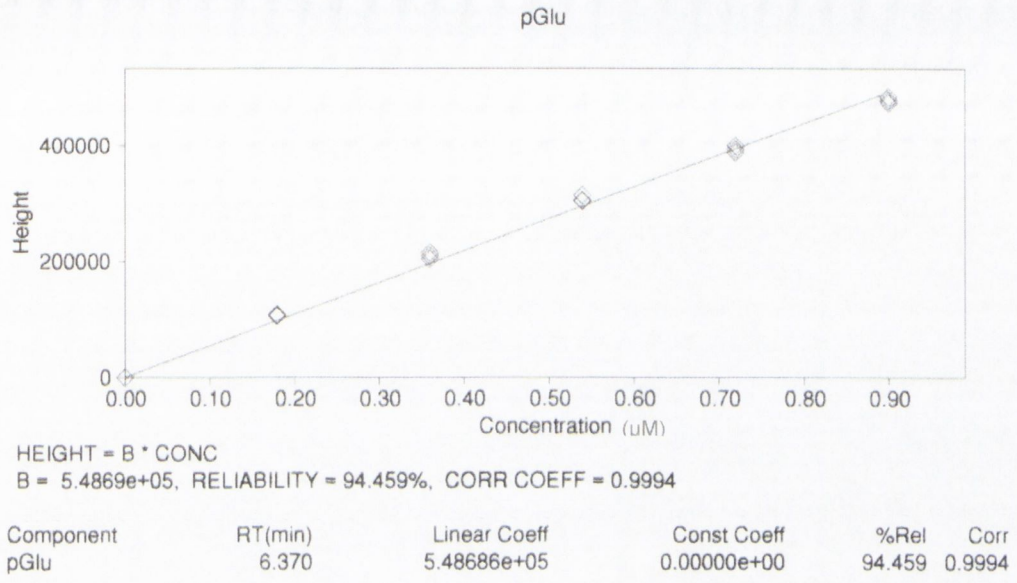

Figure 3.1 Standard curve of pyroglutamate

Five concentrations of pyroglutamate (pGlu) were eluted from a Waters column by HPLC and detected by UV absorption at 206 nm. The peak height was plotted against the concentration and the slope was calculated at 5.49 and the goodness of fit is 0.9994. The standard curve was used to determine the concentration of pGlu released from novel peptides following incubation with TRH-DE.

3.2.5 Standard curve of 7-amino-4-methylcoumarin

A standard curve of 7-amino-4-methylcoumarin (AMC) was determined with 5 µM TRH-AMC present. 0.01–1 µM of AMC concentrations were prepared and the intensity was measured fluorimetrically on a Perkin–Elmer LS-50B spectrophotofluorometer. TRH-AMC exhibits only small background fluorescence (less than 1% of the total fluorescence when TRH-AMC and AMC are present in equimolar concentrations).

The fluorescence of each concentration was measured in triplicate and was graphed using Excel, calculating an R^2 value for the data (Figure 3.2). The

slope of this line was then used for determining the amount of AMC release from TRH-AMC following incubation with TRH-DE ± potential inhibitors. The quantitative limit of detection for AMC using these parameters was found to be 0.01 μM.

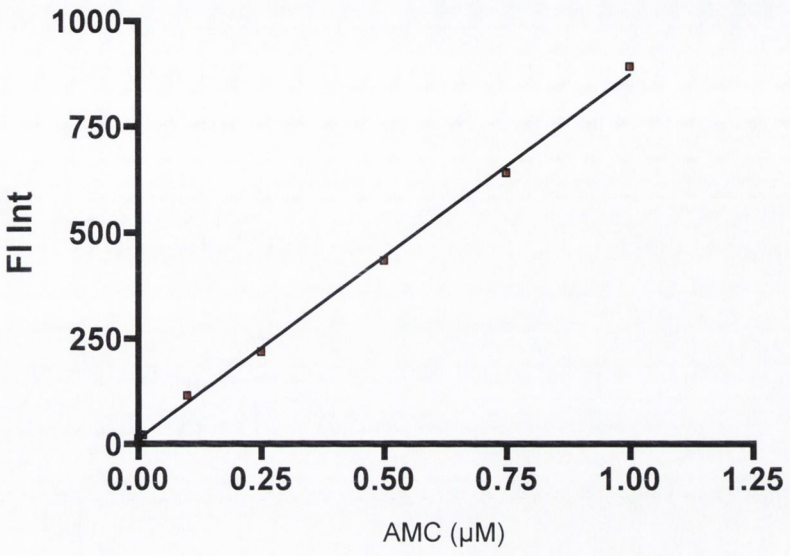

Figure 3.2 Standard curve of 7-amino-4-methylcoumarin

The fluoresce intensity of 6 concentrations (0.01–1 μM) of 7-amino-4-methylcoumarin (AMC) was measured in triplicate and a graph of concentration versus intensity was produced using Microsoft Excel, the slope of this plot was calculated to be 861.512 and is used in determining the hydrolysis of TRH-AMC. The goodness of fit was determined with an R^2 value of 0.9984. In all cases the error bars were smaller than the point sizes.

3.2.6 *Screening of novel inhibitor compounds*

Table 3.2 The novel peptide structures.

The compounds outlined below were custom synthesised (Kelly et al. 2000; Kelly et al. 2005; Scalabrino et al. 2007) as structural analogues of TRH (Glp-His-ProNH$_2$) to determine their ability to act as competitive inhibitors of TRH-DE, an enzyme highly specific for TRH.

Glp-Asn(Benzyl)-ProNH$_2$ 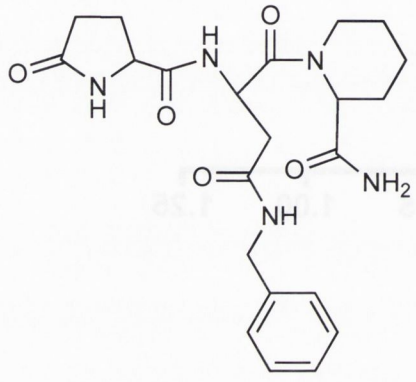	Glp-Asn(Phenyl)-ProNH$_2$ 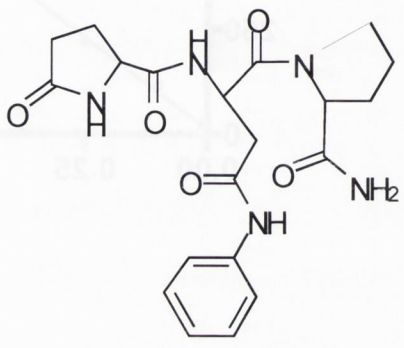
Glp-Asn-AlaNH$_2$ 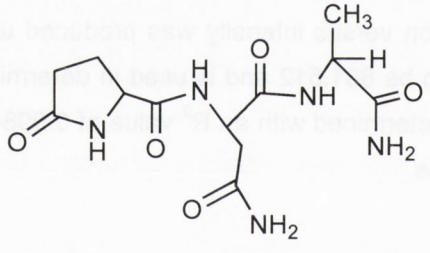	Glp-Asn-HomoProNH$_2$ 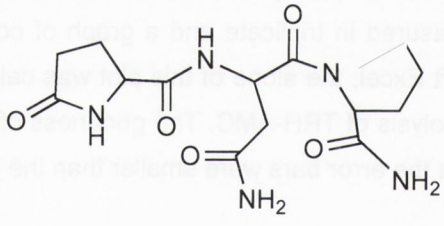
Glp-Asn-Pro(O)-Benzyl 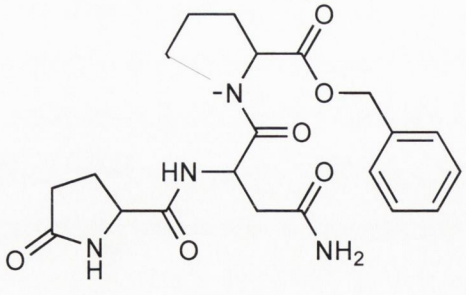	Glp-Asn-ProOMe 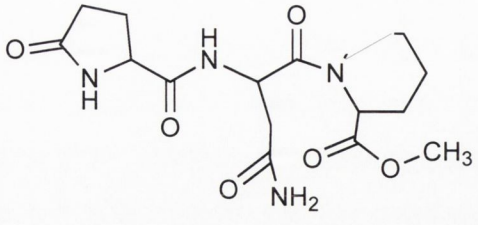

Glp-Asn-Pro-Tyr-Trp-NH_2

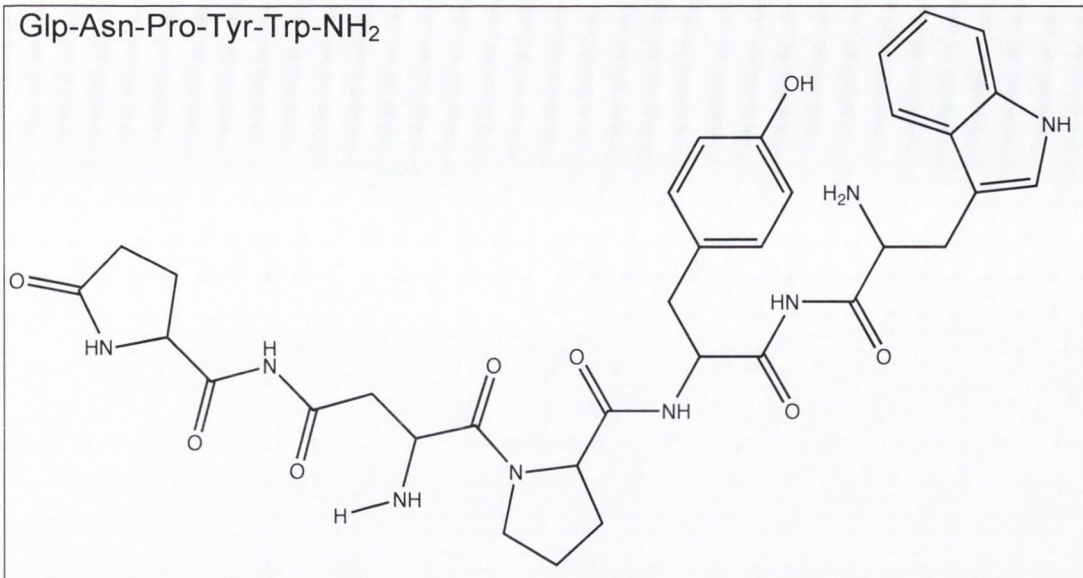

Glp-Asn-Pro-Tyr-Trp-Trp-NH_2

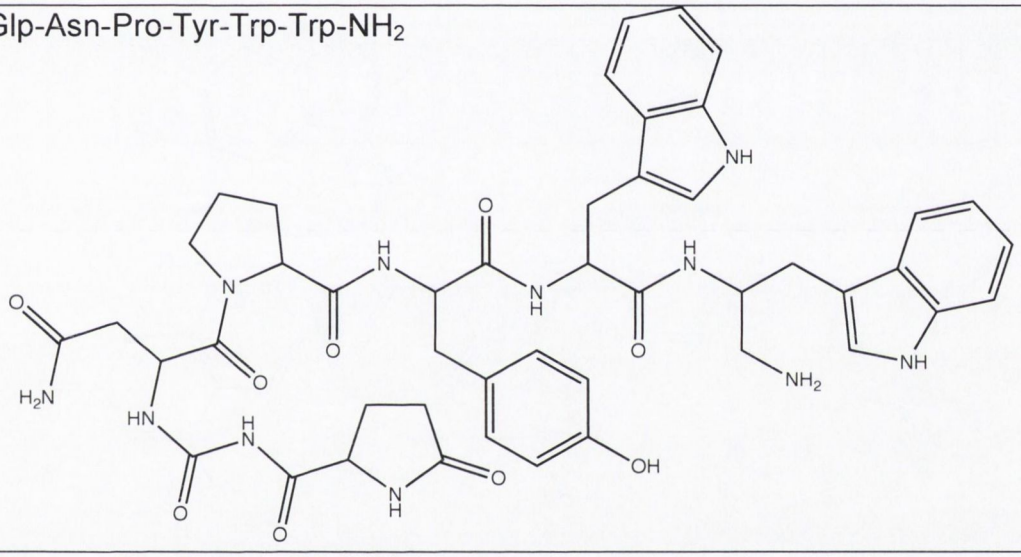

Glp-Asn-Pro-Tyr-Trp-Trp$(OMe)_2$

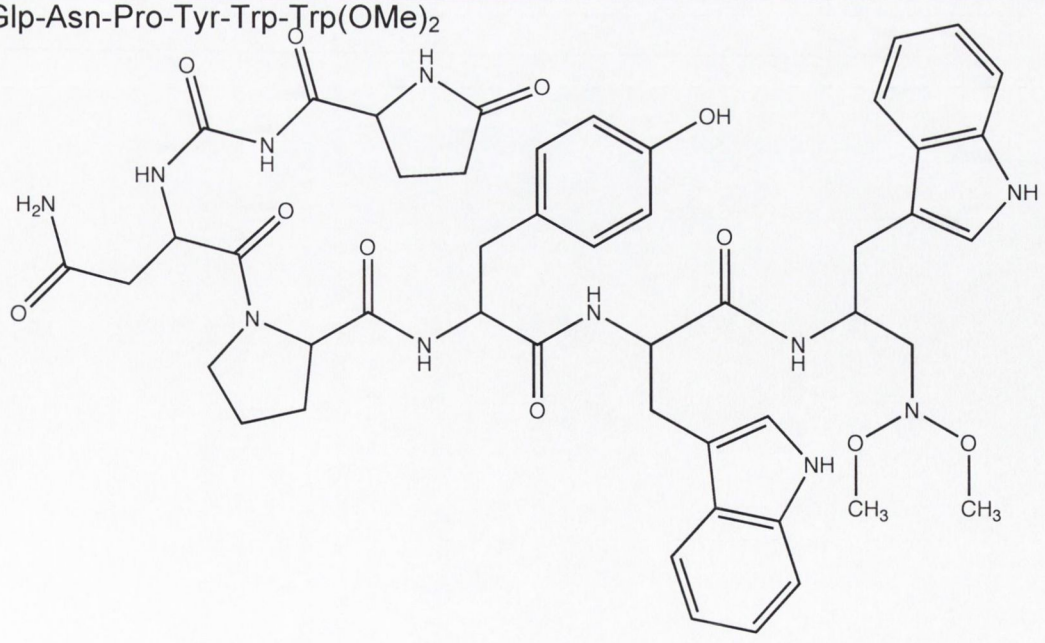

Glp-Asn-Pro-Tyr-Trp-AMC

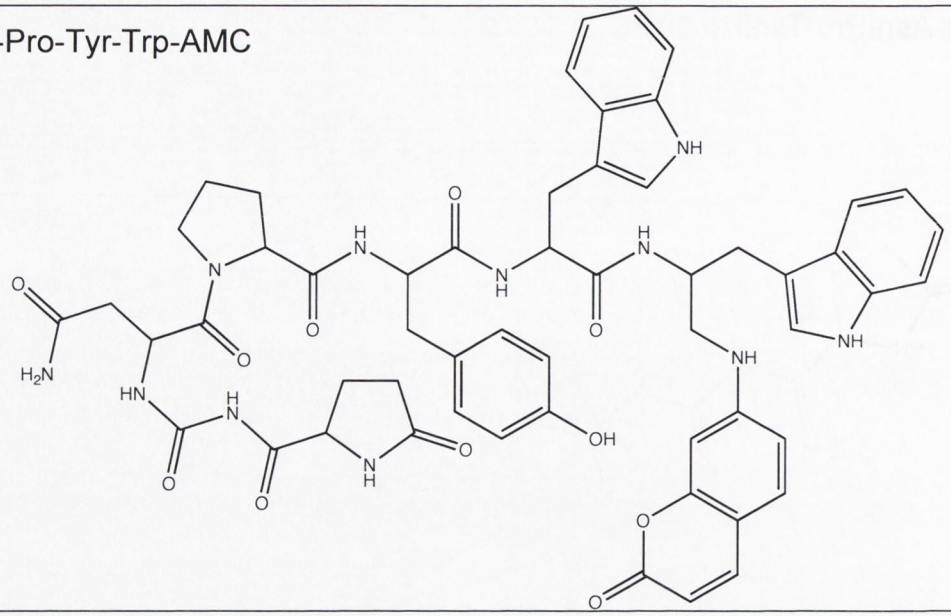

Glp-Asn-Pro-Tyr-Trp-Trp-AMC

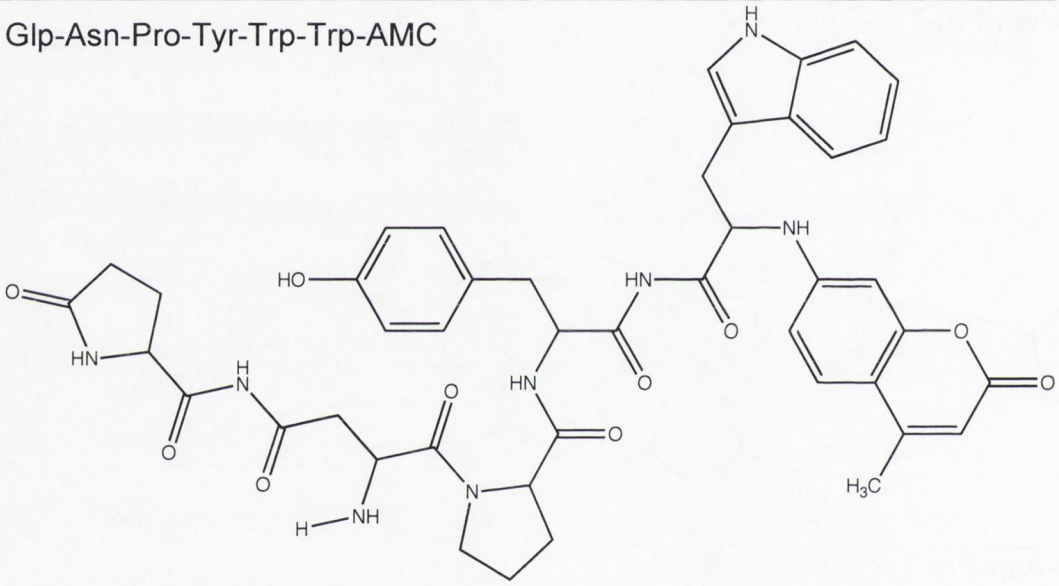

3.2.6.1 Hydrolysis of Peptides

The ability of the peptides outlined in Table 3.2 to resist hydrolysis by TRH-DE was ascertained by incubating 1 mM final concentrations of each inhibitor or TRH with 0.08 µg of TRH-DE, in a total volume of 100 µL, for 18 hours at 37°C. Controls were included, where TRH-DE was absent from the incubation. When TRH is subjected to these conditions it is completely degraded to pyroglutamate and His-Pro-diketopiperazine. Following the 18 h incubation, the reaction was terminated by the addition of trifluoroacetic acid (0.15%, v/v). The samples were then analysed by HPLC, using a reverse phase C-18 column (Waters). 40 µL of each of the incubations were loaded onto the column and TRH, the test peptides and any degradation products were separated and eluted from the column using the linear gradient outlined in Table 3.1. Elution products were detected at a UV absorbance of 206 nm. The presence of pyroglutamate in the sample indicated the peptide to be a substrate of TRH-DE.

3.2.6.2 Continuous coupled fluorometric assay

Peptides that resisted hydrolysis by TRH-DE were assayed using a continuous coupled fluorometric assay (Kelly et al. 1999). The ability of the peptides to inhibit TRH-AMC degradation by TRH-DE was measured in this assay. DPPIV is used as a coupling enzyme, with the reaction mechanism as follows:

TRH-AMC $\xrightarrow{\text{TRH-DE}}$ **pGlu + His-Pro-AMC** $\xrightarrow{\text{DPPIV}}$ **His-Pro + AMC** **Equation 3.1**

The progress of the reaction was measured by the release of AMC, with accompanying increase in fluorescence over the 10 minutes of the reaction. This was measured on a Perkin–Elmer LS-50B spectrophotofluorometer, using the time-drive function of the FL WinLab software, with 6001 data-points collected. Wavelengths for excitation and emission were set at 370 and 440nm, respectively, and with slit-widths of 10 and 5 nm, respectively.

The amount of DPPIV required as the coupling enzyme was determined by Kelly *et al.* (1999) using the equation derived by McClure (McClure 1969):

$$t = K_m' \ln(1 - F) / V' \qquad \text{Equation 3.2}$$

lag time (t) is the time required for [His-ProAMC], the reaction intermediate to reach a defined fraction (F) of the steady-state concentration and K_m and V' are the K_m and V_{max} of DPPIV.

Peptides at 16.6 µM final concentrations (except Glp-Asn-Pro-Tyr-Trp-AMC and Glp-Asn-Pro-Tyr-Trp-Trp-AMC, which were assayed at 1 µM and 0.1 µM, respectively) were analysed for inhibition potency, using 5 µM TRH-AMC substrate and 0.53 µg final concentration of TRH-DE in potassium phosphate buffer, final volume 600 µL. The TRH-AMC, peptide, DPPIV and buffer were pre-equilibrated in a quartz cuvette at 37°C for one minute prior to addition of TRH-DE. A plastic rod was used to mix the solution immediately after addition of TRH-DE. Fluorescence was measured as a function of time using the program FL WinLab, version 2.0 on a Perkin Elmer LS50B luminescence spectrometer.

In each assay the fluorescence of 5 µM TRH-AMC alone was measured to calculate background fluoresence. An initial control assay incubating TRH-AMC with DPPIV was performed, demonstrating no increase in fluorescence indicating no release of AMC. Further control assays including the solvent used to dilute the peptide of interest, e.g. MeOH, were also performed to ensure potential solvent inhibition of TRH-DE or DPPIV was accounted for. In all experiments it was ensured that the reaction, outlined in Equation 3.1 was fully coupled by increasing the amount of DPPIV added, by 50%, and demonstrating that there was no increase in the velocity of the reaction.

3.2.6.3 Discontinuous fluorometric assay

The use of DPPIV in assays is limited by any potential inhibitors of this coupling enzyme. Though TRH and TRH-AMC are not substrates of DPPIV (Kelly et al. 1999), it has been demonstrated that His-ProOH is an inhibitor (K_i of 70 µM)

and His-ProNH_2 is a substrate of DPPIV. Thus, any peptides demonstrated to be cleaved by TRH-DE during HPLC screening (Section 3.2.6.3) are potential inhibitors of DPPIV as the resulting cleavage products could inhibit AMC release from His-ProAMC should the continuous coupled assay be used. An alternative method of analysis is required that does not utilise DPPIV as a coupling enzyme.

Peptides that underwent hydrolysis in the HPLC screen were examined as competitive substrates of TRH-DE by a discontinuous method. This used an intramolecular condensation reaction, which converts His-ProAMC to the cyclised histidyl-proline diketopiperazine (His-Pro DKP) and released AMC:

$$\text{TRH-AMC} \xrightarrow{\text{TRH-DE}} \text{pGlu + His-ProAMC} \xrightarrow[\text{cyclization}]{\text{5 h, 80°C}} \text{His-ProDKP + AMC} \qquad \textbf{Equation 3.3}$$

The peptide of interest at 250 µM final concentration was incubated with TRH-AMC (5 µM) and 0.4 µg TRH-DE in 20 mM phosphate buffer in a 1250 µL total volume for 10 minutes at 37°C. TRH-DE activity was then terminated by incubating the reaction mixture at 80°C for 5 hours. The fluorescence due to AMC release was then measured using excitation and emission wavelengths of 370 and 440 nm, respectively, and excitation and emission slit widths of 10 and 5 nm, respectively.

3.2.6.4 Kinetic analysis of inhibition by non-linear regression

The kinetics of compounds that were found to resist hydrolysis and inhibited TRH-DE potently (>20% inhibition) were further examined by non-linear regression analysis of initial-rate data. In this case, the degradation of TRH-AMC by TRH-DE was measured using the continuous fluorometric assay in the presence and absence of four different concentrations of the inhibitor compound and at five concentrations of TRH-AMC.

The initial rate of the reaction was calculated from the amount of AMC released, using the slope measured by the time-drive function of FL-WINLAB and the

AMC standard curve. The Ki values were then obtained by nonlinear regression analysis of initial-rate data using Prism (GraphPad Software Inc.). Double reciprocal (Lineweaver-Burk) plots are used for illustrative purposes only.

3.3 Results

3.3.1 HPLC screening of peptides

Compounds were screened for their ability to resist hydrolysis by TRH-DE by incubating each with TRH-DE. For each assay a control was performed using 1 mM TRH to ensure TRH-DE was fully active and on all occasions it was demonstrated that all TRH was fully degraded to pyroglutamate and His-ProNH_2 and His-ProDKP. These compounds were distinguished as they eluted from the column by the absorption peaks detected at 206 nm. All peptides outlined in Table 3.2 except Glp-Asn(*N*-Bzl)-ProNH_2 were found to resist hydrolysis and were detected as a single peak.

3.3.1.1 Degradation profile of TRH

TRH elutes from a C18 column at 9.42 min and is fully degraded following an 18h incubation with TRH-DE. The resulting products, pGlu and His-Pro-diketopiperazine, elute at ~6.5 and ~10.64 min, respectively (Figure 3.3).

3.3.1.2 Glp-Asn(*N*-Bzl)-ProNH_2 is hydrolysed by TRH-DE

Glp-Asn(*N*-Bzl)-ProNH_2 acts as a weak substrate of TRH-DE. The peptide elutes as a single peak when no enzyme is present, but following 18h incubation with the enzyme, formation of pGlu was evident (Figure 3.4). The pGlu standard curve, Figure 3.1, was used to calculate that 165 µM pyroglutamate was produced due to peptide cleavage by TRH-DE. This result led to the examination of the inhibitory properties of this peptide by its use as a competitive substrate in the discontinuous fluorometric assay for the reasons outlined in Section 3.2.6.3.

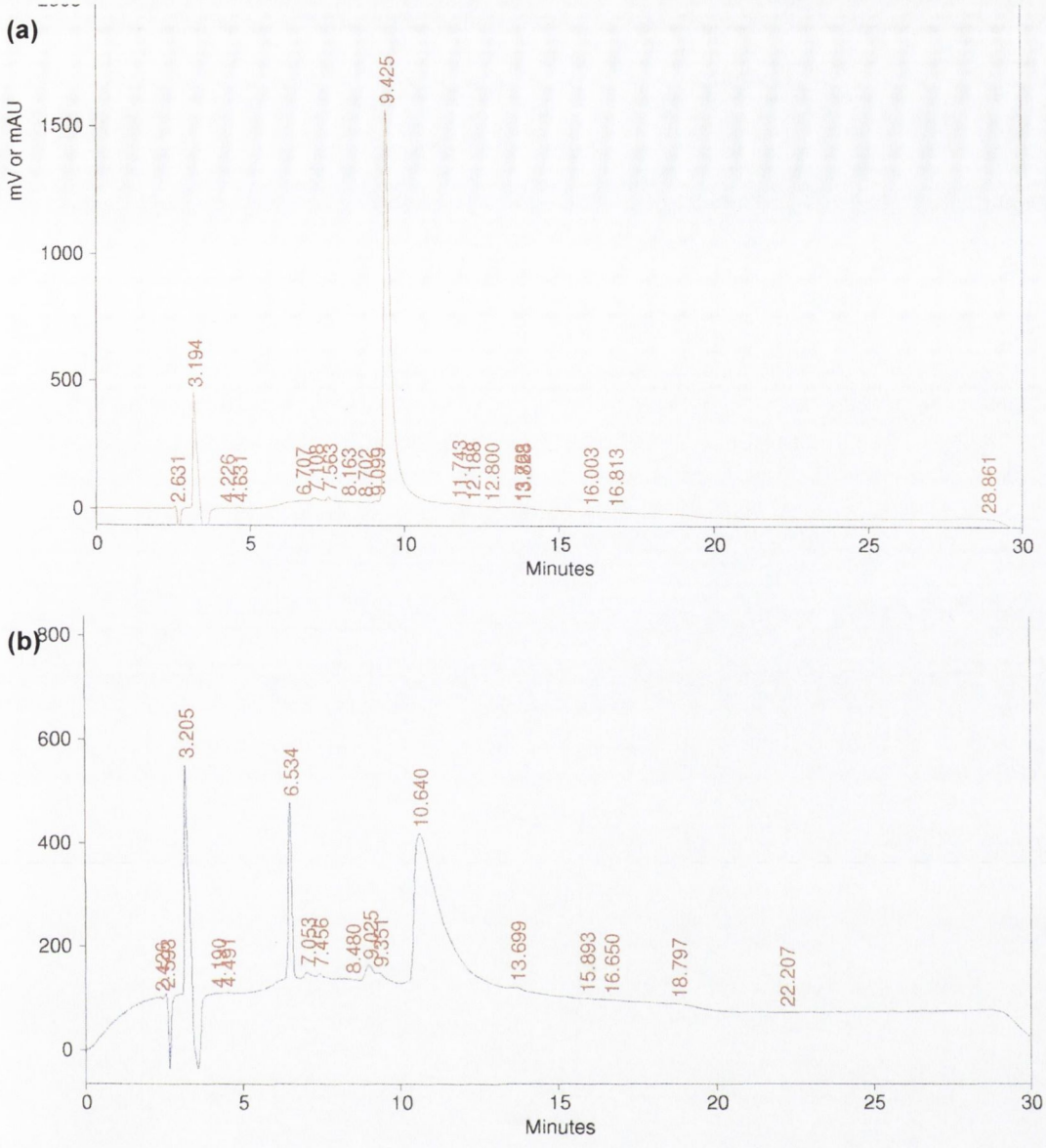

Figure 3.3 Elution profile of TRH

(a) When incubated with buffer for 18 h, TRH elutes by HPLC as a single peak and is detected by absorption at 206 nm with a retention time of ~9.4 min. (b) Following incubation of TRH with TRH-DE for 18 h, TRH is fully degraded to the products pyroglutamate and His-Pro-diketopiperazine, which elute by HPLC at ~6.5 and ~10.64 min, respectively.

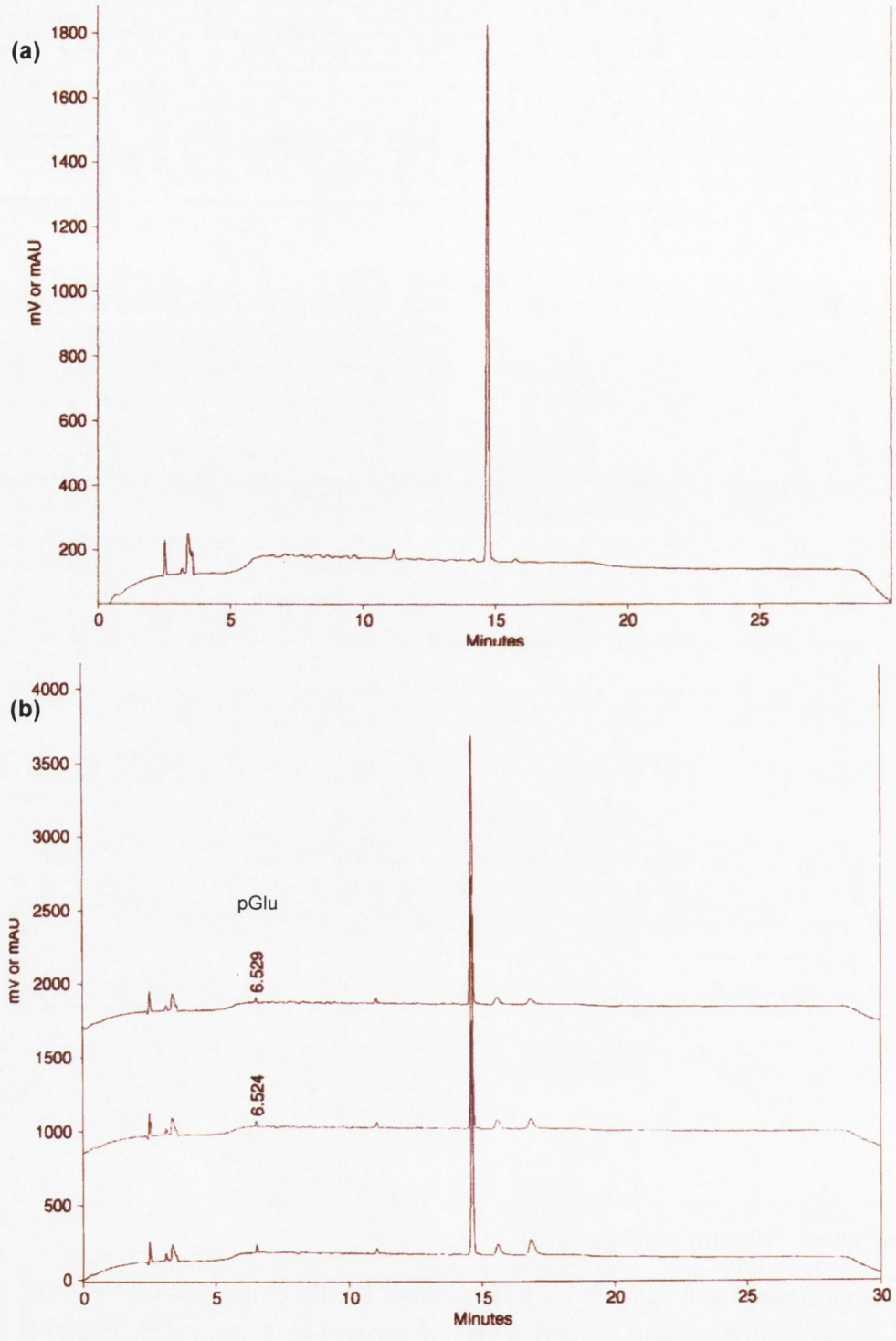

Figure 3.4 Glp-Asn(Bzl)-ProNH$_2$ following 18 h incubation

(**a**) The peptide is detected by HPLC elution as a single peak with a retention time of 15 min following incubation with buffer in the absence of TRH-DE, neither pyroglutamate nor other peaks are detected. (**b**) This peptide undergoes degradation following incubation with TRH-DE, as evidenced by the HPLC elution of pyroglutamate at 6.5 min and further degradation products eluting after the major peak at 15 min representing the peptide.

3.3.2 The kinetic parameters of TRH-AMC

The kinetic parameters of TRH-AMC as a substrate of TRH-DE in the continuous coupled enzyme assay were calculated. The release of AMC from the coupled reaction was measured fluorometrically over 10 min for 5 substrate concentrations (n=4). Initial rates were fitted to a Michaelis–Menten curve (Figure 3.5). The Michaelis constant, K_m, for TRH-AMC hydrolysis by TRH-DE was determined by non-linear regression fit analysis as 3.3 ± 0.37 μM and V_{max} was 0.101±0.005 μM/min, with goodness of fit, R^2=0.968. The double reciprocal Lineweaver-Burk plot determination confirms the linearity of the curve fit with an R^2 value of 0.9309 (Figure 3.6). The same assay was used to study the inhibition by a number of TRH analogues and representative traces showing their effects on the rates of hydrolysis are shown in Fig. 3.8.

3.3.3 Kinetic properties of peptides resistant to TRH-DE hydrolysis

The release of AMC from TRH-AMC was measured fluorometrically using the Perkin–Elmer LS-50B in the presence of the peptides shown to be resistant to hydrolysis. The slopes of each of these traces were calculated by the time-drive function of FL-WinLab. The release of AMC was decreased, evidenced by the rate of change in fluorescence (Figure 3.7). The slope due to increase in fluorescence was used to calculate the amount of product, AMC, formed using the standard curve. From this value, the rate of the reaction, v_0, could then be determined.

Then, using the K_m determined above and the equation:

$$\frac{v_i}{v_o} = \frac{[\mathrm{I}]}{[\mathrm{I}] + K_i\left(1 + \frac{[\mathrm{S}]}{K_m}\right)}$$

Equation 3.4

where v_i is the initial rate measured in the presence of inhibitor, [I] and [S] are the inhibitor and substrate concentrations, respectively, and K_i is the inhibitor constant; the percent inhibition, v_i, and an approximate K_i afforded by the

peptide were calculated. This relationship assumes inhibition to be competitive. The approximate K_i values determined for each inhibitor is outlined in Table 3.3, where each value given is the mean ± S.E.M., where n=3. The small amounts of each peptide available precluded more detailed studies.

3.3.4 Kinetic properties of peptides hydrolysed by TRH-DE

The only peptide found by HPLC analysis to be hydrolysed by TRH-DE in this study was Glp-Asn(*N*-Bzl)-ProNH_2 (Figure 3.4). This peptide was thus assayed by the stopped fluorometric assay outlined in Section 0. The amount of AMC (determined from a standard curve as above) cleaved from TRH-AMC in the presence of 250 µM Glp-Asn(*N*-Bzl)-ProNH_2 was used to determine the rates of the reaction, v_0 and v_i. The K_m of TRH-AMC catalysis by TRH-DE in the discontinuous assay was determined to be 3.4 µM. These values were inserted into the formula outlined above (Equation 3.4), where [I] is 250 µM and [S] is 5 µM, and an approximate value for K_i was found to be 99.64±7.99 µM. The K_i properties of this peptide were not investigated further, due to the unavailability of the compound.

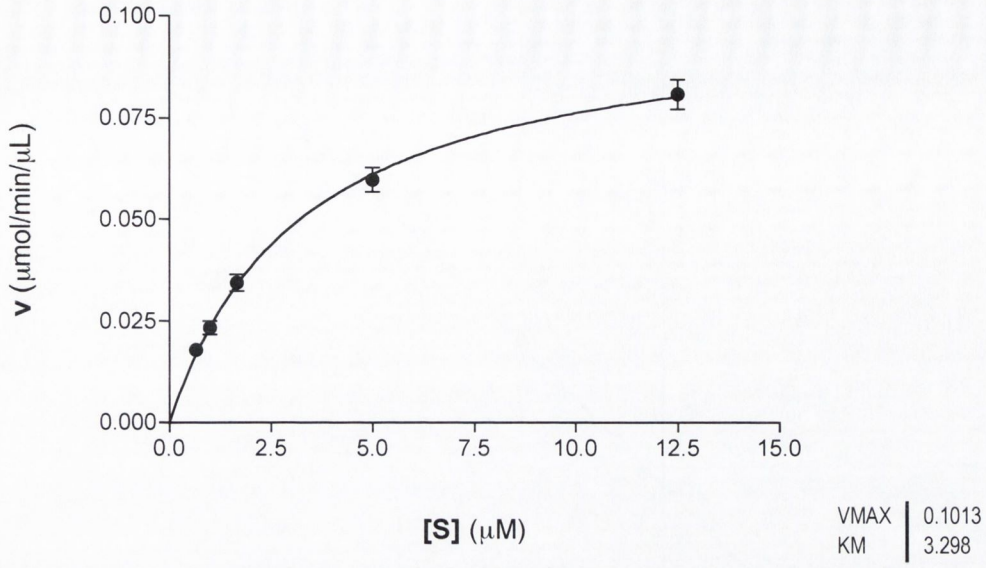

Figure 3.5 Michaelis–Menten plot of TRH-AMC as a substrate of TRH-DE

The plot of TRH-AMC at 0.66–12.5 µM substrate concentration against the initial rate of the reaction calculated from the slope of the line and using the AMC standard curve. Data points represent the mean ± S.E.M. (n=4), plotted using GraphPad Prism. Non-linear regression fit analysis indicates K_m as 3.3 ± 0.37 µM and V_{max} was calculated to be 0.101±0.005 µmol/min/µL, with a correlation coefficient of the fit of 0.9675.

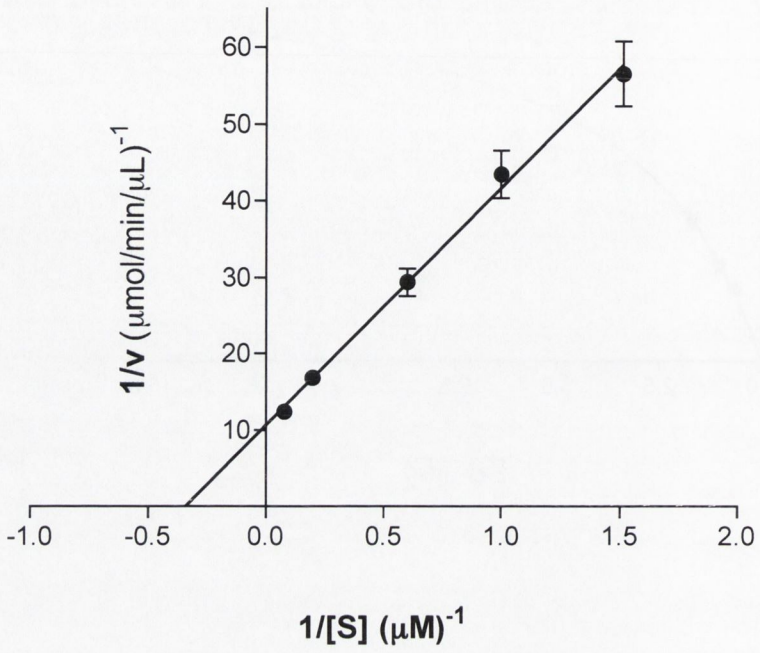

Figure 3.6 Lineweaver–Burk plot of TRH-AMC as a substrate of TRH-DE

The reciprocal values of TRH-AMC (0.66–12.5 µM) from Fig. 3.5 were replotted using GraphPad Prism. Linear regression analysis confirms the linearity of the curve fit, with an R^2 value of 0.93. K_m=2.92 ± 0.29 µM. V_{max}=0.094 ± 0.015 µM/min.

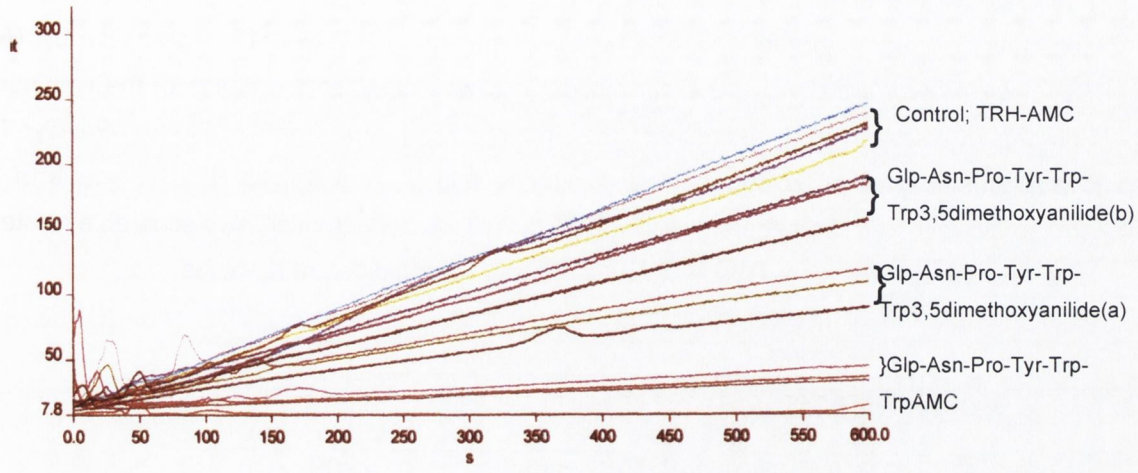

Figure 3.7 The inhibition of AMC release from TRH-AMC

Sample trace of the increase of fluorescence measured when inhibitors were present, in this case pGlu-Asn-Pro-Tyr-Trp-TrpAMC, Glp-Asn-Pro-Try-Trp-Trp(OMe)$_2$ (a) and (b). An approximate K_i afforded by the peptide were calculated using the equation $v_i/v_0=[I] / ([I] + K_i(1+[S]/K_m))$, which assumes competitive inhibition and K_m to approximate to a dissociation constant.

Table 3.3 Inhibition of TRH-DE by C-terminally extended analogues of Glp-Asn-Pro-NH_2

The percent inhibition was found using the relationship $v_i/v_0 = i = [I]/([I] + K_i(1 + [S]/K_m))$ where v_0 and v_i are the rate and inhibited rate of the reaction, respectively, [I] and [S] are the inhibitor and substrate concentration and K_m is the Michaelis constant for TRH-AMC degradation by TRH-DE, the inhibition constant K_i is determined. Data was obtained by means of the continuous fluorometric assay and represent the mean ± S.E.M. (n=3). Glp-Asn-Pro-Tyr-Trp-Trp3,5dimethoxyanilide is represented as compounds (a) and (b), as HPLC analysis of the compound revealed two separate resolved peaks, which are potentially two separable isosteres of the compound and were thus assayed separately, giving different K_i values.

Peptide	K_i μM
Glp-Asp((*N*)Analine)-ProNH_2	>200
Glp-Asn-AlaNH_2	>200
Glp-Asn-ProOMe	74.3 ± 17.2
Glp-Asn-HomoProNH_2	19.3 ± 0.8
Glp-Asn-Pro(O)-Benzyl	15.3 ± 0.4
Glp-Asn-Pro-Tyr-Trp-TrpNH_2	0.73 ± 0.07
Glp-Asn-Pro-Tyr-TrpNH_2	0.630 ± 0.001
Glp-Asn-Pro-Tyr-Trp-Trp$(OMe)_2$ **b**	0.55 ± 0.08
Glp-Asn-Pro-Tyr-Trp-Trp$(OMe)_2$ **a**	0.02 ± 0.002
Glp-Asn-Pro-Tyr-TrpAMC	0.04 ± 0.004
Glp-Asn-Pro-Tyr-Trp-TrpAMC	0.01 ± 0.00

3.3.5 Kinetic analysis of Inhibition by non-linear regression

The most potent inhibition determined by the coupled enzyme assay was elicited by the *C*-terminally extended analogues Glp-Asn-Pro-Tyr-Trp-AMC and Glp-Asn-Pro-Tyr-Trp-Trp-AMC. The apparent K_i values initially calculated at a single inhibition concentration (1 µM Glp-Asn-Pro-Tyr-Trp-AMC and 0.1 µM Glp-Asn-Pro-Tyr-Trp-Trp-AMC) were 0.04±0.004 µM and 0.01±0.0008 µM, respectively.

The kinetic parameters of the inhibition of TRH-DE by these compounds were measured by the continuous fluorometric method at five different substrate concentrations in the presence and absence of four concentrations of the peptides.

3.3.5.1 Kinetic parameters of Glp-Asn-Pro-Tyr-TrpAMC

The rate of AMC release was measured by the time-drive function of FL-WINLAB software using a Perkin–Elmer spectrometer in duplicate at 0.66–12.25 µM substrate in the presence of 0.04–0.1 µM concentrations of the inhibitor. The initial rate at each concentration was fitted to a Michaelis–Menten plot using GraphPad Prism (version 4.0c) (Figure 3.8). Non-linear regression analysis was then performed calculating the V_{max} as 0.094± 0.002 µM/min (with no significant deviation, P=0.663, analysed by one-way ANOVA), and an apparent K_m for each concentration of the inhibitor. The inhibition constant, K_i, was then found using the K_m determined from non-linear regression analysis when no inhibitor was present and the apparent K_m ($K_{m\ app}$) for each inhibitor concentration, assuming competitive inhibition, with the equation:

$$K_i = \frac{[I]}{\frac{K_{m\,app}}{K_m} - 1} \qquad \text{Equation 3.5}$$

The K_i for Glp-Asn-Pro-Tyr-TrpAMC is 0.038±0.007 µM.

The reciprocal values of substrate and initial rates were used to create a Lineweaver-Burk plot (Figure 3.9). Linear regression analysis used to fit data illustrates that the inhibitor is competitive. The V_{max} calculated for each inhibitor concentration using this plot did not alter significantly (average V_{max} is 0.078±0.006, with P=1, determined by one-way ANOVA analysis). The linearity of the curve fit by linear regression had a goodness of fit (R^2) of >0.96. Using Equation 3.5, the K_i was calculated to be 0.044±0.006 μM.

The $K_{m\ app}$ was plotted against the concentration of inhibitor (Figure 3.10), giving a K_m of 3.28 ± 0.55 μM (y-axis intercept) and a K_i for Glp-Asn-Pro-Tyr-Trp-AMC of 0.032 μM (-x-axis intercept). The goodness of fit of the linear regression is 0.98.

Linear regression analysis of the slope of a plot of V_{max} versus inhibitor concentration was not found to deviate significantly from zero (P= 0.854), which supports the interpretation that Glp-Asn-Pro-Tyr-Trp-AMC is acting as a classical competitive inhibitor of TRH-DE.

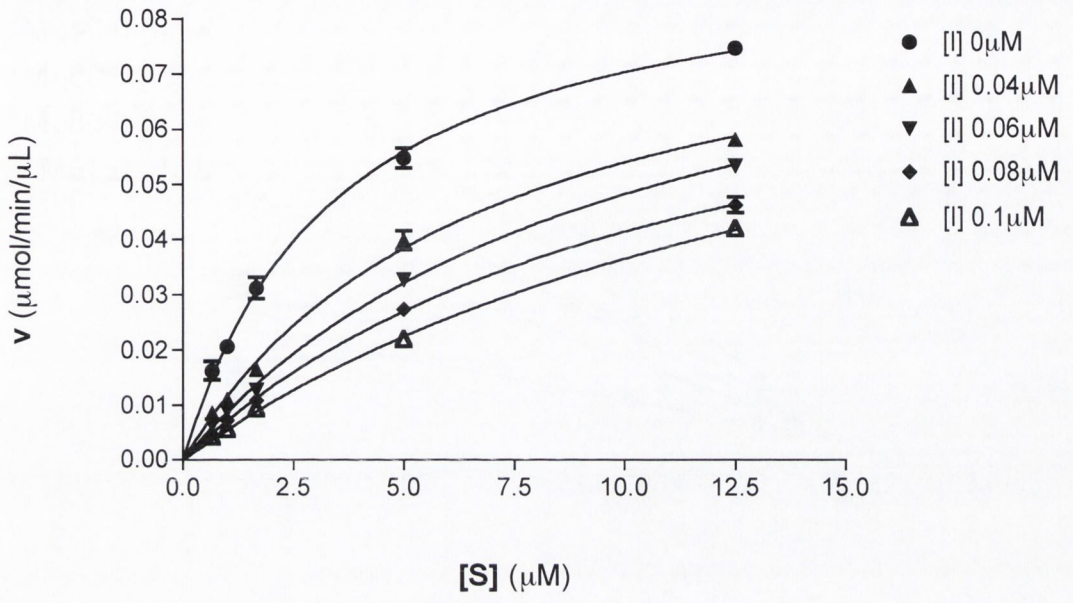

Figure 3.8 Michaelis–Menten plot in the presence of the novel inhibitor Glp-Asn-Pro-Tyr-Trp-AMC

The initial rate of TRH-DE was measured fluorometricaly at 5 substrate concentrations (0–12.5 μM) in the presence of 4 concentrations of the inhibitor Glp-Asn-Pro-Tyr-Trp-AMC (0.04–0.1 μM). The initial rate (v) versus substrate concentration ([S]) was fitted to a Michaelis–Menten plot using GraphPad Prism (version 4.0c for Mac). Non-linear regression analysis gave a V_{max} of 0.094± 0.002 μM/min (with no significant deviation, P= 0.663, analysed by one-way ANOVA). The goodness of fit of the non-linear regression is >0.99 at all inhibitor concentrations. Apparent K_m values ($K_{m\ app}$) were calculated at each of the inhibitor concentrations from non-linear regression fit and these were used to determine the inhibition constant (K_i) for Glp-Asn-Pro-Tyr-Trp-AMC using the equation $[I]/((K_{m\ app}/K_m)-1)$. The K_i calculated for Glp-Asn-Pro-Tyr-Trp-AMC is 0.038±0.007 μM.

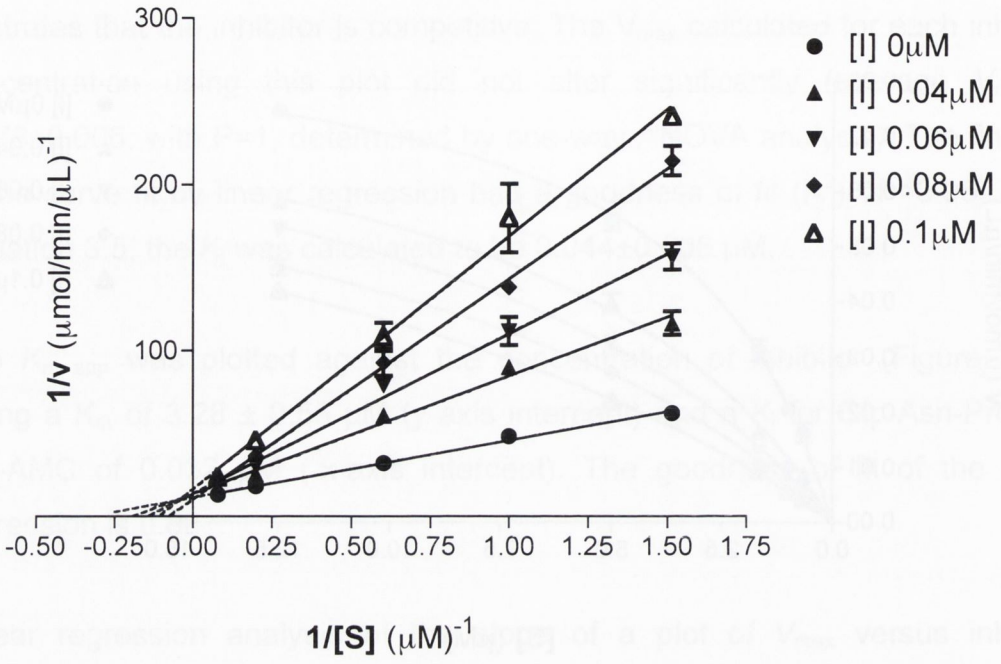

Figure 3.9 Lineweaver–Burk plot in the presence of the novel inhibitor Glp-Asn-Pro-Tyr-Trp-AMC

The double reciprocal values of substrate concentration and initial rates were fitted to a plot using GraphPad Prism. Linear regression analysis illustrates that the inhibitor is competitive. The average V_{max} is 0.078±0.006, calculated from the reciprocal of the intercept of the y-axis. There is no significant difference in this value for each inhibitor concentration (P=1, determined by one-way ANOVA analysis). The goodness of fit (R^2) of the linear regression is >0.96. The inhibition constant, K_i, was then calculated using the K_m (3.03 μM) and the apparent K_m ($K_{m\ app}$) for each inhibitor concentration (reciprocal of intercept with the x-axis) using the equation [I] / (($K_{m\ app}$/K_m) - 1). The K_i calculated for Glp-Asn-Pro-Tyr-Trp-AMC is 0.04 ±0.01 μM.

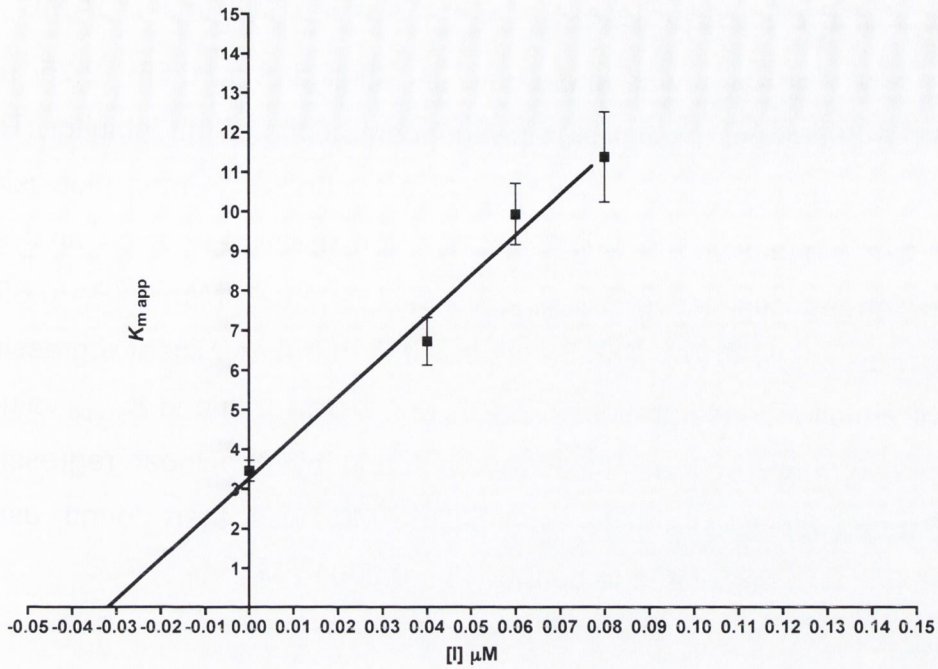

Figure 3.10 Plot of apparent K_m against the inhibitor concentration

The $K_{m\ app}$ determined from non-linear regression fit in the Michaelis–Menten plot is plotted against the concentrations of inhibitor ([I]). Linear regression analysis reveals a K_m value of 3.3 µM (intercept of the y-axis) and the intercept with the x-axis gives the $-K_i$ value, which is 0.032 µM, the goodness of fit is 0.97.

3.3.5.2 Kinetic parameters of Glp-Asn-Pro-Tyr-Trp-TrpAMC

The rate of AMC release was measured in duplicate at 0.66–12.25 μM substrate in the presence of 0.01–0.04 μM concentrations of the inhibitor. The initial rate at each concentration was fitted to a Michaelis–Menten plot using GraphPad Prism (version 4.0c) (Figure 3.11). Non-linear regression analysis was then performed calculating the V_{max} as 0.111±0.002 μM/min (P= 0.856, analysed by one-way ANOVA). The goodness of fit of the non-linear regression is >0.98 at all inhibitor concentrations. The K_m (3.16±0.14 μM) and $K_{m\ app}$ values for each concentration of the inhibitor were found by non-linear regression analysis. The K_i for Glp-Asn-Pro-Tyr-Trp-Trp-AMC was then found using Equation 3.5 and was calculated to be 0.0013 ± 0.0001 μM.

The double reciprocal values of substrate and initial rates were used to create a Lineweaver-Burk plot (Figure 3.15). Linear regression analysis used to fit data illustrates that the inhibitor is competitive. The V_{max} determined for each inhibitor concentration using this plot (the reciprocal of the intercept with y-axis) does not alter significantly (average V_{max} is 0.101±0.007, with P= 0.947 determined by one-way ANOVA analysis). The linearity of the curve fit by linear regression has a goodness of fit of >0.97. The inhibition constant, K_i, was then found using the K_m determined from the reciprocal of the intercept with the x-axis when no inhibitor was present and the $K_{m\ app}$ for each inhibitor concentration using Equation 3.5. The K_i for Glp-Asn-Pro-Tyr-Trp-Trp-AMC determined using this plot is 0.0016± 0.0009 μM.

The $K_{m\ app}$ was plotted against the concentration of inhibitor (Figure 3.15), giving a K_m of 2.99 ± 0.18 μM and a K_i for Glp-Asn-Pro-Tyr-Trp-Trp-AMC of 0.0012 μM and the goodness of fit of the linear regression is 0.99.

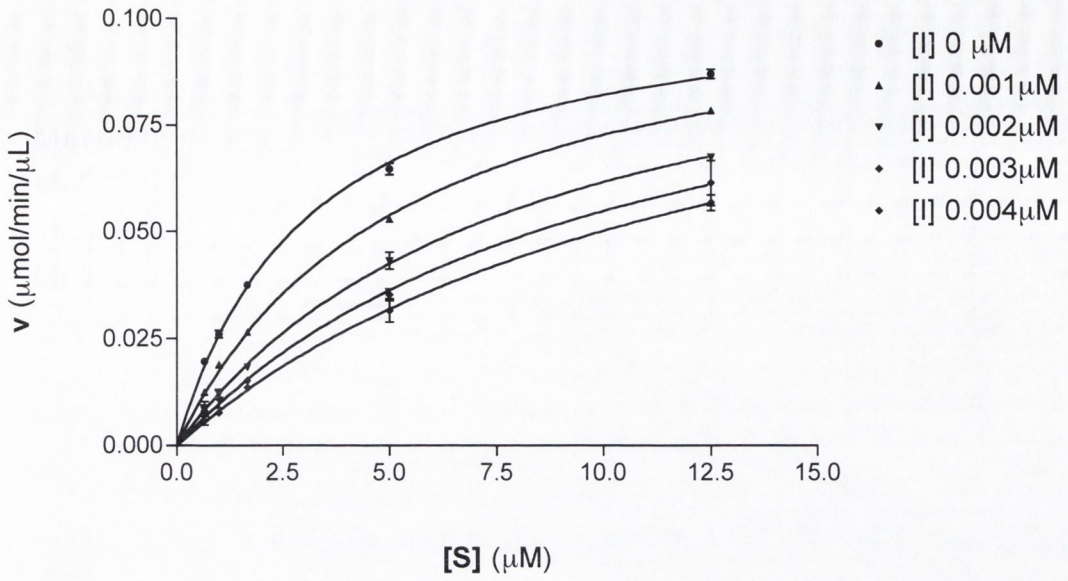

Figure 3.11 Michaelis–Menten plot in the presence of the novel inhibitor Glp-Asn-Pro-Tyr-Trp-Trp-AMC

The initial rate of TRH-DE was measured fluorometricaly at 5 substrate concentrations (0–12.5 μM) in the presence of 4 concentrations of the inhibitor Glp-Asn-Pro-Tyr-Trp-Trp-AMC (0.001–0.004 μM). The initial rate (v) versus substrate concentration ([S]) was fitted to a Michaelis–Menten plot using GraphPad Prism (version 4.0c for Mac). Non-linear regression analysis gave a V_{max} of 0.111±0.002 μM/min (with no significant deviation, P= 0.856, analysed by one-way ANOVA). The goodness of fit of the non-linear regression is >0.98 at all inhibitor concentrations. Apparent K_m values ($K_{m\ app}$) were calculated at each of the inhibitor concentrations from non-linear regression fit and these were used to determine the inhibition constant (K_i) for Glp-Asn-Pro-Tyr-Trp-Trp-AMC using the equation $[I]/((K_{m\ app}/K_m)-1)$. The K_i calculated for Glp-Asn-Pro-Tyr-Trp-Trp-AMC is 0.0013±0.0001 μM.

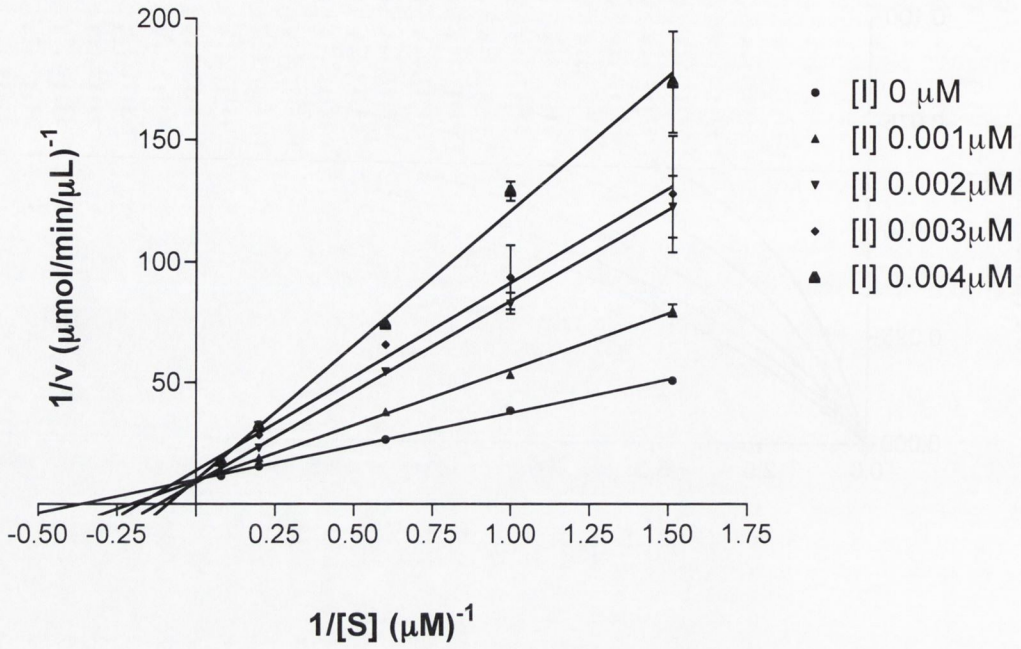

Figure 3.12 Lineweaver–Burk plot in the presence of the novel inhibitor Glp-Asn-Pro-Tyr-Trp-Trp-AMC

The double reciprocal values of substrate concentration and initial rates in the presence of increasing concentrations of Glp-Asn-Pro-Tyr-Trp-Trp-AMC were fitted to a plot using GraphPad Prism. Linear regression analysis illustrates that the inhibitor is competitive. The average V_{max} is 0.100±0.007, calculated from the reciprocal of the intercept of the y-axis. There is no significant difference in this value for each inhibitor concentration (P=0.95, determined by one-way ANOVA analysis). The goodness of fit (R^2) of the linear regression is >0.96. The inhibition constant, K_i, was then calculated using the K_m (2.79 µM) and the apparent K_m ($K_{m\ app}$) for each inhibitor concentration (reciprocal of intercept with the x-axis) using the equation [I] / (($K_{m\ app}/K_m$) - 1). The K_i calculated for Glp-Asn-Pro-Tyr-Trp-Trp-AMC is 0.0016±0.0009 µM.

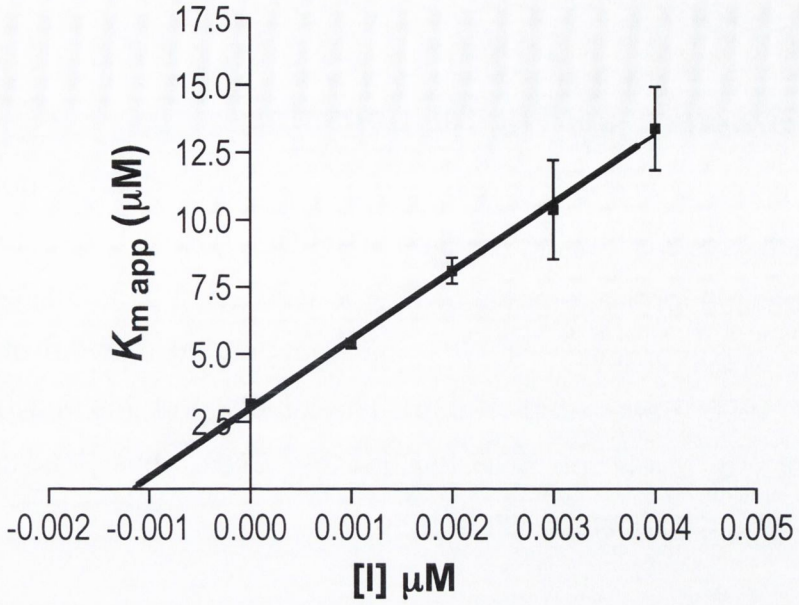

Figure 3.13 Plot of apparent K_m against the inhibitor concentration.

The $K_{m\ app}$ determined from non-linear regression fit in the Michaelis–Menten plot is plotted against the concentrations of inhibitor ([I] μM). Linear regression analysis reveals a K_m value of 2.99±0.181 μM (intercept of the y-axis) and the intercept with the x-axis gives the $-K_i$ value for Glp-Asn-Pro-Tyr-Trp-Trp-AMC, which is 0.0012 μM, the goodness of fit is 0.99.

3.4 Discussion

3.4.1 Structure–activity relationships

In the experiments described herein, the kinetic properties of novel TRH-analogues were assayed using purified TRH-DE. TRH-DE is the enzyme primarily responsible for the removal of TRH *in vivo* as it has an extremely high specificity for the conformation of TRH and is mainly an enzyme of the CNS (O'Cuinn et al. 1990; Bauer et al. 1997b). The inhibition of this enzyme should lead to increased levels of TRH within the CNS, thus leading to the neuroprotective effects described in Chapter 1.

These experiments examined the potency of inhibition afforded by compounds structurally designed on basis of the previous identification of two lead structures in TRH-DE inhibition, in which histidine residue of TRH was substituted with asparagine, Glp-Asn-ProNH_2 and Glp-Asn-ProAMC (Kelly et al. 2002). Replacement of histidine with asparagine was found to prevent the Glp-Xaa bond from being hydrolysed (Kelly et al. 2002). Unfortunately, the quantities of several of the custom-synthesised peptides used in this work were too small to allow detailed analysis of their behaviour as inhibitors, or substrates. In those cases the K_i values can only be regarded as being approximate.

3.4.2 Effects of modifications to the Asn side-chain

The involvement of the Asn side-chain amide group in TRH-DE inhibition was explored further by modifications of the asparagine residue by addition of a benzyl or phenyl moiety to create Glp-Asn(*N*-Benzyl)-ProNH_2 and Glp-Asn(*N*-Phenyl)-ProNH_2, respectively. Addition of the benzyl group resulted in a peptide that was degraded by TRH-DE, as shown by HPLC analysis. The inhibition potency was found to be poorer than that of Glp-Asn-ProNH_2 by a factor of approximately 5. This suggested that the Asn group might provide a key interaction with TRH-DE, essential in forming a stable enzyme–ligand complex. Glp-Asn-(*N*-Phenyl)-ProNH_2 was found to resist hydrolysis by TRH-DE, though

it was revealed to be a poor inhibitor, with a K_i of >200 μM. This gives further indication that the amide of asparagine is key to the enzyme interaction and that modifications of the peptide's structure can lead to major changes in potency. Such information may then feed back into the design process for further rational design of inhibitor compounds.

3.4.3 The effects of replacing or modifying the proline residue

Replacement of proline at the *C*-terminus with amidated alanine, another neutral and hydrophobic amino acid, was found to increase the K_i to >200 μM, indicating that the *C*-terminal proline residue provides an important interaction with the enzyme at this position, perhaps as a result of the unique conformation that it confers.

The substitution of proline with homoproline resulted in a peptide that resisted enzyme hydrolysis and had a K_i (19 μM) that was similar to that determined for Glp-Asn-ProNH_2, demonstrating that this substitution still confers the necessary interactions with TRH-DE for inhibition. Proline was coupled to benzyl alcohol and methyl alcohol to gain further insight into ligand–enzyme interactions. Both Glp-Ans-ProOBzl and Glp-Asn-ProOMe resisted hydrolysis by TRH-DE. The inhibitor constants were found to be 15 and 74.25 μM for Glp-Ans-ProOBzl and Glp-Asn-ProOMe, respectively. The tolerance of TRH-DE to the benzylation of proline suggests that aromatic interactions may be important for binding between this region of the inhibitor and the active site of the enzyme.

3.4.4 Carboxy terminus extension

The most substantial improvement in inhibition resulted from extension of the peptide at the carboxy terminus. The best inhibition that had been previously achieved was when an AMC functional group is attached to the proline, Glp-Asn-ProAMC has a K_i of 0.5 μM (Kelly et al. 2000). Extension of this lead structure to include the residues tyrosine and tryptophan with a terminal amide

group to give of Glp-Asn-Pro-Tyr-TrpNH_2 and Glp-Asn-Pro-Tyr-Trp-TrpNH_2 resulted in peptides that were found to resist hydrolysis by TRH-DE and to inhibit the enzyme potently, an improvement in inhibition over Glp-Asn-ProNH_2 by factors of 28 and 24 fold, respectively. Attachment of an AMC functional group to the *C*-terminus, to give Glp-Asn-Pro-Tyr-Trp-TrpAMC, yielded a compound with the most potent inhibition achieved thus far (Kelly et al. 2005). This peptide resisted hydrolysis by TRH-DE and was shown to be a competitive inhibitor (Fig. 3.14) with a K_i value of 1 nM. This indicates the tolerance of TRH-DE to the C-terminal extension of Glp-Asn-ProNH_2, suggesting a possible hydrophobic pocket at the active-site, to which the *C*-terminus of the inhibitors interacts. Further information of possible enzyme–substrate interactions was gained by replacing the AMC group of Glp-Asn-Pro-Tyr-Trp-Trp-AMC with 3,5-dimethoxyaniline. Analysis of this compound by HPLC revealed two separate resolved peaks, consistent with the presence of two isosteres (labelled (a) and (b) in Table 3.), although this has not yet been confirmed by mass spectrometry. Both compounds were found to resist hydrolysis by TRH-DE, but were poorer inhibitors than Glp-Asn-Pro-Tyr-Trp-Trp-AMC. This might indicate possible hydrogen bonding between inhibitor and residues of the active site to be important. Some of these interactions may be absent with the OMe groups of 3,5-dimethoxyaniline, resulting in the reduction of inhibitory potency.

In summary, the design of novel potential inhibitors of TRH-DE is an iterative process, with substitutions and replacements performed on the natural substrate, TRH. With each modification made, new information for further inhibitor design is provided. Modifications to and substitutions of the asparagine residue and replacement of and substitution on the proline were examined, in addition to extension of the carboxy terminus of inhibitor compounds. The properties of these substrate analogues leads to a better understanding of the active site area of TRH-DE and the interactions required to cause effective inhibition. The substantial improvement of inhibitory potency found with some of the compounds studied could provide lead compounds for therapeutic drug development (Kelly et al. 2005).

CHAPTER 4

ASSESSMENT OF NEUROTOXICITY AND NEUROPROTECTION USING *IN VITRO* MODELS

4.1 Introduction

Thyrotropin releasing hormone (TRH), which is found in the CNS, is believed to be a protective agent against toxic insult. The protective function of TRH was investigated using the neurotoxin kainate.

In vitro systems may be used to enable measurement of events that occur within cells, in order to investigate the mechanisms involved in neurotoxicity and neuronal protection. Brain slices are widely used as model systems for the study of neuronal function. In the case of the slice-superfusion system it is possible to study neurodegenerative processes over a relatively short period of time, in a preparation where glial–neuronal interactions remain intact (O'Byrne et al. 1997).

The hippocampal slice has frequently been used as a model of brain damage (Clark and Rothman 1987; Rothman et al. 1987; Feig and Lipton 1990; McBean 1990; Raley and Lipton 1990; Vornov and Coyle 1991), since it combines the advantages of an *in vitro* method with the presence of well-characterised synaptic connections. However, there are drawbacks in that these models cannot be fully correlated with *in vivo* tests (O'Byrne et al. 1997). Slices are exposed to mechanical shear trauma, vascular and related hormonal regulatory effects are lost and cellular metabolism may be altered due to the artificial conditions used. Furthermore, slices remain viable for only a relatively short period of time. Despite these disadvantages, respiring slices of rat brain have the advantage of offering mechanical stability, the extracellular medium can be controlled, as can the administration of treatments, and studies using slices require a much shorter time scale than many *in vivo* studies.

Several studies have been carried out (Jaworska-Feil et al. 2001; Faden et al. 2003; Prokai-Tatrai et al. 2003; Nie et al. 2005; Veronesi et al. 2007a) to assess the effects of TRH and its various analogues as a neuroprotective agents and this chapter describes further investigations of the effects that TRH exerts in response to a stressed environment.

As discussed in Section 1.9, excitotoxicity has been implicated in many disease states. A well-established model is to apply glutamate or one of its receptor agonists *in vitro* to induce excitotoxicicty. In the present studies, the rigid structural analogue of glutamate, kainate, was used as the excitotoxin and the protective capacity of TRH was assessed. Kainate binds to specific presynaptic and postsynaptic kainate-type receptors, which opens membrane channels, causing an influx of Ca^{2+} and Na^{+} ions. This influx of ions results in depolarisation, which, in turn, opens voltage-gated cation channels (Chung and Han 2003a). Neuronal injury results, possibly, from the release of endogenous glutamate and the depletion of neuronal energy reserves in an effort to maintain homeostasis. Damage may also be mediated partly through an indirect mechanism that may involve the overproduction of free radicals, i.e., oxidative stress, resulting in variable levels of neuronal death (Chung and Han 2003a).

In the studies described herein, kainate was administered to hippocampal slices from rat brains, and the protective ability of TRH was investigated, using indicators of cellular damage and by measuring changes in neurotransmitter concentrations.

4.2 Methods

4.2.1 The effects of a range of kainate doses on the lactate dehydrogenase (LDH) content of hippocampal slices

Male Wistar rats (200-250 g) were sacrificed and tissue slices prepared as described previously (Section 2.4). A stock solution of 10 mM kainate was prepared each day. This was diluted to concentrations ranging from 100–500 µM. Following a 30 min preincubation in which slices, incubated in triplicate in the perfusion chamber, were superfused in oxygenated (95% O_2/5% CO_2) Krebs buffer at 1 mL/min, slices were exposed to kainate for a period of 30–60 min. The slices were then returned to normal Krebs buffer for a further 30 min. Control slices were incubated for the full time period in Krebs buffer. Following superfusion, slices were homogenised and diluted 1:10 prior to determination of the protein concentration using the Bio-Rad method (Section 2.3.1). The viability of the slices was determined by assaying for the LDH content using the spectrophotometric method described in Section 2.5.1. The results are expressed as U/mg of protein.

4.2.2 The effect of TRH on viability as determined by LDH activity

Hippocampal slices were incubated in perfusion chambers and were superfused with oxygenated (95% O_2/5% CO_2) Krebs buffer at 1 mL/min for 30 min, followed by superfusion with 300 µM kainate in conjunction with 100 and 300 µM TRH for 60 min. The slices were then given a 30 min recovery period, during which superfusion was continued. Slices were then homogenised and assayed for LDH and protein content. The results were compared to the levels of LDH found in slices that were superfused with the Krebs buffer alone for the duration of the experiment. Experiments were also performed over a shorter duration, in which kainate was administered for 30 min, following an initial 30 min incubation. TRH was administered either in conjunction with kainate or in the 30 min prior to or directly following kainate superfusion.

A variation of this method was also used to determine the level of LDH released from the slices, in which slices were incubated for 30 min in a chamber containing 2 mL of Krebs buffer and maintained at 37°C. In slices undergoing TRH treatment, the Krebs buffer contained 300 µM TRH during this period. A final volume of 300 µM KA was then added to the slices, while control slices were given a sham treatment by addition of buffer. Following this 30 min period, the incubation medium was removed, slice chambers were rinsed and fresh Krebs buffer was added for a final 30 min incubation period. The incubation medium was assayed for LDH activity.

4.2.3 The effect of TRH on kainate induced apoptosis as determined by measurement of caspase activation

Hippocampal slices that underwent treatment with 300 µM kainate for 30–60 min in conjunction with either 100 or 300 µM TRH, in addition to control slices and slices treated with kainate alone, were given a recovery period of 30 min superfusion in Krebs buffer before being homogenised in lysis buffer (see Section 2.5.3.1), sonicated and stored at –80°C. The level of caspase activation was quantified fluorometrically using the method described in Section 2.5.3. Caspase activity was calculated and expressed as nM of 7-amino-4-methyl coumarin (AMC) produced per min per µg of protein contained within the slice.

4.2.4 Effects of TRH on Kainate toxicity: Amino Acid Release

The release of amino acids from the hippocampal slices into the incubation medium following incubation with kainate ± TRH over a 30 min period was determined fluorometrically following reaction with *o*–phthalaldehyde and HPLC, using the method described in Section 2.11. The separated amino acids were detected as they eluted by measuring changes in fluorescence at excitation and emission wavelengths of 340 and 455 nm, respectively, and were identified using the retention times detected for standards (Appendix B,

Figure 1) and quantified using the standard curves generated (Apppendix B, Figure 2), concentrations are expressed as µM/µg protein.

4.2.5 Effects of TRH on Kainate toxicity: Amino Acid Content

The amino acid content of homogenised hippocampal slices following superfusion with kainate ± TRH over a 30 min period was determined fluorometrically following reaction with *o*–phthalaldehyde and HPLC, using the method described in Section 2.7. The separated amino acids were detected as they eluted by fluorescence changes using excitation and emission wavelengths of 340 and 455 nm, respectively and quantified using standard curves (Figure 2.7), concentrations are expressed as µM/µg protein.

4.2.6 Effect of TRH on kainate induced loss of glial-cell viability, as determined by assay of glutamine synthase (GS) activity

Hippocampal slices that underwent perfusion with 300 µM kainate in the presence of either 100 or 300 µM TRH for 30 min, with pre- and post-superfusion periods of 30 min in Krebs buffer, were homogenised in 0.1 M sodium acetate buffer, pH 7.4. Samples were then treated as described in Section 2.2. Glutamine synthase (GS) activity was calculated and expressed as nmol l-glutamic acid γ-mono-hydroxamate (GHA) formed/mg protein/min.

4.2.7 Effect of TRH on kainate toxicity: Catecholamines, their metabolites and 5-hydroxytryptamine

Following the superfusion treatment described above, slices were homogenised using the method described in Section 2.6 and catecholamines and indoleamines were extracted. Concentrations were determined from standard curves and expressed as ng/µg protein.

4.3 Results

4.3.1 The superfusion system: Basal levels

The levels of lactate dehydrogenase (LDH) activity remaining in slices superfused with Krebs buffer for the full incubation time, i.e. 2 h, were compared to those of slices that were assayed directly without a perfusion period. As LDH is released during trauma to the cell, remaining LDH activity is an indication of survival. One unit (U) of enzyme is defined as the amount of enzyme catalysing the formation of 1 µmol of product per minute under standard conditions. Table 4.1 indicates that the loss of LDH over the incubation period was negligible. Slice superfusion did not appear to adversely affect slice viability and as such validates the procedure of the slice superfusion model (Figure 4.1).

Table 4.1 Effects of superfusion on LDH content of hippocampal slices.

Slices that had been homogenised and assayed for LDH activity directly after preparation were compared with slices that had been continuously perfused with Krebs buffer at 37°C for 2 hours and subsequently assayed. An unpaired Student's T-test revealed that there is no significant loss of LDH activity in the incubated slices. Data represent mean values ± S.E.M. (n=5 for each treatment).

Incubation period (min)	U LDH/ mg protein	P Value
0	4.835 ± 0.378	0.39
120	4.291 ± 0.470	

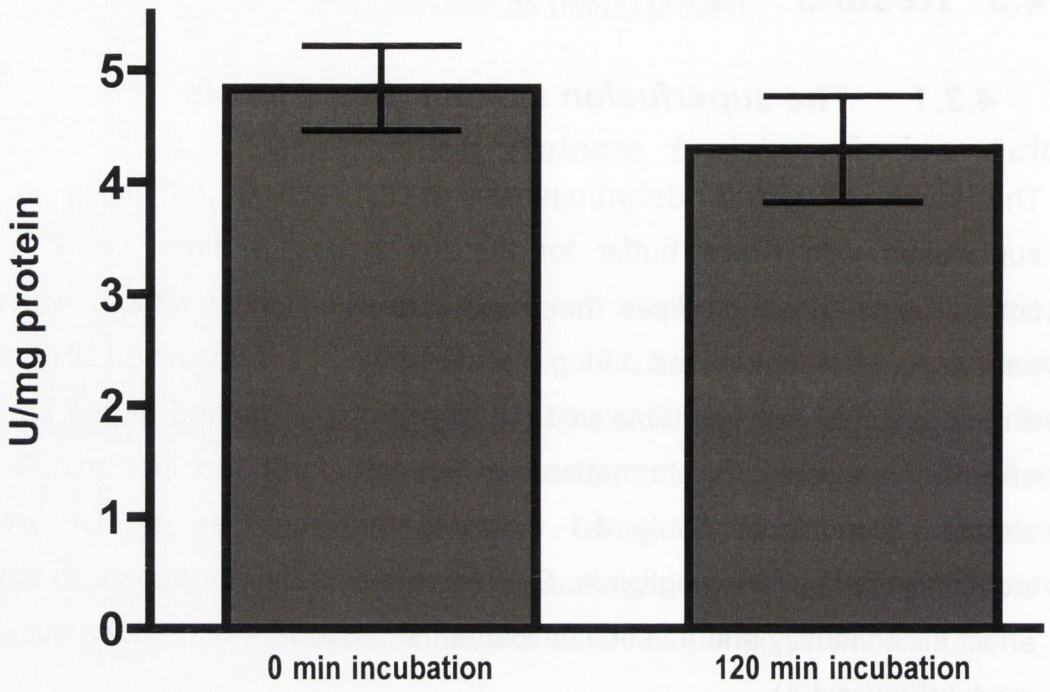

Figure 4.1 Effects of incubation of hippocampal sections on basal LDH activity.

Slices were homogenised directly after preparation and assayed for LDH activity as described in the text. Results were compared with the LDH content of sections that were perfused in oxygenated Krebs buffer for 120 min at 37°C, and subsequently assayed. The incubation period did not result in a significant loss in LDH activity. Data represent mean values ± S.E.M. (n = 5, measured in triplicate).

4.3.2 *The* in vitro *effects of a range of kainate doses on hippocampal slices*

Neurotoxicity induced by a range of kainate doses in the slice system was determined by measuring the content of LDH remaining in the perfused slices. The measurement of LDH activity within the slices is outlined in Table 4.2 and presented in Figure 4.2.

Table 4.2 The effects of a range of kainate doses on viability.

The amount of LDH remaining in slices following incubation with 200, 300 and 500 μM kainate for 60 min was determined by measuring the conversion of NADH to NAD^+ as a function of cell viability. This activity was expressed as a measure of the protein content of each slice and compared to the LDH content of control slices. Data represent mean values ± S.E.M. and were analysed using one-way ANOVA with Bonferroni's multiple comparison post-test (n=6 for each treatment). *= P value compared with control slices.

Treatment	U LDH/mg protein	Mean Diff.	P value*
Control	4.55 ± 0.56	-	-
200 μM kainate	2.78 ± 0.81	1.77	< 0.05
300 μM kainate	0.70 ± 0.19	3.85	< 0.001
500 μM kainate	0.29 ± 0.03	4.26	< 0.001

A 60 min incubation in kainate followed by a 30 min recovery period revealed that all doses resulted in a loss of slice viability. In slices treated with 200 μM kainate there is a reduction in the amount of LDH remaining to 61% of the amount present in control, untreated, slices ($P<0.05$, by one-way ANOVA with Bonferroni's post-test). This level of LDH activity was further reduced using 300 and 500 μM kainate, where the units of LDH activity were significantly lower than those found in control slices ($P<0.001$). Treatment with 300 μM kainate reduced the level of LDH to 15% of that found in control slices, and 500 μM reduced LDH content further to 6.3% of control levels. The difference between the LDH contents following treatment with either 300 or 500 μM kainate was not

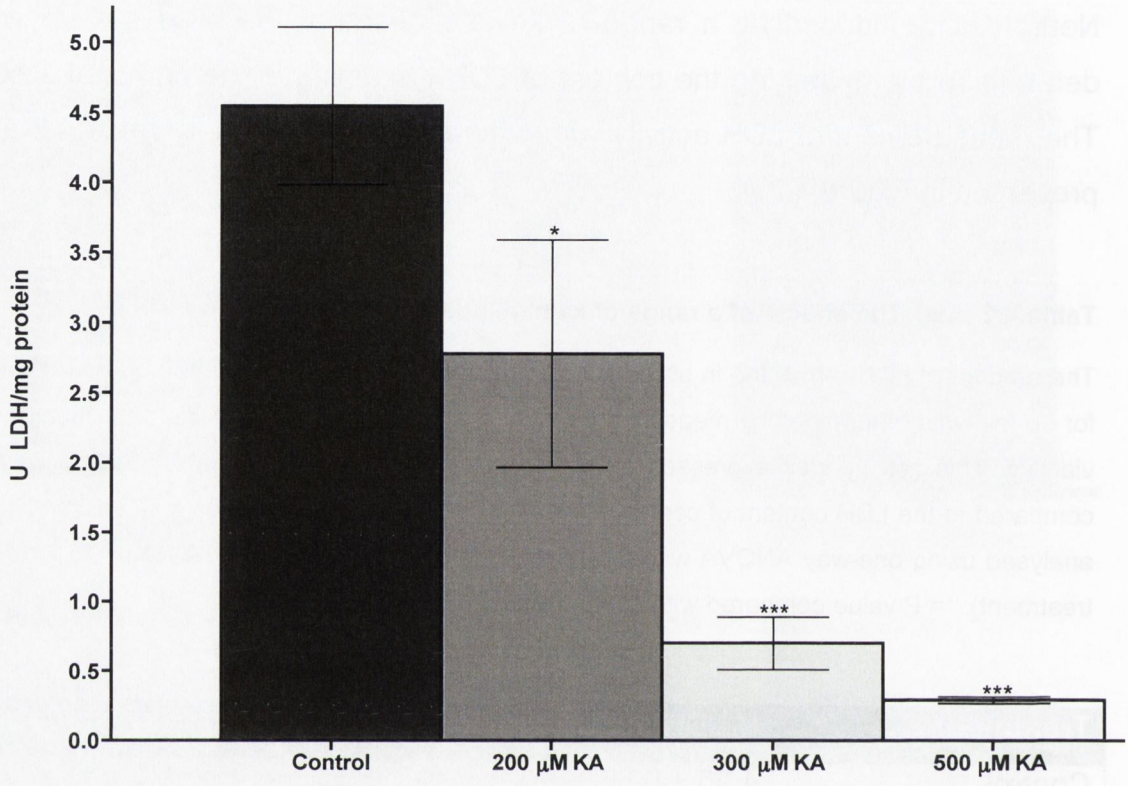

Figure 4.2 The effect of increasing concentrations of kainate on the LDH content of hippocampal slices.

Hippocampal slices were continuously superfused with Krebs buffer. Following a 30 min recovery period, 200–500 μM kainate in Krebs buffer was perfused onto the slices for 60 min. The slices were then washed and perfused with Krebs buffer for a further 30 min to allow damaged cells to die, and were then homogenized and assayed for LDH activity. Data represent mean values ± S.E.M. and were analysed by GraphPad Prism using one-way ANOVA with Bonferroni's multiple comparison test (n=6 for each treatment, measured in triplicate). *=$P<0.05$ and ***=$P<0.001$, calculated in comparison to control slices.

significant (P>0.05). Thus a dosage of 300 μM kainate is effective in inducing cell damage and cytotoxicity and this was used in further experiments.

4.3.3 The effect of TRH on viability, as determined by assay of lactate dehydrogenase activity

The release of LDH from hippocampal slices into the incubating medium in the incubation rig, described in Section 4.2.2, is depicted in Figure 4.3. This demonstrated that a basic level of cytotoxicity was occurring in untreated control slices incubated in Krebs buffer, with 0.04±0.003 U/mL of LDH released from the slices. However, slices incubated in 300 μM kainate released 92% more LDH than control slices (P<0.01, one-way ANOVA with Bonferroni's multiple comparison post-test). The co-incubation of 300 μM TRH with 300 μM kainate resulted in a significant reduction of LDH leakage into the medium in comparison to kainate-incubated slices, and loss of LDH was not significantly different from that occurring in control slices incubated in Krebs buffer only.

The effect on hippocampal slices of superfusing TRH with 300 μM kainate for 60 min was measured by assaying the LDH content of the slices. Analysis of the results was performed by one-way ANOVA with Bonferroni's multiple comparison post-test, using GraphPad Prism. The LDH content is depicted in Figure 4.4. Treatment with 100 μM TRH whilst slices were superfused with 300 μM kainate significantly reduced the leakage of LDH from hippocampal slices, in comparison to kainate treated slices (P<0.01), but did not fully attenuate kainate cytotoxicity, as the LDH content was significantly less than that of control, Krebs perfused slices (P<0.01). When 300 μM TRH was co-administered with kainate, the activity levels of LDH contained within the slices returned to the same levels found in control slices, with no significant difference between them. The effect of TRH was further investigated by superfusion of the slices with 300 μM TRH in the absence of kainate. Comparison with control slices again revealed an LDH content that was not significantly different from values obtained for control slices or from those treated with kainate plus 300 μM TRH.

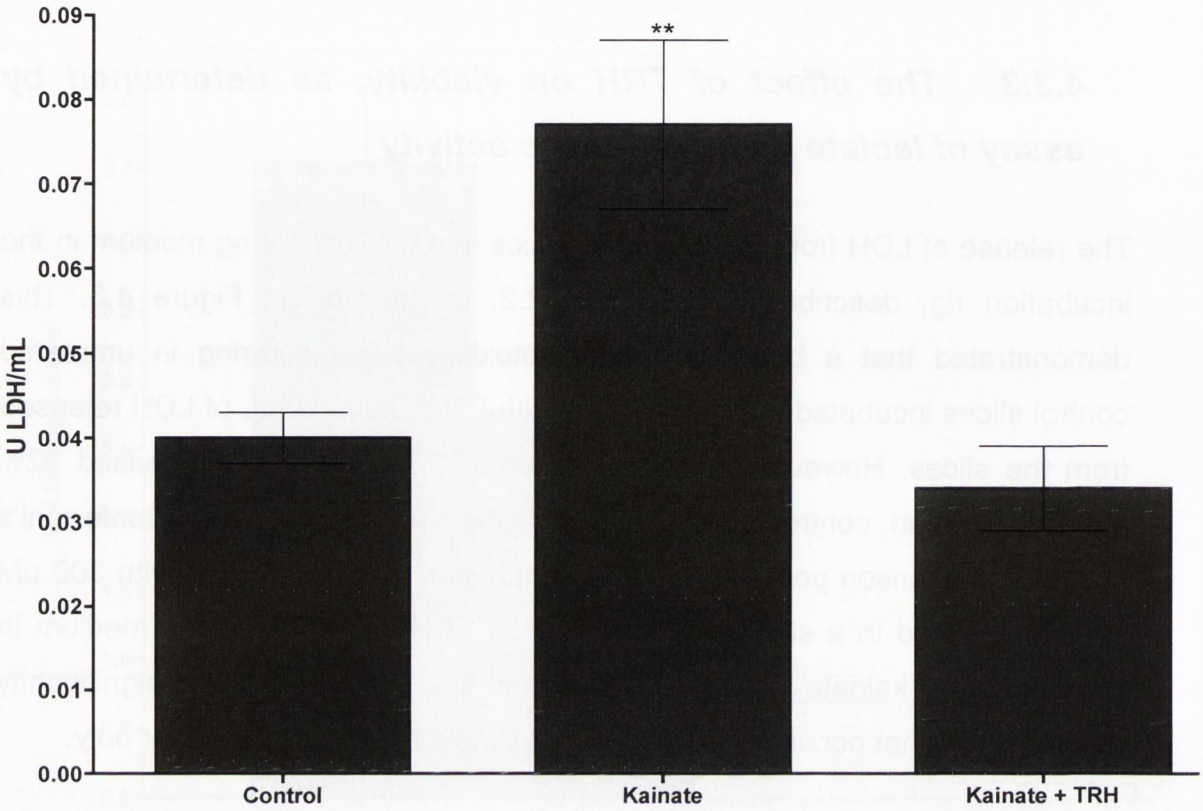

Figure 4.3 The effect of TRH on the release of LDH from hippocampal slices into the incubation medium.

Lactate dehydrogenase release from hippocampal slices incubated in 300 µM KA ± 300 µM TRH for 30 min, with 30 min pre- and post-incubation in Krebs buffer, was measured as a function of cellular integrity. Data represent the mean values (n=6, measured in triplicate) ± S.E.M. Analysis of the results was performed by one-way ANOVA with Bonferroni's post-test with **P<0.01 in comparison to control or TRH-treated slices.

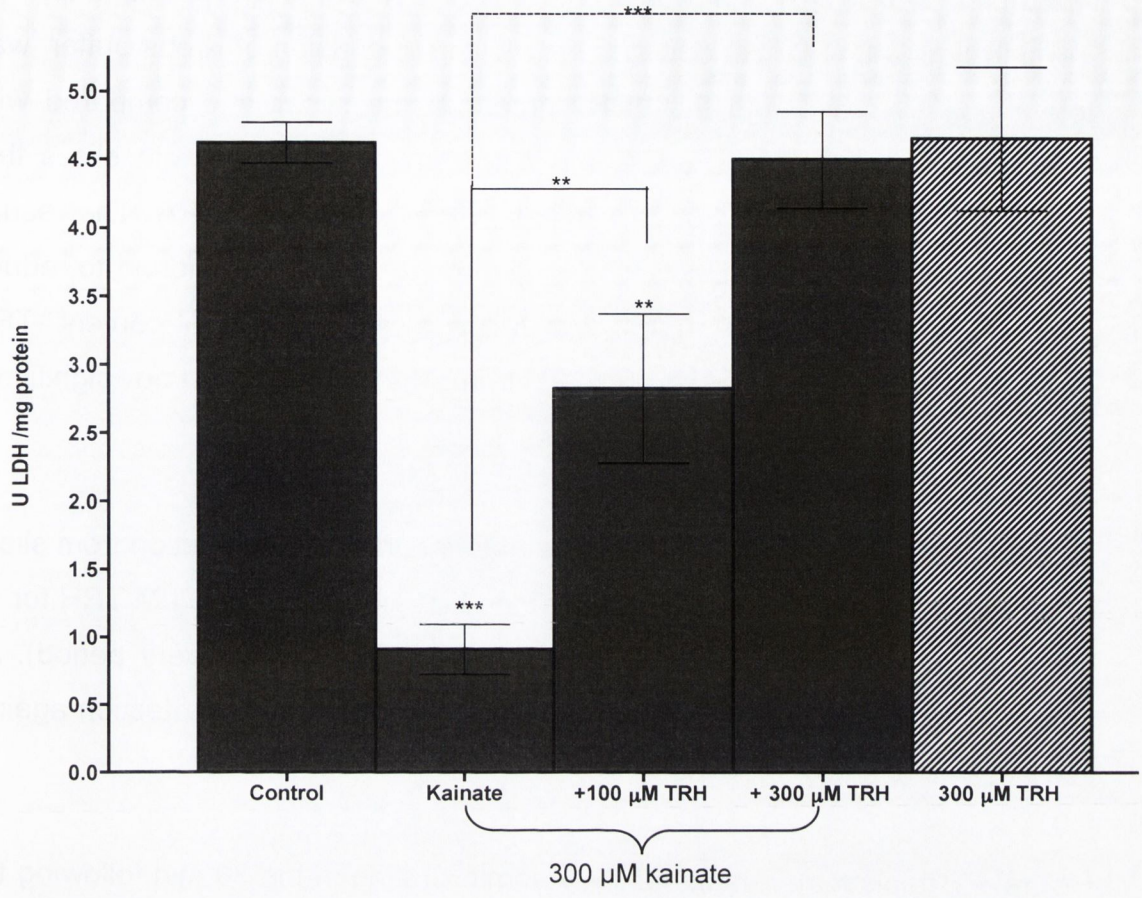

Figure 4.4 The effect of TRH on the kainate induced loss of LDH from hippocampal slices.

The LDH content of hippocampal slices was measured following superfusion of slices with 300 µM kainate for 60 min, with 30 min pre- and post-superfusion in Krebs. The effect of co-incubation of kainate with 100 and 300 µM TRH was measured spectrophotometrically and normalised using the protein content of the slice. The effect of 300 µM TRH on slices in the absence of kainate was also measured (▨). Analysis of the results was performed by one-way ANOVA analysis with Bonferroni's post-test, with *** $P<0.001$ and **$P<0.01$ in comparison to controls or, where indicated, to kainate-treated slices. Data represent mean values± S.E.M., with n values ranging from 3–6 and all values measured in triplicate.

The effect of a 30 min superfusion of 300 μM TRH with 300 μM kainate, with pre- and post-recovery periods of 30 min with superfusion of Krebs buffer, was determined by measuring the LDH content of the slices and compared with slices superfused in Krebs buffer for the entire duration and with slices that underwent treatment with 300 μM kainate in the absence of TRH. The results are shown in Figure 4.5. Incubation of kainate for 30 min was found to reduce LDH levels significantly ($P<0.05$), with levels at 41% of control content. TRH prevented kainate-induced loss LDH from the slices, with no significant difference in comparison to control slices.

The effect of TRH protection against kainate-induced LDH depletion from slices was compared to the values found in slices that were given 300 μM TRH for 30 min prior to superfusion with 300 μM kainate (the initial recovery period). As shown in Figure 4.6, pre-treatment with TRH also resulted in protection against LDH loss induced by kainate.

Figure 4.7 depicts the results of TRH administration in the 30 min following the 30 min superfusion with kainate (the final recovery period). There was a significantly greater LDH loss from slices, in comparison to controls ($P<0.01$), than the other treatment schedules, although there was still significant protection against kainate toxicity ($P<0.01$).

The effects of co-, pre-and post-superfusion of TRH with kainate were compared in Figure 4.8. The data were analysed by Bonferroni's post-test, which demonstrated that TRH affords the same level of protection when given prior to or in conjunction with kainate treatment ($P>0.05$). Incubation of slices with TRH in the 30 min period following kainate administration resulted in significantly less protection against LDH release ($P<0.05$).

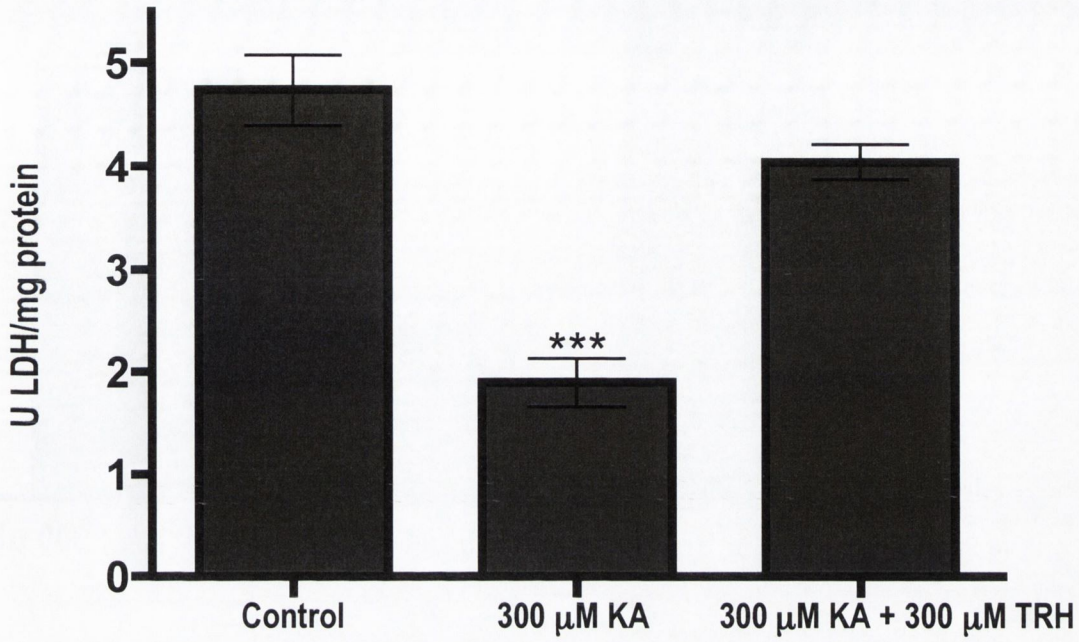

Figure 4.5 The effect of TRH on the kainate induced loss of LDH from hippocampal slices over 30 minutes.

The LDH content of hippocampal slices was measured following superfusion of slices with 300 μM kainate for 30 min, with 30 min pre- and post-superfusion in Krebs buffer. The effect of co-incubation of kainate with 300 μM TRH was measured spectrophotometrically and normalised using the protein content of the slice. Comparison of the results was performed by one-way ANOVA analysis with Bonferroni's post-test, with *** =$P<0.001$ when compared with control and TRH treated slices. Data represent mean values ± S.E.M. (n=6, measured in triplicate).

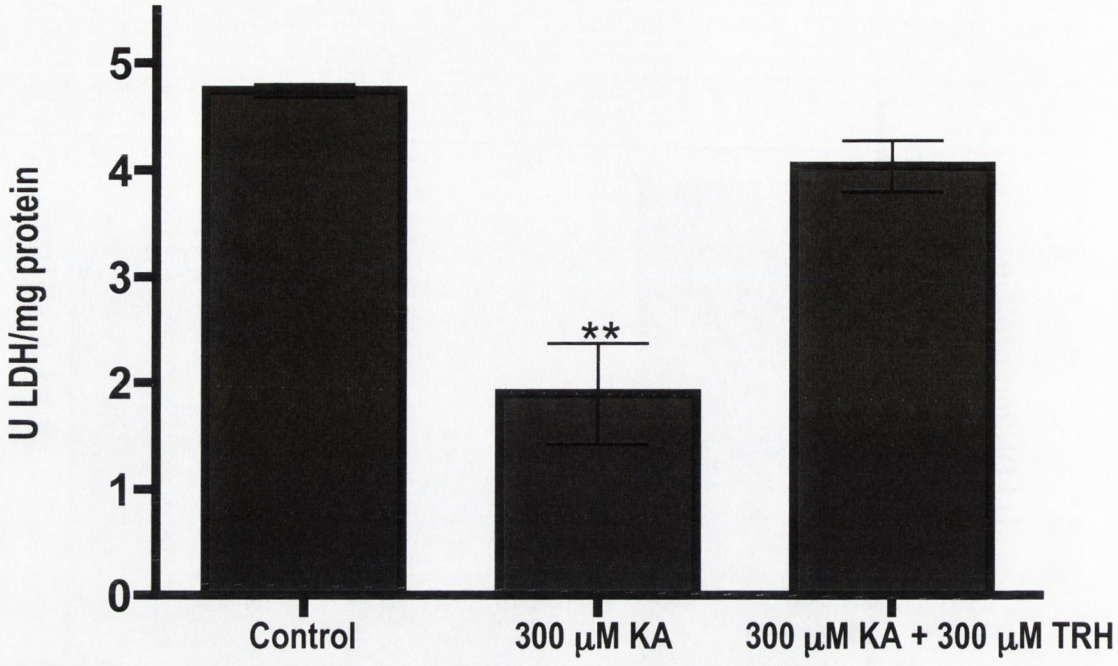

Figure 4.6 The effect of pre-perfusion with TRH on the kainate induced loss of LDH from hippocampal slices.

The LDH content of hippocampal slices was measured spectrophotometrically and normalised using the protein content of the slice. Slices undergoing TRH treatment were superfused with 300 μM TRH for 30 min, followed by superfusion with 300 μM kainate for 30 min, followed by 30 min post-superfusion in Krebs buffer. Control slices were superfused with Krebs buffer for 90 min and slices that underwent kainate treatment were superfused with Krebs buffer for 30 min, 300 μM kainate for 30 min and Krebs buffer for the final 30 min. Comparison of the results was performed by one-way ANOVA analysis with Bonferroni's post-test, with **=$P<0.01$ when compared to control and TRH-treated slices. Data represent mean values ± S.E.M. (n=6, measured in triplicate).

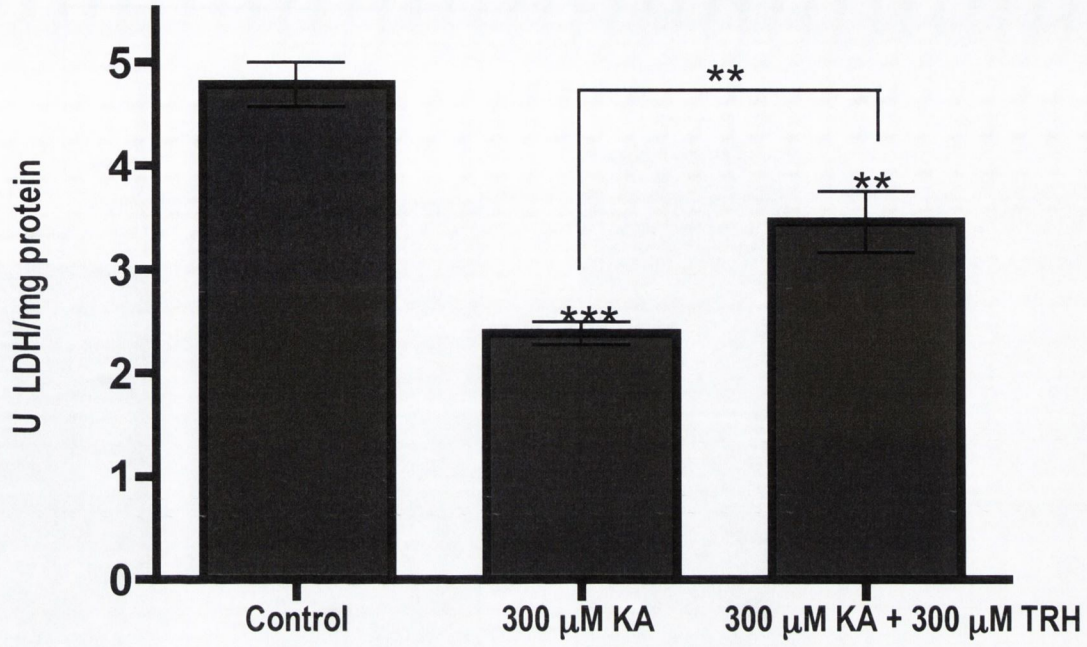

Figure 4.7 The effect of post-perfusion with TRH on the kainate-induced loss of LDH from hippocampal slices.

The LDH content of hippocampal slices was measured spectrophotometrically and normalised using the protein content of the slice. Slices undergoing TRH treatment were superfused with Krebs buffer for 30 min, 300 μM kainate for 30 min and 300 μM TRH for the final 30 min. Control slices were superfused with Krebs buffer for 90 min and slices that underwent kainate treatment were superfused with Krebs buffer for 30 min, 300 μM kainate for 30 min and Krebs buffer for the final 30 min. Comparison of the results was performed by one-way ANOVA analysis with Bonferroni's post-test, with *** =$P<0.001$ and **$P<0.01$ in comparison to control slices or, where indicated, to kainate-treated slices. Data represent mean values ± S.E.M. (n=6, measured in triplicate).

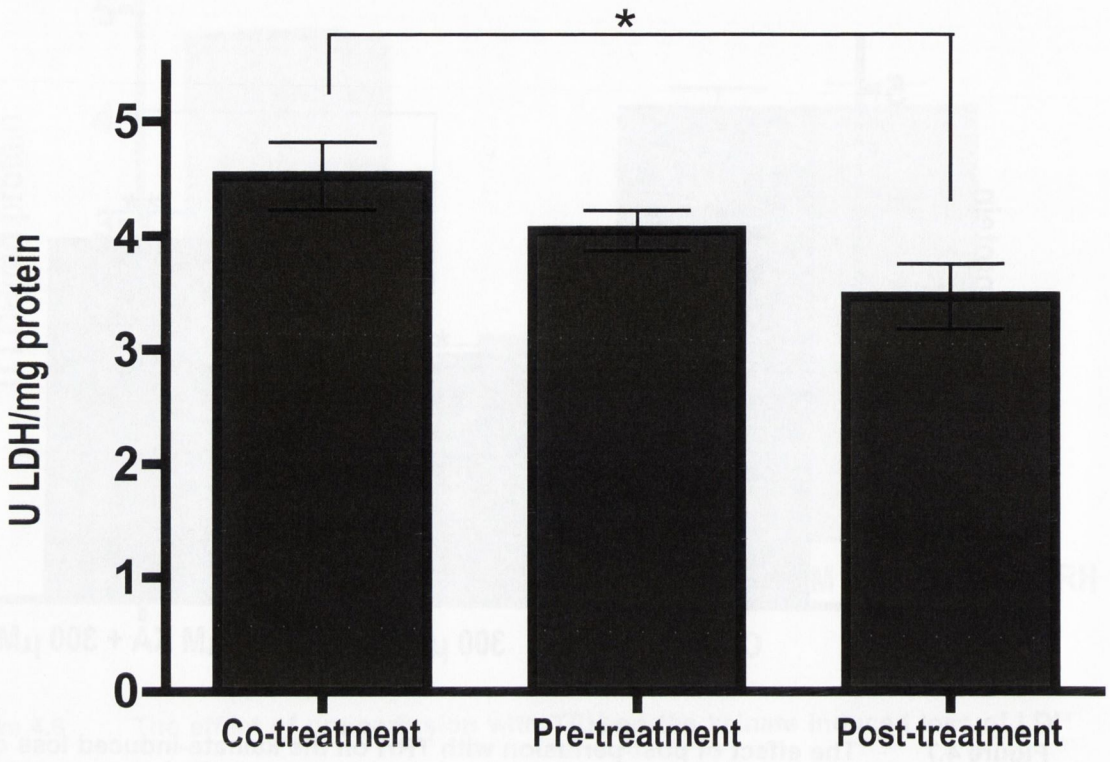

Figure 4.8 Comparison of pre-, post- and co-treatment of TRH with the administration of kainate

The effects of time of administration of TRH on kainate-induced loss of LDH from hippocampal slices (Figures 4.5–4.7) were compared by the by one-way ANOVA with Bonferroni's post-test, with *=P<0.05. Data represent mean values (n=6) ± S.E.M.

Table 4.3 The effect of TRH on the loss of LDH activity in hippocampal slices due to kainate.

Kainate induced loss of LDH from hippocampal slices was measured using two incubation processes by coupling the conversion of NADH to NAD^+ with the enzymatic conversion of pyruvate to lactate. Analysis was performed by one-way ANOVA with Bonferroni's post-test using GraphPad Prism. Data represents mean values ± S.E.M. In (a) slices were incubated in a static, continuously oxygenated medium containing 300 µM kainate alone or kainate with 300 µM TRH for 30 min. All treatments underwent a 30 min recovery period prior to and following treatment. The leakage of LDH from cytotoxic cells was compared with control slices incubated in Krebs buffer for the duration of the experiment and are expressed as U/mL. In (b) following an initial 30 min recovery, slices were superfused with the treatments outlined for 60 min, given a 30 min recovery period and then homogenised and assayed for LDH content. Results are expressed as units of enzyme per mg of protein.

(a)

Treatment	LDH release U/mL	% Change	P value
Control	0.040 ± 0.003	–	–
300 µM KA	0.077 ± 0.010	+ 92%	<0.01
300 µM KA + 300 µM TRH	0.034 ± 0.005	−15%	>0.05

(b)

Treatment	LDH content U/mg protein	% Change	P value
Control	4.621 ± 0.15	–	–
300 µM TRH	4.653 ± 0.529	+ 0.7%	>0.05
300 µM KA	0.911 ± 0.182	− 80%	<0.001
300 µM KA + 100 µM TRH	2.826 ± 0.547	− 39%	<0.05
300 µM KA + 300 µM TRH	4.498 ± 0.355	− 2.7%	>0.05

4.3.4 The effect of kainate on apoptosis as determined by measurement of caspase activation

The induction of apoptosis in the slices following kainate treatment was measured by the level of caspase activity in slices homogenised following perfusion treatment. The results were determined fluorometrically by measuring the release of AMC from the caspase substrate (as described in Section 2.5.3, with AMC standard curve shown in Figure 2.3), and were normalised to the protein content of each slice. The rate of caspase activity found in each slice are presented in Table 4.6 and are depicted in Figure 4.9.

A basal level of caspase activity, of 79.26±3.6 nM/min/µg protein, was found in untreated control slices. This caspase activity was increased by ~18% by superfusion with 300 µM kainate for 30 min, although one-way ANOVA with Bonferroni's post-test revealed this difference was not significant. However, caspase activity was significantly increased by treatment with 300 µM kainate for 60 min, to an activity that was almost double that found in the control slices ($P<0.001$).

4.3.5 The effect of TRH on kainate induced apoptosis

The increase in caspase activity induced by 300 µM kainate was not reversed by treatment with 100 µM TRH. Caspase activity levels were higher than those found in slices treated with kainate alone (157.0±6.2 nM/min/µg protein), although this change was not significant. In contrast, co-incubation of the slices with 300 µM TRH, resulted in caspase activity levels (83.5±12.51 nM/min/µg protein) that were not significantly different from those found in the control slices.

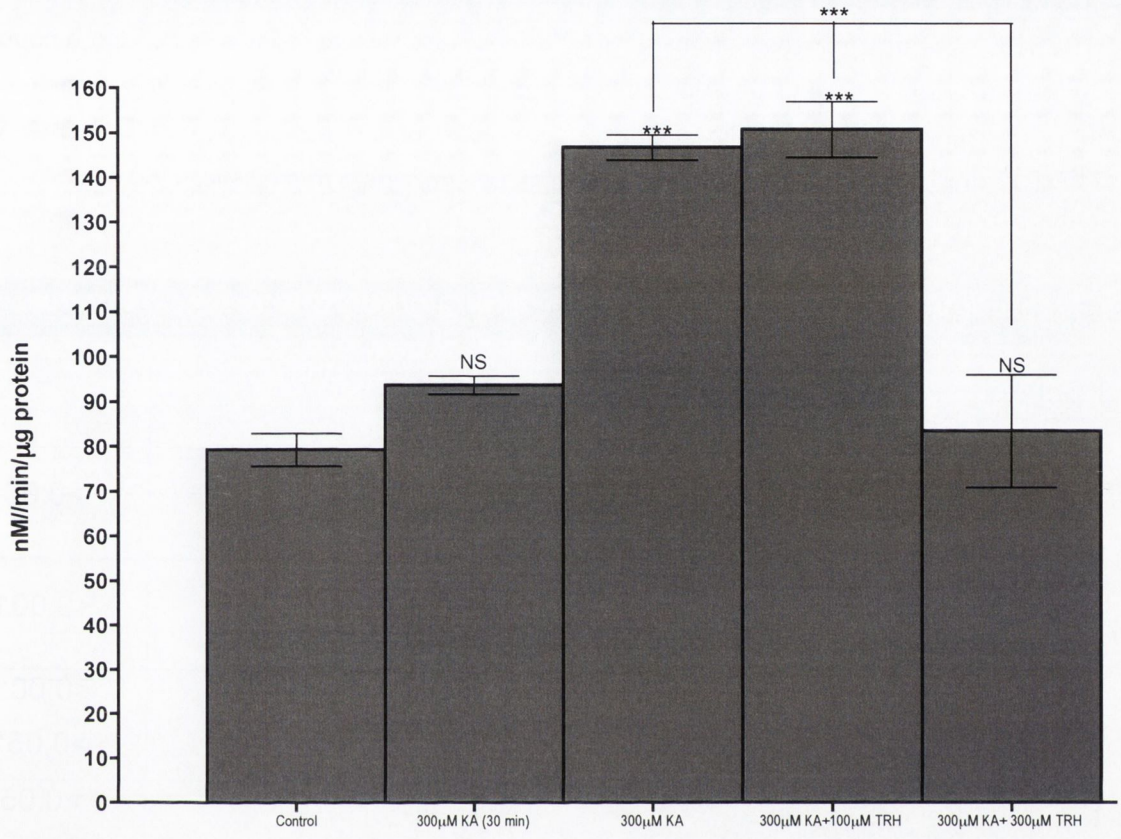

Figure 4.9 Caspase activation in hippocampal slices.

Homogenised hippocampal slices were assayed for caspase activity following superfusion in Krebs buffer, Krebs buffer with 100 or 300 µM KA or Krebs buffer with 300 µM KA and either 100 or 300 µM TRH. The rate of caspase activity per mg of protein is presented here, determined by the release of AMC from the caspase substrate, *N*-acetyl-Asp-Glu-Val-Asp-AMC (Ac-DEVD-AMC) using the AMC standard curve (Figure 2.3). Data represent the mean ± S.E.M. with n=6, with each value measured in triplicate for each treatment group. Statistical analysis was performed by one-way ANOVA with Bonferroni's post-test, with NS=not significant and ***=$P<0.001$ in comparison to controls or, where indicated, to kainate-treated slices.

Table 4.4 Apoptosis activation following kainate treatment.

Caspase activity in homogenised slices incubated with kainate or with kainate, and 100 or 300 µM TRH, was determined fluorometrically. Caspase activity was normalised to the amount of protein in each slice and an AMC standard curve (Figure 2.3) was used to determine the enzyme rate. Analysis of the caspase rates was performed by one-way ANOVA with Bonferroni's post-test, with *=P values in comparison to kainate-treated slices (60 min).

Treatment	nM/min/µg protein	P value
Control	79.26 ± 3.613	-
300 µM KA – 30 min	93.70 ± 2.045	>0.05
300 µM KA – 60 min	146.8 ± 2.819	<0.001
300 µM KA+100 µM TRH	157.0 ± 6.183	<0.001 >0.05*
300 µM KA+300 µM TRH	83.51 ± 12.51	>0.05 <0.001*

4.3.6 TRH prevents an increase in the release of glutamine from hippocampal slices

The release of amino acids from hippocampal slices into the incubating medium was measured by *o*–phthalaldehyde (OPA) derivitisation, followed by HPLC separation and detection with an FL2000 fluorescence detector. The elution profiles for each of the incubation treatments; slices incubated in 300 µM kainate or in 300 µM TRH and 300 µM kainate for 30 min followed by a 30 min recovery period were compared with those that underwent incubation in Krebs buffer for the same period. The elution profiles are depicted in Figure 4.10.

The major peak in each of these profiles represents glutamine, determined from the elution profile of amino acid standards (Appendix B, Figure 1) and by spiking the samples with glutamine. Glutamine was released from the slices in a greater concentration than each of the other amino acids. The areas were integrated, using the PC1000 system software. The glutamine was then quantified using the glutamine standard curve described in Chapter 2 (presented in Appendix B, Figure 2), to determine the concentration (µM) of glutamine released into the incubation medium. Statistical analysis of the glutamine released from the slices by one-way ANOVA with Bonferroni's test and the mean concentrations ± S.E.M. (n=4) are depicted in Figure 4.11.

Incubation of the slices in 300 µM kainate resulted in a three-fold increase in the concentration of glutamine released into the incubation medium when compared with the glutamine released by control slices. When slices were treated with 300 µM TRH in conjunction with kainate, the glutamine release was significantly lower than that found in slices incubated in kainate alone ($P<0.01$), with the level of release returning to that of control slices ($P>0.05$).

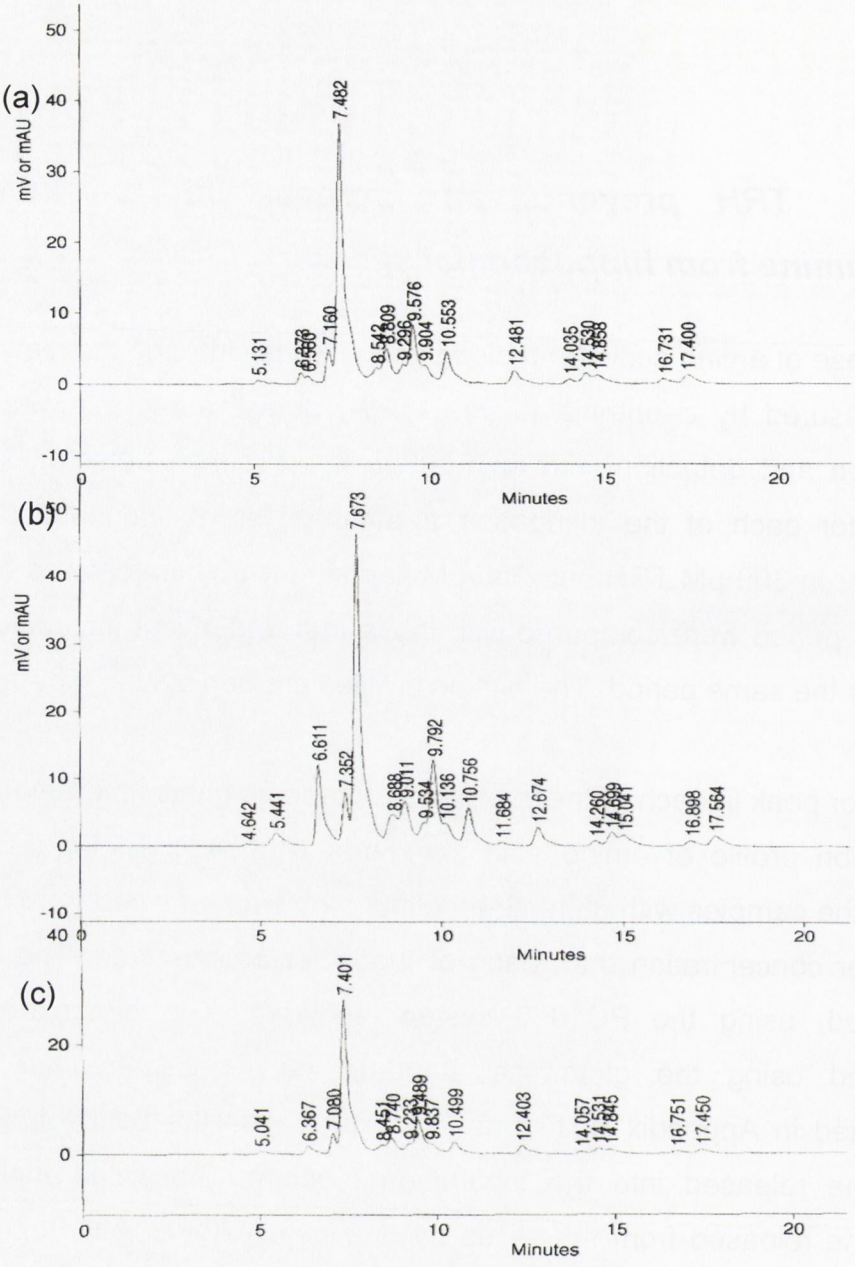

Figure 4.10 Elution profile of amino acids released from hippocampal slices

The amino acids released from hippocampal slices incubated in Krebs buffer (a), 300 µM kainate (b) or 300 µM kainate with 300 µM TRH (c) for 30 min followed by a 30 min recovery period were identified by *o*–phthalaldehyde (OPA) derivitisation, HPLC separation and fluorometric detection. Peaks were identified using the elution profile of a mix of amino standards (Appendix B, Figure 1). The major peak at ~7.4 min represents glutamine, confirmed by spiking samples with glutamine.

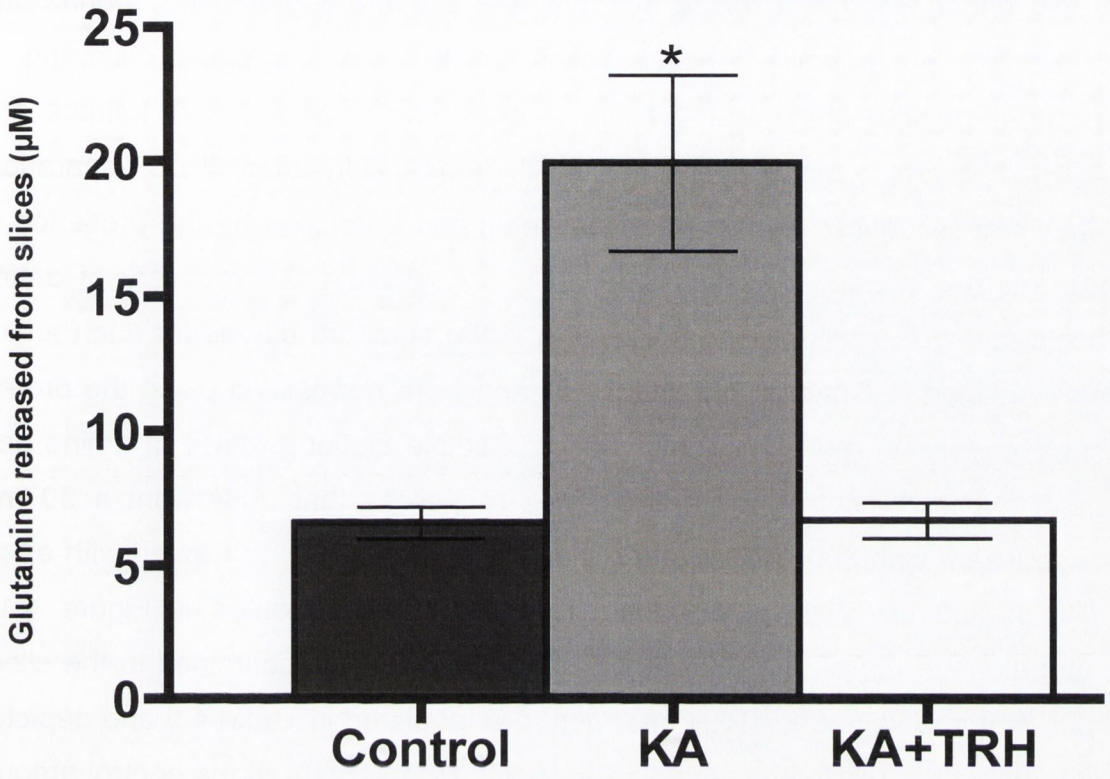

Figure 4.11 The release of glutamine from hippocampal slices

The concentration of glutamine released into the incubating medium from hippocampal slices that were incubated in 300 µM kainate or in kainate along with 300 µM TRH for 30 min followed by a 30 min recovery period was compared with the release of glutamine from control slices incubated in Krebs buffer for the same duration. The level of glutamine was assayed by *o*–phthalaldehyde (OPA) derivatisation, followed by HPLC separation and fluorometric detection at 330 and 440 nm (excitation and emission wavelengths, respectively; Figure 4.10). The resulting fluorescence peaks were integrated with a standard curve of glutamine (Appendix B, Figure 2) and the mean glutamine concentrations ± S.E.M. were calculated, with n=4. Analysis was performed by one-way ANOVA, with *=$P<0.05$ in comparison to control and TRH-treated slices.

4.3.7 *Effects of TRH on KA toxicity: alterations in the level of amino acids*

The presence of the amino acids glutamate, aspartate, glutamine, taurine and GABA in homogenised hippocampal slices was examined following a superfusion time of 90 min (30 min of which in the presence of kainate and TRH). The amino acids were detected fluorometrically after HPLC separation. They were identified by the retention times and quantified by the presence of the internal standard, cysteic acid, used to calculate the recovery of amino acids during the preparation process, and the standard curves for each amino acid outlined in Chapter 2, section 2.7, and were normalised using the protein concentration of the homogenised slice. Sample elution profiles of amino acid detection from control, untreated slices (a), slices that underwent a 30 min superfusion with 300 μM kainate (b) and those that were co-treated with either 100 or 300 μM TRH plus kainate (c and d) are presented in Figure 4.12. Alterations in the amount of each of these amino acids contained in the slices as a result of kainate or TRH treatment are tabulated in Table 4.5 and depicted in Figure 4.13, with the amino acid amounts as a percent of the control amount in Figure 4.14.

It was found that superfusion with 300 μM kainate for 30 min resulted in depletion of each of the amino acids examined, with glutamine undergoing the greatest loss (levels reduced by 71% in comparison to the control; $P<0.01$. Aspartate was reduced to 49% of control levels ($P<0.01$), glutamate to 45% ($P<0.01$) with taurine and GABA reduced to 37 and 34% of control levels, respectively (both $P<0.01$). Treatment of the slices with 100 μM TRH and kainate resulted in levels of aspartate, glutamine and GABA unchanged compared with slices that underwent kainate treatment only and values were significantly lower than control slices. Superfusion of 300 μM TRH along with 300 μM kainate resulted in significant protection against the loss of amino acids, returning the concentrations to levels found in control slices. The only exception was GABA, the levels of which remained significantly lower than the controls and not significantly different from those of slices that underwent treatment with kainate alone or kainate and 100 μM TRH.

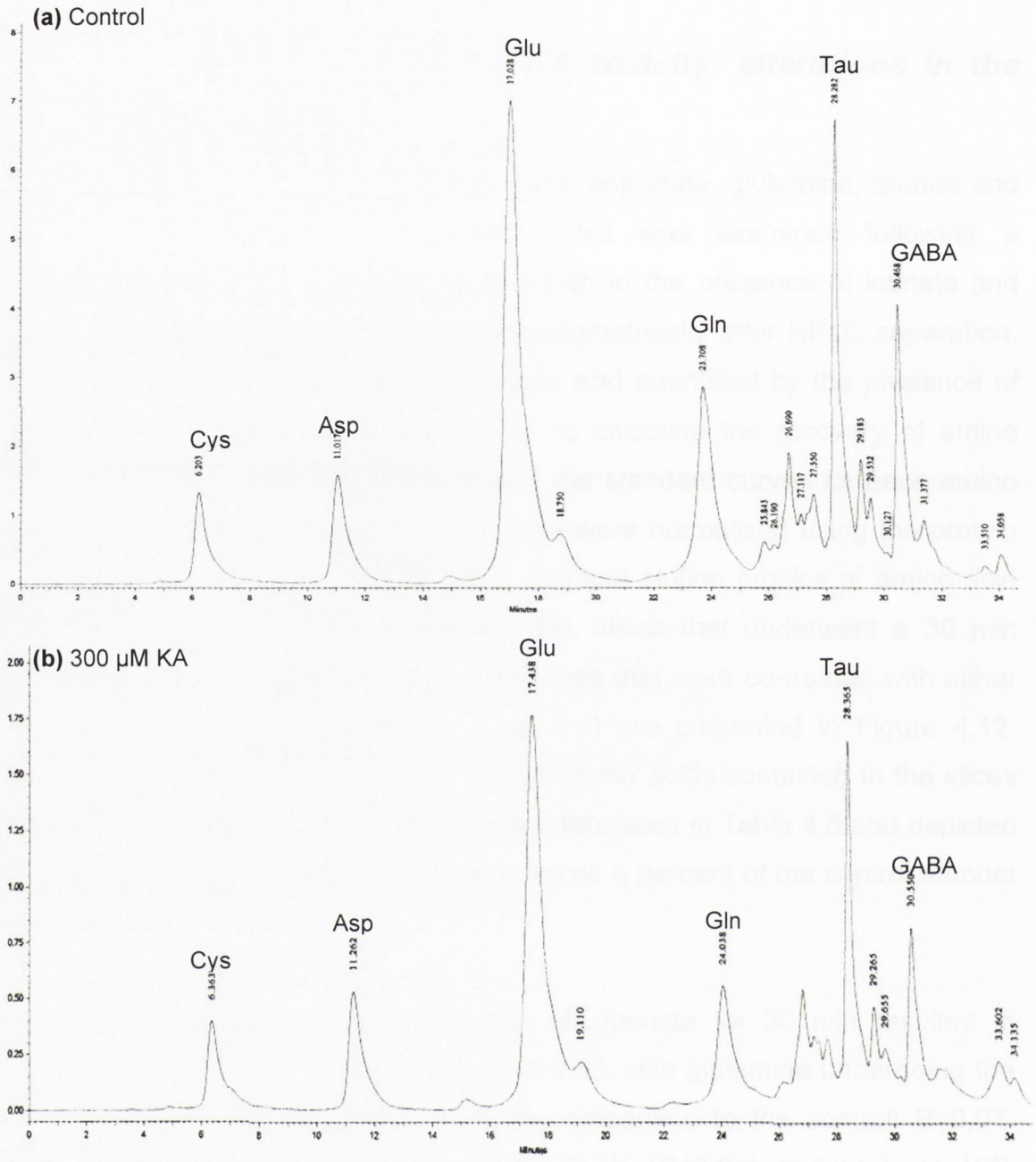

Figure 4.12 Elution profiles of amino acid detection in homogenised hippocampal slices following superfusion experiments.

Hippocampal slices were superfused in Krebs buffer for 30 min, after which slices were superfused with either 300 µM kainate (b), or with kainate plus either 100 µM (c) or 300 µM TRH (d) for 30 min, followed by a 30 min recovery period. Control slices (a) were included in the experiment and these were perfused with Krebs buffer for the same time period. Slices were then homogenised in 0.05 M HCl containing 10 µM cysteic acid as an internal standard.

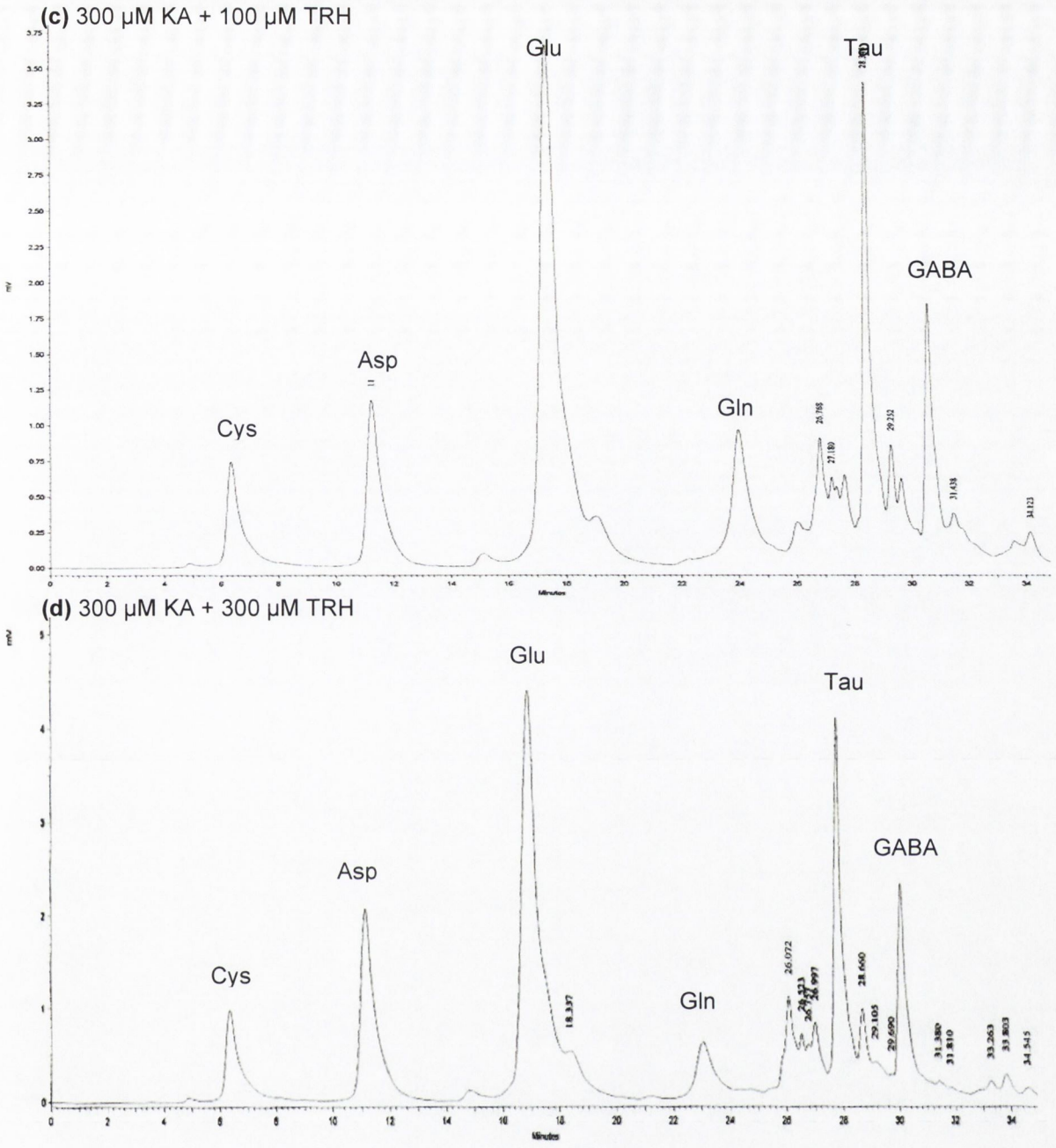

The homogenates were sonicated and filtered through Microcon® centrifugal filter devices. Dervatised samples were separated and detected by HPLC and fluorescence detection. The internal standard is present in all samples at 6.3 min. Cys=Cysteic acid, Asp=Aspartate, Glu= Glutamate, Gln=Glutamine and Tau=Taurine.

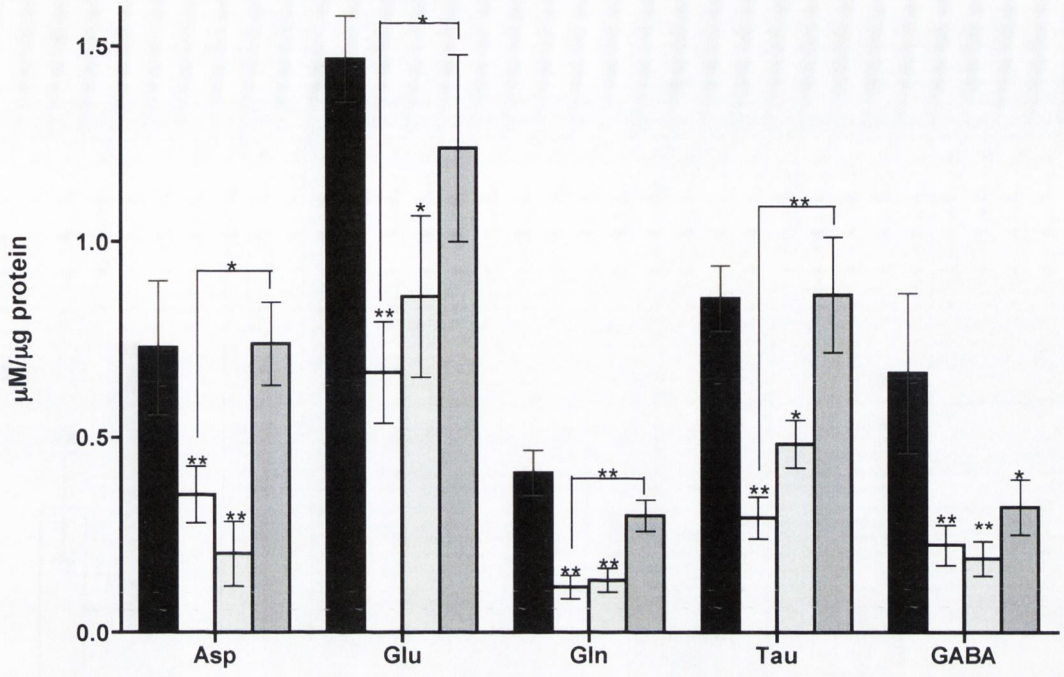

Figure 4.13 The effect of TRH on kainate induced alterations of the levels of amino acid within hippocampal slices.

The amount of each amino acid contained in hippocampal slices following superfusion with Krebs buffer (■) 300 µM kainate (□), kainate and 100 µM TRH (□) or kainate and 300 µM TRH (■) was determined by HPLC separation with fluorometric detection. The peak area and a standard curve for each amino acid was used to calculate the amount contained in each slice and was normalised using the protein content of that slice. Data represent mean ± S.E.M. (n is at least 3 for all treatments). Significant differences were determined by one-way ANOVA with Bonferroni's post-test, with *=P<0.05, **=P<0.01 in comparison to control slices, or to kainate-treated slices where indicated.

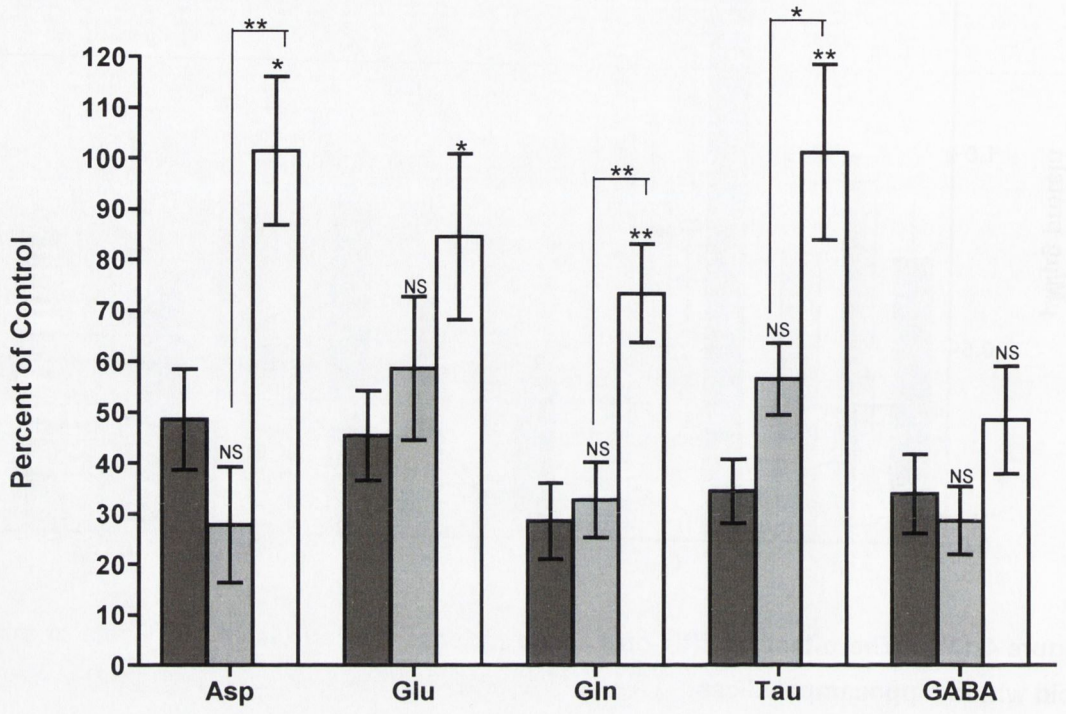

Figure 4.14 Effect of TRH on kainate induced depletion of excitatory amino acids.

The levels of excitatory amino acids within hippocampal slices following superfusion with 300 μM kainate in the absence of TRH (=■); 300 μM kainate with 100 μM TRH (=▨); or 300 μM kainate with 300 μM TRH (=□) shown in Figure 4.13 are replotted here and expressed as a percentage of the levels found in control slices that were superfused with buffer for the same time period. Data represent mean values ± S.E.M. (where n is at least 3), data analysis was performed by two-way ANOVA analysis with Bonferroni's post test with NS=no significant difference, *=P<0.5 and **=P<0.01 in comparison to kainate treated slices.

Table 4.5 Amino acid release from hippocampal slices.

The levels of amino acids contained in hippocampal slices following perfusion experiments were analysed by HPLC. The concentration of each amino acid was then normalised to the concentration of protein found within the slice. Data represent the mean value ± the S.E.M., with n=3 or 4 for each treatment group. The results were analysed by one-way ANOVA with Bonferroni's post-test, with *=P<0.05, **=P<0.01 in comparison to control slices and †=P<0.05 and ††=P<0.01 in comparison to kainate treated slices.

Treatment	Aspartate (μM/μg protein)	Glutamate (μM/μg protein)	Glutamine (μM/μg protein)	Taurine (μM/μg protein)	GABA (μM/μg protein)
Control	0.729±0.171	1.47±0.11	0.410±0.058	0.855±0.084	0.664±0.204
300 μM KA	0.354±0.072**	0.667±0.13**	0.117±0.031**	0.295±0.054**	0.225±0.052**
300 μM KA + 100 μM TRH	0.202±0.083**	0.860±0.207*	0.134±0.030**	0.483±0.061*	0.191±0.044*
300 μM KA + 300 μM TRH	0.740±0.107†	1.240±0.24†	0.300±0.040††	0.865±0.148††	0.322±0.070*

4.3.8 *The effect of TRH and kainate on glial-cell viability*

Perfusion of hippocampal slices with 300 μM kainate caused a significant reduction of glial cell viability, as determined by the levels of glutamine synthetase (GS) in the hippocampal slices as a function of the protein content (Table 4.5, Figure 4.15). Kainate perfusion for 30 min caused a 60% reduction in the enzyme activity in slices. Co-administration of 100 μM TRH with 300 μM kainate, increased the level of enzyme activity slightly, by 16%, though this increase was not significantly different from kainate only slices ($P>0.05$) and the level remained at least 50% of that found in control tissue slices ($P<0.01$). The level was significantly increased with the co-administration of 300 μM TRH, with glutamine synthetase levels of these hippocampal slices was found to be 11% greater than those of the control tissue, although this increase was not found to be significant, with respect to control, by one-way ANOVA analysis with Bonferroni's post-test. Slices that underwent treatment with 300 μM TRH also demonstrated significantly greater glutamine sythetase levels than kainate and kainate with 100 μM TRH treated slices by the same analysis ($P<0.01$ for both).

Table 4.6 Glutamine synthetase activity in hippocampal slices

Glial-cell viability was determined by measuring GS activity in homogenised hippocampal slices following perfusion with 300 μM kainate alone or in conjunction with either 100 or 300 μM TRH for 30 min, followed by a recovery period of 30 min. Statistical analysis was performed using GraphPad Prism by one-way ANOVA and Bonferroni's post-test. Data represent mean values ± S.E.M., with n=4, for each treatment group (measured in triplicate). P values presented represent comparison of treated cells to control, untreated slices, and P* values are in comparison with kainate treated slices.

Treatment	nmoles/ mg protein/min	% of Control	P value
Control	53.39 ± 7.69		-
300 μM KA	21.32 ± 1.91	39.9	<0.01
300 μM KA + 100 μM TRH	24.83 ± 0.83	46.5	<0.01 >0.05*
300 μM KA + 300 μM TRH	59.28 ± 9.82	111	>0.05 <0.01*

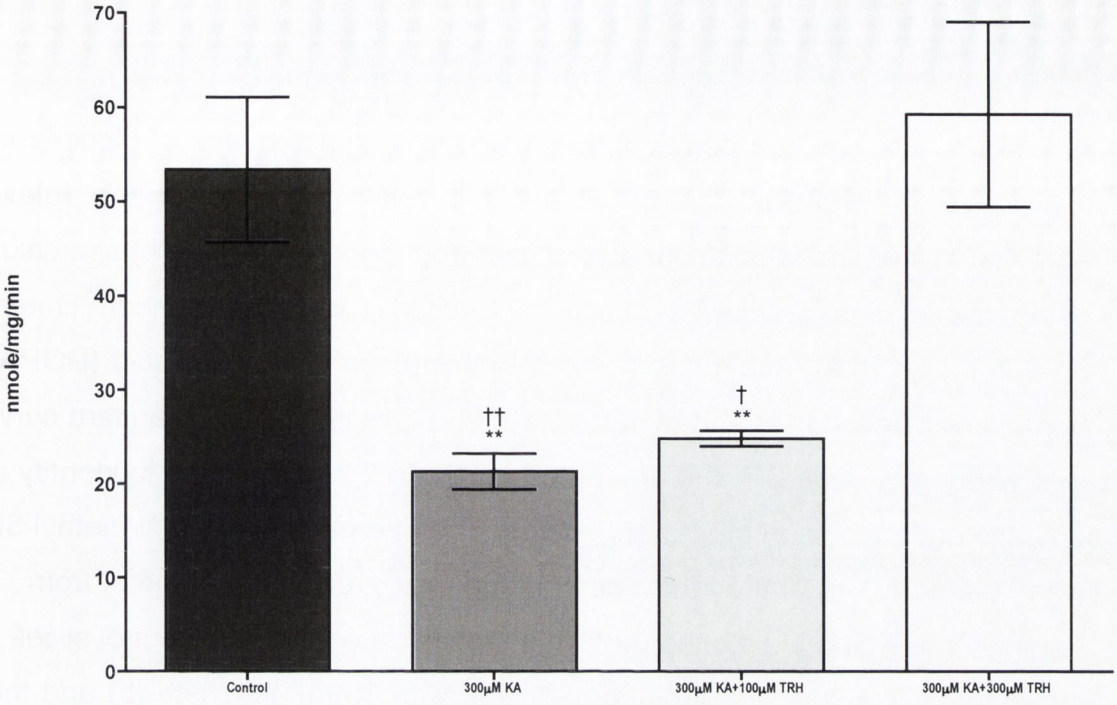

Figure 4.15 The level of glutamine synthetase activity in hippocampal slices

Glial-cell viability was measured by determining the level of glutamine synthetase (GS) activity in homogenised hippocampal slices following a 90 min perfusion experiment. Activity was measured spectrophotometrically using a standard curve of L-glutamic acid γ-monohydroxamate to calculate product formation. Data represent mean values ± S.E.M. (n =4) and data analysis was performed by one-way ANOVA analysis with Bonferroni's post test, **= $P<0.01$ in comparison to control slices, †=$P<0.05$ and ††=$P<0.01$ compared to 300 μM kainate + 300 μM TRH slices.

4.3.9 *Effects of TRH on kainatate toxicity: Biogenic amine levels*

In order to identify the alterations in levels of biogenic amines of hippocampal slices it was necessary to determine the retention times of the relevant catecholamines, metabolites and serotonin from the C18 reverse phase column using the elution gradient outlined in Section 2.6. The retention times of noradrenaline (NA), dopamine (DA), 3,4-dihydroxyphenylacetic acid (DOPAC), homovanilic acid (HVA) and of serotonin (5-HT), as well as the standard curves, described in Section 2.6 and presented in Figure 2.7, were used to identify and quantify each amine in the homogenates. The internal standard, *N*-methyl-5HT, was used to quantify the percentage recovery of amines from the homogenates. Sample elution profiles of amine detection from control slices (a), slices that underwent a 30 min superfusion with 300 µM kainate (b) and those that were co-treated with either 100 µM (c) or 300 µM (d) TRH plus kainate are also shown in Figure 4.16. The levels of amines present in the slices following incubation with kainate in the presence and absence of TRH were compared using one-way ANOVA with Bonferroni's post-test (Figure 4.17). Kainate was found to cause a significant reduction in the levels of dopamine ($P<0.01$; Figure 4.18) and serotonin ($P<0.05$) compared to control slices and the levels of the dopamine metabolites DOPAC and HVA were significantly elevated compared to controls (both $P<0.05$). The serotonin metabolite 5HIAA was also significantly depleted by kainate. Kainate had no effect on noradrenaline levels, however 300 µM TRH with kainate was found to cause a significant reduction in noradrenaline compared to both control ($P<0.01$) and kainate-treated slices ($P<0.05$). Treatment with 100 µM TRH with kainate did not demonstrate this loss, with levels the same as both controls and kainate-treated slices. The levels of dopamine, DOPAC, HVA and serotonin in slices treated with 300 µM TRH with kainate were the same as control slices and were significantly different from slices incubated with kainate alone. Changes in the amount of each of these biogenic amines contained in the slices are tabulated in Table 4.7 and presented as percentages of control levels in Figure 4.19.

(a) Control

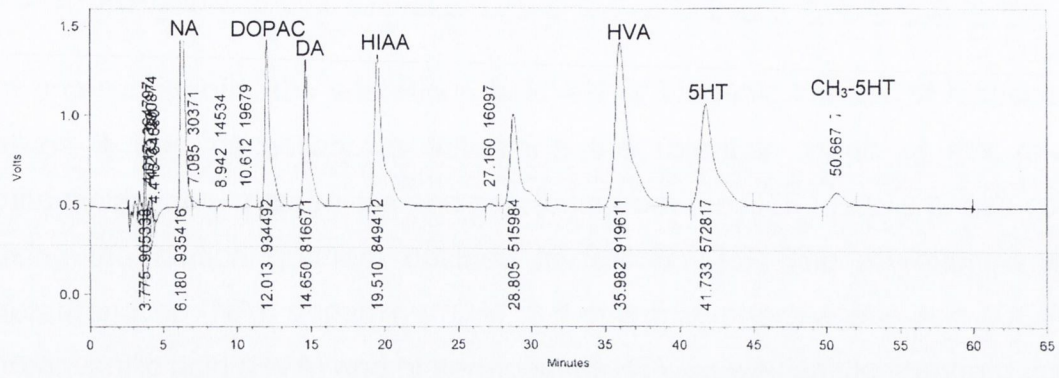

(b) 300 µM KA

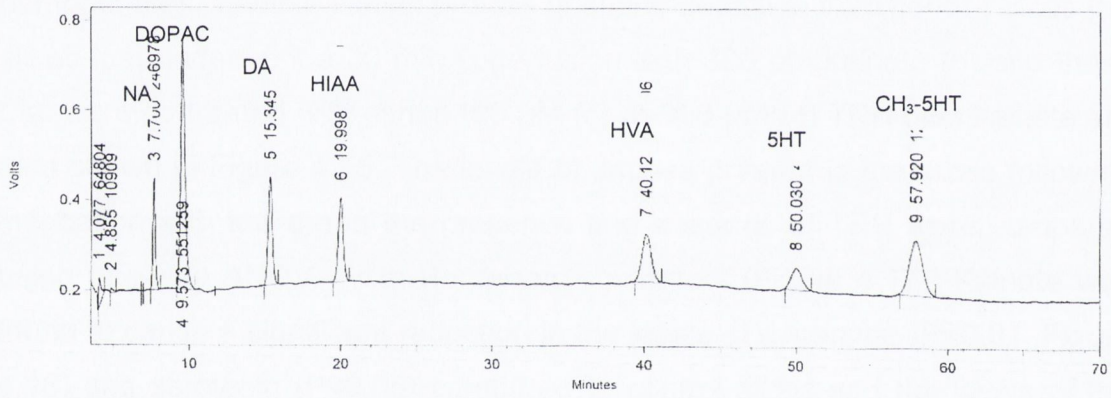

Figure 4.16 Elution profiles of biogenic amine detection in homogenised hippocampal slices following superfusion experiments.

Hippocampal slices were superfused in Krebs buffer for 30 min, after which slices were superfused with either (a) krebs buffer, (b) 300 µM kainate, (c) kainate plus 100 µM TRH or (d) kainate plus 300 µM TRH for 30 min, followed by a 30 min recovery period. Slices were then homogenised in mobile phase containing methyl-serotonin as an internal standard, as described in Chapter 2, Section 2.6.2. The homogenates were then sonicated and filtered through Microcon® centrifugal filter devices. Samples were then separated and detected by HPLC and electrochemical detection, described in Chapter 2, Section 2.6.2.

(c) 300 µM KA + 100 µM TRH

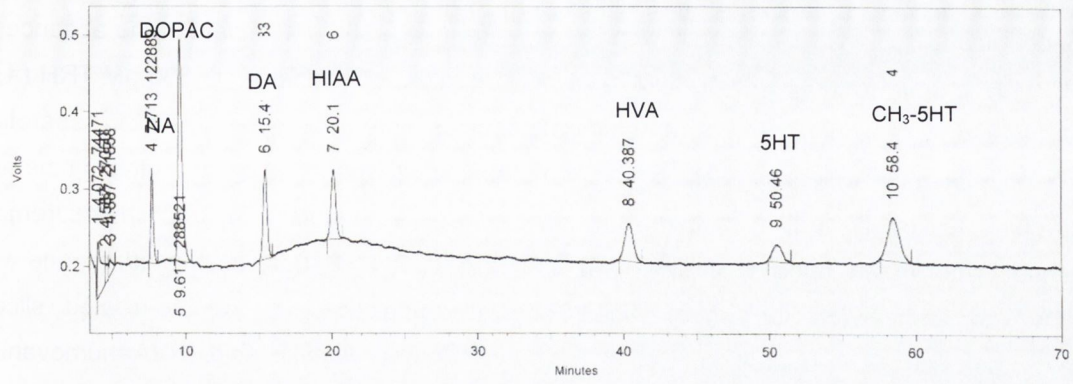

(d) 300 µM KA + 300 µM TRH

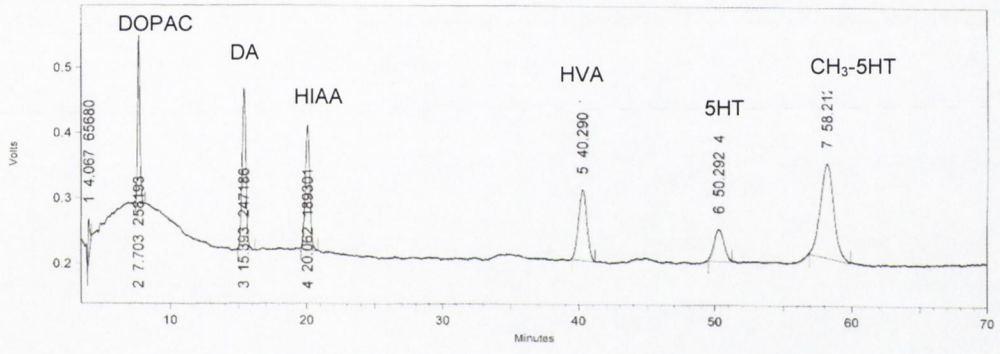

The amines and their metabolites were identified by the retention times of standards (see Chapter 2, Figure 2.6) and quantified using standard curves of the amines (Chapter 2, Figure 2.7), the amount of protein in each slice and the recovery of the internal standard *N*-methyl-serotonin. NA=Noradrenaline, DOPAC=3,4-Dihydroxyphenylacetic acid, DA=Dopamine, HIAA=5-Hydroxyindoleacetic acid, HVA=Homovanillic acid and 5-HT=5-Hydroxytryptamine or serotonin. The internal standard, *N*-methyl-serotonin (CH_3-5-HT) is present in all samples at ~58 min.

Figure 4.17 The effect of TRH on kainate-induced changes to the levels of amines and their metabolites in hippocampal slices.

Hippocampal slices were superfused with Krebs buffer (=■), 300 μM kainate in the absence of TRH (=■); 300 μM kainate with 100 μM TRH (=□); or 300 μM kainate with 300 μM TRH (=□) and the amount of biogenic amines and their metabolites were determined by HPLC separation and electrochemical detection. Each amine or metabolite was identified by its retention time and was quantified by its peak area using the standard curves (Figure 2.7). Each measurement represents the mean value ± S.E.M. (n=4) and *=P<0.05, **=P<0.01 calculated by one-way ANOVA in comparison to control slices, or where indicated, to kainate-treated slices. (NA=noradrenalin, DA=dopamine, DOPAC=3,4-dihyroxyphenylacetic acid, HVA=homovanillic acid, 5HT=5-hydroxytryptamine (serotonin) and HIAA=5-hydroxy-indoleacetic acid).

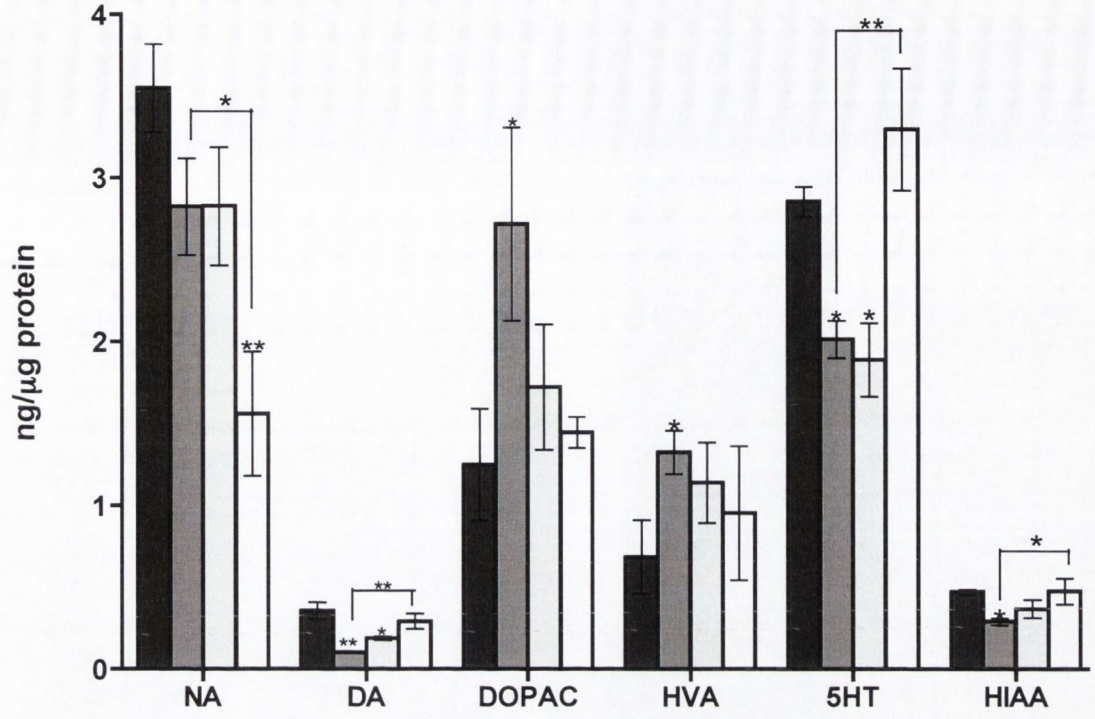
ng/µg protein
4
3
2
1
0
NA
DA
DOPAC
HVA
5HT
HIAA

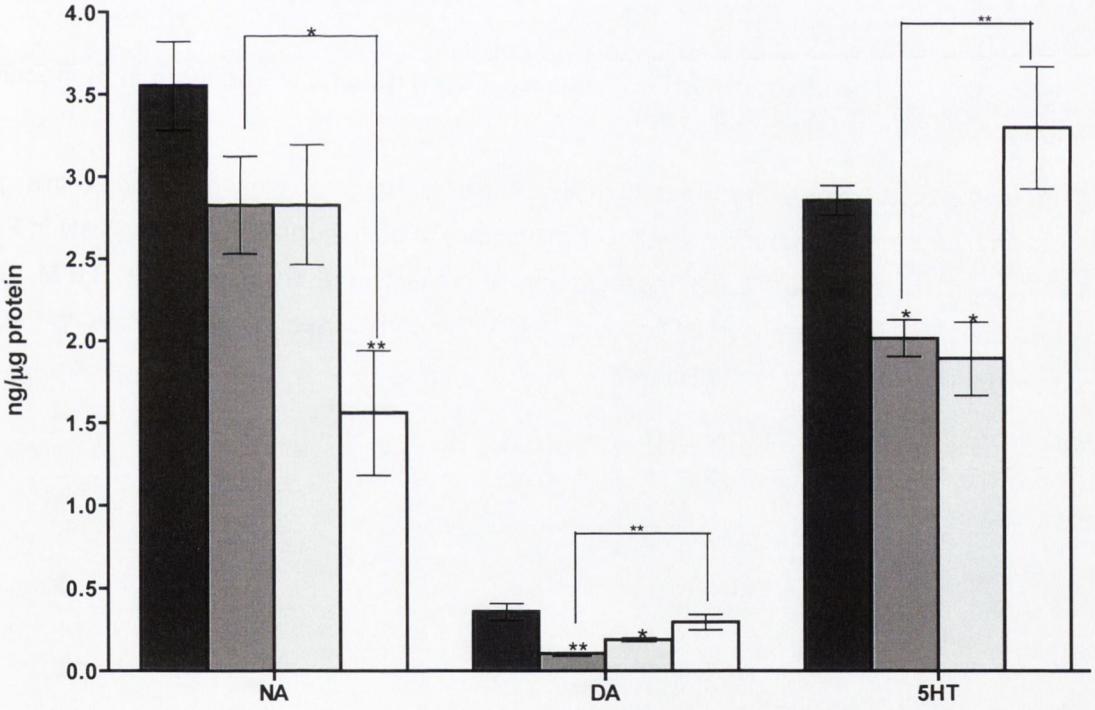
ng/µg protein
4.0
3.5
3.0
2.5
2.0
1.5
1.0
0.5
0.0
NA
DA
5HT

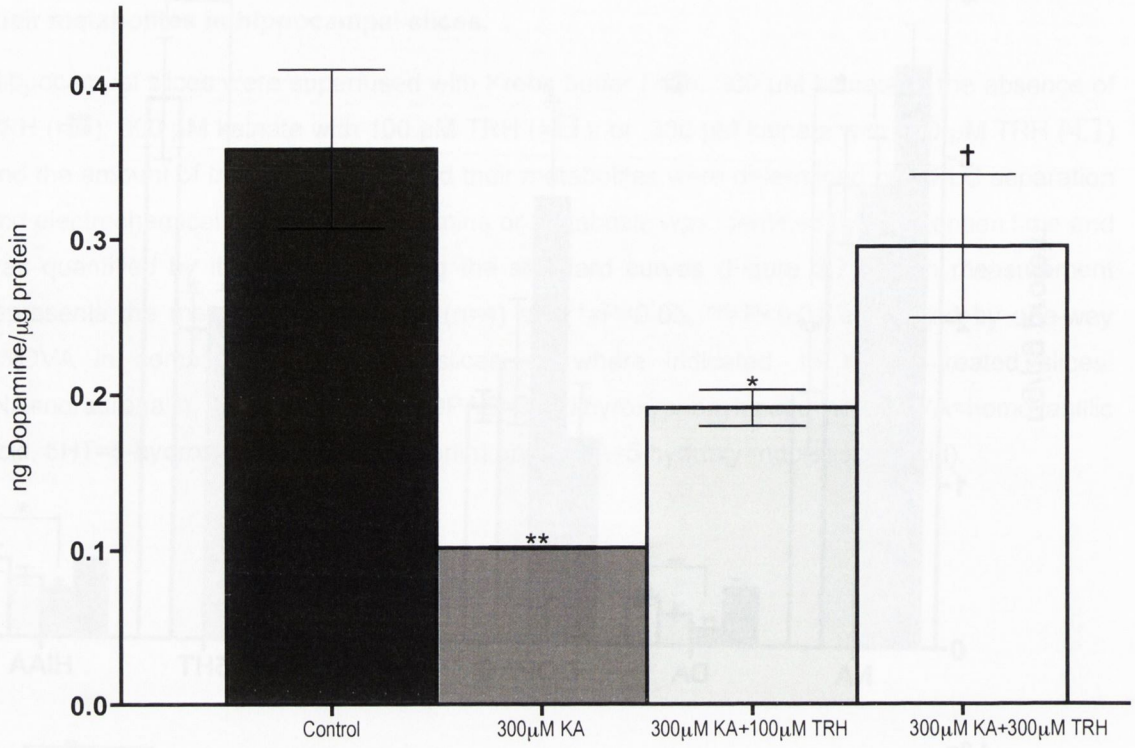

Figure 4.18 The effect of TRH on kainate-induced dopamine depletion in hippocampal slices

The levels of dopamine are lower than the levels of the other biogenic amines; this graph depicts hippocampal dopamine levels per microgram of protein (presented previously in Figure 4.17 on a larger scale). Each measurement represents the mean value ± S.E.M. (n=4). *P<0.05, **P<0.01 determined by one-way ANOVA in comparison to control slices, †=P<0.001 in comparison to kainate treated slices.

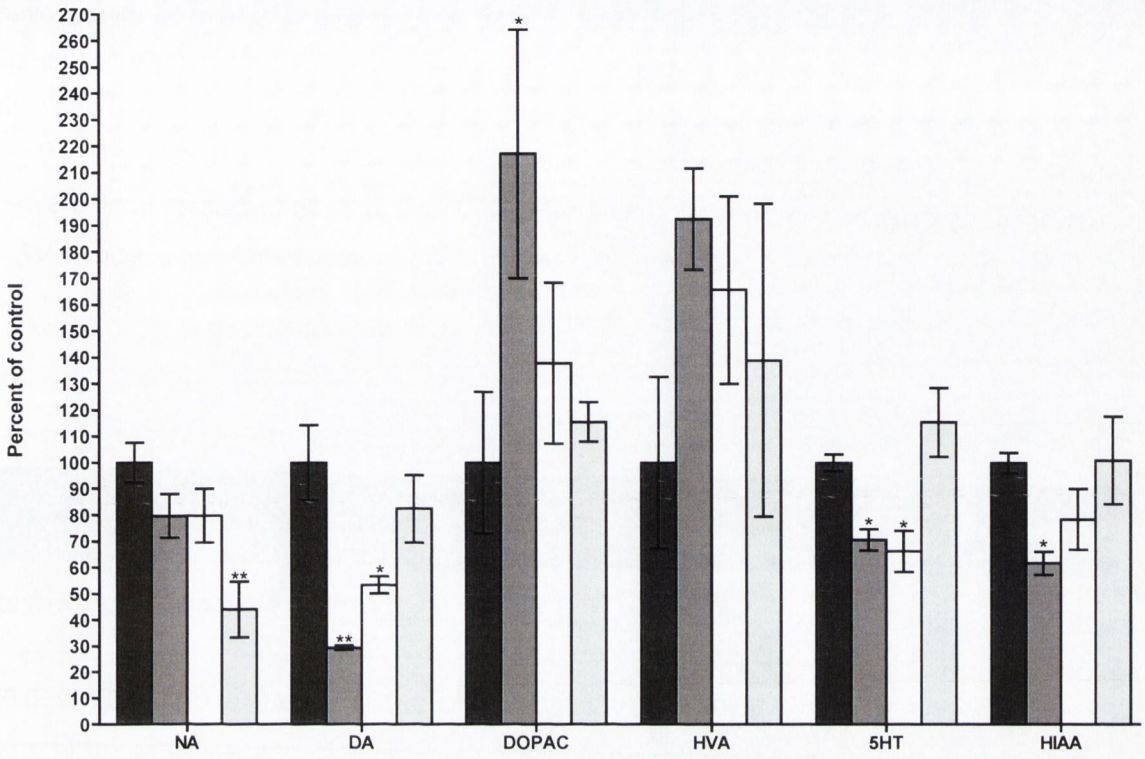

Figure 4.19 The effect of TRH on kainate-induced changes to levels of amines and their metabolites.

Hippocampal slices were incubated with 100 or 300 µM TRH during exposure to 300 µM kainate for 30 min. Amines and metabolites were assayed by HPLC and levels obtained are expressed as a percentage of the levels found in control slices that were superfused with buffer for the duration of the kainate and TRH exposure. 300 µM kainate in the absence of TRH (=■); 300 µM kainate with 100 µM TRH (=□); and 300 µM kainate with 300 µM TRH (= ▨). Data represent the mean values ± S.E.M. (n=4) and were analysed by one-way ANOVA with Bonferroni's post-test, with *=P<0.05 and **=P<0.01 in comparison to control slices.

Table 4.7 Effects of kainate and TRH on amine and metabolite levels in hippocampal slices.

Following a 30 min pre-incubation, hippocampal slices were superfused with 300 µM kainate or 300 µM kainate with either 100 or 300 µM TRH for 30 min and given a further 30 min recovery period. The level of amines and metabolites in homogenised slices was assayed by HPLC. Results are expressed as ng/µg protein. Data represent mean values ± S.E.M. (n=4) and were analysed by one-way ANOVA and Bonferronis post-test, with *=P<0.05 and **=P<0.01 in comparison to controls and †=P<0.05 and ††=P<0.01 in comparison to kainate-treated slices. (NA = noradrenaline, DA = dopamine, DOPAC = 3,4-dihydroxyphenylacetic acid, HVA = homovanilic acid and 5HT = serotonin).

Treatment	NA (ng/µg)	DA (ng/µg)	DOPAC (ng/µg)	HVA (ng/µg)	5HT (ng/µg)	HIAA (ng/µg)
Control	3.552±0.29	0.358±0.05	1.253±0.34	0.689±0.23	2.86±0.09	0.474±0.02
300 µM KA	2.827±0.29	0.105±0.00**	2.720±0.59*	1.327±0.13*	2.016±0.11*	0.292±0.02*
300 µM KA + 100 µM TRH	2.830±0.36	0.191±0.01*	1.727±0.38	1.142±0.22	1.891±0.22	0.371±0.06
300 µM KA + 300 µM TRH	1.563±0.39**†	0.300±0.05††	1.448±0.09	0.957±0.41	3.299±0.37††	0.478±0.08†

4.4 Discussion

A disadvantage of the use of brain slices is that a variable amount of tissue is destroyed at the cut surfaces of the slices during preparation. In the slice-incubation method there is a loss of cellular integrity, which is reflected in the basal levels of lactate dehydrogenase (LDH), a cytosolic enzyme that is released from damaged cells, and of glutamine released from the control, untreated slices (Figures 4.3 and 4.11). Some caspase activation was also evident is the slice superfusion system. Control slices were affected by cell damage in the preparation process, probably as a result of membrane disruption, destabilisation and anoxia during the slicing process. However, the amount of LDH and glutamine released from control slices was significantly less than that released by slices treated with kainate, which validates the use of the method for determining the protective effects of TRH. It was demonstrated that superfusing the slices for 2 h did not induce any significant level of damage. Comparison of the LDH content of slices following perfusion with slices homogenised directly revealed no significant depletion due to the perfusion process.

In determining the appropriate concentration of kainate to apply to the slices, a dose response experimental range of 200–500 μM kainate was used to measure the efflux of LDH from damaged cells. Levels remaining in the slices were used as an indicator of the extent of damage induced by kainate, it was found that 200 μM kainate induced a level of toxicity reflected by a 40% reduction of the LDH content of hippocampal slices following a 60 min incubation. The higher doses of 300 and 500 μM kainate further increased cytotoxicity. A kainate concentration of 300 μM, which reduced the amount of LDH within the slices by 60% and 85% when incubated for 30 min and 60 min, respectively, was chosen as the appropriate dose to induce excitotoxicity in further experiments. This concentration of kainate is comparable to those used by others to induce cell death (McBean 1990; McBean et al. 1995; Wallin et al. 1999), but is greater than that used to evoke physiological effects such as depolarization or ion fluxes (Vornov and Coyle 1991).

It was found that 100 μM TRH has some neuroprotective effect against kainate toxicity, as demonstrated by a reduction in the loss of LDH content from superfused slices. This concentration of TRH did not fully reduce the extent of cell death induced by kainate in the slice system, as the levels of LDH remain significantly lower than those of the control slices. In addition, it had no effect in preventing the activation of apoptosis, as measured by caspase activation, or glial cell impairment, as measured by loss of glutamine synthase activity.

Previously, Nie et al. (2005), who examined TRH-protection by release of LDH from hippocampal and dentate gyrus slices following glutamate-stimulated excitotoxicity (10 mM), reported no protection at the lower TRH concentration of 10 μM. However, Jaworska-Feil et al. (2001) found that pre-treatment of rat cortical neurons with 1, 10 and 100 μM TRH significantly reduced the level of LDH release from cells caused by a subsequent application of 150 μM kainate, although the level of LDH release remained greater than in the control, untreated, cells, indicating that the protection against kainate was not complete.

The present studies demonstrated that the higher concentration of TRH fully protects against LDH leakage when given at the same time as, or prior to administration of the toxin. It also affords a significant level of protection when given after the toxic insult. This demonstrates the ability of TRH to maintain the integrity of the hippocampal cells against excitotoxic trauma. Pizzi et al (1999) also reported 100 μM TRH to completely prevent neurotoxicity caused by NMDA exposure of hippocampal slices. However, they determined viability by counting the ratio of viable and lesioned cells in stained slices. Unlike LDH release, their method does not account for dying or damaged cells. This may account for the need for higher concentration of TRH in the present studies.

The release of LDH from the slices functions as a marker of neuronal integrity, in order to understand the mechanism of TRH protection more fully, the initiation of programmed cell death, apoptosis, was measured by determining caspase activation. Kainate is known to induce apoptosis (Simonian et al. 1996) and, in the present studies, the activation of caspases was clearly demonstrated following exposure of hippocampal slices to kainate. Slices

exposed to 300 μM kainate, for 60 min, reveal an almost two-fold increase in activity but the application of 100 μM TRH had no significant effect on this. Treatment with 300 μM TRH, however, effectively reduces the level of caspase activity to that seen in control slices with no significant difference observed. TRH has been reported to suppress the genes of proapoptotic Bcl-2-associated protein X, Bcl-xL/ Bcl-2-associated death promoter and Fas in pancreatic cell cultures (Luo and Yano 2005). Further work would be required to show whether similar effects occur in the neuronal system used in the present work.

Examination of the derivatised amino acids released from incubated hippocampal slices revealed that a relatively large amount of glutamine was discharged from the slices regardless of the incubation conditions. Glutamine was released in a concentration that was far greater than that of any other amino acid detected. This may reflect progressive anoxia during the incubation (Ogata et al. 1992). There was, however, an appreciable increase in the level of glutamine release due to kainate treatment, with levels in the incubation medium being almost three-fold greater than those of controls. TRH (300 μM) fully counteracted this release. Superfusion of hippocampal slices with kainate resulted in a depletion of each of the amino-acid transmitters contained within the tissue. The kainate induced amino acid loss from slices ranged from 29–48% of control levels. This variable effect on the loss of amino acids may indicate that changes in cell signalling are also contributing to loss. Indeed, this kainate-evoked response was considerably greater than the cell death determined by LDH release.

Again, the greatest change was in glutamine levels, which were only 29% of the levels found in the controls. The kainate-induced loss of glutamate from slices resulted in a fall to 45% of the levels in the controls. Glutamate release from brain slices as a result of trauma has been previously described (Faden et al. 1989; Montoliu et al. 2002) and is calcium-independent (Nicklas et al. 1980; Ferkany et al. 1982; Krespan et al. 1982; McBean et al. 1995). This loss of glutamate could arise by its leakage from the neuronal cytoplasm as a result of energy depletion (Pocock et al. 1988; Nie et al. 2005).

TRH has been reported to be an up-regulator of neurotransmitter systems in various loci of the brain (Nillni and Sevarino 1999; Gary et al. 2003). In this hippocampal slice system, however, TRH afforded significant protection against kainate-stimulated loss of aspartate and glutamate. The concentrations of aspartate and glutamate, in addition to glutamine and taurine, were returned to levels found in control slices. In the presence of TRH, the levels of aspartate and glutamate were significantly greater than those found in kainate-treated slices, with the levels of aspartate being returned to control values whilst glutamate was at 85% of control values. The loss of taurine and glutamine was also prevented by TRH. Protection against hippocampal depletion of glutamate and aspartate has also been described in potassium-induced slice depolarisation (Nie et al. 2005), which is a calcium-dependent process, suggesting that TRH is a homeostatic regulator of neurotransmitter release by both calcium-dependent and –independent mechanisms. As discussed in Chapter 1, excess excitatory amino acid activity has been implicated in the pathophysiolgoy of many cognitive and neurodegenerative disorders, thus this homeostatic function of TRH may indicate a role for TRH analogues as a preventative treatment for such disorders.

It appears that TRH had no effect on the kainate-induced reduction of GABA levels. GABA is the primary inhibitory neurotransmitter of the CNS and TRH has been reported to regulate GABA function in the hippocampus (Kachidian et al. 1991; Heuer et al. 2000; Deng et al. 2006). A contributing factor to the failure of TRH to affect the kainite-evoked depletion of GABA in the hippocampal slices may be that administration of TRH under normal circumstances has been previously shown to increase GABA release in the hippocampus (Deng et al. 2006). The reduced concentration of GABA in kainate-treated cells probably results from a combination of kainate-stimulated release, energy depletion and leakage from dying cells as the membrane looses integrity. TRH may protect against GABA loss from the slices because of the improved cellular integrity, demonstrated by protection against apoptosis and LDH release, but these effects may enhance the direct TRH-stimulated GABA release. This TRH evoked release of the inhibitory GABA is probably a homeostatic response to the over-excitation due to kainate. This excitation by glutamatergic mechanisms

may function through an increase in cGMP, which GABA-receptor activation, caused by the TRH stimulus, then inhibits (Nakayama et al. 1996).

The prevention of glutamate and aspartate loss may, in part, be due to TRH-enhanced glial uptake (Nie et al. 2005), indicating that neuroprotection by TRH may function through glial cells. The ability of TRH to protect glial cells was, therefore, investigated. Glial cells are central to regulation of glutamate conversion to non-toxic glutamine. As previously mentioned, kainate functions as a toxin by activating glutamate receptors, this in turn causes an excessive release of glutamate within the cell, disturbing the glutamate–glutamine regulatory cycle and inducing excitotoxicity. Glia probably function to decrease the effective concentration of glutamate by a high-affinity, high-capacity transport system and most of the transport sites for glutamate are present on the glial cells and, therefore, the initial effects of kainate may be exerted in glial cells (Garthwaite and Garthwaite 1985; Vornov and Coyle 1991; McBean et al. 1995). It has previously been shown that glial cells are susceptible to kainate toxicity (Kollegger et al. 1991; McBean et al. 1995), and kainate receptors have been identified in microglial cells (Noda et al. 2000).

Assaying for glutamine synthetase (GS), an enzyme found only in glial cells, serves as a marker for glial-cell viability. This enabled the measurement of the protective effects of TRH on the glial-cell population of the hippocampal slices. Kainate susceptibility was confirmed in these studies, which showed that 300 µM kainate reduces the level of GS activity in slices by 60%. This loss of glial viability by kainate treatment could explain the significant increase in glutamine leakage from the hippocampal slices, shown in Figure 4.11.

Co-treatment with 100 µM TRH did not significantly improve this loss of GS activity, with levels of GS remaining at just over 50% of the levels found in control hippocampal slices. The loss of glial-cell viability could, however, be reversed by treatment with 300 µM TRH, which lead to levels of activity at normal, control, limits. This protective effect on glial cells coincides with the observation that incubation with 300 µM TRH prevented kainate-induced release of glutamine from hippocampal slices, and maintained glutamine levels

within slices, consistent with TRH protecting glia from kainate induced loss of viability. Astrocytes have previously been demonstrated to express receptors for TRH (Fernandez-Agullo 2001), which could explain the capacity for TRH to exert this protective effect.

Alterations in the levels of biogenic amines and their metabolites in hippocampal slices following superfusion with kainate may be due to the loss of cell integrity, however, the variable effect of kainate on the level of amines and their metabolic products suggests that alterations in the cell-signalling processes may also contribute. Kainate had the smallest impact on noradrenaline, with levels remaining at 80% of controls and not significantly different to control levels. The level of dopamine within slices was reduced by greater than 3-fold. The level of the indoleamine serotonin was reduced to 70% of control values following exposure to kainate, whilst the metabolite HIAA was reduced to 62% of control levels. Interestingly, the levels of the dopamine metabolites, DOPAC and HVA, did not appear to be altered to the same degree as dopamine. The levels of the dopamine metabolites within the slices doubled. This indicates that some of kainate-released dopamine stores or its metabolites were released into the perfusate. Dopamine depletion was greater than cell death assessed by the LDH assay, whereas the loss of noradrenaline and serotonin was less. Thus the kainate-evoked depletion of these molecules may involve both cellular signalling as well as leakage of these substances from damaged cells.

Kainate treatment had no significant effect on the noradrenaline levels of the hippocampus. Treatment with TRH, however, resulted in significant depletion of this catecholamine, an effect that has also been elicited *in vivo* by microdialysis. It is thought that, among monoaminergic neurons, the noradrenerigic system may be most sensitive to TRH (Itoh et al., 1994a). TRH and noradrenaline co-localise throughout the CNS (Lechan and Kakucska, 1992, Kolk et al., 2002, Itoh et al., 1994a). The stimulatory effect of TRH on the release of noradrenaline may be of benefit in the treatment of locomotor disorders.

When TRH (300 μM) was co-administered with kainate, it completely prevented the depletion of dopamine, serotonin and their metabolites caused by kainate alone. The ability of TRH to prevent loss or altered metabolism of neurotransmitters could be caused by the endogenous functions of TRH being mediated through these amines. TRH is known to co-localise with serotonin, noradrenaline and dopamine in certain neuronal populations (Section 1.8), and previous studies have demonstrated that TRH-analogues appear to function *in vivo* through serotonin and dopamine release (Fukuchi et al., 1998, McCreary and Handley, 1999, Tanabe et al., 2007), implying the involvement of these amine neurotransmitters in the actions of TRH. Further studies should examine the effects of TRH on this system in the absence of kainate, to confirm these conclusions.

In summary, kainate was shown to be neurotoxic in the system studied, leading to increased levels of cell death, both by apoptosis and necrosis, and neurotransmitter release which may involve altered cell signalling as well as cell damage and death. TRH was shown be neuroprotective.

The anatomical relationship between the TRH signalling elements in the hippocampus is not yet fully understood. TRH has been detected in the dentate gyrus and the TRH receptor is expressed in the molecular layer and the dentate gyrus, whereas TRH-DE is widely expressed in the pyramidal-cell layer (Heuer et al. 2000). It has been postulated that TRH is neuroprotective in a manner that is independent of the TRH receptors (Faden et al. 2003a), both by phosphorylation through protein kinase C (Pizzi et al. 1999) and by preventing glutamate-stimulated increases to levels of intracellular calcium (Koenig et al. 1996).

The preservation of cell viability, as indicated, may be the major mechanism by which TRH promotes functional neuronal recovery in brain trauma. TRH inhibits excitotoxically mediated cell loss, which suggests that it could be of value in the treatment of brain injury and neurological diseases associated with excitotoxic cell death. TRH appears to function as a homeostatic regulator of the neurotransmitters glutamate, aspartate, taurine, dopamine and serotonin. This

is a conclusion that may be of significance in the treatment of the many diseases thought to result from excessive glutamatergic signalling.

Despite reports on the short life span of TRH, due to rapid degradation primarily by TRH-DE, which is present in the hippocampus, the protective effects of TRH endured for the time-periods used in these experiments, ranging from 30–60 min from the conclusion of TRH application. This is most likely to explain the high concentration of TRH (300 μM) that were found to be necessary for obtaining neuroprotection. The application of effective TRH-DE inhibitors might be expected to reduce the effective TRH concentrations.

Overall, these findings demonstrate that TRH protects hippocampal cells from kainate-induced toxicity in a concentration-dependent manner *in vitro*. This paradigm should permit further in-depth investigations into the downstream molecular mechanism(s) involved in this TRH effect.

CHAPTER 5

STUDIES ON THE PROTECTIVE EFFECT OF TRH AGAINST CELLULAR INSULTS

5.1 Introduction

Studies with cultured cells compliment the results obtained with brain slices (Chapter 4) in the study of cytotoxicity and protection. It is possible to estimate the contributions of apoptosis and necrosis to cell death. Furthermore, much longer periods of exposure to toxins and TRH were possible than with the brain slices. The cell-culture system also allowed the effect of TRH to be measured directly in a homogenous tissue type, and a wider range of toxins, which operate by different primary mechanisms, were used in these studies, to facilitate further elucidation on the method of TRH protection.

SH-SY5Y cells provided the *in vitro* system used in this section. These cells have a neuroblastoma morphology and were initially biopsy-derived from metastasis to bone marrow from a human Caucasian, 4-year old female. They are a thrice-cloned sub-line of the bone marrow neuroepithelioma cell line SK-N-SH (ECACC No. 86012802). These cells express many features of mature noradrenergic neurons; they have sodium-dependent glutamate/aspartate and noradrenaline transporters and express both ionotropic and metabotropic glutamate receptors (Naarala et al. 1993; O'Neill et al. 1994). Activation of both the ionotropic and metabotropic receptors increases free intracellular Ca^{2+} concentration ($[Ca^{2+}]_i$), however it is the ionotropic (particularly the NMDA) receptors that predominate in the increase in $[Ca^{2+}]_i$ (Naarala et al. 1993), a crucial factor triggering excitotoxic and apoptotic cascades. These cells have dopamine-beta-hydroxylase activity and can also convert glutamate to GABA (Naarala et al. 1993; Tetich et al. 2004).

The toxins used in this study to induce cell death were staurosporine, 1-methyl-4-phenylpyridinium (MPP^+) and kainate. The effects of kainate in inducing death by excitoxicity are described in detail in Chapter 1, Section 1.9. Briefly, kainate binds to ionotropic glutamate receptors, this causes depolarisation of the cell membrane and release of Ca^{2+} from intracellular non-mitochondrial calcium stores and into the cytoplasm increasing $[Ca^{2+}]_i$ levels, with subsequent

activation of protein kinases, including protein kinase C and calmodulin-dependent kinases (Naarala et al. 1993; Song et al. 2008).

Staurosporine is a microbial alkaloid that was originally isolated in 1977 from the bacterium *Streptomyces staurosporeus*. It functions by inhibition of protein kinases through the prevention of ATP binding to the kinase (Schnier et al. 1996; Chae et al. 2000). This is achieved through the stronger affinity of staurosporine to the ATP-binding site on the kinase. It is one of the most potent, but non-specific protein kinase inhibitors with IC_{50} values in the nanomolar range. This protein kinase inhibition means staurosporine is a strict apoptosis inducer – arresting the cell cycle at the G1 phase (Schnier et al. 1996; Weil et al. 1996). It induces apoptosis in all cells except red blood cells due to their anucleation. It has biological activities ranging from anti-fungal to anti-hypertensive.

MPP^+ is the dihydropyridine oxidised metabolite of 1-methyl-4phenyl-1,2,3,6-tetrahydropyridine (MPTP). It can be readily taken into dopaminergic cells via the dopamine re-uptake transporter. It is cytotoxic due to its accumulation by mitochondria, where it inhibits Complex I of the mitochondrial electron transport chain, thus causing depletion in ATP levels and, consequently, increases in cytosolic Ca^{2+} concentration and ROS formation and, eventually, death of the neurone. It also inhibits the synthesis of catecholamines, catalysed by tyrosine hydroxylase, leading to reduced levels of dopamine and noradrenaline (Lotharius and O'Malley 2000).

Cell culture assays provide a simple and direct approach to measuring toxicity and function at the cellular level under varying conditions. In these studies the cells were exposed to toxins in conjunction with TRH for varying time periods and well-established viability assays were performed to quantify the protection afforded by TRH.

Alteration of protein kinase activity is a common factor in the processes of cell death instigated by each of these toxins, as depicted in Figure 5.1. Kainate and MPP^+ cause increases the levels of $[Ca^{2+}]_i$, which may induce death by itself or by initiating cellular signal transduction processes, a number of which are

regulated by the level of $[Ca^{2+}]_i$, including the activation of protein kinase C and calcium/calmodulin-dependent protein kinase, whereas staurosporine functions as an inhibitor of protein kinase.

The studies described in Chapter 4 showed TRH to be neuroprotective against excitotoxicity induced by kainate in hippocampal slices. The aim of the studies described herein was to investigate if TRH could afford protection against cell death instigated by different toxins, which have different primary actions, which initiate overlapping signalling events that ultimately cause cell death. The possible protective effects of TRH were studied in order to assess the level(s) at which it might act.

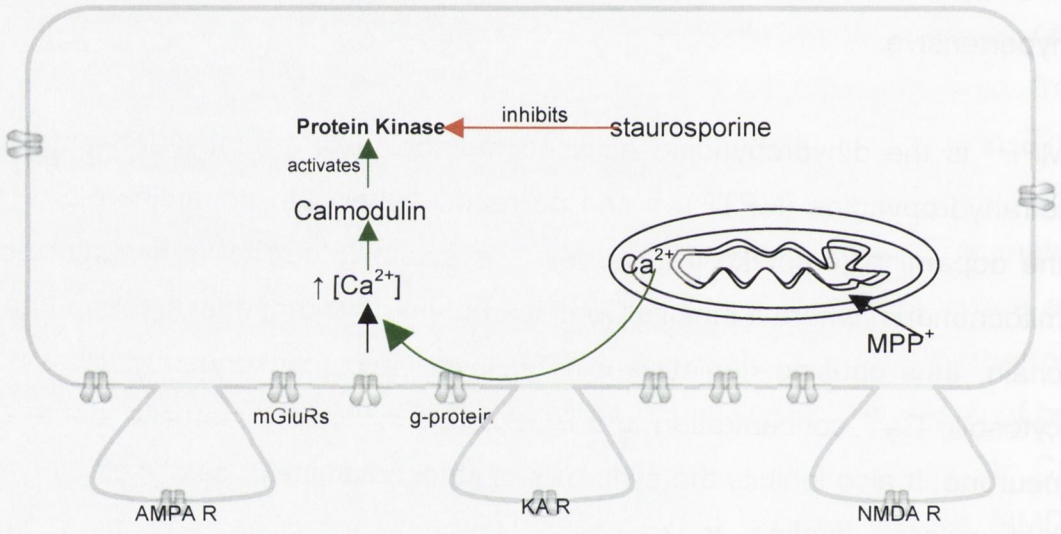

Figure 5.1 The effects of staurosporine, kainate (KA) and MPP^+ have on intracellular events.

Schematic representation of the overlapping events that occur within the cell following administration of each type of cell toxin. The common theme between cell toxicity events is an alteration in $[Ca^{2+}]_i$, and an alteration of protein kinase activity – activated by kainate and MPP^+ and inhibited by staurosporine.

5.2 Methods

5.2.1 Culturing

Human neuroblastoma SH-SY5Y cells obtained from ATCC (CRL-2266) grow as a mixture of floating and adherent cells that aggregate and can form floating clumps. They form clusters of neuroblastic cells with multiple, short, fine cell processes (neurites). The cells were cultured in tissue culture flasks (15 x 8.5 x 3.5 cm, with a 75 cm^2 surface area), in a 1:1 mixture of Ham's F12 nutrients and essential medium (MEM) supplemented with 10% fetal bovine serum (FBS), glutamine, non-essential amino acids, sodium pyruvate and sodium bicarbonate with 100 IU/ml penicillin and 100 µg/ml streptomycin. All cells were maintained in humidified 5% CO_2 atmosphere at 37°C. The medium was replaced every 4–7 days, depending on cell density. For subculturing, the medium was removed with the floating cells, and these cells were recovered by centrifugation. The adherent cells were covered with 3 mL of fresh 0.25% trypsin, 0.53 mM EDTA solution and incubated for 4 min in the hood, until the cells detached. Fresh medium was then added and the culture-flask rinsed, this was then aspirated and centrifuged to obtain the cell pellet, and sub-cultured into new flasks at a ratio of about 1:5.

5.2.2 Cell Counting

Trypan Blue exclusion of non-viable cells was used to determine cell number, by viable cell counting using a haemocytometer and a light microcscope and the number of cells/mL was determined (before plating).

5.2.3 Cell Plating

Cells were resuspended after counting in plating medium – the same medium as above, but not supplemented with serum. Cells were then plated at 1×10^4 cells/100 µL/well on a 96 well plate, leaving the first row (a) as a blank, cell free, containing serum-free medium, cells in the second row (b) were control cells.

The cells were left to adhere for 24 hours prior to initiation of experiments. Cells rows c–h were treated with toxins ± doses of TRH, in triplicate at various time points, as laid out in Figure 5.2.

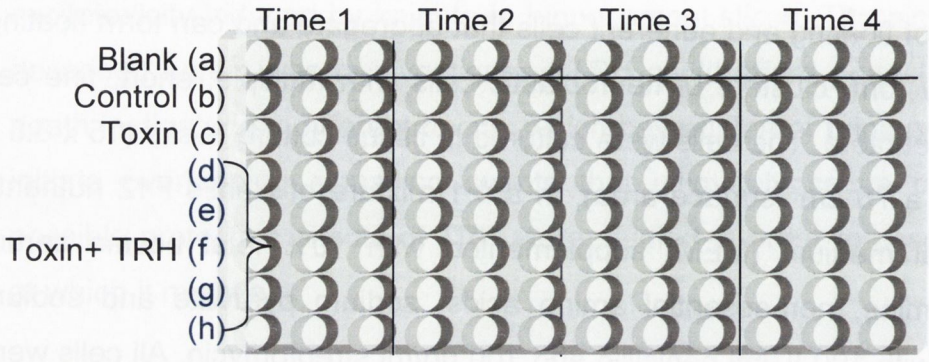

Figure 5.2 Cell culture assay setup

Cells were plated in rows b–h at a density of 1×10^4 cells/100 µL/well on 96 well plates in serum-free medium and left for a 24 h period before initiation of toxicity studies. Toxins were added to the wells over a range of time periods and TRH was co-administered in the appropriate wells. All treatments were made in triplicate.

5.2.4 Cell toxicity studies

Kainate, MPP^+ or staurosporine were added to the cells and incubated for varying time periods to induce cell death by their differing mechanisms. TRH was administered to measure its ability to protect against cell death.

5.2.5 Cell Viability

5.2.5.1 The MTT viability assay

In this assay the ability of reductase enzymes of viable cells to convert the yellow tetrazolium salt, 3-(4,5-Dimethylthiazol-2-yl)-2,5-diphenyltetrazolium bromide (MTT) to formazan, resulting in a purple colour, was measured on a microplate reader spectrometer at an absorption of 540 nm with a reference wavelength of 630 nm. This redox activity measurement indicated the level of cytotoxicity induced by a range of concentrations of each of the toxins studied

following incubation over 2–48 h. MTT was dissolved in phosphate-buffered saline (PBS) at a concentration of 5 mg/mL and filtered through 0.22 µm filters, 10 µL of this solution was added to each well and incubated for 4–6h, the plates were then centrifuged at 2000 rpm for 10 min and the medium removed, leaving behind formazan crystals, which were dissolved by addition of 100 µL DMSO and the absorption measurement was taken within 5 min. A reference using 120 µL cell medium with 10 µL MTT solution was used as a blank. Control cells were assumed to have 100% viability and the viabilities of cells that underwent treatment were calculated as a percentage of control cells.

5.2.5.2 Propidium iodide

The propidium iodide assay measured the damage or leakage of the plasma membrane. The assay was used to identify late apoptotic or necrotic cells that lost membrane integrity as the propidium iodide penetrated dying cells and bound to DNA, emitting a red fluorescence. Cells were stained with 50 µM propidium iodide (PI) solution in PBS at room temperature for 15 min in the dark. The fluorescence at 536 nm and 590 nm (excitation and emission, respectively) was measured to give the first reading (F), with a background reading made for medium + PI (blank). A second fluorescence reading was made following cell lysis with 160 µM digitonin for 20 min to obtain the fluorescence of the permeabilised cells. This second (F_{max}) reading was used to determine the percentage viability, calculated as $100-((F-\text{blank})\div(F_{max}-\text{blank}))\times100$.

5.2.5.3 Lactate dehydrogenase release

As a measure of the release of cytosolic proteins and loss of plasma membrane integrity, the amount of lactate dehydrogenase (LDH) released into the culture supernatant in 96-well plates and that remaining within lysed cells was measured. LDH release is a reliable index of membrane failure because of the enzyme's high intracellular activity and high stability in the extracellular medium. LDH activity was determined spectrophotometrically, by the conversion of pyruvate to lactate and simultaneous oxidation of NADH to NAD^+,

with the rate of decrease in NADH directly proportional to the LDH activity. Plates were centrifuged at 4000 rpm for 5 min and 25 µL of the medium was removed from each well to a new plate to measure the LDH released from cells. Viable cells adherent to the plate were lysed with 0.1% ice-cold Triton-X100 and 25 µL of this lysed cell fraction was used to measure the LDH content of the cells. The LDH activity of each fraction was measured by addition of 25 µL 10 mM sodium pyruvate to each well, followed by 100 µL of 0.3 mg/ml NADH solution and reading the OD was immediately started on the microplate reader at an absorbance 340 nm. The total amount of LDH in each well was determined by adding the value of the LDH released from cells into the incubation medium with that found in lysed cells. The LDH released from the cells into each well was then calculated as a percent of the total amount of that well.

5.2.5.4 Caspase

Initiation of apoptosis in cells was analysed by assaying for caspase activity (caspases -3, -6, -7, -8 and -10) following incubation of the cells with toxin in the presence and absence of TRH. The method is outlined in Chapter 2, Section 2.9.3. Briefly, 10 µL of cell lysates were transferred to wells of a black 96-well plate, 100 µL of 1.65 µM substrate (*N*-acetyl-Asp-Glu-Val-Asp-7-amino-4-methylcoumarin; Ac-DEVD-AMC) was added to each sample and the controls. Production of fluorescent free-7-amino-4-methylcoumarin (AMC), released by caspase activity, was monitored over 60 min at 37°C using a microplate fluorimeter (Spectra Max Gemini, Molecular Devices) at excitation and emission wavelengths of 360 and 460 nm, respectively. An AMC standard curve (Chapter 2, Figure 2.3) was used to calculate caspase activity and expressed as AMC formed/mg protein/min. The protein concentration was determined by the BioRad method (Section 2.3.1).

5.3 Results

5.3.1 Dose–dependant and time-dependant effects of toxins on SH-SY5Y death

The MTT method was used to determine the level of cytotoxicity induced by a range of concentrations of each of the toxins following incubation over 2–48 h and the results are shown in Figures 5.3–5.5.

Statistical analysis was performed for each data-set by two-way ANOVA with Bonferroni's post-test, comparing the values to the controls, to determine the effect of incubation time and the concentration of toxin used. The appropriate concentration of each toxin and incubation period required to induce approximately 50% cell death was thus determined. This concentration of toxin was then used in further experiments to determine the level of protection afforded by a range of doses of TRH.

The concentration of staurosporine for use was determined to be 10 μM, which at 2 h resulted in a 15% loss of viability in comparison to control cells and decreased to 45% cell viability following 12 h incubation. The range of incubation periods with staurosporine for future experiments was performed within this 2–12 hour time frame.

Kainate caused substantial loss of viability at concentration ranges of 300–500 μM following incubation for 24 h, with no further increase in death at 48 h. Comparison of the viabilities following 8–48 h incubations in kainate revealed no significant difference due to the concentrations used, thus 300 μM kainate was used to induce toxicity in future experiments, with time periods of 8–48 h.

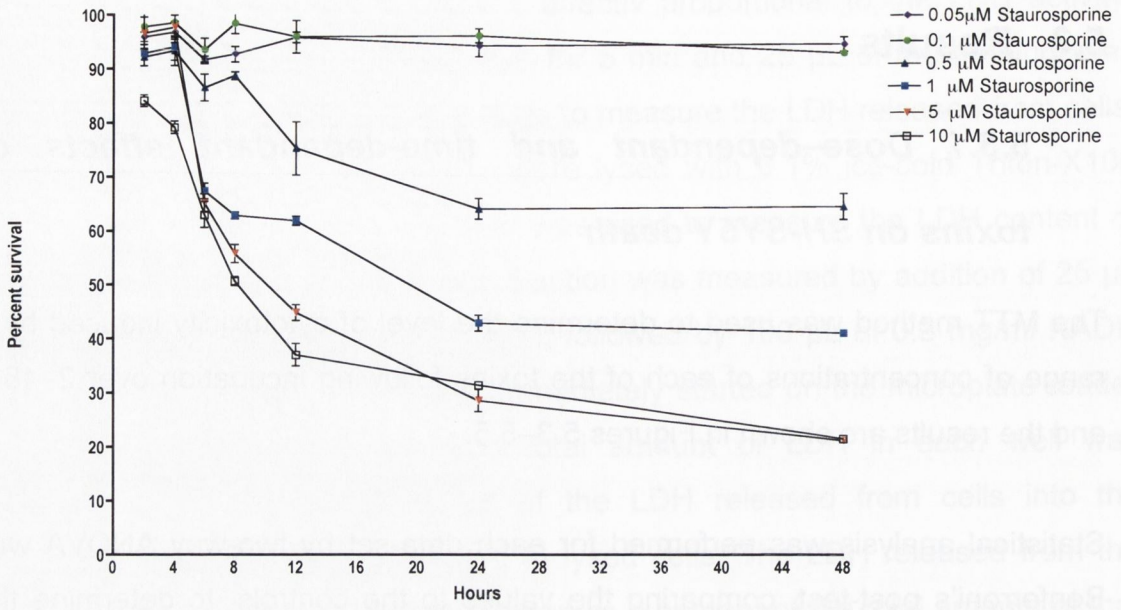

Figure 5.3 Cell viability following incubation of cells with staurosporine

SH-SY5Y cells were incubated with 0.05–10 μM concentrations of staurosporine for times periods of 2–48 h. The viability of the cells as a percentage of control, untreated cells incubated for the same periods was determined by the MTT assay. Values represent mean ± S.E.M. with n=3.

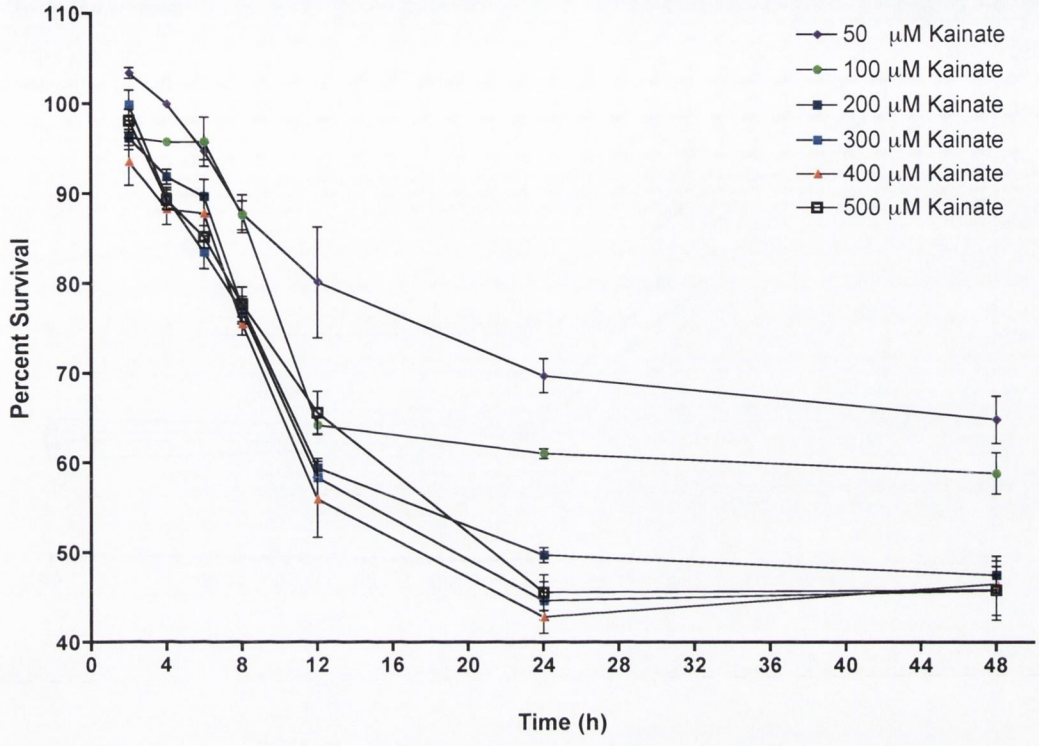

Figure 5.4 Cell viability following incubation of cells with kainate

SH-SY5Y cells were incubated with 50–500 μM concentrations of kainate for times periods of 2–48 h. The viability of the cells as a percentage of control, untreated cells incubated for the same periods was determined by the MTT assay. Values represent mean ± S.E.M. with n=3.

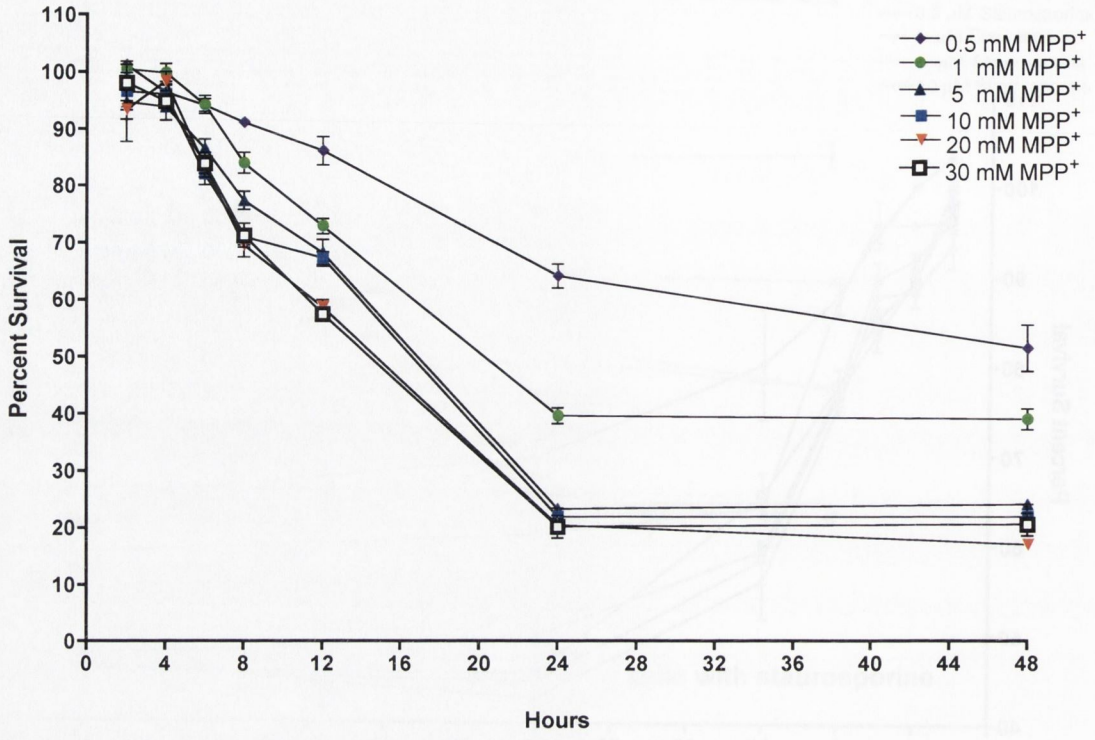

Figure 5.5 Cell viability following incubation of cells with MPP^+

SH-SY5Y cells were incubated with 0.5–30 mM concentrations of MPP^+ for a period of 2–48 h. The viability of the cells as a percentage of control, untreated cells incubated for the same periods was determined by the MTT assay. Values represent mean ± S.E.M. with n=3.

Concentration ranges of 0.5–30 mM MPP^+ on cells for incubation periods of 2–48 h were used to induce cell death. Concentrations of 10, 20 and 30 mM induced the greatest cell death, with 30% decrease in viability following an 8 h incubation and viability reduced to 20% of controls following 24 h, with no further reduction at 48 h. There was no significant change in the effect due to increasing the MPP^+ concentration from 10 mM and this was thus used to cause cell death over 6–48 h periods in further experiments.

Table 5.1 The effective concentration and incubation period of toxins

Incubation of SH-SY5Y cells with kainate, staurosporine and MPP^+ was performed over a range of time periods. The viability of the cells was then determined by the MTT assay. The survival of the cells as a percentage of the control cells was used to determine the concentration of each toxin required to give 50% cell death and the period of incubation necessary.

Toxin	Concentration	Incubation Times
Kainate	300 µM	12–48 h
Staurosporine	10 µM	2–9 h
MPP^+	10 mM	6–48 h

5.3.3.1 The effect of TRH on staurosporine toxicity

MTT viability studies

The viability of SH-SY5Y cells following incubation in 10 µM staurosporine with a range of concentrations of TRH and for a range of times was measured and the results are shown in Figure 5.3. In determining the effect due to the concentration of TRH and the period of exposure to staurosporine with TRH, two-way ANOVA analysis was performed, with comparison of the viabilities to control cells at each time, assumed to be 100% viable, and also with cells that were incubated with staurosporine alone. It was found that the degree of protection conferred by TRH depended on both the concentration of TRH

(P<0.0001, accounting for 51.9% of the variance) and the incubation time (P<0.0001, with 24.98% of the variance).

Cell viability, depicted in Figure 5.6, was significantly decreased by staurosporine after the 2 h incubation (P<0.05) and continued to decrease over each incubation period thereafter (P<0.01–0.001). Cells that were incubated with TRH and staurosporine also exhibited a decrease in viability over the times used (Figure 5.6). Cells that were incubated with 400 and 600 μM TRH with staurosporine were not significantly different to control cells initially (3 and 6 h incubations), but were significantly reduced in comparison to controls following the 9 h incubation (P<0.001), although the viabilities of cells that were incubated in the presence of 400 and 600 μM TRH with staurosporine were significantly greater than those treated with staurosporine alone after 6 and 9 h incubations (P<0.001). 300 μM TRH also showed protection against staurosporine following 6 and 9 h incubations, with significantly improved viability compared with cells treated only with staurosporine (P<0.05 and 0.01, respectively). The viabilities of cells incubated with 100 and 200 μM TRH plus staurosporine were not significantly different from those incubated with staurosporine alone after any of the incubation periods. For clarity, the effects of staurosporine and TRH are shown individually for each time period in Figure 5.7 (a–d) and analysis, performed by one-way ANOVA, revealed that treatment with 300, 400 and 600 μM TRH resulted in significant improvement in viability at 6 and 9 hours in comparison to cells incubated in staurosporine alone (P<0.05–0.001). At 2 and 3 h incubations, when the level of cell death due to staurosporine was not as great, only 600 μM TRH gave significantly improved viability (P<0.05).

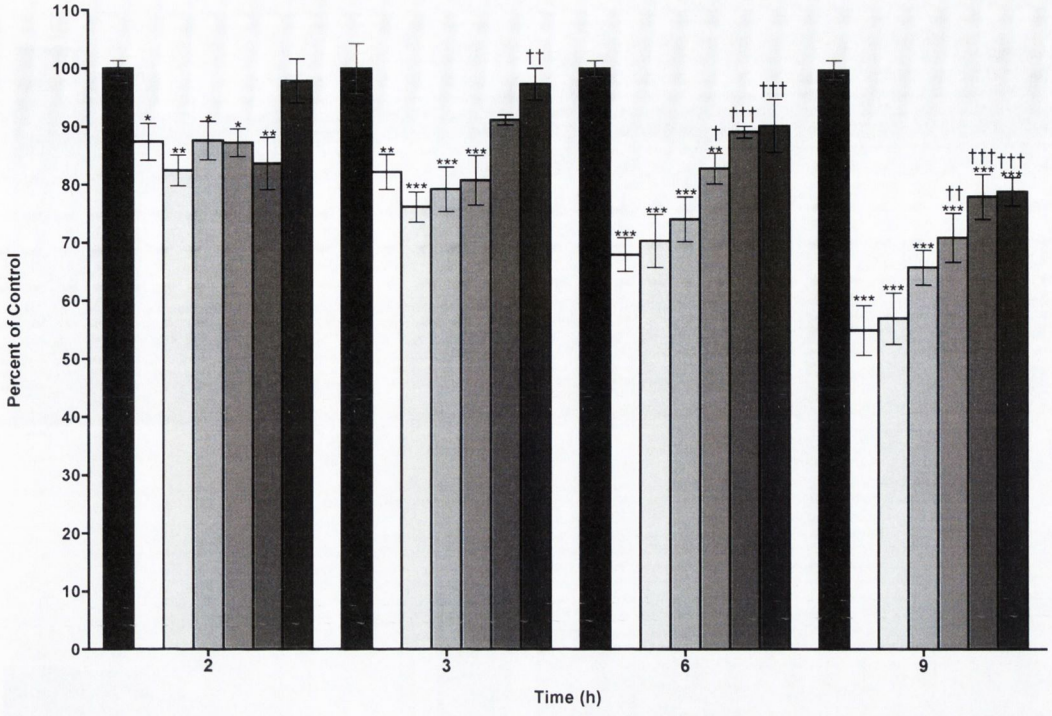

Figure 5.6 Viability of cells during incubation with staurosporine in the presence of TRH assessed by the MTT procedure

The viability of cells was determined colourimetrically by MTT conversion to formazan following 2–9 hour incubations. The viability was calculated as a percentage of that obtained for controls (■). The effect of co-incubating TRH at concentrations of 100 (□), 200 (▨), 300 (▩), 400 (■) and 600 (■) μM with 10 μM staurosporine was measured. Two-way ANOVA with Bonferroni's post-test was performed, with ***=P<0.001, **=P<0.01 and *=P<0.05, in comparison of the viabilities of control cells and †=P<0.05, ††=P<0.01 and †††=P<0.001 in comparison to cells incubated with staurosporine (▭). Data represent the mean values ± S.E.M. (n=3).

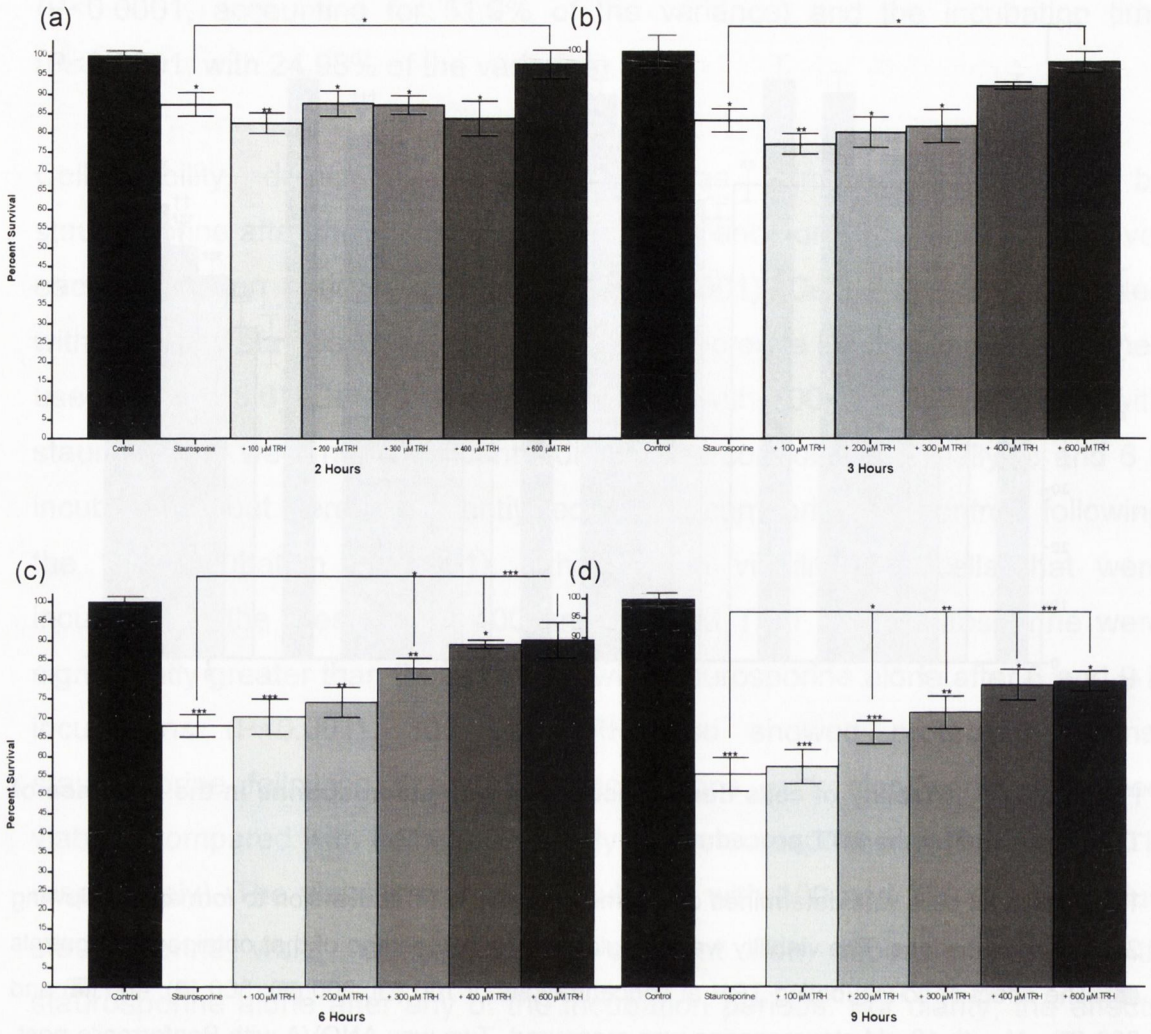

Figure 5.7 TRH protects against staurosporine-induced cell death assessed by the MTT assay

The data shown in Figure 5.6 are graphed individually for (a) 2, (b) 3, (c) 6 and (d) 9 hour incubations in 10 µM staurosporine (□), 10 µM staurosporine with 100 µM TRH (□), 10 µM staurosporine with 200 µM TRH (■), 10 µM staurosporine with 300µM TRH (■), 10 µM staurosporine with 400 µM TRH (■), 10 µM staurosporine with 600µM TRH (■) and control cells (■). The viability of cells was determined as a percentage of control, untreated cells for each incubation time and analysis was performed by one-way ANOVA with Bonferroni's post-test, with ***=P<0.001, **=P<0.01 and *=P<0.05 in comparison to control cells or, where indicated, to cells incubated with staurosporine alone. Data represent the mean values ± S.E.M. (n=3).

5.3.3.2 Propidium Iodide studies

The viabilities of cells following incubation times of 2, 3, 6 and 9 h in the presence of 10 μM staurosporine and with the addition of 100–600 μM TRH were also determined by the propidium iodide exclusion assay and the results are shown in Figure 5.8 and Figure 5.9. Statistical analysis of the viability detected for each treatment at each incubation time was calculated by two-way ANOVA with Bonferroni's post-test. Following 2 h incubation with staurosporine, 21% cell death was detected, and the staurosporine-induced cell death increased significantly between 3 and 6 h and again between 6 and 9 h (both $P<0.05$). After the 2 h incubation, there was no significant difference between staurosporine treated cells and those where TRH was also present. However, after 3 h, the level of cell death was significantly reduced in cells that had received 300 ($P<0.05$), 400 ($P<0.01$) or 600 ($P<0.05$) μM TRH with staurosporine in comparison to cells incubated with staurosporine alone. This increased level of viability detected for the 3 highest concentrations of TRH was maintained throughout the 6 and 9 h incubation periods ($P<0.001$). The lower concentrations of TRH (100 and 200 μM) had no significant protective effect at any time point. Overall, the incubation time accounted for 57.67% of the total variance and the concentration of TRH accounted for 27.15% of the variance, and both had an extremely significant effect on the viability of the cells ($P<0.0001$). Figure 5.10 shows the cell viability following treatment with staurosporine compared directly with that of cells that were treated with 600 μM TRH with staurosporine. This shows that staurosporine-treated cells had an almost linear decline in viability ($r^2=0.8499$, slope=−2.93), however this rate was attenuated by 600 μM TRH ($r^2=0.485$, slope=−0.665).

Comparison of the effects of staurosporine, assessed in the MTT assay with that from propidium iodide assay (Figure 5.11) indicated that there was no significant difference between the viabilities calculated by either method ($P=0.399$, by paired T-test). Furthermore, there was no significant difference in the level of viability resulting from the inclusion 600 μM TRH with staurosporine detected by the two different methods ($P=0.1062$, by paired T-test).

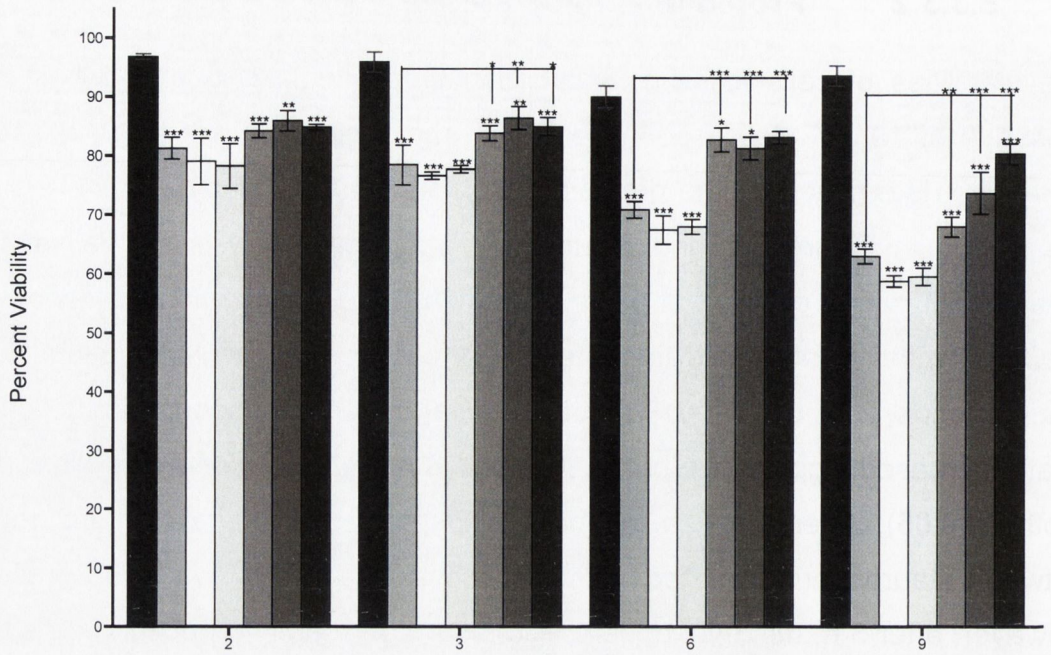

Figure 5.8 Protection by TRH against staurosporine-induced loss of viability in SH-SY5Y cells assessed by the propidium iodide exclusion procedure

The propidium iodide exclusion assay was used to determine the viability of SH-SY5Y cells as a function of the fluorescence of fully permeabilised cells, with data representing mean values ± S.E.M. (n=3). Cells were incubated for 2–9 h in 10 μM staurosporine (□), 10 μM staurosporine with 100 μM TRH (□), 10 μM staurosporine with 200 μM TRH (■), 10 μM staurosporine with 300 μM TRH (■), 10 μM staurosporine with 400 μM TRH (■), 10 μM staurosporine with 600 μM TRH (■) and the viability was compared by two-way ANOVA with Bonferroni's post-test to control cells (■), and where indicated, to cells treated with staurosporine in the absence of TRH, with *=P<0.05, **=P<0.01 and ***=P<0.001.

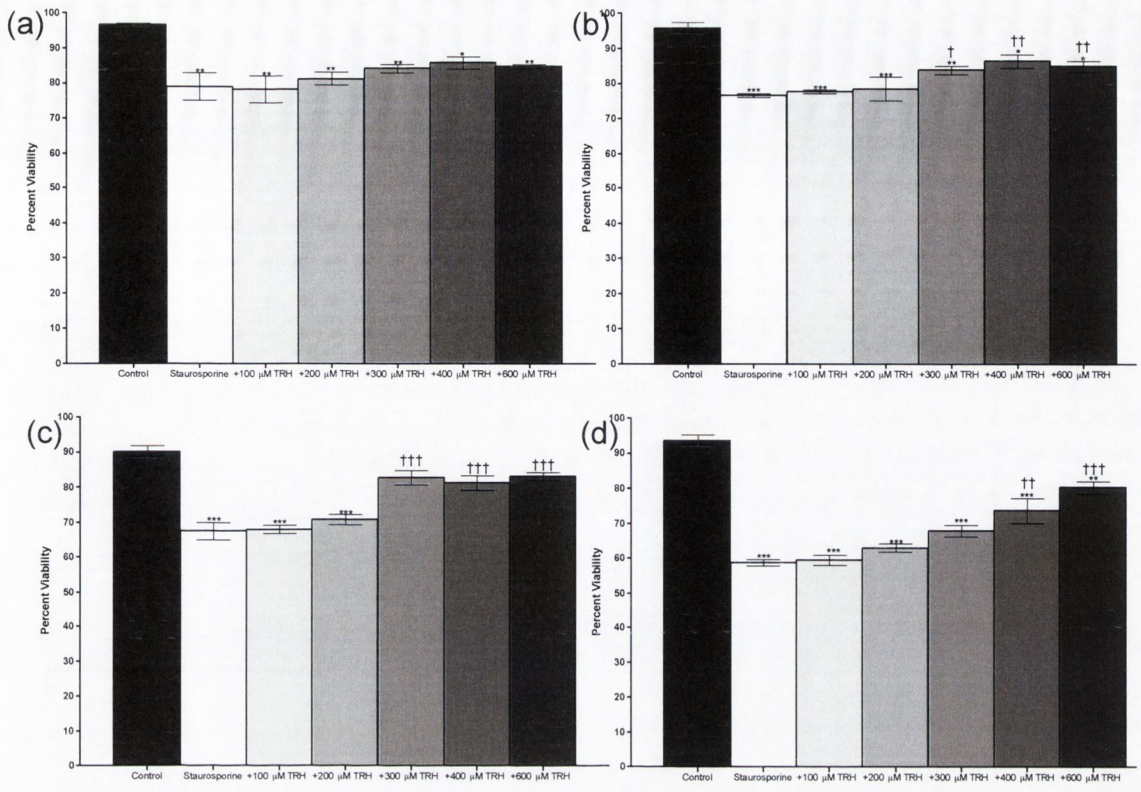

Figure 5.9 TRH protects against staurosporine-induced cell death using the propidium iodide assay

Data shown in Figure 5.8 are graphed for the individual incubations of (a) 2, (b) 3, (c) 6 and (d) 9 hour in 10 μM staurosporine (□), 10 μM staurosporine with 100 μM TRH (□), 10 μM staurosporine with 200 μM TRH (□), 10 μM staurosporine with 300 μM TRH (■), 10 μM staurosporine with 400 μM TRH (■), 10 μM staurosporine with 600 μM TRH (■) and control cells (■). The viability of cells was determined as a percentage of control, untreated cells for each incubation time and analysis was performed by one-way ANOVA with Bonferroni's post-test, with ***=P<0.001, **=P<0.01 and *=P<0.05 in comparison to control cells and †=P<0.05, ††=P<0.01 and †††=P<0.001 in comparison to cells incubated with staurosporine alone. Data represent the mean values ± S.E.M. (n=3).

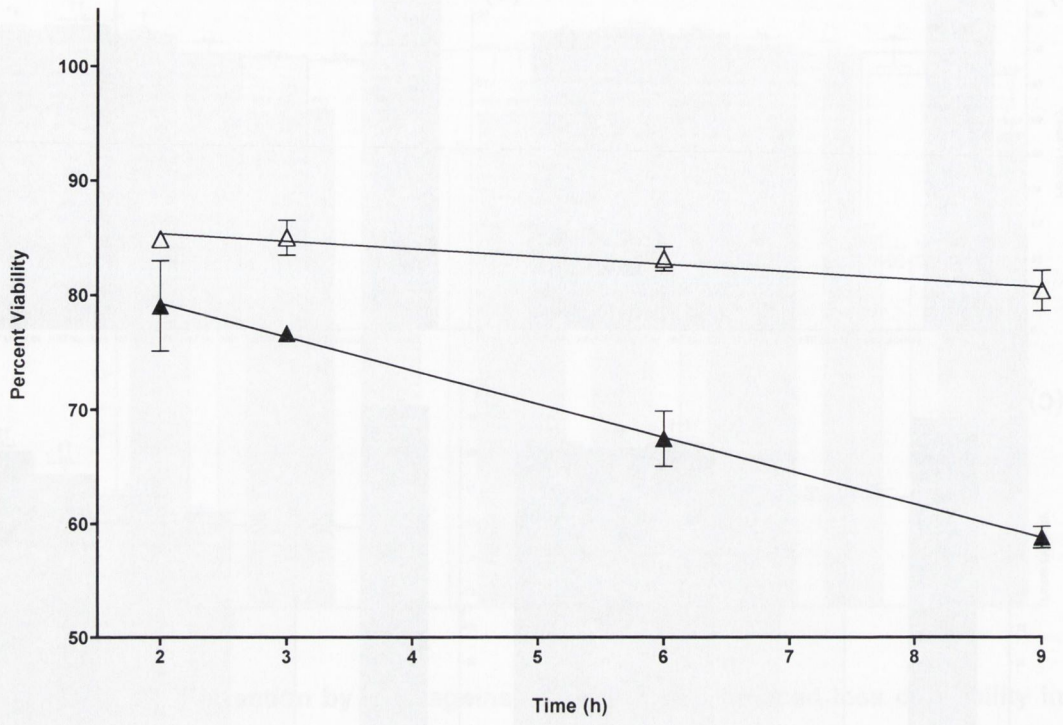

Figure 5.10 Incubation with 600 μM TRH and staurosporine protects against staurosporine-induced death, as assessed by the propidium iodide assay

The viability data (Figure 5.8) for staurosporine-treated cells (▲) and those that were co-incubated with 600 μM TRH (△) are replotted to show the decline in viability over the incubation periods (2–9 h). Data represent mean values ± S.E.M. (n=3) and linear regression analysis was performed.

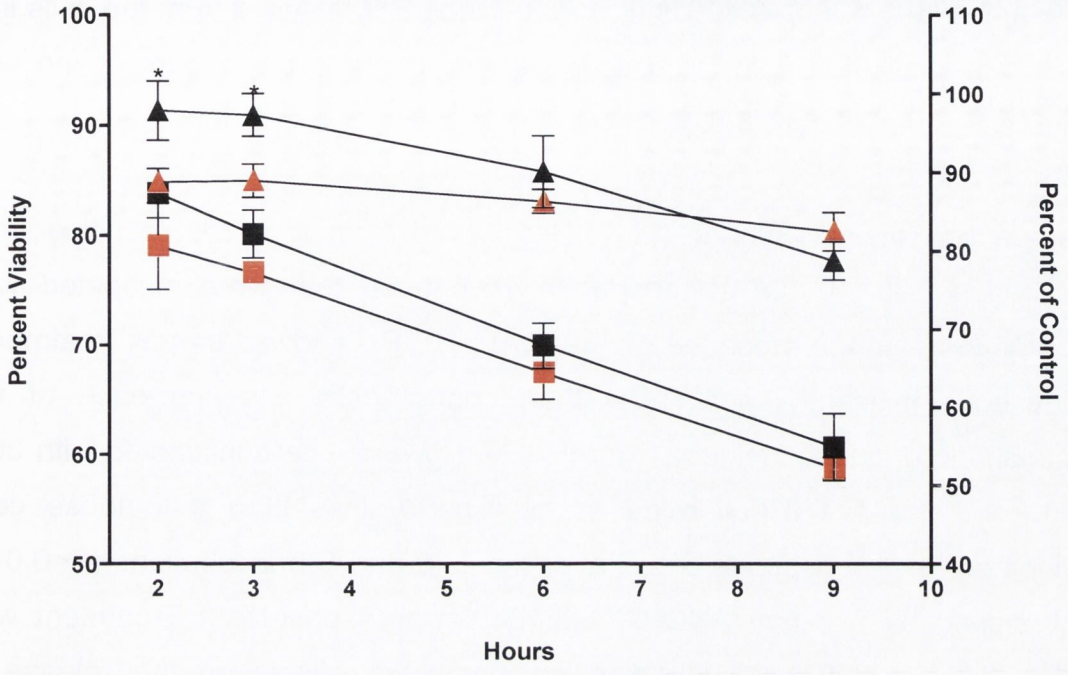

Figure 5.11 Comparison of the cell viability due to staurosporine treatment detected by MTT and propidium iodide exclusion assays

The cell viability measured by both reductase-activity (MTT; Figure 5.6) and membrane integrity (PI; Figure 5.8) due to treatment with staurosporine (PI=■; MTT=■) and with staurosporine in the presence of 600 µM TRH (PI=▲; MTT=▲) were replotted for comparison of the effect of the viabilities detected by each assay. Two-way ANOVA analysis was performed comparing PI with MTT values for staurosporine in the absence of TRH (■ vs. ■) and comparing PI with MTT in the presence of TRH (▲vs. ▲), with *=P<0.05.

5.3.2.3 Effect of TRH and staurosporine on LDH release

The total amount of LDH did not vary significantly between wells, with an average value of 58.3±0.49 U/mL (n=63). The LDH released from the cells into each well was then calculated as a percent of the total amount of the well (Figure 5.12 and Figure 5.13).

Comparison of the amounts of LDH released from the cells resulting from incubation with 10 μM staurosporine with those that were incubated with staurosporine in the presence of 100–600 μM TRH showed that all treatments released significantly more LDH than control cells following each of the incubation periods examined (Figure 5.12). However, cells incubated with 300, 400 or 600 μM TRH all released significantly less LDH than those cells incubated in staurosporine alone after the 3, 6 and 9 h incubations ($P<0.001$, determined by two-way ANOVA with Bonferroni's post-test). Treatment with either 100 or 200 μM TRH had no significant effects on the release in comparison with cells treated with staurosporine alone. For clarity, the data shown in Figure 5.12 were replotted in Figure 5.13 as individual bar-charts at each of the incubation periods.

5.3.2.4 Caspase activity following staurosporine treatment

Initiation of apoptosis in cells was analysed by assaying for caspase activity following incubation of the cells with staurosporine alone or with 100–600 μM TRH for 3, 6 and 9 h periods (Figure 5.14 and Figure 5.15). Two-way ANOVA analysis revealed that both time and treatment affected the activation of apoptosis; with the concentration of TRH used accounting for 80.9% of the variation ($P<0.0001$) and the length of exposure influencing 6.96% of the variation ($P<0.0001$). Cells incubated with staurosporine alone or in conjunction with 100, 200 or 300 μM TRH had significantly greater caspase activity than control cells. However, inclusion of 600 μM TRH and staurosporine gave significant protection, there being no significant difference in caspase activity in comparison to the control cells after each of the incubation periods.

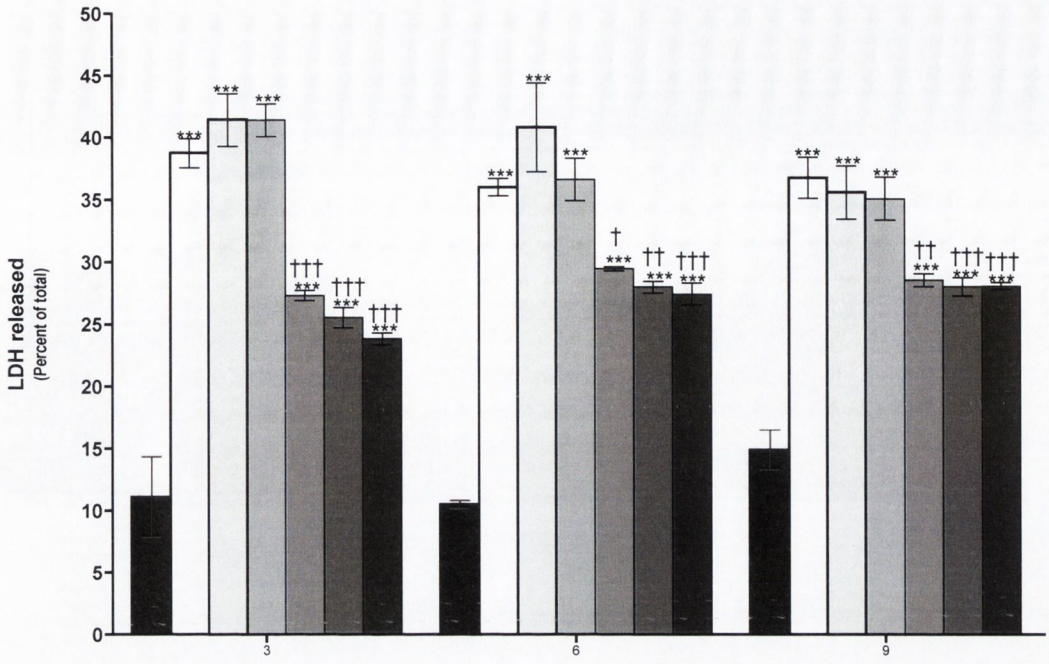

Figure 5.12 The release of lactate dehydrogenase from SH-SY5Y cells resulting from incubation with staurosporine

The release of lactate dehydrogenase (LDH) from cells was measured as a percentage of the total amount of LDH contained in each well (calculated by addition of the LDH found in the medium with the amount contained in lysed cells). Statistical analysis was performed by two-way ANOVA with Bonferroni's post-test (n=3 for all treatments). The release of LDH from control cells (■) and from cells incubated with 10 μM staurosporine (□) was compared with the LDH released from cells that were incubated with staurosporine and 100μM TRH (□), 200 μM TRH (□), 300 μM TRH (■), 400 μM TRH (■) or 600 μM TRH (■). With ***=P<0.001 in comparison to controls and †=P<0.05, ††=P<0.01 and †††=P<0.001 in comparison to cells incubated with staurosporine alone.

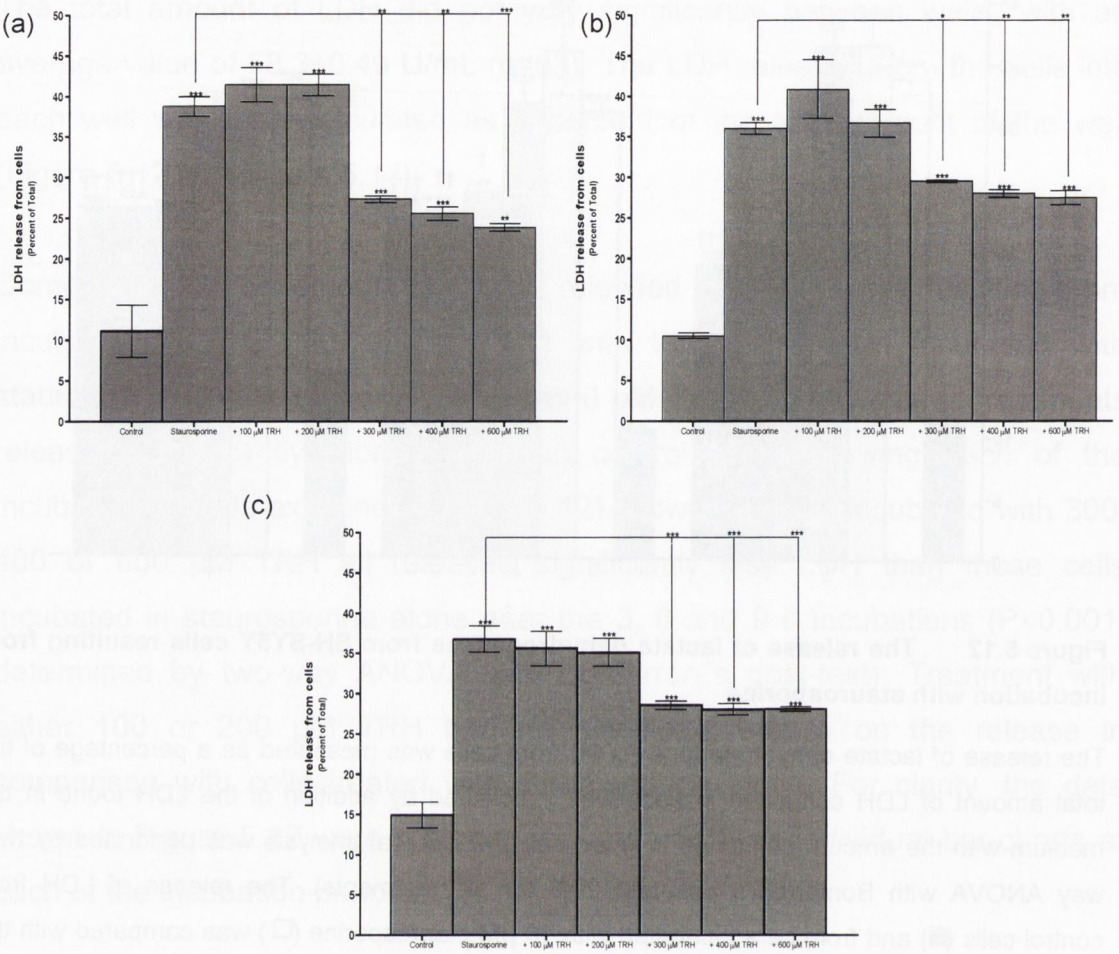

Figure 5.13 TRH attenuates staurosporine-induced lactate dehydrogenase release from SH-SY5Y cells

The data presented in Figure 5.12 are replotted for clarity as the percent of LDH released from cells incubated with 10 µM staurosporine with 100–600 µM TRH following (a) 3, (b) 6 and (c) 9 h incubations. One- way ANOVA with Bonferroni's post-test (n=3 for all treatments) was performed comparing the LDH released due to staurosporine with TRH incubation with the LDH released from cells incubated with staurosporine alone, and in comparison to control cells where indicated.

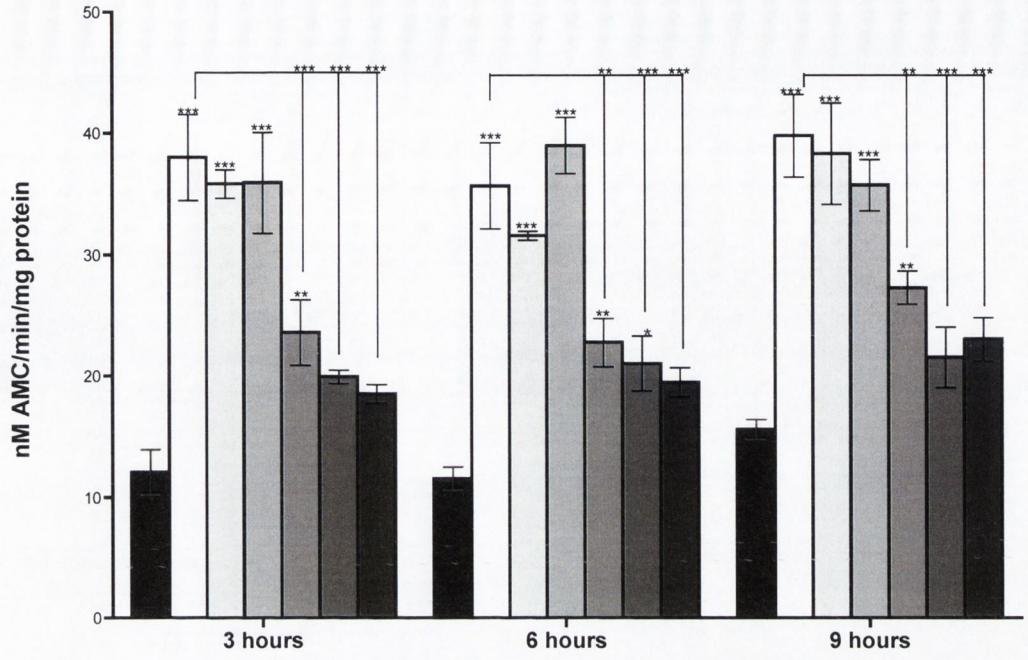

Figure 5.14 Caspase activation in cells following incubation in staurosporine

Cultures of SHSY-5Y cells treated with 10 μM staurosporine (□), and staurosporine with 100 μM TRH (□), 200 μM TRH (□), 300 μM TRH (■), 400 μM TRH (■) and 600 μM TRH (■), in addition to control cells incubated in medium (■) for 3–9 h were assayed for caspase activity. Statistical analysis was performed by two-way ANOVA with Bonferroni's post-test (n=3 for all treatments), to compare the effect of TRH and the length of incubation, with **=P<0.01 and ***=P<0.001 in comparison to cells incubated with staurosporine alone.

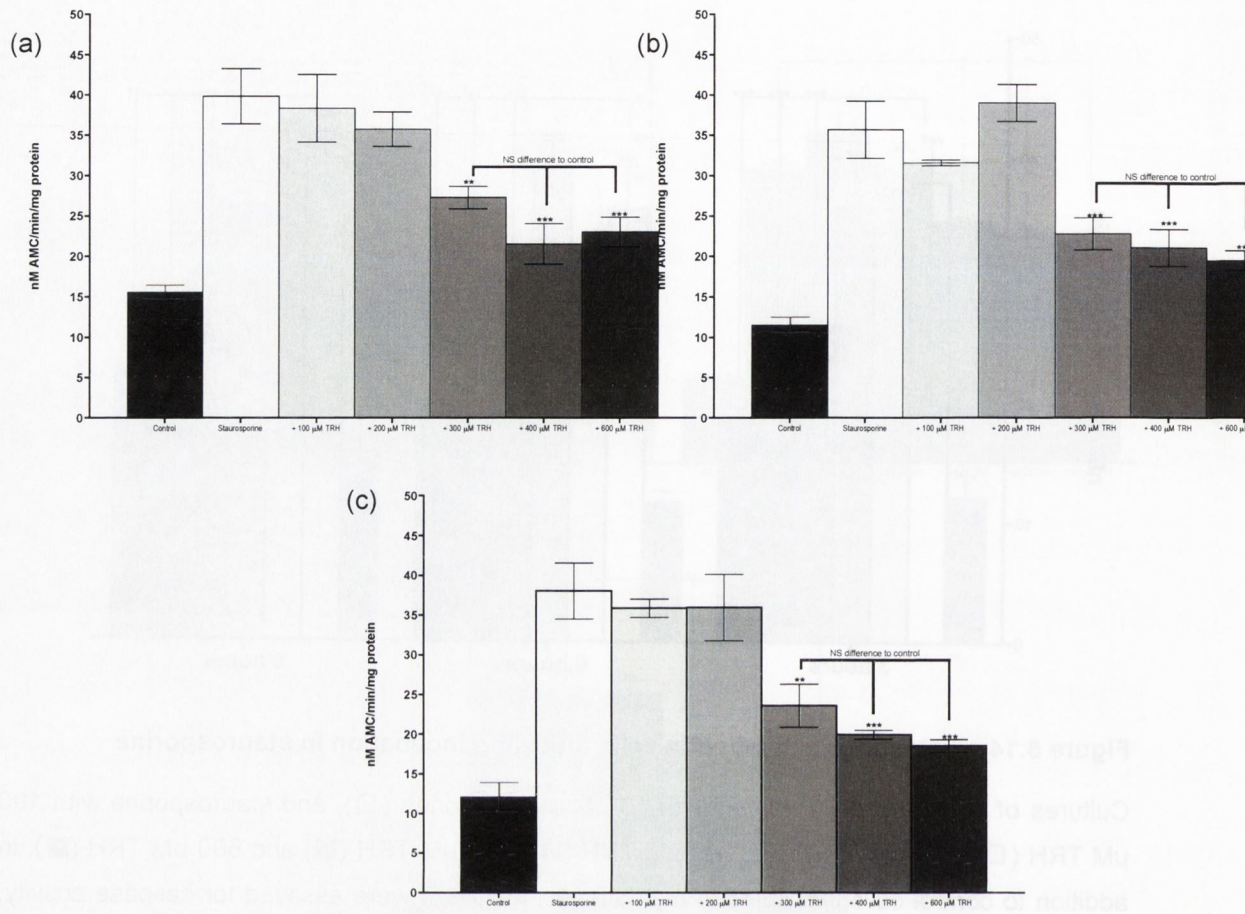

Figure 5.15 TRH prevents apoptosis in SH-SY5Y cells following exposure to staurosporine

Cultures of SHSY-5Y cells treated with 10 µM staurosporine (□), and staurosporine with 100 µM TRH (□), 200 µM TRH (□), 300 µM TRH (□), 400 µM TRH (■) and 600 µM TRH (■), in addition to control cells incubated in medium (■) for (a) 3, (b) 6 and (c) 9 h were assayed for caspase activity. Statistical analysis was performed by one-way ANOVA with Bonferroni's post-test (n=3 for all treatments), to compare the effect of TRH and the length of incubation, with **=P<0.01 and ***=P<0.001 in comparison to cells incubated with staurosporine alone and with control cells where indicated.

Although incubation with 300 μM TRH plus staurosporine resulted in greater caspase activity than control cells, the level detected following 3 ($P<0.001$), 6 ($P<0.01$) and 9 ($P<0.01$) h incubations was significantly less than the activity found in cells incubated in staurosporine alone. Treatment with TRH concentrations of 400 and 600 μM TRH also resulted in significantly less caspase activity than the staurosporine treated cells following each of the incubation periods used ($P<0.001$ in each case). The data from Figure 5.14 were replotted, for clarity, with each incubation period shown individually (Figure 5.15). One-way ANOVA analysis with Bonferroni's post-test was used to compare caspase activity following incubation with staurosporine for (a) 3, (b) 6 and (c) 9 h in comparison to the effects of co-incubation of TRH (100–600 μM) with staurosporine and the caspase activity measured in control cells. This analysis showed that following each of the incubation periods, the caspase activity in cells treated with the three highest TRH concentrations (300, 400 and 600 μM) did not significantly differ from control cells, and that the caspase activity levels were significantly lower than those of cells incubated with staurosporine alone (P values ranged from <0.01 to <0.001).

5.3.2.5 Comparison of the different detection procedures

The effects of incubation with staurosporine in the presence and absence of TRH over time measured by the different assay methods was compared, initially by comparison of the MTT and propidium iodide methods (Figure 5.11), and subsequently by comparison of the percentage cell death measured by propidium iodide and the release of LDH, both determined as percentages of the total cell number and plotted on the same y-axis with the rate of caspase activity plotted on the opposite y-axis (Figure 5.16). This comparison is for illustrative purposes. It shows the protection due to the highest concentration of TRH used (600 μM) in incubations with staurosporine. Two-way ANOVA with Bonferonni's post-test comparison of the effects of staurosporine incubation show that the cell death due to apoptosis measured by caspase activity did not differ from that assessed by the release of LDH, nor was there a difference between these measurements and the level of cell death, measured by propidium iodide exclusion, following 6 or 9 h incubations. However, when cells

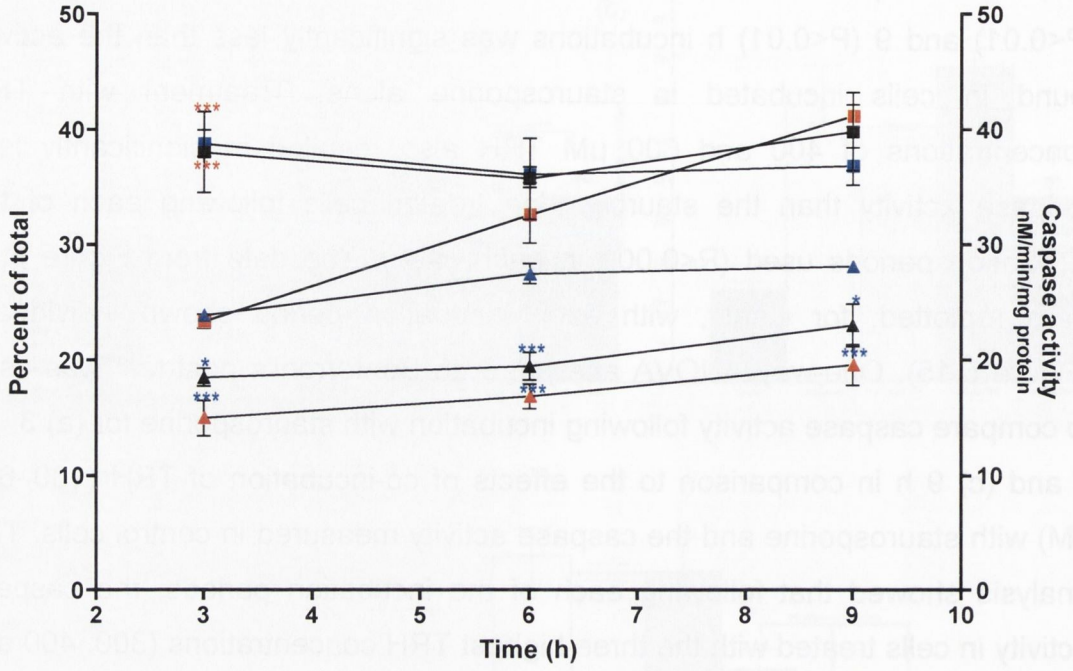

Figure 5.16 The effect of staurosporine in the presence and absence of 600 µM TRH measured by propidium iodide exclusion, release of LDH and caspase activity

The data for cells incubated with staurosporine from the propidium iodide assay=■ (Figure 5.8), release of LDH =■ (Figure 5.12) and measurement of caspase activity=■ (Figure 5.14) and cells incubated with the highest concentration of TRH (600 µM; ▲=propidium iodide, ▲= LDH release and ▲=caspase activity) are grouped here for comparison of the results. Cell death measured by propidium iodide was measured as a function of the total cell number and the release of LDH was measured as the percentage of the total LDH, and is thus a function of the total cell number, and both are plotted on the left y-axis. Caspase activity was determined as the rate of AMC released as a function of protein and is plotted as such on the right y-axis. Data represent mean values ± S.E.M. (n=3) and analysis was performed by two-way ANOVA with Bonferroni's post-test and comparison was made between the data obtained in the absence of TRH, with ***=P<0.001 in comparison to the propidium iodide assay. Data from the incubation of cells with staurosporine with 600 µM TRH were analysed in the same manner with *=P<0.05 compared to caspase activity and **=P<0.01 and ***=P<0.001 compared to LDH release.

were incubated with 600 μM TRH plus staurosporine there was a significant difference between the levels of caspase activity and LDH release following 3, 6 and 9 h incubations ($P<0.05$, <0.001 and <0.05, respectively), unlike cells that did not receive TRH-treatment. There was no difference between propidium iodide detected cell death and caspase activity. Unlike cell incubation with staurosporine alone, the co-incubation with 600 μM TRH resulted in significant differences between the levels of propidium iodide detected cell death and the release of LDH from cells ($P<0.001$ following each incubation). The overall effects of 300, 400 and 600 μM TRH incubation with staurosporine on the viabilities assessed by each of the assays is summarized in Table 5.2.

Table 5.2 Comparison of the effects of staurosporine in the absence and presence of TRH

The effect of 10 μM staurosporine on SH-SY5Y cells with 0–600 μM TRH was measured by the MTT, propidium iodide, LDH release and caspase activation procedures following incubation for 3, 6 and 9 h. This table summarises the results obtained from these assays, presented in Figures 5.6–5.14, excluding the data obtained for 100 and 200 μM TRH which had no significant effects, when compared to staurosporine. The data of all assays were analysed by two-way ANOVA with Bonferroni's post-test, with comparison made to control cells (*=P<0.05, **=P<0.01 and ***=P<0.001) and comparison of cells incubated with TRH and staurosporine to cells incubated in staurosporine alone (†=P<0.05, ††=P<0.01 and †††=P<0.001) and -=no significant difference detected.

Assay type	Staurosporine (10 μM)				Staurosporine (10 μM) + TRH (300 μM)				Staurosporine (10 μM) + TRH (400 μM)				Staurosporine (10 μM) + TRH (600 μM)			
Time (h)	2	3	6	9	2	3	6	9	2	3	6	9	2	3	6	9
MTT	*	**	***	***	* -	*** -	** †	*** ††	** -	- -	- †††	*** †††	- -	- ††	- †††	*** †††
PI	***	***	***	***	*** -	*** †	* †††	*** ††	** -	** ††	* †††	*** ††	*** -	*** †	- †††	*** †††
%LDH Release	/	***	***	***	/	*** †††	*** †	*** ††	/	*** †††	*** ††	*** †††	/	*** †††	*** †††	*** †††
Caspase Activity	/	***	***	***	/	** †††	** ††	** ††	/	- †††	* †††	- †††	/	- †††	- †††	- †††

5.3.3 The effect of TRH on kainate induced toxicity

5.3.3.1 Viability studies with MTT assay

The viability of SH-SY5Y cells following incubation in 300 μM kainate with a range of concentrations of TRH for a range of times was measured by the MTT assay. The incubation periods, 8–48 h, were determined in Figure 5.6. The effects of TRH on the viability of the cells are shown in Figure 5.17 and Figure 5.18. Analysis of Figure 5.17 by two-way ANOVA revealed that both the incubation time and the concentration of TRH affected cell viability, with time accounting for about 13% of the variance and the amount of TRH accounting for about 70%, with significant interaction between the incubation period and concentration of TRH, which accounts for about 10% of the variance.

The data presented in Figure 5.17 showed that cell viability was significantly decreased by kainate after 8 h and continued to decrease over the incubation period. It was found, by Bonferroni's post-test following two-way ANOVA, that neither incubations in 100 nor 200 μM TRH with kainate had any effect on the decrease in cell viability at any of the time points examined. Cells treated with 300, 400 and 600 μM TRH with kainate had significantly improved viabilities compared to cells that were incubated in kainate alone at 8, 12 and 24 h. Following the 48 h incubation two-way ANOVA analysis revealed the 300 μM TRH did not differ from kainate treated cells, although both 400 and 600 μM TRH were significantly more viable ($P<0.05$ and $P<0.01$, respectively). The data presented in Figure 5.17 were then reanalysed by one-way ANOVA with Bonferroni's post-test for each incubation length [Figure 5.18 (a–d)]. Cells that were co-incubated with 300, 400 or 600 μM TRH as well as kainate were not significantly different to control cells after 8 and 12 h, although they were significantly less viable following the 24 and 48 h periods ($P<0.001$ for each comparison). However, these higher concentrations of TRH resulted in significantly improved viabilities, compared to those cells that were incubated in kainate alone following these incubation periods (for 24 h incubation, $P<0.001$ for each of the three concentrations, for the 48 h incubation, $P<0.01$ for 400 and $P<0.05$ for 600 μM TRH).

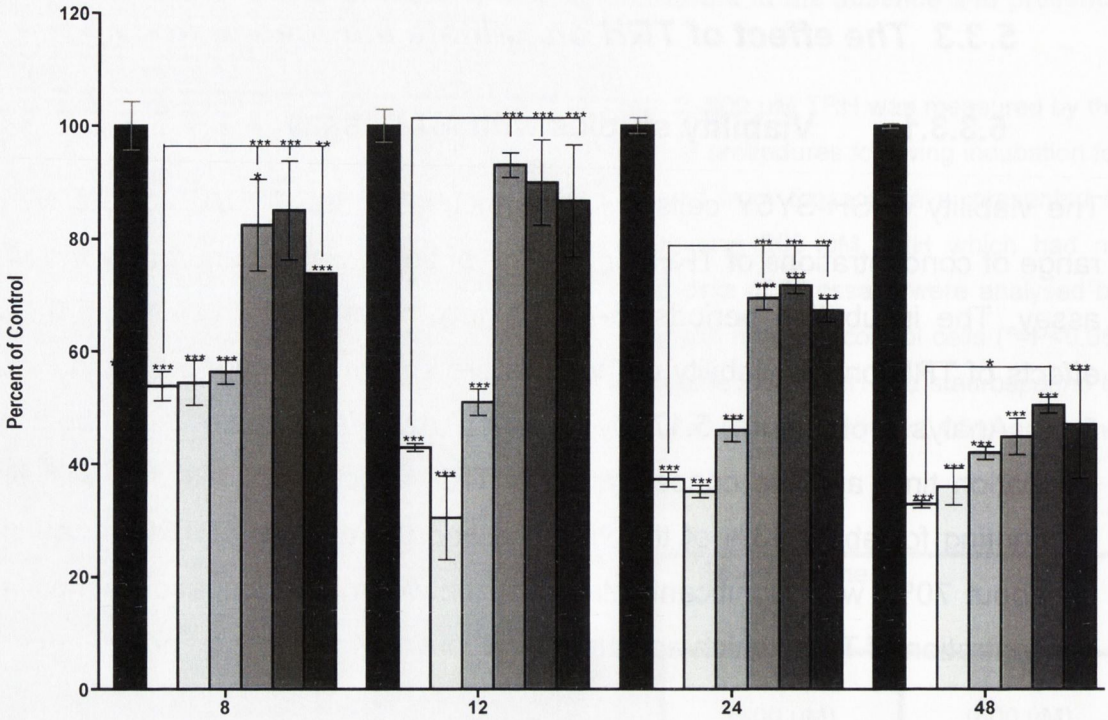

Figure 5.17 Cell viability following incubation with kainate in the presence of TRH as assessed by the MTT procedure

The viability of SH-SY5Y cells was determined colorimetricly by MTT conversion to formazan following 8–48 hour incubations in 300 μM kainate (□), 300 μM kainate with 100 μM TRH (□), 300 μM kainate + 200 μM TRH (▒), 300 μM kainate + 300 μM TRH (▒), 300 μM kainate + 400 μM TRH (■), 300μM kainate + 600μM TRH (■) and controls (■). Two-way ANOVA with Bonferroni's post-test was used to compare the viability of TRH-treated cells to control cells and, where indicated, to kainate-treated cells. Data points represent the mean values ± S.E.M. (n=3), with ***=P<0.001, **=P<0.01 and *=P<0.05.

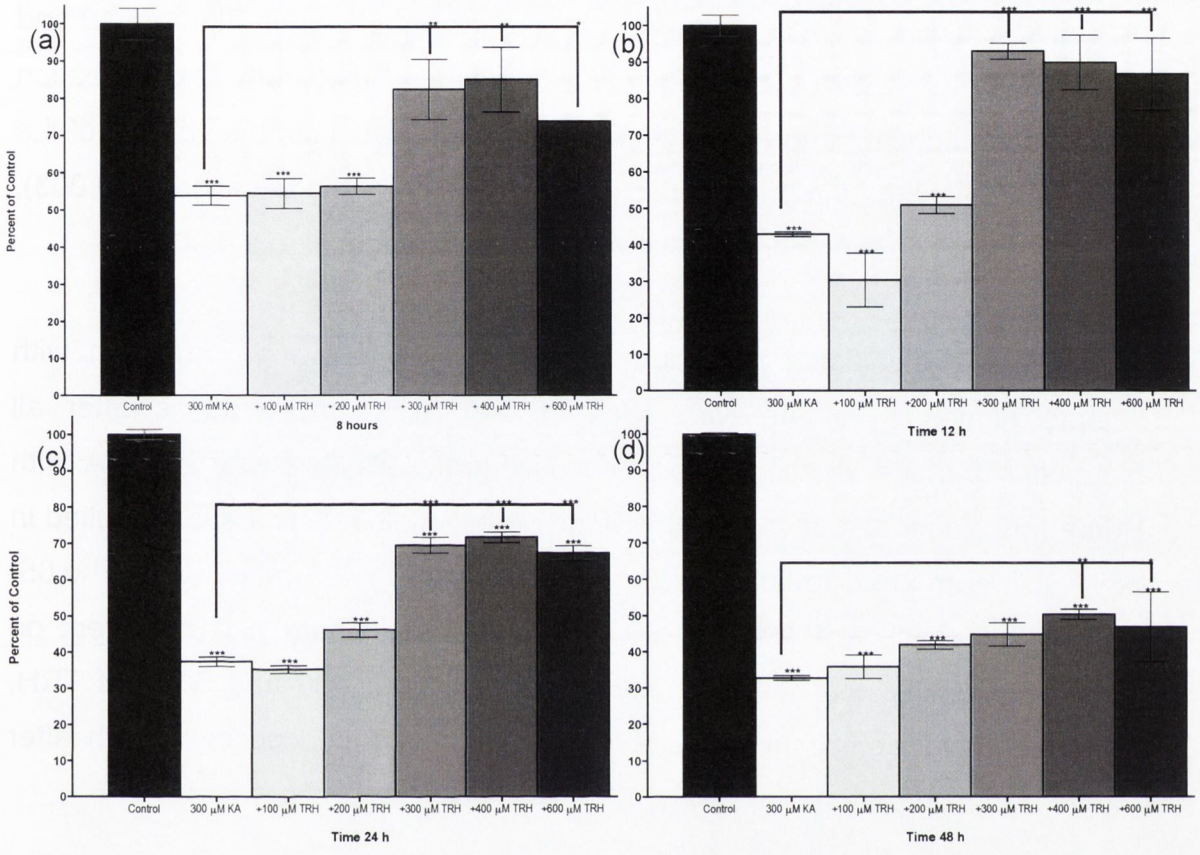

Figure 5.18 TRH attenuates kainate-induced cell death using the MTT assay

The viability of SH-SY5Y cells, plotted in Figure 5.17, is presented here for the individual incubation periods of (a) 8, (b) 12, (c) 24 and (d) 48 h. 300 µM kainate =□, 300 µM kainate with 100 µM TRH=□, 300 µM kainate with 200 µM TRH=□, 300 µM kainate with 300 µM TRH=□, 300 µM kainate with 400 µM TRH=□, 300 µM kainate with 600 µM TRH=■ and control cells (■). The viability of cells was determined as a percentage of control, untreated cells for each incubation time. One-way ANOVA with Bonferroni's post-test was performed for each plot to compare the viability of TRH-treated cells to control cells and, where indicated, to cells treated with kainate alone. Each bar representing the mean of n=3 ± S.E.M, with *=P<0.5, **=P<0.01 and ***=P<0.001.

5.3.3.2 Propidium iodide exclusion

The viabilities of cells following treatment times of 8, 12, 24 and 48 h with 300 μM kainate in the presence of 100–600 μM TRH were determined by the propidium iodide exclusion assay and the results are shown in Figure 5.19 and Figure 5.20. Analysis by two-way ANOVA revealed that both the incubation time and the concentration of TRH used significantly affected the viability of the cells with the incubation period accounting for ~2.9% of the variation ($P=0.003$), and TRH concentration accounts for ~86.3% of the variation ($P<0.0001$).

There was a significant reduction in cell viability following incubation with kainate alone or kainate with each of the TRH concentrations after all incubation periods when compared with control cells (two-way ANOVA with Bonferroni's post-test gave $P<0.001$ in all cases). Kainate incubation resulted in 35% cell death after 8 h incubation, which declined to 46% after 48 h ($P<0.05$) and the incubation of 100 or 200 μM TRH with kainate had no effect on protecting against the cell loss. Treatment with 300, 400 and 600 μM TRH, however, gave significant protection against kainate-induced cell death after each incubation period.

A pairing of the loss of cell viability determined due to kainate obtained in the MTT assay with that from propidium iodide demonstrated that there was a significant difference between the viabilities calculated by the two methods (P0.006, by paired t-test; Figure 5.20). However, comparison of the viabilities due to incubation with 600 μM TRH with kainate showed that those measured by the MTT and propidium iodide procedures gave cell viability values that did not significantly differ.

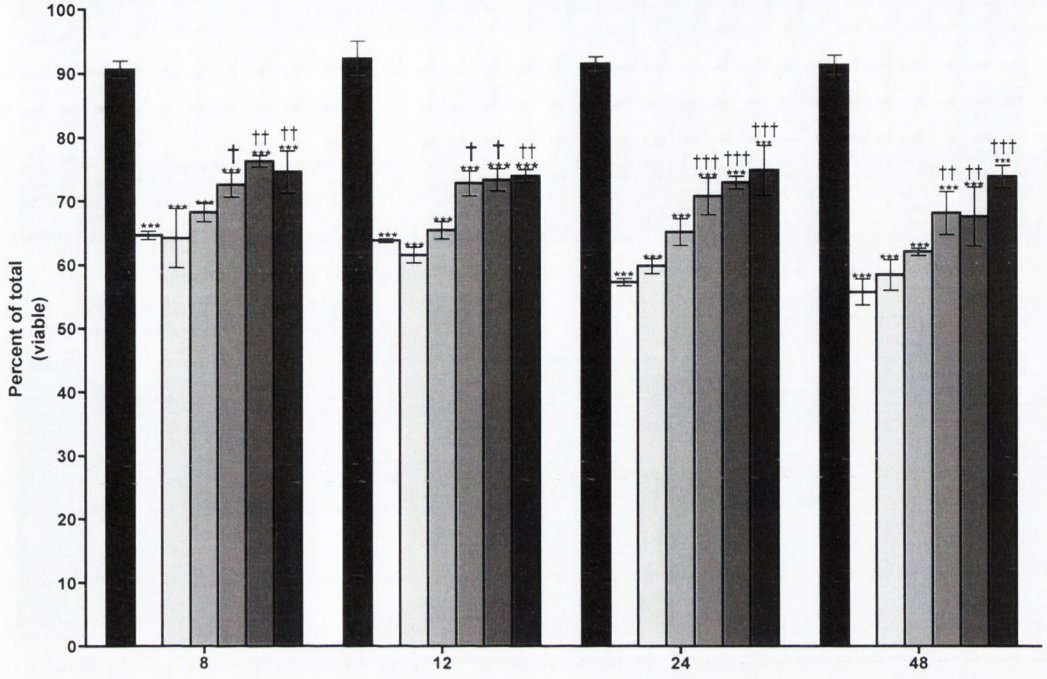

Figure 5.19 Protection by TRH against kainate-induced loss of viability in SH-SY5Y cells as assessed by the propidium iodide procedure

Cell viability was determined by propidium iodide exclusion following 8–48 hour incubation of the cells in medium (■), 300 μM kainate (□), 300 μM kainate with 100 μM TRH (□), 300 μM kainate with 200 μM TRH (□), 300 μM kainate with 300 μM TRH (□), 300 μM kainate and 400 μM TRH (■), 300 μM kainate and 600 μM TRH (■). Data represent the mean ± S.E.M. (n=3). Two-way ANOVA with Bonferroni's post-test was performed for each time point, with ***=P<0.001, **=P<0.01 and *=P<0.05 in comparison to control cells and †=P<0.05, ††=P<0.01 and †††=P<0.001 compared to cells incubated with kainate alone.

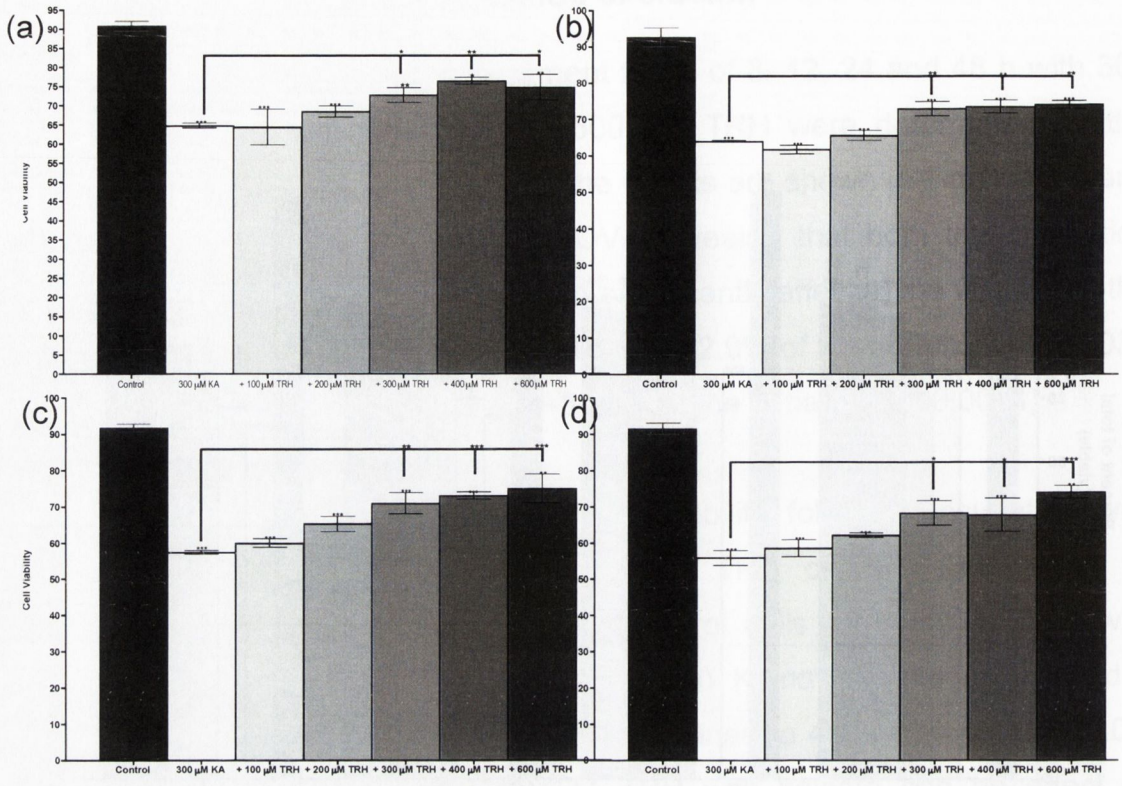

Figure 5.20 TRH protects against kainate-induced cell death in the propidium iodide assay

The viability of SH-SY5Y cells, plotted in Figure 5.19, is presented here for the individual incubation periods of (a) 8, (b) 12, (c) 24 and (d) 48 h. One-way ANOVA with Bonferroni's post-test was performed for each plot to compare the viability of TRH-treated cells to control cells and, where indicated, to cells treated with kainate alone. Each bar representing the mean of n=3 ± S.E.M, with *=P<0.5, **=P<0.01 and ***=P<0.001. 300 µM kainate (□), 300 µM kainate with 100 µM TRH (□), 300 µM kainate and 200 µM TRH (□) , 300 µM kainate and 300 µM TRH (□), 300 µM kainate and 400 µM TRH (■), 300 µM kainate and 600 µM TRH (■) and control cells (■).

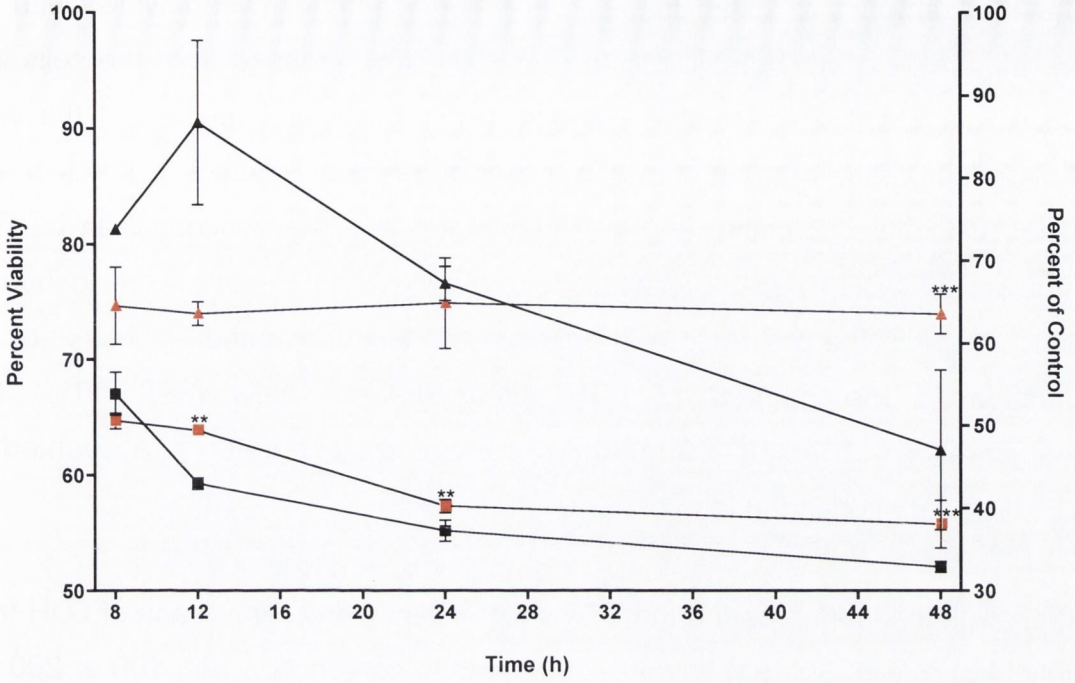

Figure 5.21 Comparison of the cell viability due to kainate treatment detected by MTT and propidium iodide exclusion assays

The cell viability measured by both reductase-activity (MTT; Figure 5.17) and membrane integrity (PI; Figure 5.19) due to treatment with kainate (PI=■; MTT=■) and with kainate in the presence of 600 µM TRH (PI=▲; MTT=▲) were replotted for comparison of the measurement of the cell viability determined by each of the assays. Two-way ANOVA analysis was performed comparing PI with MTT values for kainate in the absence of TRH (■ vs. ■) and comparing PI with MTT in the presence of TRH (▲vs. ▲), with **=P<0.01 and ***=P<0.001.

5.3.3.3 Effect of TRH and kainate on LDH release

The total amount of LDH did not vary significantly between wells, with an average value of 68.7±1.3 U/mL (n=63). The LDH released from the cells into each well was then calculated as a percent of the total amount of the well. Comparison of the amount of LDH released from cells (Figure 5.22) by two-way ANOVA showed both the length of incubation and the concentration of TRH affected the LDH release. The length of time (12–48 h) cells were incubated with kainate in the presence and absence of TRH accounted for 14.7% of the variation in the amount of LDH released from cells ($P<0.0001$). The concentrations of TRH (0–600 μM) that cells were incubated with accounted for 42.6% of variation in the loss of LDH.

After each incubation period there was significantly greater release of LDH from cells treated with 300 μM kainate, or kainate in conjunction with 100 or 200 μM TRH compared to LDH lost from control cells. Cells co-incubated with 300, 400 or 600 μM TRH in the presence of kainate showed no significant increase in LDH release compared to the control cells after 12 h incubation, although after 24 and 48 h incubations the release of LDH was significantly greater than control cells. These three higher concentrations of TRH significantly reduced the loss of LDH from cells compared to cells that were incubated with kainate alone after both 12 and 48 h incubations ($P<0.01$ and $P<0.001$, respectively).

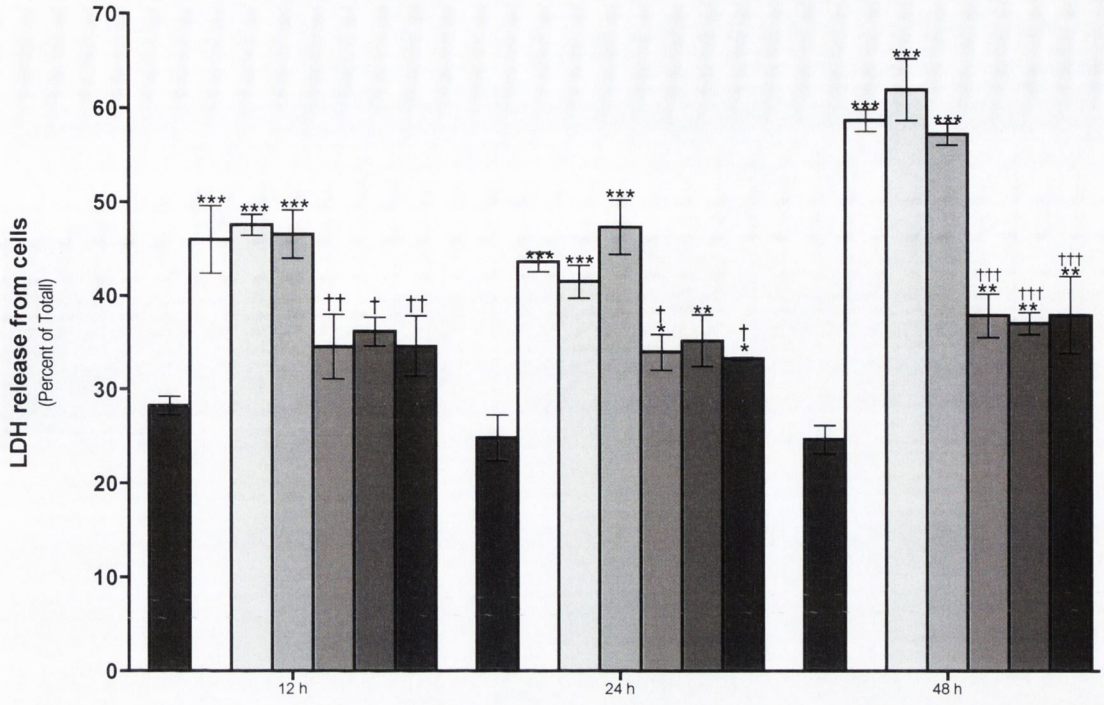

Figure 5.22 The release of LDH from SH-SY5Y cells due to incubation with kainate

Cells were incubated for 12–48 h in medium (■), 300 μM kainate (□), 300 μM kainate with 100 μM TRH (□), 300 μM kainate and 200 μM TRH (□), 300 μM kainate and 300 μM TRH (□), 300 μM kainate and 400 μM TRH (■), 300 μM kainate and 600 μM TRH (■). The release of LDH as a percent of the total amount of LDH was analysed by two-way ANOVA with Bonferroni's post-test to compare the LDH released during TRH incubation with kainate to the LDH released from control cells (*=P<0.05, **=P<0.01 and ***=P<0.001) and to the LDH released from cells incubated in kainate alone (†=P<0.05, ††=P<0.01 and †††=P<0.001). Data represent mean values ± S.E.M. (n=3).

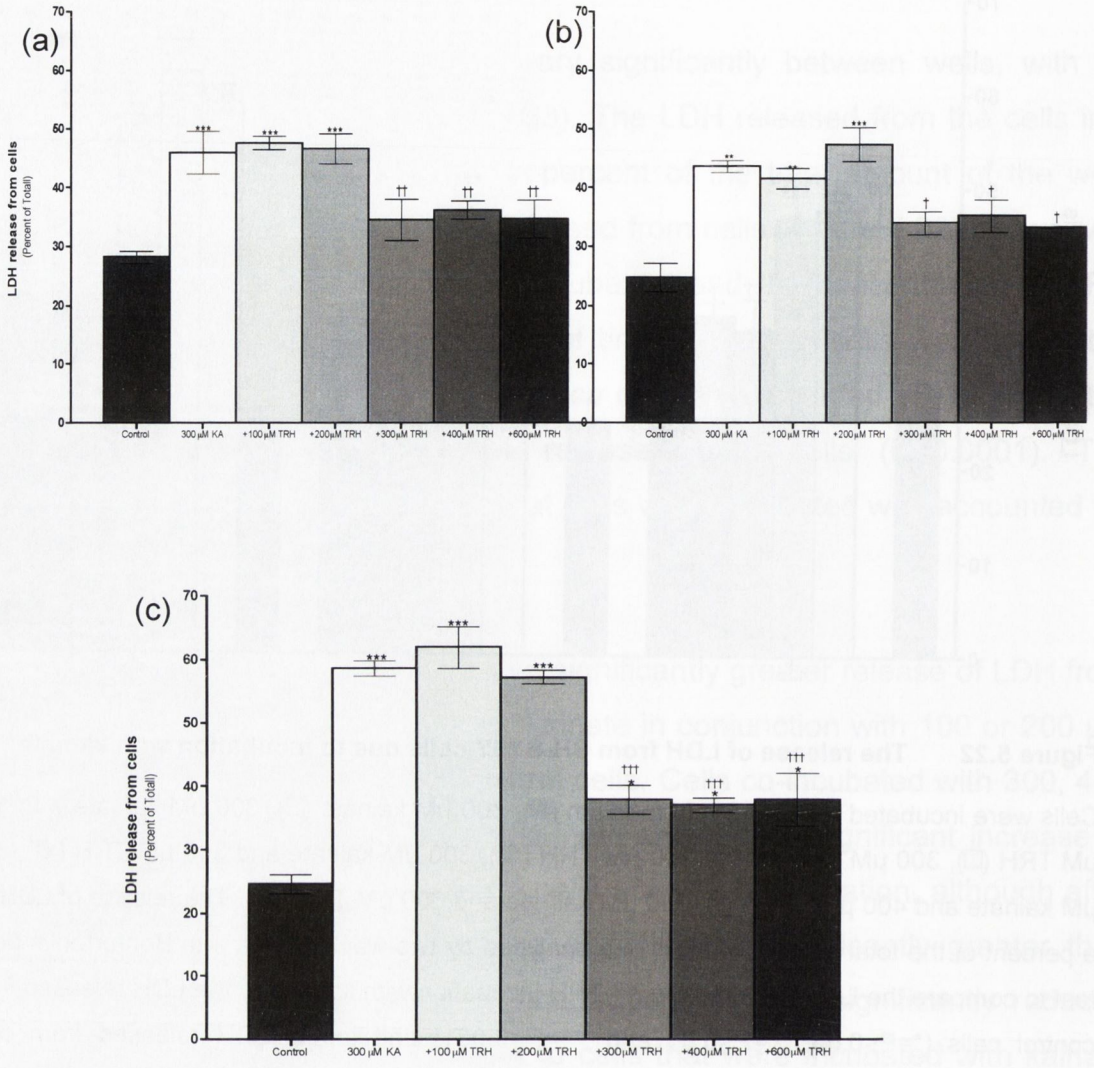

Figure 5.23 The release of LDH from SH-SY5Y cells due to incubation with kainate

The data in Figure 5.22 were plotted as individual incubation periods; (a) 12 h, (b) 24 h and (c) 48 h. The LDH release after each incubation due to 300 μM kainate (□) or kainate with 100 μM TRH (□), 200 μM TRH (▨), 300 μM TRH (▨), 400 μM TRH (■), or 600μM TRH (■) was analysed by one-way with Bonferroni's post-test. The release of LDH when TRH was present with kainate was compared with the release from control cells (■; *=P<0.05, **=P<0.01 and ***=P<0.001) and with LDH released from cells incubated in kainate alone (†=P<0.05, ††=P<0.01 and †††=P<0.001). Data represent mean values ± S.E.M. (n=3).

5.3.3.4 Caspase activity following kainate treatment

Initiation of apoptosis in cells was analysed by assaying for caspase activity following incubation of the cells with kainate alone or with 100–600 μM concentrations of TRH for 8, 12 and 48 h periods (Figure 5.24). Two-way ANOVA analysis of the activity revealed that both time and treatment affected the activation of apoptosis; with the concentration of TRH used accounting for 79.8% of the variation ($P<0.0001$) and the length of exposure influencing 3.5% of the variation ($P=0.0069$).

Comparison of the caspase activity after each treatment showed that cells incubated with kainate alone or with 100 or 200 μM TRH had significantly greater caspase activity than control cells ($P<0.001$ for each incubation, two-way ANOVA with Bonferroni's post-test). However, co-treatment of 300, 400 or 600 μM TRH with kainate revealed that there was no significant difference in caspase activity compared to the control cells at each of the incubation periods and that the caspase activity was significantly less than the activity found in cells incubated with kainate alone (P values ranged from <0.01 to <0.001).

The data from Figure 5.24 were replotted for clarity, with each incubation period shown individually (Figure 5.25). One-way ANOVA analysis with Bonferroni's post-test was performed to compare changes in caspase activity following (a) 12, (b) 24 and (c) 48 h co-incubations of TRH (100–600 μM) with kainate with the caspase activity measured in control cells. This analysis showed that following each of the incubation periods, the caspase activity in cells treated with the three highest TRH concentrations (300, 400 and 600 μM) did not significantly differ from control cells, and that the activity levels were significantly lower than the caspase activity of cells incubated with staurosporine alone (P values ranged from <0.01 to <0.001).

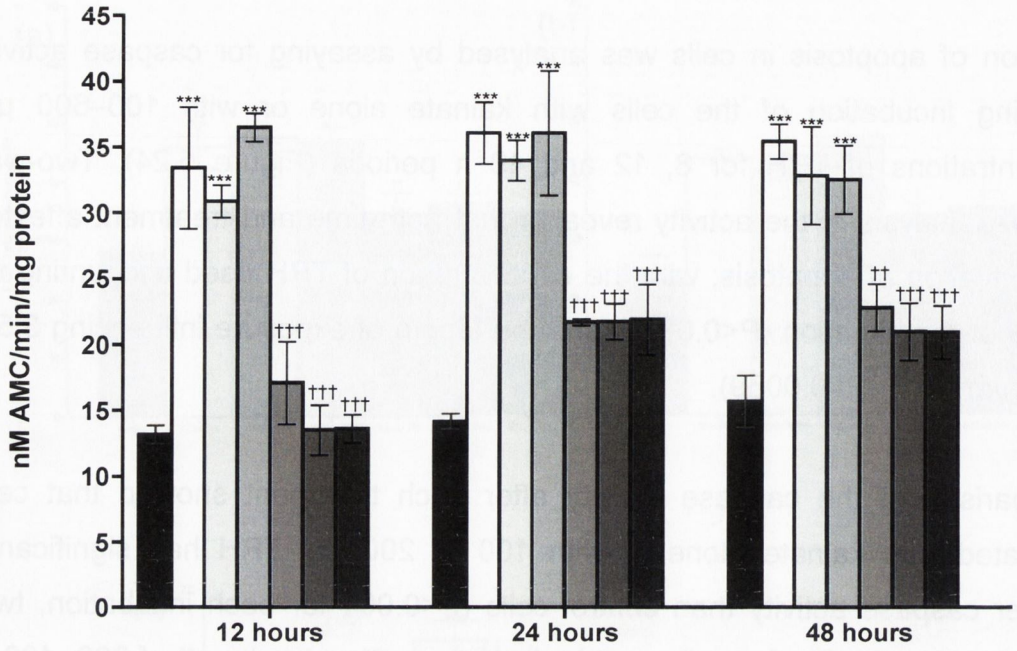

Figure 5.24 Caspase activation in SH-SY5Y cells following kainate incubation

Cultures of SHSY-5Y cells treated with 300 μM kainate (□), and kainate with 100 μM TRH (□), 200 μM TRH (□), 300 μM TRH (□), 400 μM TRH (■) and 600 μM TRH (■), in addition to control cells incubated in medium (■) were lysed following 12–48 h incubations and assayed for caspase activity. Statistical analysis was performed by two-way ANOVA with Bonferroni's post-test (n=3 for all treatments), to compare the effect of TRH with control cells (***=P<0.001) and to cells incubated with kainate alone (††=P<0.01 and †††=P<0.001).

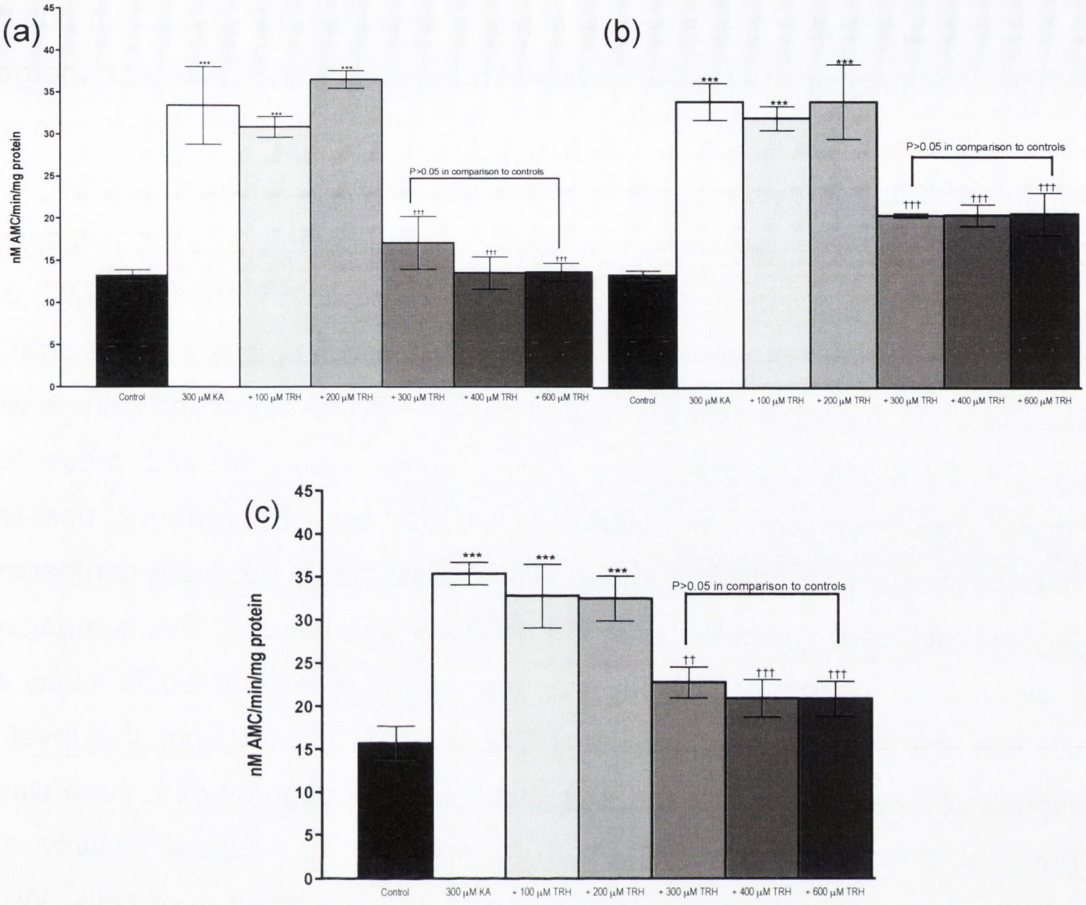

Figure 5.25 TRH attenuates apoptosis activation in SH-SY5Y cells following kainate treatment

The data presented in Figure 5.24, in which cells treated with 300 μM kainate (□), and kainate with 100 μM TRH (□), 200 μM TRH (□), 300 μM TRH (■), 400 μM TRH (■) and 600 μM TRH (■), in addition to control cells incubated in medium (■) are graphed individually for (a) 12, (b) 24 and (c) 48 h incubation periods. Statistical analysis was performed by one-way ANOVA with Bonferroni's post-test (n=3 for all treatments), to compare the effect of TRH for each incubation period with control cells (***=P<0.001) and with cells treated with kainate alone (††=P<0.01 and †††=P<0.001).

5.3.3.5 Comparison of the different detection procedures

In order to correlate the measurements determined by propidium iodide exclusion, release of LDH and activation of caspases the data was merged together onto a single graph (Figure 5.26). The cell death measured by propidium iodide exclusion and the release of LDH were both determined as a percentage of the total and were thus plotted on the same y-axis (left), caspase activity in the cells was measured as the rate of product formation, AMC, per min as a function of the protein content of cells and was plotted on the right y-axis. For clarity, only the data for incubation with kainate alone and kainate with 600 µM TRH, the highest concentration, were compared and presented. Analysis was performed by two-way ANOVA with Bonferroni's post-test comparing results for cells incubated with kainate and a separate comparison was made for cells incubated with 600 µM TRH with kainate. This comparison shows that the percent cell death measured by the propidium iodide assay did not differ from the percent release of LDH from cells or from the level of caspase activity following 12 and 24 h incubations, though by 48 h there was a significant difference, with $P<0.05$ in comparison to caspase activity and $P<0.001$ in comparison to the percentage of LDH released from cells. When 600 µM TRH was incubated with kainate on cells there was a significant difference between release of LDH from cells and the percent cell death (propidium iodide inclusion) following all incubations ($P<0.05$ following 12 and 24 h, rising to $P<0.001$ following 48 h) and also significant differences between the LDH release and the caspase activity ($P<0.001$, <0.01 and <0.001 for 12, 24 and 48 h respectively). The level of caspase activity and percentage of cell death differed only following 12 h incubation ($P<0.001$). To summarise the data collected by incubation of cells with kainate and 300, 400 or 600 µM TRH by the four types of assays (MTT, propidium iodide exclusion, release of LDH and caspase activity), Table 5.3 outlines the significant differences obtained by comparison of the results due to incubation with TRH with control cells and with cells incubated with kainate alone.

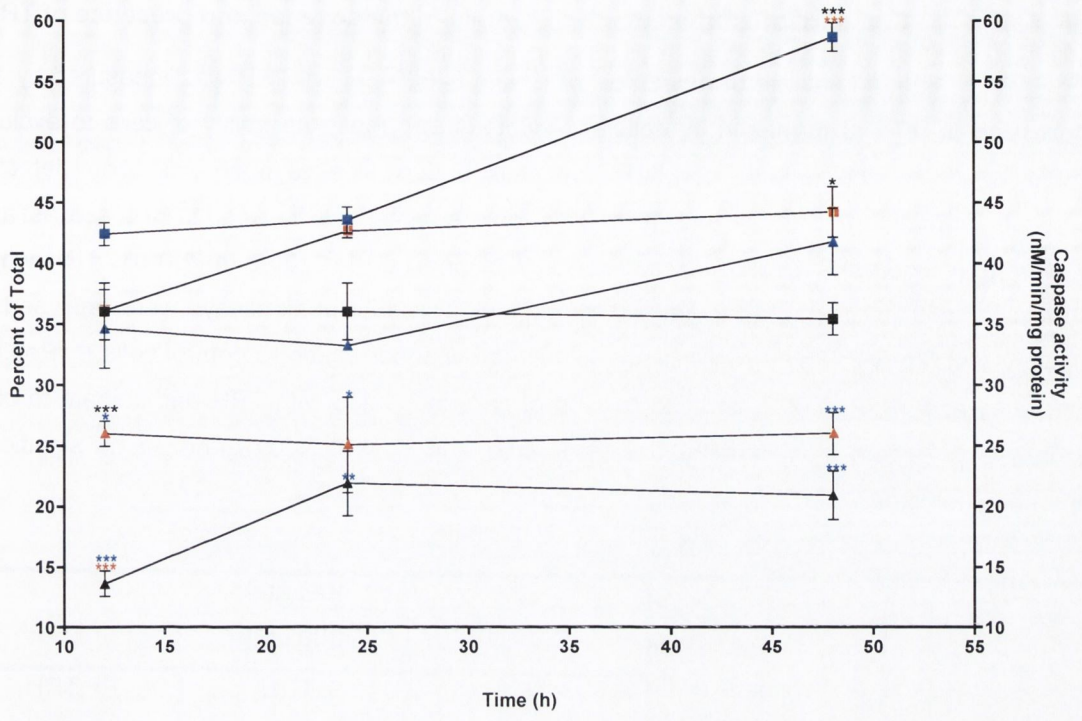

Figure 5.26 The effect of kainate and kainate with 600 µM TRH, measured by propidium iodide exclusion, LDH release and caspase activity

The cell death due to incubation of cells with kainate, measured by propidium iodide exclusion (Figure 5.19; ■), LDH release (Figure 5.22; ■) and caspase activity (Figure 5.24; ■), are grouped together for analysis. The comparison was repeated for results obtained for cells treated with kainate in the presence of 600 µM TRH (Propidium iodide exclusion=▲, caspase activity=▲ and LDH release=▲). The release of LDH was measured as a percent of total LDH and cell death was determined by propidium iodide exclusion as a function of the total cell number and both on plotted on the left y-axis as percentages of the total. Caspase activity was determined as the rate of AMC release from the substrate as a function of the protein content of the cells and is plotted on the right y-axis. Data represent the mean ± S.E.M. (n=3). Data were compared by two-way ANOVA analysis with Bonferroni's post-test. Significant differences are indicated as *=P<0.05, **=P<0.01 and ***=P<0.001, compared to caspase activity, *=P<0.05, **=P<0.01 and ***=P<0.001, compared to LDH release and *=P<0.05, **=P<0.01 and ***=P<0.001, compared to cell death detected by the propidium iodide assay.

Table 5.3 Comparison of the effects of kainate in the absence and presence of TRH

The effect of 300 μM kainate on SH-SY5Y cells with 0–600 μM zdhTRH was measured by the conversion of MTT to formazan by cellular reductase enzymes, the ability of cells to exclude propidium iodide, the release of LDH from cells and by the caspase activation detected following incubation for 12, 24 and 48 h. This table summarises the results of these assays, presented in Figures 5.16–5.24, excluding the data obtained for 100 and 200 μM TRH which had no effect when compared to kainate throughout. The data of all assays were analysed by two-way ANOVA with Bonferroni's post-test, with comparison made to control cells (*=P<0.05, **=P<0.01 and ***=P<0.001) and comparison of cells incubated with TRH and kainate to cells incubated in kainate alone (†=P<0.05, ††=P<0.01 and †††=P<0.001), and –= no significant difference detected.

Assay type	Kainate (300 μM)				Kainate (300 μM)											
					+ TRH (300 μM)				+ TRH (400 μM)				+ TRH (600 μM)			
Time (h)	8	12	24	48	8	12	24	48	8	12	24	48	8	12	24	48
MTT	***	***	***	***	*	-	***	***	-	-	***	***	***	-	***	***
					†††	†††	†††	-	†††	†††	†††	†	††	†††	†††	-
PI	***	***	***	***	***	***	***	***	***	***	***	***	***	***	***	***
					†	†	†††	††	††	†	†††	††	††	††	†††	†††
%LDH Release	/	***	***	***	/	-	*	**	/	-	**	**	/	-	*	**
						††	†	†††		†	-	†††		††	†	†††
Caspase Activity	/	***	***	***	/	-	-	-	/	-	-	-	/	-	-	-
						†††	†††	††		†††	†††	†††		†††	†††	†††

5.3.4 The effect of TRH on MPP^+-induced toxicity

5.3.4.1 Studies with the MTT assay

A concentration of 10 mM MPP^+ was used in incubations of 6–24 h to measure the ability of TRH to maintain cellular viability (Figure 5.27 and Figure 5.28). It was found by two-way ANOVA analysis of Figure 5.27 that the degree of protection conferred by TRH depended on both the concentration of TRH and the incubation time. Time accounted for 23.9% of the variance and the amount of TRH accounted for 58.6%, with significant interaction between the incubation period and concentration of TRH, which accounted for 12% of the variance.

After the shortest incubation (6 h) cells treated with MPP^+ alone or MPP^+ with 100 or 200 µM TRH had significantly reduced viabilities when compared to the control cells ($P<0.001$ in each case, determined by two-way ANOVA with Bonferroni's post-test). Cells that were co-incubated with MPP^+ plus 300, 400 or 600 µM TRH did not significantly differ from the viability of control cells following 6 h incubation. However, after 12 h incubation none of these TRH concentrations gave significant protection against MPP^+ toxicity. After incubation for 24 h the viability of cells incubated in MPP^+ alone had decreased significantly in comparison to that detected after 12 h incubation ($P<0.05$), although the viabilities of cells that underwent treatment with 300, 400 or 600 µM TRH with MPP^+ did not differ from the values detected for each after 12 h incubation. The viabilities of the cells incubated with 400 or 600 µM TRH plus MPP^+ after 24 h were significantly greater than cells incubated for 24 h in MPP^+ alone ($P<0.001$), although significantly less than control cells ($P<0.001$). After 48 h the viabilities of cells incubated with 400 or 600 µM TRH with MPP^+ were significantly decreased in comparison to the viabilities for each treatment detected after 24 h ($P<0.001$) and did not differ from cells incubated with MPP^+ alone.

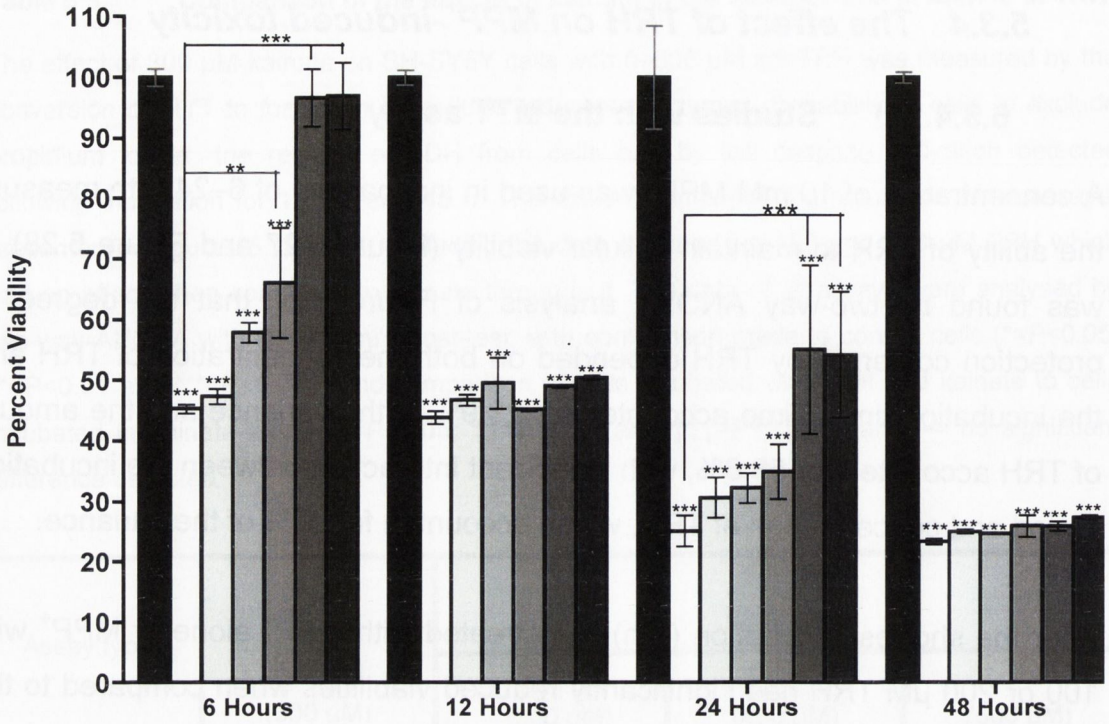

Figure 5.27 Cell viability following incubation with MPP^+ and TRH, measured by MTT assay

The survival of SH-SY5Y cells incubated for 6–48 h with 10 mM MPP^+ (□) and MPP^+ in the presence of 100 µM TRH (□), 200 µM TRH (□), 300 µM TRH (■), 400 µM TRH (■) and 600 µM TRH (■) and control cells (■) incubated in medium for the duration of the experiments was measured by the MTT assay, with viabilities calculated as percent of control cells. Two-way ANOVA with Bonferroni's post-test was used to compare the effect of TRH on cell viability with the viability of control cells and, where indicated, with the viability of cells incubated in MPP^+ alone. Data represent the mean of n=3 ± S.E.M., with *=P<0.05, **=P<0.01 and ***=P<0.001.

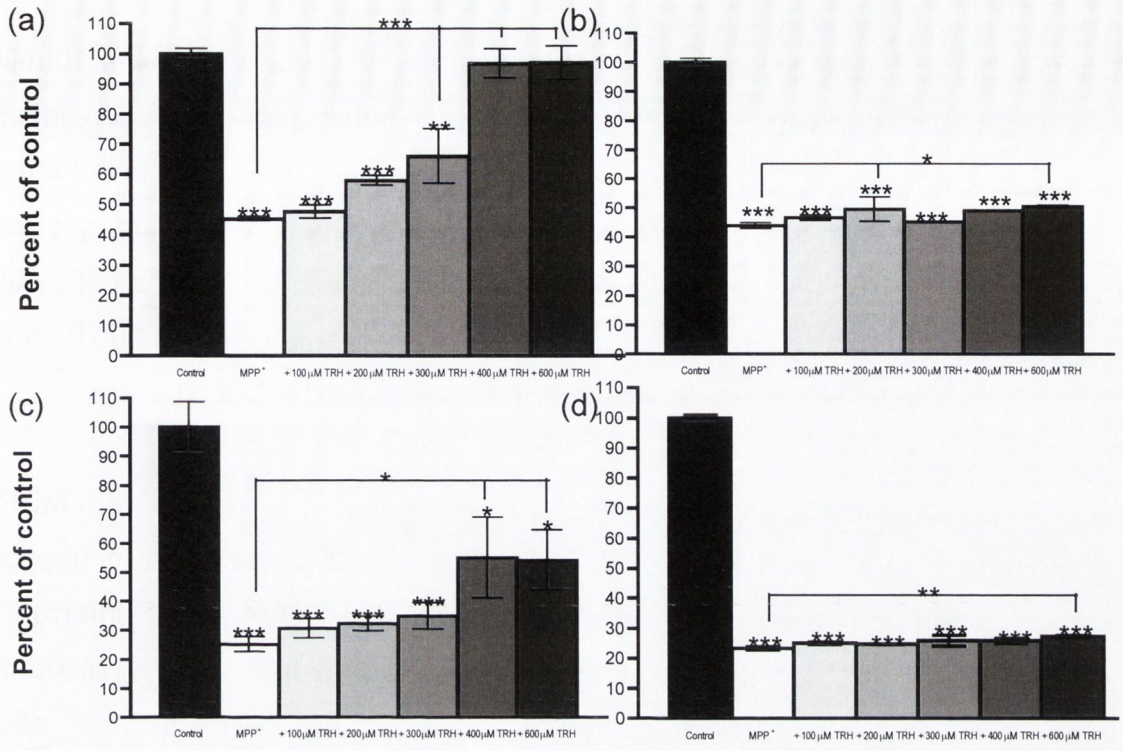

Figure 5.28 TRH protected cell viability, measured by MTT assay, following incubation with MPP^+

The data in Figure 5.28 were plotted as separate graphs for (a) 6, (b) 12, (c) 24 and (d) 48 h incubation periods. Cells were incubated in 10 mM MPP^+ (□) and MPP^+ with 100 (□), 200 (▩), 300 (▩), 400 (■) or 600 (■) μM TRH. Analysis of the viabilities was performed by one-way ANOVA with Bonferroni's post-test to compare the viability of TRH-treated cells with control cells (■) and, where indicated, to cells incubated in MPP^+ alone. Data represent mean values ± S.E.M. (n=3), with *=P<0.05, **=P<0.01 and ***=P<0.001.

5.3.4.2 Propidium iodide exclusion studies

The viability of cells following treatment times of 6, 12, 24 and 48 h with 10 mM MPP^+ in conjunction with 100–600 μM TRH was determined by the propidium iodide exclusion assay, with the results are shown in Figure 5.29 and Figure 5.30. Analysis by two-way ANOVA revealed that both the incubation length and the concentration of TRH used significantly affected the viability of the cells with the incubation period accounting for ~13.2% of the variation ($P<0.0001$), and TRH concentration accounts for ~75.2% of the variation ($P<0.0001$).

There was a significant reduction in cell viability following incubation with MPP^+ alone or with MPP^+ plus each of the TRH concentrations after all incubation periods, when compared with control cells (two-way ANOVA with Bonferroni's post-test gave $P<0.01$ in all cases). MPP^+ incubation resulted in 58% cell death after 6 h incubation and the incubation of 100 or 200 μM TRH with MPP^+ after showed no significant protective effects after any of the incubation periods. Treatment with 300, 400 and 600 μM TRH, however, gave significant protection against MPP^+-induced cell death after 6 h ($P<0.01$, $P<0.001$ and $P<0.001$, respectively). After 12, 24 and 48 h there was no protection against cell loss achieved by 300 μM TRH with MPP^+ ($P>0.05$ in comparison to MPP^+-treated cells) but 400 and 600 μM TRH with MPP^+ resulted in significantly greater cell viability after 12 and 24 h compared to cells incubated in MPP^+ alone ($P<0.01$ after 12 h and $P<0.05$ after 24 h). After 48 h incubation cells incubated with 600 μM TRH and MPP^+ were significantly more viable than cells incubated with MPP^+ ($P<0.01$).

Comparison of the viabilities due to MPP^+, obtained in the MTT assay with that from propidium iodide assay (Figure 5.31) indicated that there was no significant difference between the viabilities calculated by either method ($P=0.6188$, by paired T-test). In addition, there was no significant difference in the level of viability due to the inclusion 600 μM TRH with MPP^+ detected by either methods ($P=0.9744$, by paired T-test), though the viabilities at 48 h of cells incubated with 600 μM TRH with MPP^+ differed significantly ($P<0.001$ by two-way ANOVA with Bonferroni's post-test).

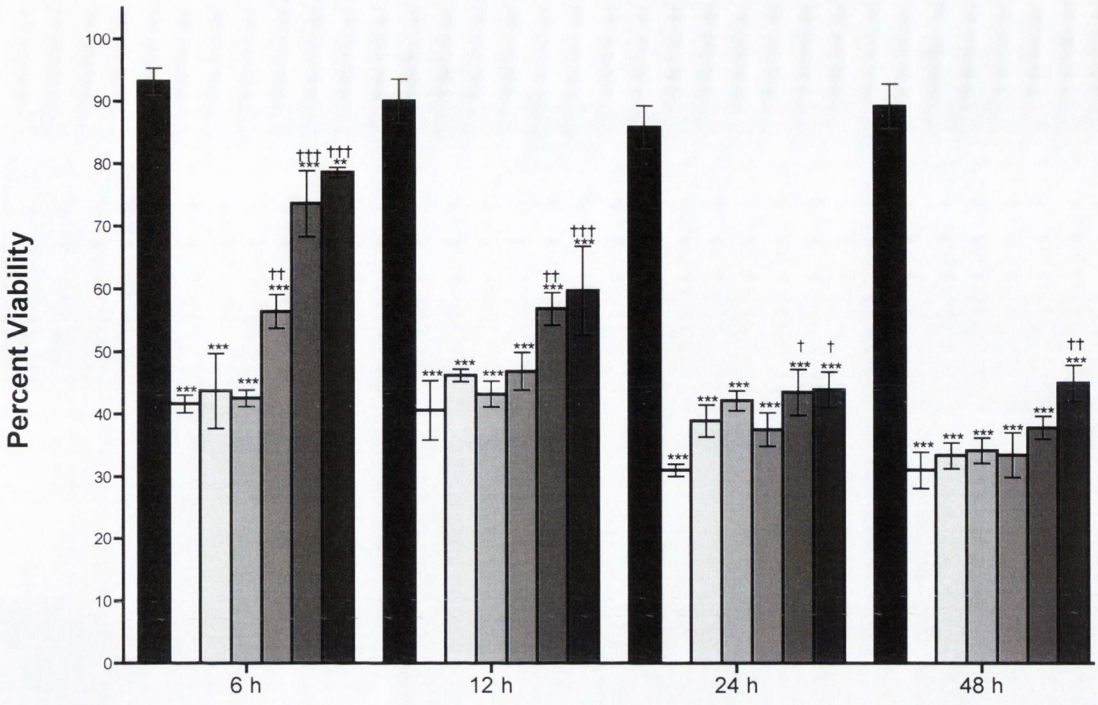

Figure 5.29 Cell survival determined by propidium iodide exclusion following incubation of SH-SY5Y cells with TRH and MPP^+

Cell survival was determined by propidium iodide exclusion following 6–48 hour incubations of the cells in medium (■), 10 mM MPP^+ (□), 10 mM MPP^+ with 100 µM TRH (□), 10 mM MPP^+ with 200 µM TRH (▒), 10 mM MPP^+ with 300 µM TRH (▒), 10 mM MPP^+ with 400 µM TRH (■), 10 mM MPP^+ with 600 µM TRH (■). The percent survival was determined using the equation $100-(F/F_{max})\times100$, where F_{max} is a function of cell number, obtained by permeablising all cells with digitonin. Data represent the mean ± S.E.M. (n=3). Two-way ANOVA with Bonferroni's post-test was performed for each time point, with TRH-treated cells compared to control cells (**=P<0.01 and ***=P<0.001) and to cells treated with MPP^+ alone (†=P<0.05, ††=P<0.01 and †††=P<0.001).

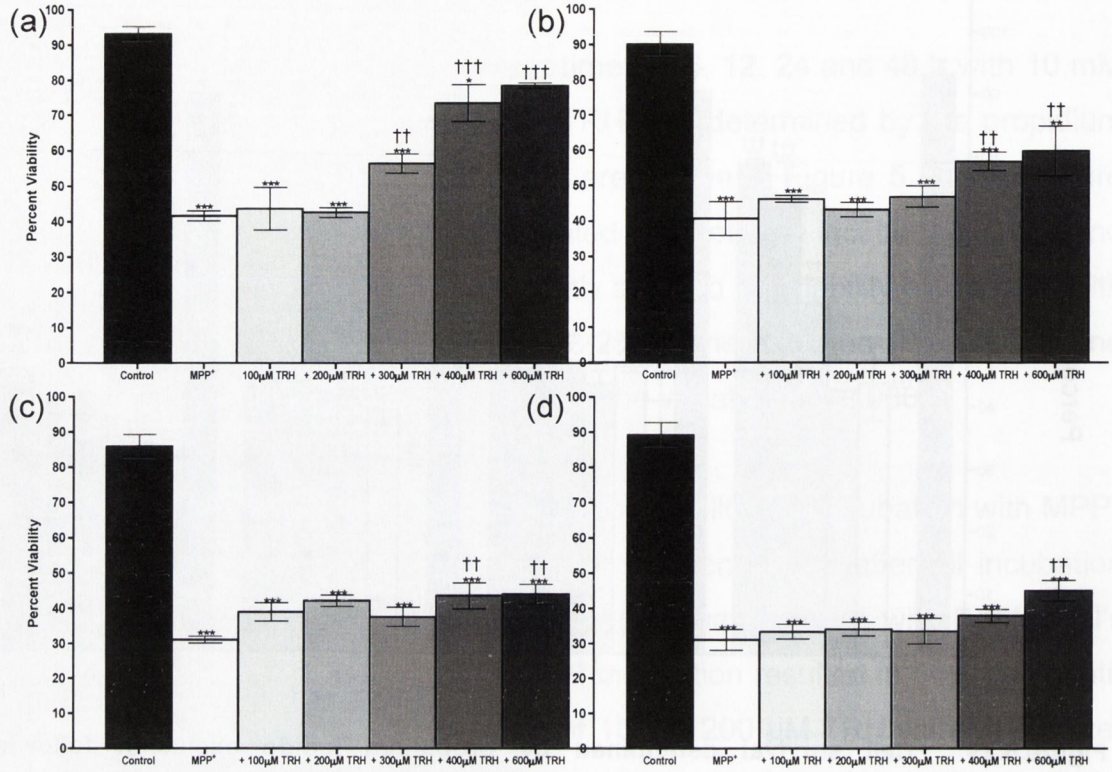

Figure 5.30 TRH protected cell viability following incubation with MPP^+ measured by propidium iodide assay

The data in Figure 5.29 were plotted as separate graphs for (a) 6, (b) 12, (c) 24 and (d) 48 h incubation periods. Cells were incubated in 10 mM MPP^+ (□) and MPP^+ with 100 (□), 200 (▨), 300 (▩), 400 (▩) or 600 (■) μM TRH. Analysis of the viabilities was performed by one-way ANOVA with Bonferroni's post-test to compare the viability of TRH-treated cells with control cells (■ ;*=P<0.05, **=P<0.01 and ***=P<0.001) and to cells incubated in MPP^+ alone (†=P<0.05, ††=P<0.01 and †††=P<0.001). Data represent mean values ± S.E.M. (n=3).

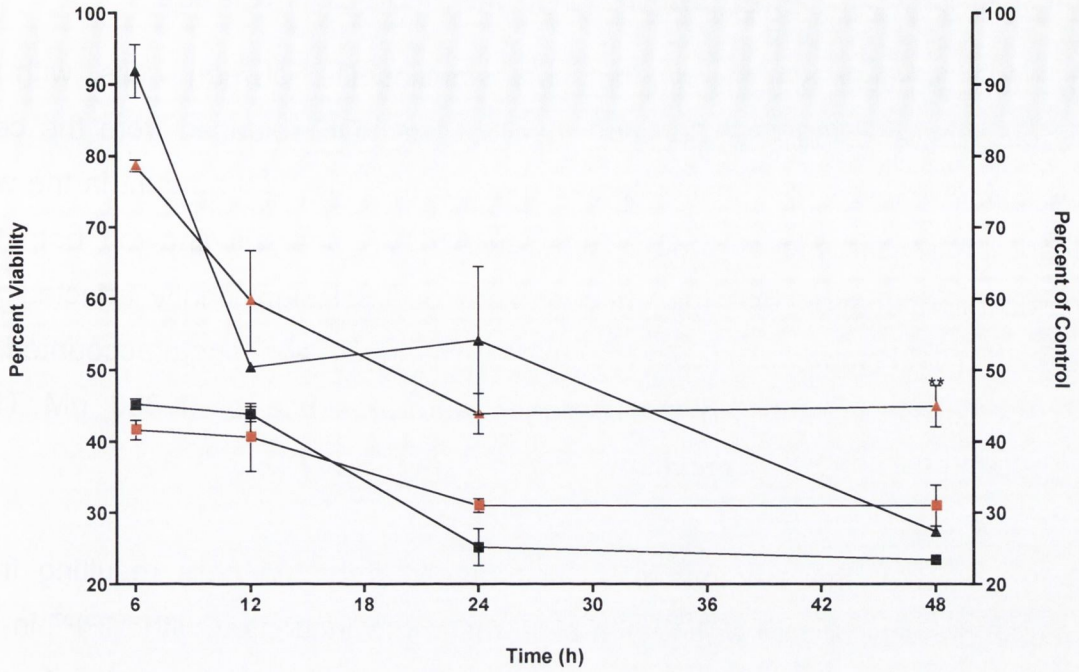

Figure 5.31 Comparison of the cell viability due to MPP^+ treatment detected by MTT and propidium iodide exclusion assays

The cell viability measured by both reductase-activity (MTT; Figure 5.27) and membrane integrity (PI; Figure 5.29) due to treatment with MPP+ (PI=■; MTT=■) and with MPP^+ in the presence of 600 µM TRH (PI=▲; MTT=▲) were replotted for comparison of the measurement of the cell viability determined by each of the assays. Data represent mean values ± S.E.M (n=3). Two-way ANOVA analysis was performed comparing PI with MTT values for MPP^+ in the absence of TRH (■ vs. ■) and comparing PI with MTT in the presence of TRH (▲vs. ▲), with **=P<0.01.

5.3.4.3 Effect of TRH and MPP^+ on LDH release

The total amount of LDH did not vary significantly between wells, with an average value of 56.77±0.86 U/mL (n=63). The LDH released from the cells into each well was then calculated as a percent of the total amount in the well (Figure 5.32 and Figure 5.33). Two-way ANOVA analysis showed both the period of incubation and the concentration of TRH significantly affected the release of LDH from cells (both $P<0.0001$). The incubation length accounted for ~5.3% of the variation in LDH release and presence of 0–600 µM TRH accounted for ~90.2% of variation.

Comparison of the amounts of LDH released from the cells resulting from incubation with 10 mM MPP^+ with cells that were incubated with MPP^+ in the presence of 100–600 µM TRH showed that all treatments released significantly more LDH than control cells following each of the incubation periods examined (Figure 5.32). However, cells incubated MPP^+ plus 400 or 600 µM TRH released significantly less LDH than those cells incubated in MPP^+ alone after the 12, 24 and 48 h incubations ($P<0.001$, determined by two-way ANOVA with Bonferroni's post-test). Treatment with either 100 or 200 µM TRH with MPP^+ had no significant effects on the LDH release in comparison with cells treated with MPP^+ alone. Cells incubated with 300 µM TRH with MPP^+ released significantly less LDH than MPP^+-treated cells at 24 and 48 h ($P<0.01$ and 0.001, respectively). For clarity, the data shown in Figure 5.32 were replotted, in Figure 5.33 as individual bar-charts at each of the incubation periods.

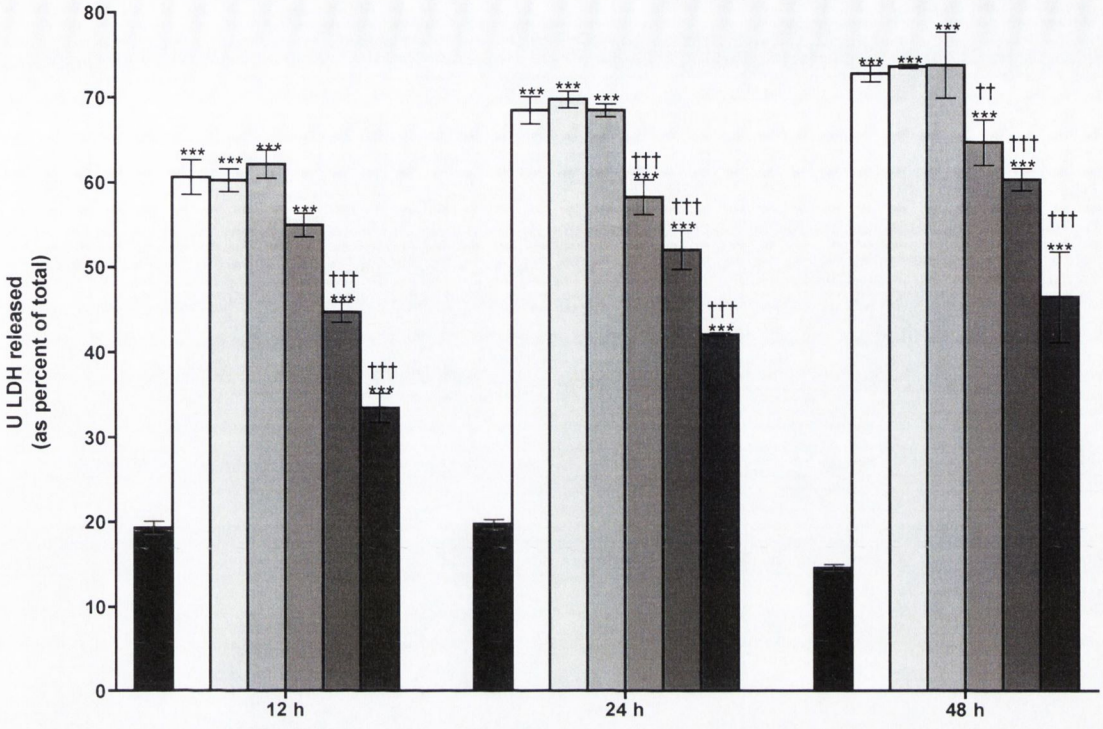

Figure 5.32 The release of LDH from SH-SY5Y cells due to incubation with MPP^+

Cells were incubated for 12–48 h in medium (■), 10 mM MPP^+ (□), 10 mM MPP^+ with 100 µM TRH (□), 10 mM MPP^+ with 200 µM TRH (□), 10 mM MPP^+ with 300 µM TRH (■), 10 mM MPP^+ with 400 µM TRH (■), 10 mM MPP^+ with 600 µM TRH (■). The release of LDH as a percent of the total amount of LDH was analysed by two-way ANOVA with Bonferroni's post-test to compare the LDH released during TRH incubation with MPP^+ to the LDH released from control cells (***=$P<0.001$) and to the LDH released from cells incubated in MPP^+ alone (††=$P<0.01$ and †††=$P<0.001$). Data represent mean values ± S.E.M. (n=3).

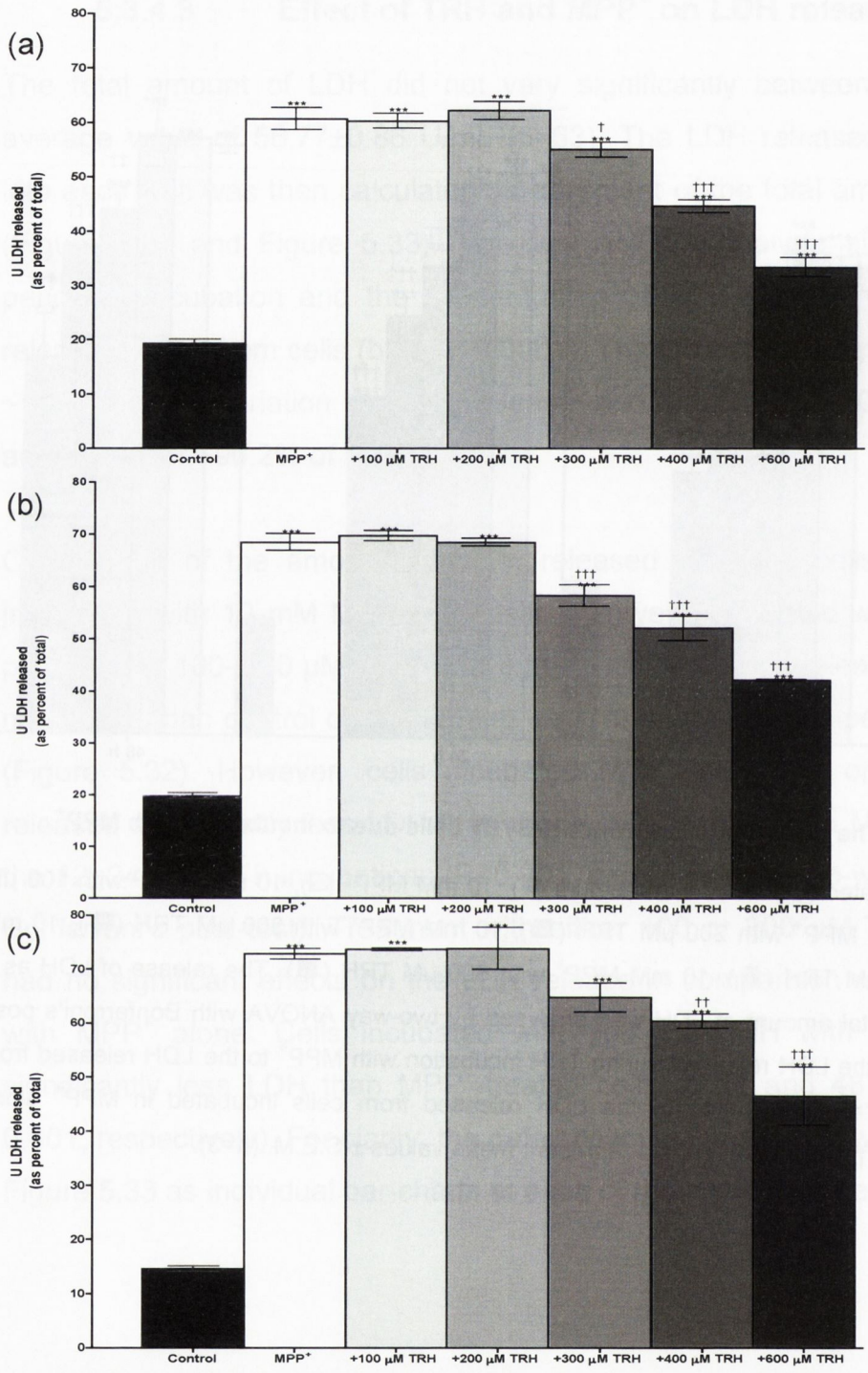

Figure 5.33 TRH attenuates MPP^+-induced LDH release from SH-SY5Y cells

The data in Figure 5.32 were plotted as individual incubation periods; (a) 12 h, (b) 24 h and (c) 48 h. The LDH release after each incubation due to 10 mM MPP+ (□) or MPP+ with 100 µM TRH (□), 200 µM TRH (■), 300 µM TRH (■), 400 µM TRH (■), or 600µM TRH (■) was analysed by one-way with Bonferroni's post-test. The release of LDH when TRH was present with MPP+ was compared with the release from control cells (■; ***=P<0.001) and with LDH released from cells incubated in kainate alone (†=P<0.05, ††=P<0.01 and †††=P<0.001). Data represent mean values ± S.E.M. (n=3).

5.3.4.4 Caspase activity following MPP^+ treatment

Caspase activity was measured following incubation of the cells with MPP^+ alone or with 100–600 µM concentrations of TRH for 12, 24 and 48 h periods (Figure 5.34 and Figure 5.35). Two-way ANOVA analysis of the activity revealed that both time and treatment affected the activation of apoptosis; with the concentration of TRH used accounting for ~86% of the variation ($P<0.0001$) and the length of exposure influencing 3.5% of the variation ($P<0.0001$).

Comparison by two-way ANOVA with Bonferroni's post-test of the caspase activity due to each treatment showed that cells incubated with MPP^+ alone or with TRH had significantly greater caspase activity than control cells after all incubation times ($P<0.001$ for 100–400 µM TRH, $P<0.05$ for 600 µM TRH at 12 and 24 h and $P<0.01$ at 48 h; Figure 5.34). There was no significant reduction in caspase activity when 100 or 200 µM TRH was incubated with MPP^+ compared to MPP^+ alone, after any of the incubation times. Treatment with 300 µM TRH resulted in significantly less caspase activation after 12 and 24 h, compared to cells incubated with MPP^+ alone, but there was no significant effect after 48 h. Incubation of cells with MPP^+ in the presence of either 400 or 600 µM TRH resulted in significantly less caspase activity than cells incubated with MPP^+ alone after 12 ($P<0.05$ and $P<0.001$ for 400 and 600 µM, respectively), 24 ($P<0.001$) and 48 ($P<0.001$) h incubation periods.

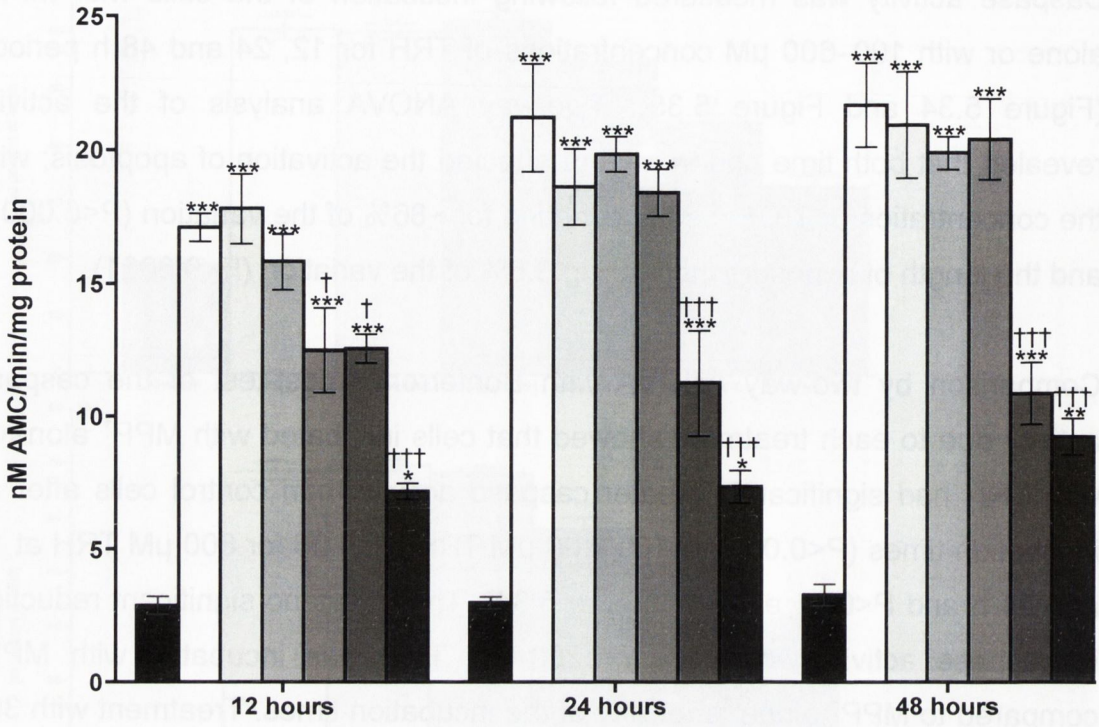

Figure 5.34 Caspase activation in SH-SY5Y cells following MPP^+ treatment

Cultures of SHSY-5Y cells treated with 10 mM MPP^+ (□), and MPP^+ with 100 µM TRH (□), 200 µM TRH (□), 300 µM TRH (■), 400 µM TRH (■) and 600 µM TRH (■), in addition to control cells incubated in medium (■) for 12, 24 and 48 h were lysed and assayed for caspase activity. Statistical analysis was performed by two-way ANOVA with Bonferroni's post-test (n=3 for all treatments), to compare the effect of TRH for each incubation period with control cells (*=P<0.05, **=P<0.01 and ***=P<0.001) and with cells treated with MPP^+ alone (†=P<0.05 and †††=P<0.001).

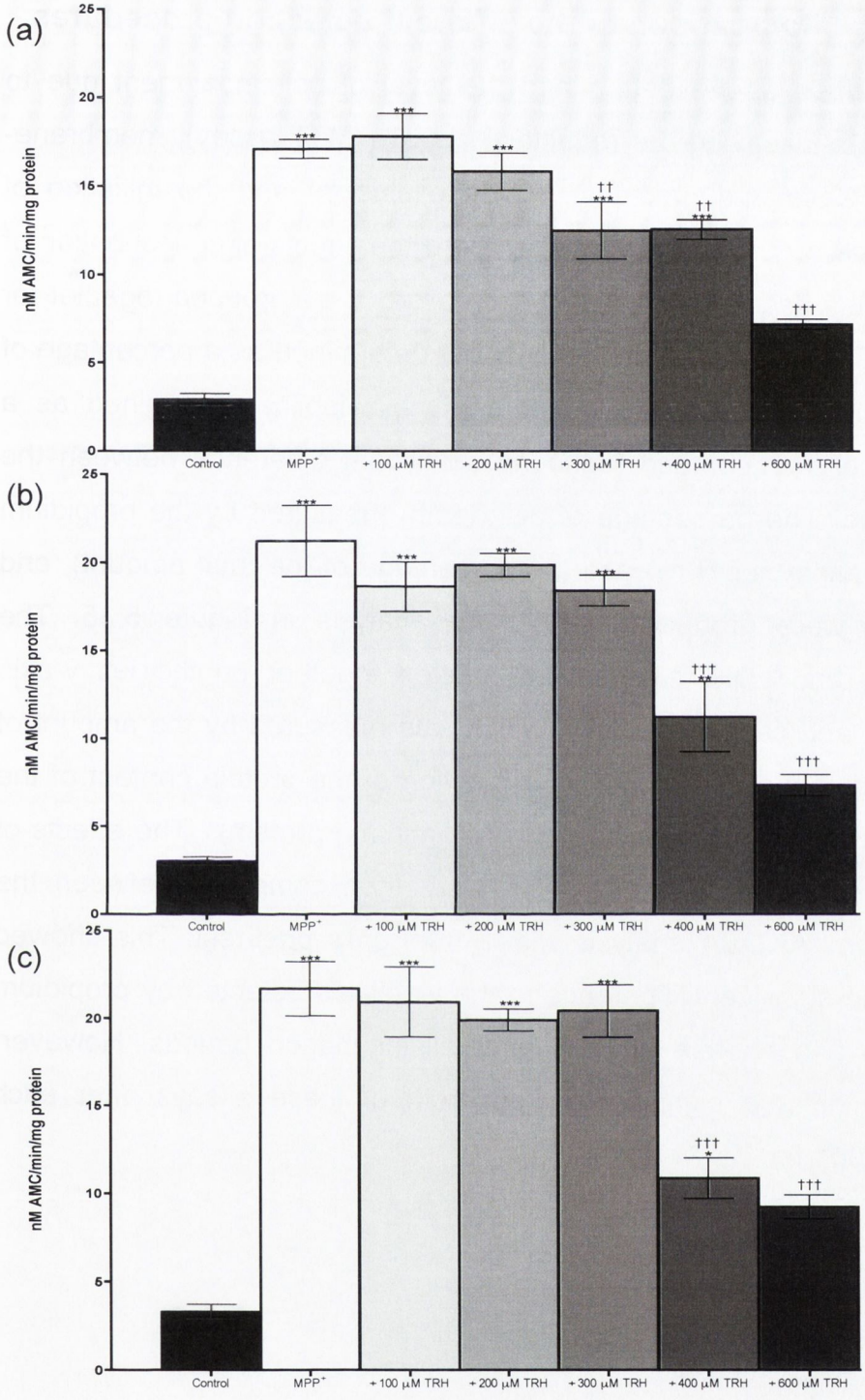

Figure 5.35 TRH attenuates caspase activation due to MPP^+ treatment

The data presented in Figure 5.34, in which cells treated with 10 mM MPP^+ (□), and MPP^+ with 100 μM TRH (□), 200 μM TRH (□), 300 μM TRH (□), 400 μM TRH (■) and 600 μM TRH (■), in addition to control cells incubated in medium (■) for (a) 12, (b) 24 and (c) 48 h were lysed and assayed for caspase activity. Statistical analysis was performed by one-way ANOVA with Bonferroni's post-test (n=3 for all treatments), to compare the effect of TRH for each incubation period with control cells (*=P<0.05, **=P<0.01 and ***=P<0.001) and with cells treated with MPP^+ alone (††=P<0.01 and †††=P<0.001).

5.3.4.5 Comparison of the different detection procedures

The results described above determined the level of cell-impairment due to MPP^+ incubation by assaying the reductase activity (MTT assay), membrane-integrity (LDH release and propidium iodide exclusion) and the initiation of apoptosis (caspase activity). In order to compare the effects of co-incubation of TRH with MPP^+, the data determined by each assay were grouped together for analysis. Figure 5.31 compared the cell viability determined as a percentage of the controls by MTT assay with the percent cell viability determined as a function of the cell number and found no significant difference between the viabilities detected. The percentage of cell death, measured by the propidium iodide exclusion assay, LDH release (as percentage of the total amount), and caspase activity were grouped together for analysis in Figure 5.35. The propidium iodide and LDH release were plotted together on the left y-axis (percent of total) and caspase activity, which was measured by the amount of product (AMC) released per minute as a function of the protein content of the cells, was plotted on the right y-axis (nM AMC/min/mg protein). The effects of MPP^+ in the absence of TRH over time were then compared between the assays by two-way ANOVA analysis with Bonferroni's post-test. This showed that there was no significant difference in the viabilities detected by propidium iodide exclusion and release of LDH after all incubation periods. However, caspase activity differed significantly from both of these assays after each incubation ($P<0.001$ for 12, 24 and 48 h).

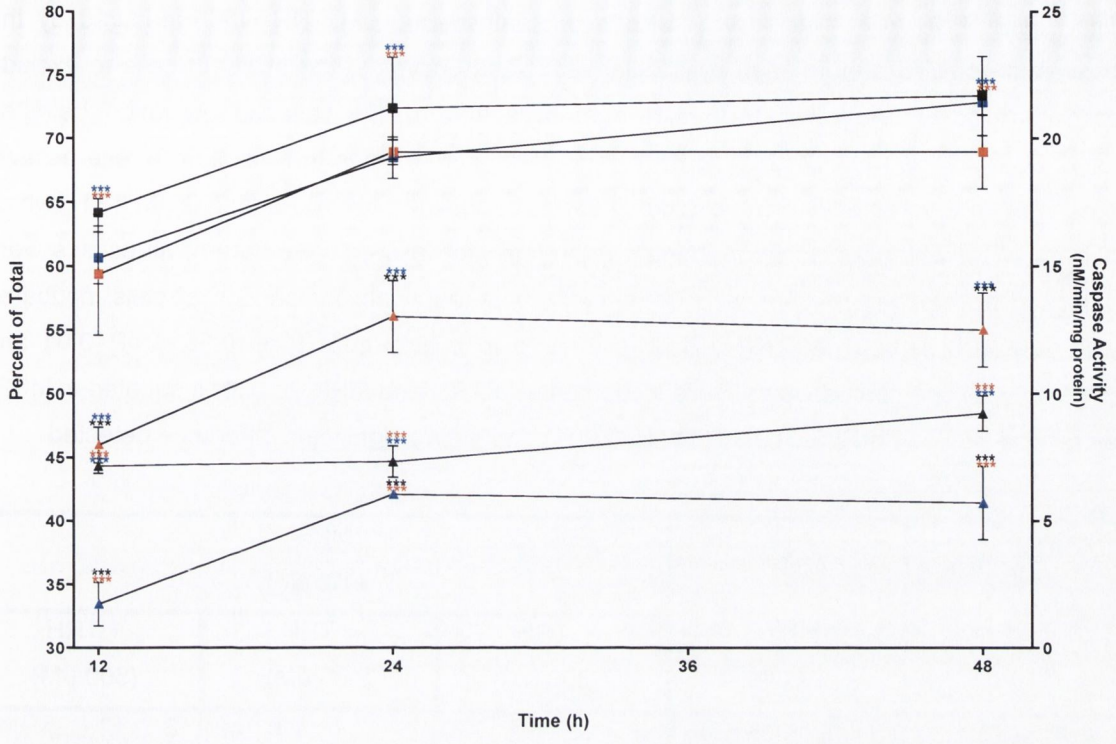

Figure 5.36 Comparison of the effects of MPP^+ determined by propidium iodide assay, LDH release and caspase activity

The cell death due to incubation of cells with MPP^+ measured by propidium iodide exclusion (■), caspase activity (■) and LDH release (■) presented in Figures 5.29–5.35 were compared by two-way ANOVA analysis with Bonferroni's post-test. The release of LDH was measured as a percent of total LDH and cell death was determined by propidium iodide exclusion as a function of the total cell number and both on plotted on the left y-axis as percentages of the total. Caspase activity was determined as the rate of AMC release from the substrate as a function of the protein content of the cells and is plotted on the right y-axis. The effect of MPP^+ in the presence of 600 μM TRH was also compared by the same analysis (propidium iodide=▲, caspase=▲, LDH release=▲). Data represent the mean ± S.E.M. (n=3) with significant differences indicated as *=P<0.05, **=P<0.01 and ***=P<0.001, compared to caspase activity, *=P<0.05, **=P<0.01 and ***=P<0.001, compared to LDH release and *=P<0.05, **=P<0.01 and ***=P<0.001, compared to cell death detected by the propidium iodide assay.

Table 5.4 Comparison of the effects of MPP^+ in the absence and presence of TRH

The effect of 10 mM MPP^+ on SH-SY5Y cells with 0–600 μM TRH was measured by the conversion of MTT to formazan by cellular reductase enzymes, the ability of cells to exclude propidium iodide, the release of LDH from cells and by the caspase activation detected following incubation for 12, 24 and 48 h. This table summarises the results of these assays, presented in Figures 5.26–5.34, excluding the data obtained for 100 and 200 μM TRH, which had no effect when compared to kainate throughout the assays. The data of all assays were analysed by two-way ANOVA with Bonferroni's post-test, with comparison of cells incubated with 300, 400 or 600 μM TRH with MPP^+ made to control cells (*=P<0.05, **=P<0.01 and ***=P<0.001) and comparison of cells incubated with TRH and MPP^+ to cells incubated in MPP^+ alone (†=P<0.05, ††=P<0.01 and †††=P<0.001) and – = no significant difference detected.

Assay type	MPP^+ (10 mM)				MPP^+ (10 mM) + TRH (300 μM)				MPP^+ (10 mM) + TRH (400 μM)				MPP^+ (10 mM) + TRH (600 μM)			
Time (h)	6	12	24	48	6	12	24	48	6	12	24	48	6	12	24	48
MTT (% of control)	***	***	***	***	*** ††	*** -	*** -	*** -	- †††	*** -	*** †††	*** -	- †††	*** -	*** †††	*** -
Propidium Iodide exclusion (% of total)	***	***	***	***	*** ††	*** -	*** -	*** -	*** †††	*** ††	*** †	*** -	*** †††	*** †††	*** †	** ††
LDH Release (% of total)	/	***	***	***	/	*** -	*** †††	*** ††	/	*** †††	*** †††	*** †††	/	*** †††	*** †††	** †††
Caspase Activity (nM/min/mg protein)	/	***	***	***	/	*** †	*** -	*** -	/	*** †	*** †††	*** †††	/	* †††	* †††	** †††

5.4 Discussion

The use of a tissue culture enabled a longer exposure to toxins and assessment of the neuroprotective effect of TRH over hours and days, rather than the more limited time frame necessary with the hippocampal slice model described in Chapter 4.

Measurement of cytotoxicity was performed by four different methods, each of which measures a different aspect of cell death. The MTT assay is a measure of the redox activity of the cell and, as such, is an indicator of cellular integrity, whereas measurement of propidium iodide exclusion demonstrated plasma membrane integrity and is, thus, a marker for late apoptosis and necrosis. Similarly, measuring the release of LDH from cells acted as a marker of loss of plasma membrane integrity and the release of cytosolic proteins in general. The measurement of caspase activity within the cells identified apoptotic cells. The use of each of the toxins used, staurosporine, kainate and MPP^+, resulted in significant loss of cell viability when determined by each of these methods ($P<0.001$ after all incubations used for each toxin, compared to controls).

The incubation of kainate on the cell cultures represents a direct excitotoxic insult, and is a toxicity model dependent on the over-activation of the kainate subtype of the glutamate receptor family. Kainate insult is known to provoke an influx of calcium ions into the cell, either directly through calcium and sodium conducting glutamate receptors, or indirectly (through the secondary activation of voltage-gated calcium channels) (Fern and Moller 2000). This increased calcium influx leads to increased oxidative and metabolic stress and is a principal death-signalling event involved in both necrosis and apoptosis (Syntichaki and Tavernarakis 2003). Cytotoxicity due to kainate was observed using each of the viability methods outlined. Kainate was shown to induce greater than 50% reduction in reductase activity over a 24 h period by the MTT assay (Figure 5.4). Damage to the plasma membrane, measured by propidium iodide binding to DNA revealed that by the same period (24 h), cell death was

at 43%, which correlated with the release of LDH from the cells, which occurred at 42% of the total amount (Figures 5.18 and 5.21).

It is believed that mitochondrial dysfunction with subsequent impairment of energy metabolism is an initiating condition that causes the development of several neurodegenerative diseases (Beal 1996; Volbracht et al. 2006). The neurotoxin MPP^+ is an inhibitor of mitochondrial respiratory chain Complex I, causing impairment of mitochondrial function and energy failure, leading to a loss of intracellular Ca^{2+} homeostasis and reactive oxygen species production (Nicklas et al. 1985; Storey et al. 1992; Volbracht et al. 2006). The incubation of MPP^+ with SH-SY5Y cells resulted in significant impairment of cellular reductase activity, with a depletion of 80% being found after 24 h incubation, in comparison to control cell activity (Figure 5.5). The cell death due to MPP^+-caused mitochondrial dysfunction was found to be at an advanced stage, with almost 70% of cells either at the late apoptotic stage or in necrosis, as demonstrated by the inability plasma membrane to exclude propidium iodide dye (Figure 5.29) and the leakage of LDH from the cells into the medium (68.5% of the total LDH; Figure 5.32).

Kainate toxicity, under the conditions used, caused a smaller loss of redox activity than observed following treatment with MPP^+. The correlation between a reduction in redox function and loss of membrane integrity observed following treatment with MPP^+ (Figure 5.31) was not evident with kainate toxicity (Figure 5.21). This indicates that the kainate treated cells were at an earlier stage of the cell death process, where cellular metabolism was impaired, but the membranes remained more intact. In comparison to control cells, however, kainate treatment resulted in significant loss of redox activity, significant reduction in the ability to exclude propidium iodide from the nucleus and significant loss of LDH from the cells ($P<0.001$). Both toxins induced a level of apoptosis though this was not the main route of cell death induced by either toxin, as demonstrated by the correlation of LDH release from cells with propidium iodide uptake into the cells when incubated with kainate or MPP^+, which did not correlate with the caspase activity in the cells, which differed significantly from the membrane integrity assays across all incubations with

MPP^+ and following 24 and 48 h incubations with kainate. Furthermore, the caspase activity in cells following incubation for 12 h with kainate or MPP^+ did not significantly increase with longer incubation times, although the release of LDH from cells, uptake of propidium iodide and decrease in viability by the MTT assay did. This would suggest that initial apoptotic cell death was superseded by necrosis.

An apoptosis inducer, staurosporine, was also used in order to investigate the mechanism of neuroprotection by TRH. As with several other cell types, caspase activation has been shown to be a critical step in SH-SY5Y apoptosis (Nath et al, 1998) and cells had a level of caspase activity of almost 40 nM/min/mg protein after a 9 h incubation with staurosporine. At which point there was a 45% reduction in redox activity and the membrane integrity was 40% decreased (Figures 5.6 and 5.8). The loss of cytosolic proteins due to the loss of membrane integrity was demonstrated by the leak of LDH, of which 36% was lost from the cells (Figure 5.12). The caspase activity of cells incubated with staurosporine correlated with the loss of LDH from cells across all incubations and with cell death measured by propidium iodide uptake following 6 and 9 incubations.

The routes of cell death induced by each of these toxins were therefore shown to operate by loss of redox control, loss of membrane integrity and apoptotic mechanisms and TRH demonstrated neuroprotection against each of the mechanisms. This neuroprotection was time dependant and had a variable level of protection against each of the death mechanisms. The lower concentrations of TRH had no effect on any measurement of cell viability, but 300–600 μM TRH had a protective effect against the cell death induced by each toxin, which diminished over time. However, the protection against toxicity afforded by TRH against toxicity varied with the impairment measured and also on the toxin used, as summarised in Tables 5.2, 5.3 and 5.4.

The protective effect of TRH, at concentrations of 300, 400 and 600 μM, against staurosporine, which has a primary mechanism of inducing cytotoxicity via apoptosis, was significant after incubations for 3, 6 and 9 h. 300 μM TRH

did not fully protect against cell death, with significant decreases in viability measured compared to control cells detected by each assay. However, there were significant improvements in viability detected by each assay compared to cells incubated with staurosporine alone. Thus, some staurosporine-induced death continued in the presence of 300 μM TRH, but significantly less than in its absence. Incubation with the two highest concentrations of TRH resulted in decreased staurosporine-induced caspase activity, to levels observed in control cells and significantly below that of staurosporine-incubated cells.

Despite this prevention of apoptosis, cells remained under staurosporine-induced stress, demonstrated by the significantly increased release of LDH from the cells and propidium iodide uptake compared to control cells, indicating that though cells were protected against programmed cell death by the presence of TRH, some level of necrotic death was occuring, even after the shortest, 3 h, incubation. This was, however, significantly less than that of cells incubated in the absence of TRH. The redox capacity of cells was also diminished by staurosporine, even in the presence of TRH, though unlike the membrane impairment, 400 and 600 μM TRH maintained the reductase activity at control levels after the 3 and 6 h incubations and this did not decrease significantly until after 9 h. Even at this point the activity was at a level significantly greater than cells incubated with staurosporine in the absence of TRH.

Although the route of cell death due to kainate is primarily necrotic, a significant level of apoptosis was also observed following 12–48 incubations, this was entirely prevented by 300, 400 and 600 μM TRH. However significant damage to the cell membranes and perturbation of the redox activity of the cell by kainate was not entirely prevented. Furthermore, there was no significant protection after the 48 h incubation, with either 300 or 600 μM TRH.

Apoptosis was also produced by MPP^+, at a lower level than that caused by kainate. However, unlike kainate, apoptosis remained significantly elevated when TRH was included in the incubation, although again the three higher TRH concentrations gave a reduction in apoptosis compared with cells incubated

with MPP^+ in its absence. Similar to kainate incubation with TRH, TRH incubation with MPP^+ protected against membrane damage, evidenced by the reduced loss of LDH and the exclusion of propidium iodide from cells compared to cells incubated with MPP^+ alone, but the duration of this protection was more short-lived than with kainate, with 300 µM TRH-protection evident following 6 h incubation only determined by the propidium iodide and MTT assays. The effects of TRH with MPP^+ on the redox activity of cells was also more variable than when incubated with kainate, with significant loss of regulation, determined by MTT assay, in comparison to controls with all TRH concentrations following 12–48 h incubations, where with kainate and TRH incubation control levels of regulation were demonstrated after 12 h incubation and did not decrease relative to controls until after 24 and 48 h incubations.

The neuroprotective mechanism of TRH is, to date, not yet elucidated. SH-SY5Y cells express both the TRH-receptor and TRH-degrading enzyme (TRH-DE) (Dr. Amanda Tivnan, personal communication), which would provide a means for TRH to exert the neuroprotective effect found in these studies. The expression of TRH-DE may explain the high concentrations of TRH required to exert protection and also the decrease in the effect of TRH against cytotoxicity over time. It is also possible that the effect of TRH is elicited through an receptor-independent mechanism, as studies have shown that TRH analogues demonstrated significant protection against glutamate-induced cell death, yet appeared not to bind to any known TRH receptors (Faden et al. 1999; Faden et al. 2003a; Faden et al. 2005).

The protective effects of TRH measured in this study were strongest against excitotoxicity, but were also observed in relation to cell death induced by staurosporine and against the mitochondrial damage caused by MPP^+. Furthermore, TRH operated to prevent multiple cell perturbations, i.e., the loss of cytosolic proteins, permeability of cell membranes, irregularities in metabolic control, as well as the initiation of programmed cell death. Thus TRH may possibly either function as a regulator of a number of cell signals, or to regulate a mechanism common to the initiation of all the above processes. The mechanisms of cell death induced by each of the toxins were illustrated in

Figure 5.1, and the regulation of protein kinases appears to be common to each toxin. Staurosporine is a direct inhibitor of protein kinases, whilst both kainate and MPP^+ cause increases in intracellular calcium levels, which in turn activate protein kinases. Thus, a plausible mechanism of the protection demonstrated in these studies is that TRH functions as a homeostatic regulator of protein kinase activity, or by a process that results in protein kinase regulation. This protective mechanism of TRH may begin with regulation of $[Ca^{2+}]_i$; it is known that TRH prevents glutamate stimulated increases in calcium (Koenig et al. 1996; Faden et al. 2004), and was shown in the present studies to protect against kainate and MPP^+-induced cell death, both of which cause increases in $[Ca^{2+}]_i$, which activate calmodulin-dependent protein kinases (CaM-K) which in turn can phosphorylate subunits of the NMDA and AMPA receptors (Song et al. 2008), further potentiating toxicity. CaM-K is central in regulating neuronal processes, with both increases and decreases in its activity reported to cause neuronal damage (Waxham et al. 1996). Inhibition of protein kinase C activity has been shown to prevent TRH-mediated neuroprotection against NMDA-mediated cell death (Pizzi et al. 1999).

In parallel to the inhibitory role against excess accumulation of $[Ca^{2+}]_i$ by TRH, which functions through calcium-channel inhibition (Kramer et al. 1991) and subsequent over-activation of CaM-K, TRH is also an activator of phospholipase C (PLC) through $G\alpha_{q/11}$ signalling causing an increase in $[Ca^{2+}]_i$, by inositol triphosphate-triggered calcium mobilisation with subsequent activation of protein kinase C (PKC) (Schledermann et al. 2001; Smith et al. 2001). This would explain the counter effects of TRH against staurosporine, a protein kinase inhibitor. This dual function of TRH to either increase or block excessive increases in $[Ca^{2+}]_i$, with resulting activation or inhibition of protein kinases may explain the protective nature of TRH against multiple cytotoxic events. It is of note that metabotropic glutamate receptors use the same signalling cascade as TRH, and thus activation of the TRH cascade may result in the inactivation of that initiated by excitotoxicity (Veronesi et al. 2007).

In conclusion, the protective effect of TRH against different toxins over time, with different cell death mechanisms, was demonstrated. The effects elicited by

TRH point to a complex mechanism of action. The neuroprotective efficacy of TRH was dependent on the neurotoxic agents studied. Compared to the direct excitotoxic insult with kainate, TRH displayed slightly lower potency in the staurosporine and MPP^+ models, although TRH facilitated cell viability and protected against the cell damage criteria leading to cell death in a concentration- and time-dependent manner. This study should permit further investigations into the molecular mechanism involved in these TRH effects and the protection conferred suggests the potential usefulness of TRH-related therapeutics in the treatment of neurodegenerative diseases.

CHAPTER 6

ASSESSMENT OF NEUROTOXICITY AND NEUROPROTECTION USING *IN VIVO* MODELS

6.1 Introduction

In the development of novel therapeutics, the use of *in vitro* assays is an essential first step. Chapter 3 reported the development of inhibitors to TRH-DE, initial analysis and K_i determination was carried out using purified enzyme. Further information on TRH was then obtained using the model systems described in Chapters 4 and 5, i.e. hippocampal slices and cell culture studies. However *in vitro* assays cannot provide an overall picture of a potential treatment's action, therefore a suitable mechanism for analysing TRH and its analogues *in vivo* is necessary. The modelling of specific disorders, such as epilepsy, and cognitive processes, such as spatial learning, may be useful to ascertain the benefits of these inhibitors.

6.1.1 *Kainate toxicity* in vivo

Ionotropic glutamate receptors are important mediators of excitotoxic neuronal death (Ha et al. 2002). The neuronal injury caused by kainate is likely to be caused by the release of endogenous glutamate due to the activation of the presynaptic kainate receptors, or because of reactive oxygen species (ROS) production (Chung and Han 2003b). A number of neurotransmitter systems are thought to be involved with this kainate-induced syndrome (Shytle et al. 1995). The hippocampus is most affected by kainate administration (Ben-Ari 1985). The striatum is particularly vulnerable to excitotoxicity, due to excessive activation of ionotropic glutamate receptors. Kainate has been shown to increase production of reactive oxygen species, mitochondrial dysfunction, and apoptosis in neurons in many regions of the brain (Wang et al. 2005).

Movement disorders such as Parkinson's disease and Huntington's disease have been traced to basal ganglia dysfunction, a group of sub-cortical nuclei involved in the control of movement and various cognitive functions. The neostriatum is a major relay station for cortical information flow through the basal ganglia. Striatal neuronal sub-types are differentially susceptible to hypoxic/ischemic, excitotoxic and oxidative insults. Excitotoxicity may contribute to oxidative stress, leading to the selective neuronal degeneration that occurs in

many neurodegenerative disorders (Skaper et al. 1999; Chung and Han 2003a; Gras et al. 2006).

Systemic or central administration of kainate can induce behavioural autisms such as limbic motor seizures, including wet dog shakes (WDS), paw tremor (PT), facial myoclonia (FM), whole body tremor, excessive salivation aggression and hyperactivity in rats. These symptoms are associated with brain neurotoxicity with the hippocampus and amygdala complex most affected (Ben-Ari 1985). These induced seizures manifest with behavioural and neurologic similarities to seizures in humans with temporal lobe epilepsy (TLE), which are thought to result from neuronal damage particularly in the hippocampus and amygdala complex. Kainate administration is used as an animal model to induce pathological changes similar to those caused by brain infarction, human temporal lobe epilepsy and neurodegenerative diseases because of both the behavioural and neurological similarities (Ben-Ari 1985; Virgili et al. 1992; Williams et al. 1993; Liu et al. 1996; Wang et al. 2005).

6.1.1.1 Free radical toxicity

Reactive oxygen species (ROS) are believed to play a vital role in the genesis and progression of many diseases, including neurodegenerative diseases, such as Parkinson's and Alzheimer's diseases, ischemia and cardiac arrest (Skaper et al. 1999; Wang et al. 2005). Although ROS, such as H_2O_2 or $O_2^{\bullet-}$, have low toxicity, their reaction with transition metal complexes leads to the formation of highly reactive oxygen species (hROS):

$$Fe^{2+} + H_2O_2 \rightarrow Fe^{3+} + hROS + HO^-$$

The products of this so-called Fenton reaction, the free hydroxyl radical $HO^{\bullet}$ or a ferryl (Fe (IV))-oxo species (see for e.g., Freinbichler, et al., 2008a) are associated to cellular oxidative stress. The excitotoxic cell death may also be associated with ATP depletion, a consequence of prolonged and repeated depolarisations, and subsequent failure of the transmembrane ion-dependent ATPases (Dykens et al. 1987; Del Rio et al. 2007)

6.1.2 *TRH effects* in vivo

Since TRH is involved in the modulation of epileptic seizures (Knoblach and Kubek 1994) and TRH and TRH-analogues have been shown to be anticonvulsant in multiple animal and human models of seizures (Jaworska-Feil et al. 2001; Koenig et al. 2001; Kubek and Garg 2002), the use of kainate was studied in this chapter to investigate the neuroprotective properties of TRH. The peripheral administration of TRH has effects on the arousal and locomotor activity of animals (O'Dowd et al. 2000; Colson and Gershengorn 2006).

6.1.3 *Microdialysis*

Microdialysis, a method originally developed by Ungerstedt and colleagues in the 1970s (see Klaus et al., 2004 for review), to measure neurotransmitter concentrations in the brain, allows monitoring of the extracellular concentration of neuroactive chemicals, simultaneously to behaviour studies. Alterations in neurotransmitter release and production of ROS following treatments can be determined.

6.1.4 *Short-term working memory*

The memory of the rats undergoing microdialysis was tested by a two-animal social discrimination test (Engelmann et al. 1995). The social recognition test in rats is a test in novelty processing and the ability to retrieve information at a later time (Prediger et al. 2005; De Leonibus et al. 2006; Squires et al. 2006). It is used as a model of short-term working memory that depends on olfactory memory, which is dopamine mediated. The memory study is a form of novelty processing based on 2 components:

Motivational → arousal to react to stimuli

Cognitive → process stimuli information

Therefore the animals must be initially motivated to react to a novel event in their environment, in this case the introduction of a juvenile rat to the cage, and should retain the memory of the initial introduction upon reintroduction. This memory requires the stimulating information to be processed and the ability to

retrieve this information later, and is thus a test of hippocampus function. Signals are mediated between the olfactory bulb and the hippocampus by vasopressin and oxytocin.

6.1.5 Water Maze spatial task

Rats have a good spatial learning ability, and the water maze is widely used to assess this property of rats and mice. The water maze task is based on the premise that animals have evolved an optimal strategy to explore their environment and escape from the water with a minimum of effort, i.e. swimming the shortest distance possible. The technique allows rats to draw inferences about the position of a stable platform in a swimming pool in the absence of local cues which would indicate the location of the platform (Morris 1984). The integrity of the hippocampal formation is essential for spatial learning, thus normal animals can learn the location of the platform very quickly and deficits in this learning ability can be monitored and compared due to kainate treatment and the effect of TRH on the learning process measured.

Microdialysis and social learning experiments were carried out in the laboratory of Professor Laura della Corte, Dipartimento di Farmacologia Preclinica et Clinica "M. Aiazzi Mancini", Viale G. Pieraccini 6, Università degli Studi di Freinze, Firenze, Italy. This work in Italy was supported by the EU Socrates and COST D13 grants. The water-maze studies were carried out in the Department of Psychology in Trinity College Dublin in collaboration with Doctor Oliviero Gobbo.

6.2 Methods

6.2.1 Microdialysis Animal Studies

6.2.1.2 Surgery and microdialysis procedure

All experiments involving laboratory animals were performed according to the Italian Guidelines for Animal Care (D.L. 116/92), which were also in accordance with the European Communities Council Directives (86/609/EEC). The experiments were performed on male Wistar rats (250 g) (Morini, S. Plo d'Enza, Italy). They were housed in groups of five in a 12 h light/dark cycle under controlled conditions of temperature and humidity with free access to food and water. The rats were anaesthetised with chloral hydrate (400 mg/kg, i.p.) and placed in a stereotaxic frame to allow implantation of a microdialysis guide cannula. The stereotaxic coordinates were: Anterior 0.7, Lateral 3.2, dorsoventral 2.5 mm, according to the atlas of Paxinos and Watson (2004). The single cannula microdialysis probe was implanted vertically into the striatum (3 mm probe tip; see Figure 6.1). The guide was anchored to the skull with a stainless-steel screw and dental cement. After surgery, animals were housed individually in plexiglass cages (32×24 cm) and given ad libitum access to food and water.

The animals were allowed to recover and the microdialysis experiments were initiated 72 h later. The dialysis probes of the now freely-moving rats, were perfused with artificial cerebrospinal fluid (aCSF) consisting of: 138 mM NaCl, 3 mM KCl, 1.2 mM $CaCl_2$, 1 mM $MgCl_2$, 1.2 mM Na_2HPO4, 0.27 mM NaH_2PO_4 and 7.2 mM glucose with 1mM sodium terephthalate (pH 7.4) via polyethylene tubing (i.d. 0.38 mm) connected to a 1 ml syringe mounted on a microinfusion pump (CMA/100, CMA/Microdialysis AB, Stockholm, Sweden), at a rate of 3 µl/min. Following a 1 h stabilization period, perfusates were collected every 20 min over a 4–5 h period.

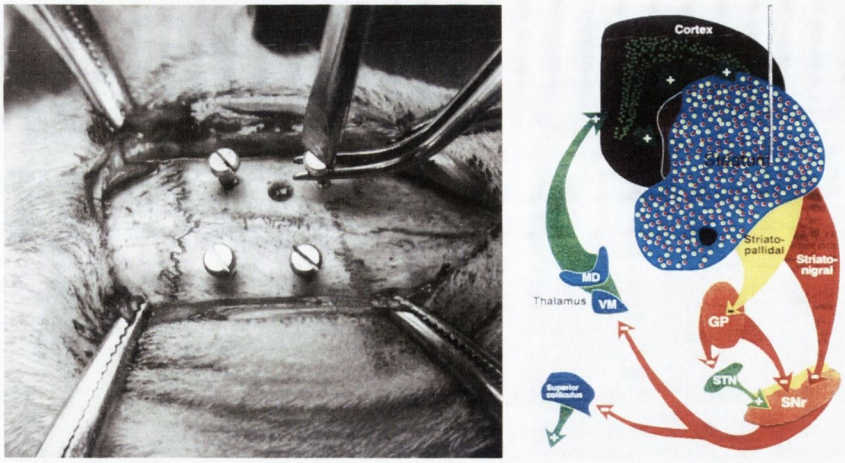

Figure 6.1 Microdialysis prope insertion procedure

The head of rats was shaved and the skull exposed and using the coordinates of the rat brain atlas (Paxinos and Watson 2004) a single cannula microdialysis probe was inserted vertically into the striatum. Three other drill-holes of a narrower bore were made through the skull in which screws were placed to stabilize the insertions. Dental cement was then used to cover the skull and to anchor the probe (Diagram courtesy of Laura Della Corte).

After a collection period of 40 min (two fractions), the striatum was exposed to 100 mM potassium (K^+) stimulation for 20 min (one fraction). In the fourth fraction collection following potassium stimulation injections of either saline or TRH (10 mg/kg) were made intraperitonially (i.p.). Animals were anaesthetised 20 min later with chloral hydrate and over the following 20 min the striatum was exposed to 100 µM kainate. Fraction collection was continued for a further 120–160 min.

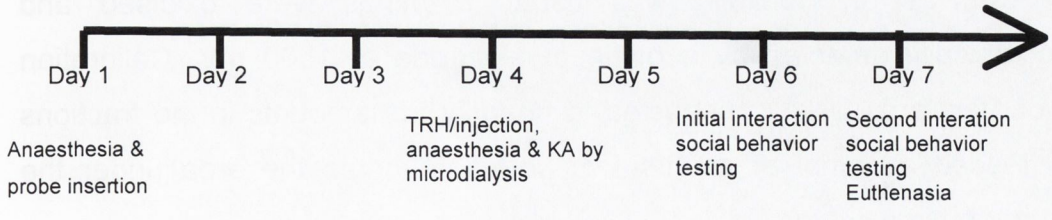

Figure 6.2 Timeline of treatment of animals undergoing microdialysis

6.2.1.2 Measurement of amino acid release

The perfusion fractions were frozen and stored at −20°C. The content of aspartate, glutamate, GABA and taurine in microdialysis perfusates was measured by high-performance liquid chromatography with fluorimetric detection, as described by Bianchi et al., 1999. Briefly, the amino acids were derivatised with mercaptoethanol and *o*-phthalaldehyde (OPA). The OPA derivatives were then separated on a 5 µm reverse phase Nucleosil C18 column (250×4 mm; Machery–Nagel, Duren, Germany) kept at room temperature, using a mobile phase consisting of methanol and potassium acetate (0.1 M, pH adjusted to 5.52 with glacial acetic acid) at a flow rate of 0.9 ml/min in a three linear steps gradient (from 25% to 90% methanol). The levels of amino acid in the perfusate fractions were expressed as pmol of amino acid/µl of perfusate or as the area under the concentration–time curve.

6.2.1.3 Measurement of biogenic amine release

The release of biogenic amines dopamine, its metabolites homovanillic acid (HVA) and 3,4-dihydroxy-phenylacetic acid (DOPAC) and the serotonin metabolite 5-hydroxyindoleacetic acid (5HIAA) were measured in the perfusion fractions by HPLC separation with electrochemical detection, as described by Rakovska et al., 1998. Amines were separated on a cation exchange column, prepared by loading a reverse phase column (Chromospher 5 C18, Chrompack, Middleburg, The Netherlands) with sodium lauryl sulfate (0.5 mg/ml). The mobile phase consisted of 0.2 M phosphate buffer, pH 8.0, containing 5 mM KCl, 1 mM tetramethylammonium (TMA), and 0.3 mM EDTA. A flow rate of 0.75 ml/min was used. Amines were oxidised and electrochemically detected by a platinum electrode at 1500 mV. Calibration curves of standards were constructed to quantify the amounts in the fractions and expressed as pmol of amine/µl of perfusate or as the area under the concentration–time curve.

6.2.1.4 Measurement of free radicals

The release of reactive oxygen species was detected simultaneously with amino acid detection, using the procedure of Freinbichler *et al.*, 2008(b). By inclusion of terephthalic acid (TA^{2-}) with the aCSF during microdialysis highly reactive oxygen species (hROS) were hydroxylated to 2-hydroxy terephthalate (OH-TA). The formation of OH-TA was detected following HPLC elution at ~3.3 min fluorometrically at excitation and emission wavelengths of 315 and 435 nm, respectively, with fluorescence linearly dependent on the concentration of OH-TA, which in turn in linearly dependent on the hROS concentration.

6.2.2 Social recognition study

The test is a model of short-term working memory, based on novelty processing and retrieval of this information at a later time (Prediger et al. 2005; De Leonibus et al. 2006; Squires et al. 2006). On day 6 after surgery and probe insertion and 2 days after kainate challenge a juvenile rat was introduced into the cage of each of the animals undergoing study for a 5 min period (Figure 6.2). The time spent investigating (nosing, pawing, sniffing, grooming) the juveniles by each rat was measured. The juvenile rat was then removed and was reintroduced 24 hours later and the level of investigation by the adult was again measured.

6.2.3 Water Maze Task

The water-maze task is based on the premise that animals have evolved an optimal strategy to explore their environment and escape from the water with a minimum of effort, i.e. swimming the shortest distance possible. The technique allows rats to draw inferences about the position of a stable platform in a swimming pool in the absence of local cues, which would indicate the location of the platform (Morris 1984).

Male Wistar rats of approx. 250 g were used. The rats were randomly assigned to different experimental groups after arrival. Animals were kept in groups of three, in cages of dimensions 44 × 28 × 17 cm. The animals were housed

under standard conditions, in a temperature-controlled (20°C), laminar airflow cupboard and maintained on a 12 hour light–dark cycle (lights on at 7 am). All testing was carried out during the light phase. Food and water were provided *ad lib*.

6.2.3.1 Experimental treatment of animals

Animals were randomly assigned to three experimental groups; control, kainate-treated and kainate with TRH treated. Kainate (10 mg/kg) was administered intraperitonially and reliably induced an acute behavioural syndrome, which included wet dog shakes and seizures, from mild forehead nodding to severe limbic convulsions with rearing and foaming at the mouth. Animals that did not undergo kainate treatment were injected with saline i.p. Animals receiving TRH were injected two hours later (10 mg/kg i.p.) others were injected with saline. TRH was administered a second time 6 hours after the first administration. TRH was administered once/day for five consecutive days. Testing began 3 days after kainate injection. The time-line of the treatment to each group is outlined in Figure 6.3.

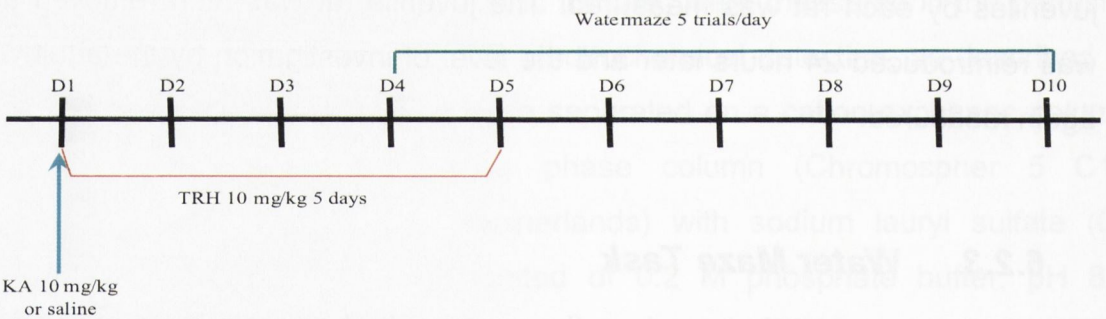

Figure 6.3 The experimental treatment of animals that underwent the Morris water-maze study

The timeline of the treatment of the three groups of animals that were studied by the Morris water-maze swim test. Control animals were injected intraperitonially (i.p.) with saline and those administered kainate were injected i.p. with 10 mg/kg. Animals in the TRH group received 10 mg/kg TRH i.p. 6 h later and once a day thereafter, to day 5. Saline was administered to the control and kainate group. Water-maze trials were initiated on day 4 and continued to day 7.

Rodents were trained to escape from water by swimming to a hidden platform, the location of which could be found by a learned sequence of movements which brought it to the platform using distal extra maze cues [a spatial strategy (D'Hooge and De Deyn 2001)]. The watermaze was a black circular pool filled with water at room temperature, diameter 200 cm, height 35 cm. The pool was located in a room with extra maze cues. The platform had a diameter of 9.5 cm and a height of 29 cm, thus submerged 2 cm below water level (for diagram, see Figure 6.4). Animals were placed in the pool facing the wall and the trial started as soon as the rat was released, if the rat did not find the platform within 60 seconds, the animal was guided to the platform where it remained for 15 seconds. Rats were given 5 trials per day. The maze was divided into theoretical North West (NW), South West (SW), North East (NE) and South East (SE) quadrants, with the platform centred in the NW quadrant (Figure **6.5**). The velocity, escape latency, total distance swam were recorded by EthoVision image analysing system from Noldus Information Technology (Wageningen, Holland).

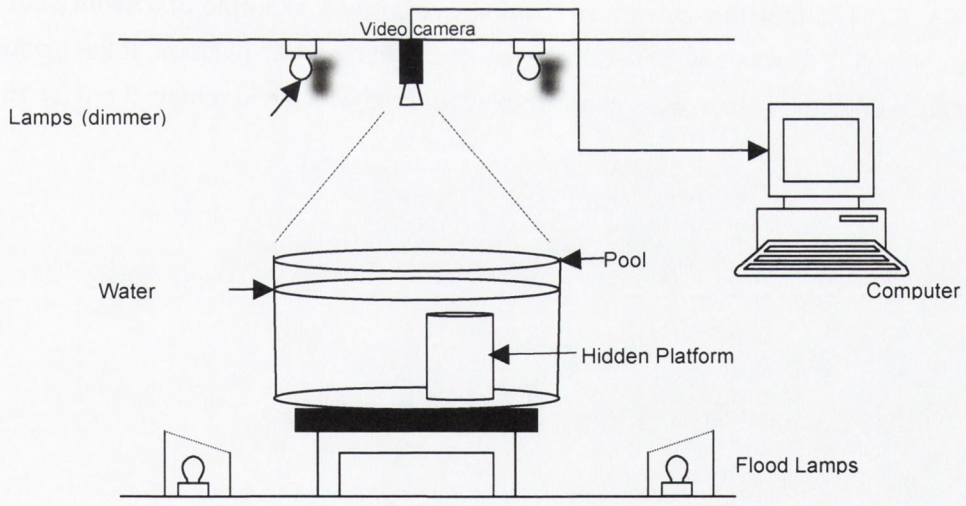

Figure 6.4 Diagram of the Morris water-maze setup A submerged platform was located in the NW quadrant of the pool and animals were placed into the pool at a random location and the time taken to locate the platform (escape latency) and the distance swam in the pool were measured by EthoVision image analysing system from Noldus Information Technology (Wagenheim, Netherlands).

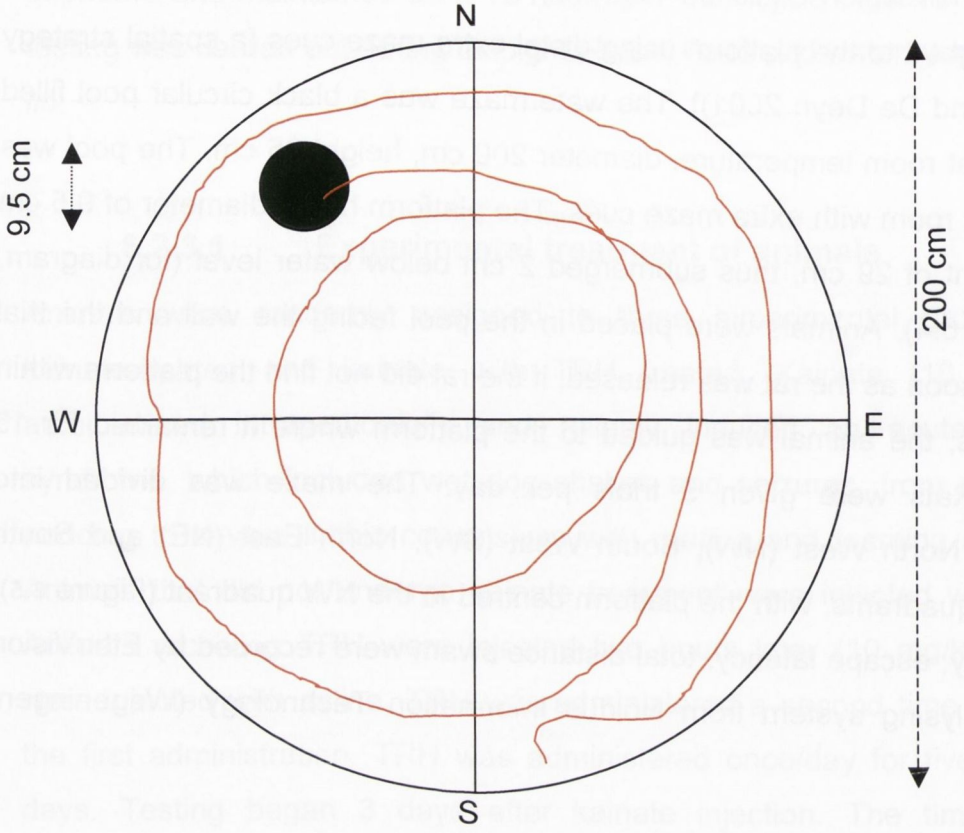

Figure 6.5 The Morris water-maze from above with an example of a swim path

Animals underwent 5 trials/day, with 60 s to locate the submerged platform. If the platform was not located at 60 s, the animal was guided to platform and was left to remain there for 15 s.

6.3 Results

6.3.1 The effect of TRH on kainate challenge to the striatum

6.3.1.1 In vivo monitoring of amino acid release during kainate challenge

The alteration in amino acid release due to 100 μM kainate infusion in the absence and presence of TRH (injected i.p.) was monitored by the collection of microdialyses fractions for 20 min periods over 320 min (Figure 6.6). The increase in amino acid release due to 100 mM potassium stimulation (over 20 min) was evident. The time of injection with TRH or saline (100 min), of anaesthetic administration (120 min) and kainate perfusion (120 min) are indicated on the graphs. The quantities of amino acids detected are expressed as pmol/μL and were analysed by two-way ANOVA with Bonferroni's post-test. Due to the hyper-excitability kainate induces in animals, animals were anaesthetised (chloral hydrate at 400 mg/kg, i.p.) prior to the kainate-challenge. For analysis purposes, the fractions collected during this period were used as the pre-kainate basal level and all subsequent fractions were collected while the animals were under anaesthesia and used to calculate the kainate-stimulated release.

Kainate administration had no effect on the release of aspartate, glutamate or GABA. It did however result in a significant increase in taurine release, which was significantly elevated in fractions collected during kainate administration and subsequently to 240 min ($P<0.001$ compared to control animals). This effect was not prevented by TRH as this group also demonstrated significantly elevated taurine release, and TRH did not affect taurine release as animals injected with TRH but not administered kainate showed the same level of taurine release as controls. The effect of the kainate challenge was further analysed by comparison of the basal, pre-challenge level of amino acid release with the release stimulated by kainate (Figure 6.7). Two-way ANOVA comparison of the data with Bonferroni's post-test showed that the basal and

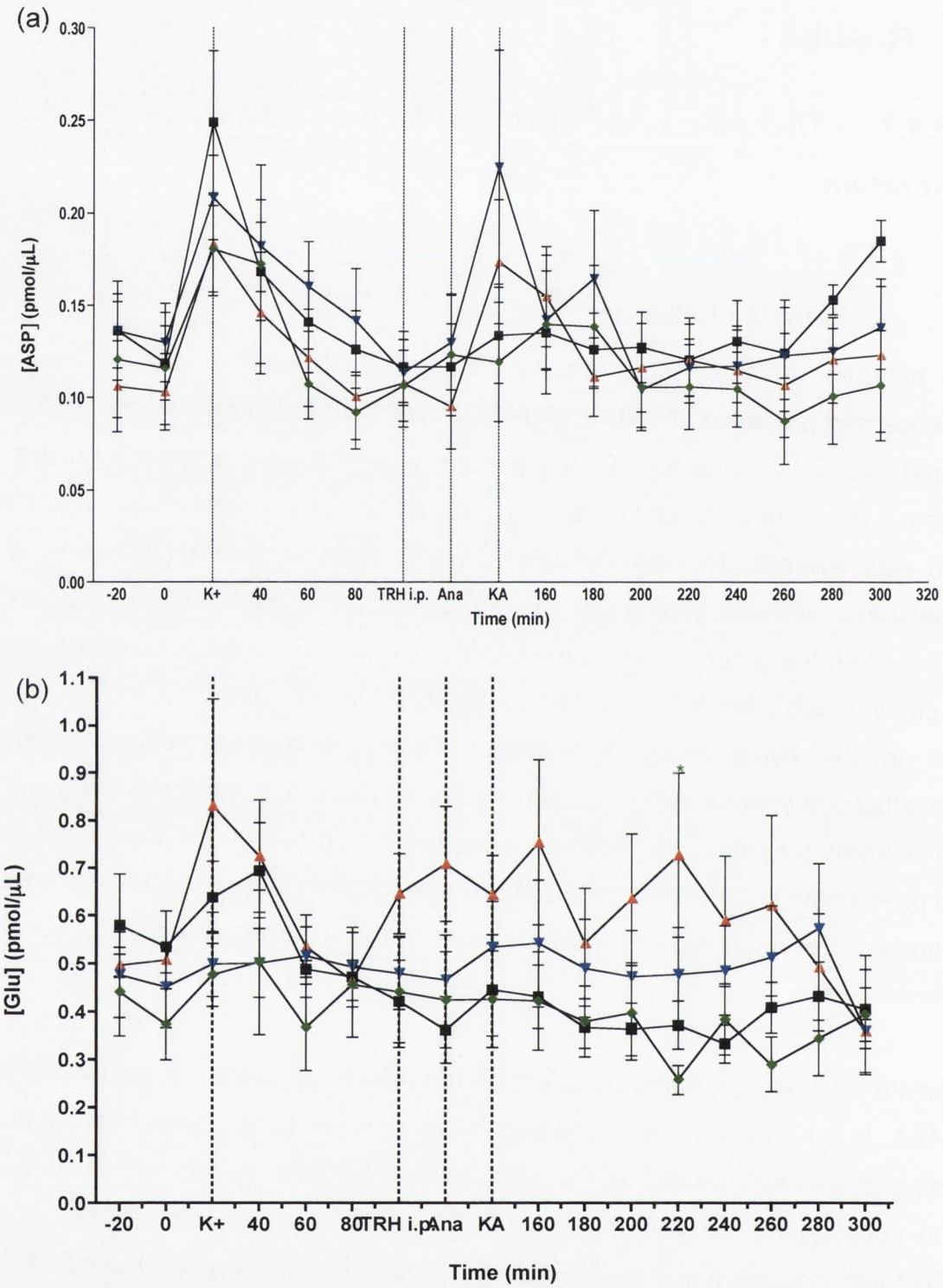

Figure 6.6 Effects of kainate and TRH on amino acid release from the striatum

Microdialyses fractions were collected at 20 min intervals from control, saline injected rats (■), rats injected with TRH (●), animals that underwent microdialysis with kainate (▲) and rats that were injected with TRH and underwent microdialysis with kainate (▼). The amino acid content of these fractions were analysed by derivatisation followed by HPLC separation.

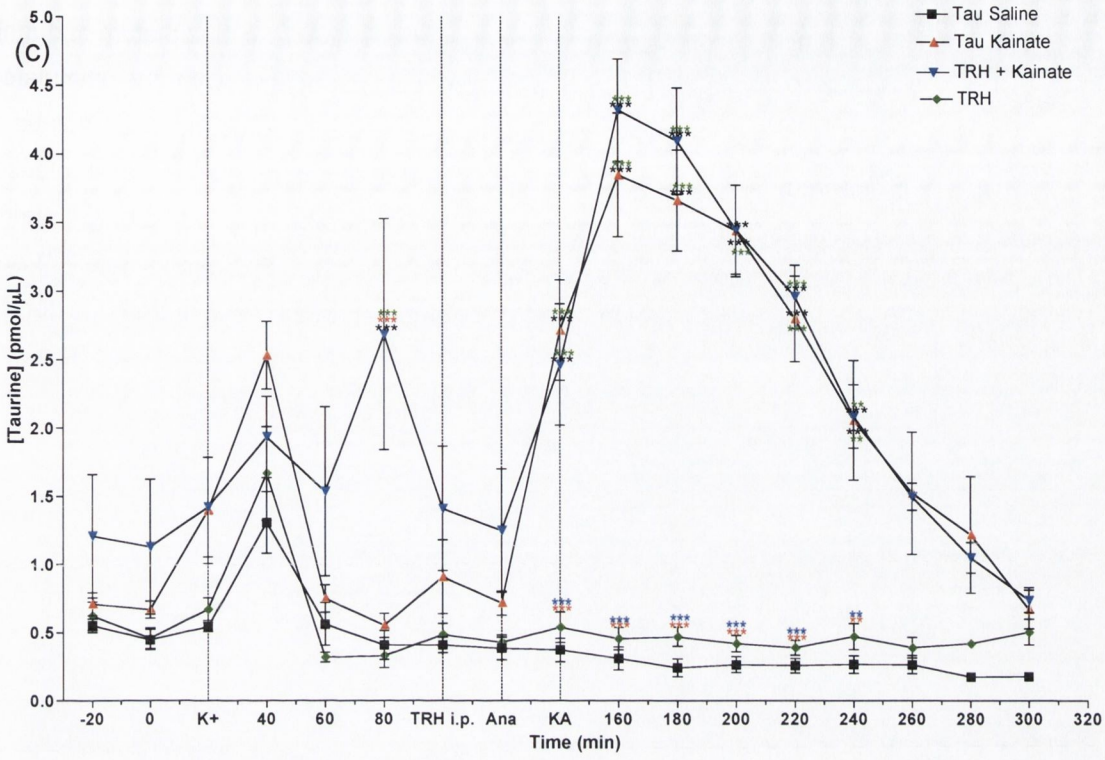

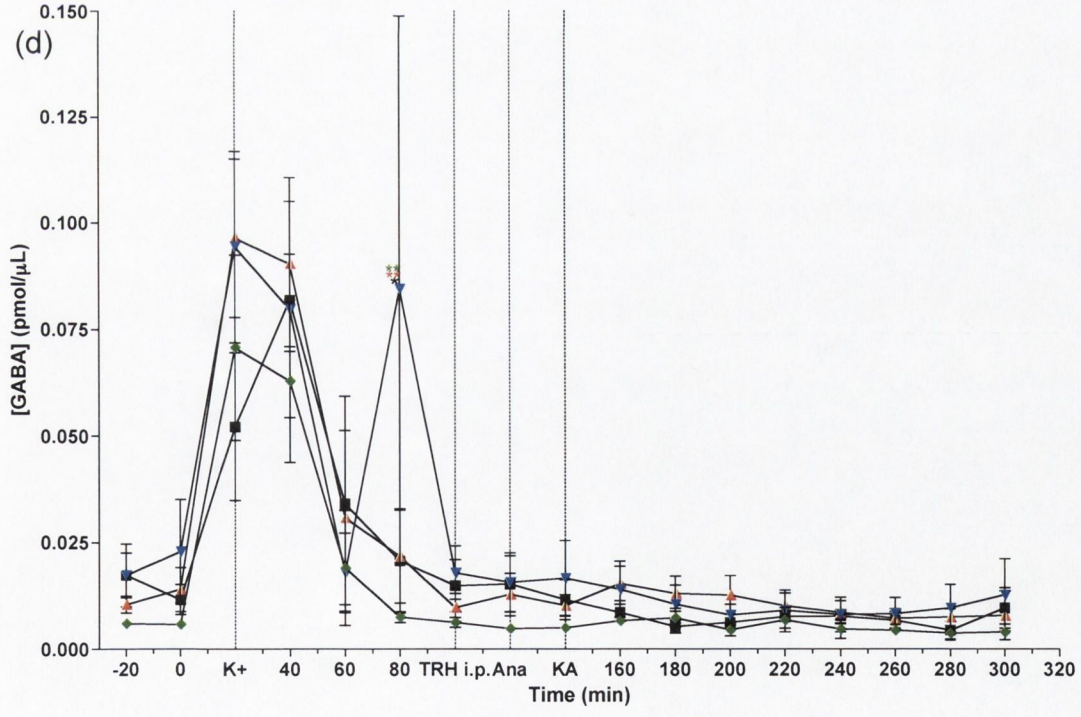

Data represent mean ± S.E.M. (n=5–9), with (a) aspartate release, (b) glutamate release, (c) taurine release and (d) GABA release. Analysis was performed by two-way ANOVA with Bonferroni's post-test and significant difference are indicated by *=P<0.05, **=P<0.01 and ***=P<0.001 and are colour-coded with reference to the group compared with.

Figure 6.7 Comparison of the basal and kainate-stimulated level of amino acid release from striatum

The release of (a) aspartate, (b) glutamate, (c) taurine and (d) GABA from the striatum of during the basal period (■; during anesthetic administration) was compared with the stimulated release (□) by two-way ANOVA with Bonferroni's post-test. Data represent mean values ± S.E.M. (n values range from 5–8) with **=P<0.01 and ***=P<0.001 compared to basal release. The basal release and the kainate-stimulated release of (e) aspartate, (f) glutatmate, (g) taurine and (h) GABA were compared between the control (■), kainate (□), TRH with kainate (▪) and TRH only (▪) groups, with *=P<0.05 and ***=P<0.001 compared to the release from the control group.

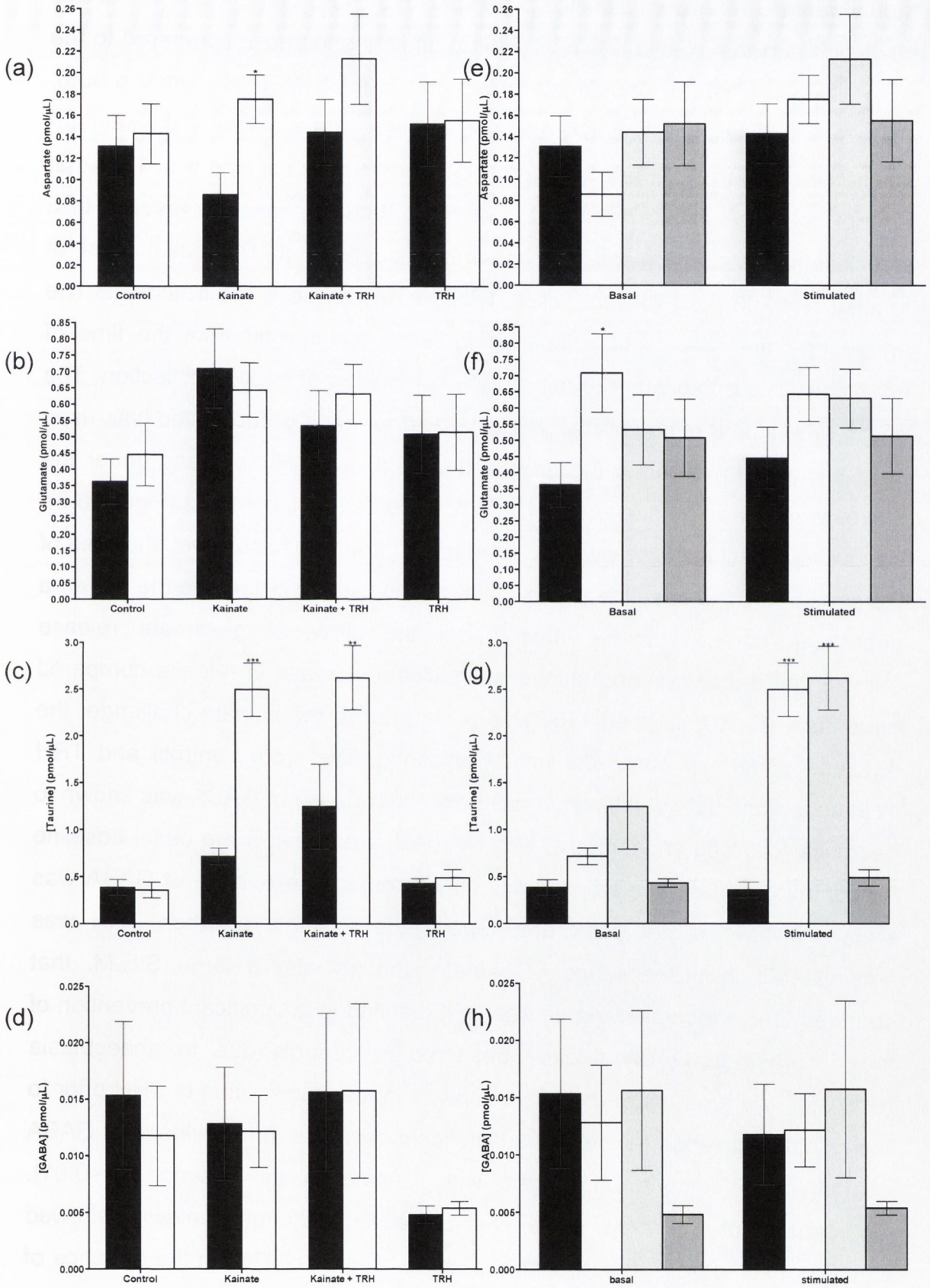
(a)
Aspartate (pmol/µL)
0.26
0.24
0.22
0.20
0.18
0.16
0.14
0.12
0.10
0.08
0.06
0.04
0.02
0.00
*
Control
Kainate
Kainate + TRH
TRH
(e)
Aspartate (pmol/µL)
Basal
Stimulated
(b)
Glutamate (pmol/µL)
0.85
0.80
0.75
0.70
0.65
0.60
0.55
0.50
0.45
0.40
0.35
0.30
0.25
0.20
0.15
0.10
0.05
0.00
Control
Kainate
Kainate + TRH
TRH
(f)
*
Glutamate (pmol/µL)
Basal
Stimulated
(c)
[Taurine] (pmol/µL)
3.0
2.5
2.0
1.5
1.0
0.5
0.0
***
**
Control
Kainate
Kainate + TRH
TRH
(g)
[Taurine] (pmol/µL)
***
***
Basal
Stimulated
(d)
[GABA] (pmol/µL)
0.025
0.020
0.015
0.010
0.005
0.000
Control
Kainate
Kainate + TRH
TRH
(h)
[GABA] (pmol/µL)
basal
stimulated

kainate-stimulated levels of glutamate and GABA release were not changed, though taurine underwent significant increase in animals that underwent kainate challenge and the injection of TRH did not affect the increase compared to the basal release ($P<0.001$ for kainate group and $P<0.01$ for TRH-treated group). Taurine release was significantly elevated in these groups following the kainate-challenge compared to the control group and to animals injected with TRH that did not undergo kainate treatment ($P<0.001$). Kainate-challenge resulted in a significantly elevated release of aspartate compared to the basal level of release ($P<0.05$), not evident when TRH was given as a pre-treatment. The area under the curve was calculated for each amino acid from the time of anaesthesia (8th fraction, 120 min) to the completion of fraction collection. The basal, pre-kainate release of each amino acid for each group tested was used as a baseline to calculate the area and comparisons of the areas under the curves were made by one-way ANOVA with Bonferroni's post-test (Figure 6.8). Where amino acids decreased in concentration from the basal level, the area of the peak below the baseline was calculated and used to determine the net area under the curve. The net area under the curve of glutamate release demonstrated that kainate induced a significant increase in release compared to controls ($P<0.05$). When TRH was given prior to the kainate challenge, the net area under the curve did not significantly differ from controls and TRH treatment alone did not differ from controls. The release of GABA was shown to decrease following anaesthesia, with net peak areas below the basal baseline for controls, kainate and kainate with TRH groups. The release of GABA was shown to have a net peak area above the basal level when TRH was administered in the absence of kainate, though with a large S.E.M. that spanned GABA increase and decrease; it resulted in a significant prevention of the decrease in GABA release observed in controls due to anaesthesia ($P<0.05$). The area under the curve showed that administration of TRH prior to the kainate challenge resulted in a significant decrease in the release of GABA compared to animals challenged with kainate in its absence ($P<0.01$). Comparison of the area under the curve for glutamate release showed significant standard errors, though the administration of TRH in the absence of kainate resulted in significantly reduced glutamate release compared to the

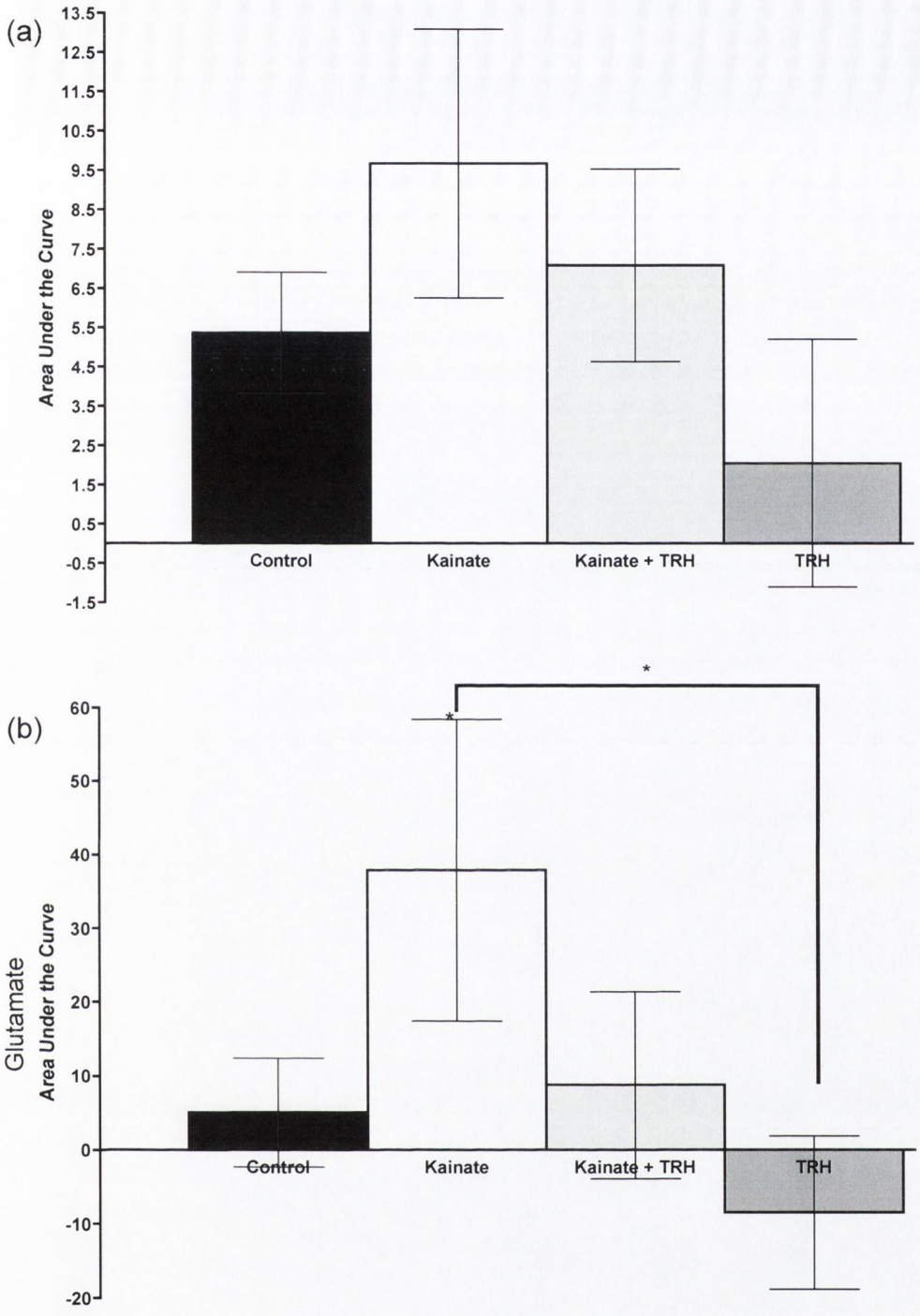

Figure 6.8 Analysis of the area under the curve of amino acid release during kainate challenge with TRH

The area under the curve of amino acid release from 120 min in Figure 6.6 using the release level of each amino acid in the fraction collected during anaesthesia as the baseline. Peaks due to the decline of amino acid release were used to calculate the net area. The areas due to each treatment (control=■, kainate treated animals in the absence of TRH=□, kainate treated animals that were injected with TRH= and animals injected with TRH in the absence of

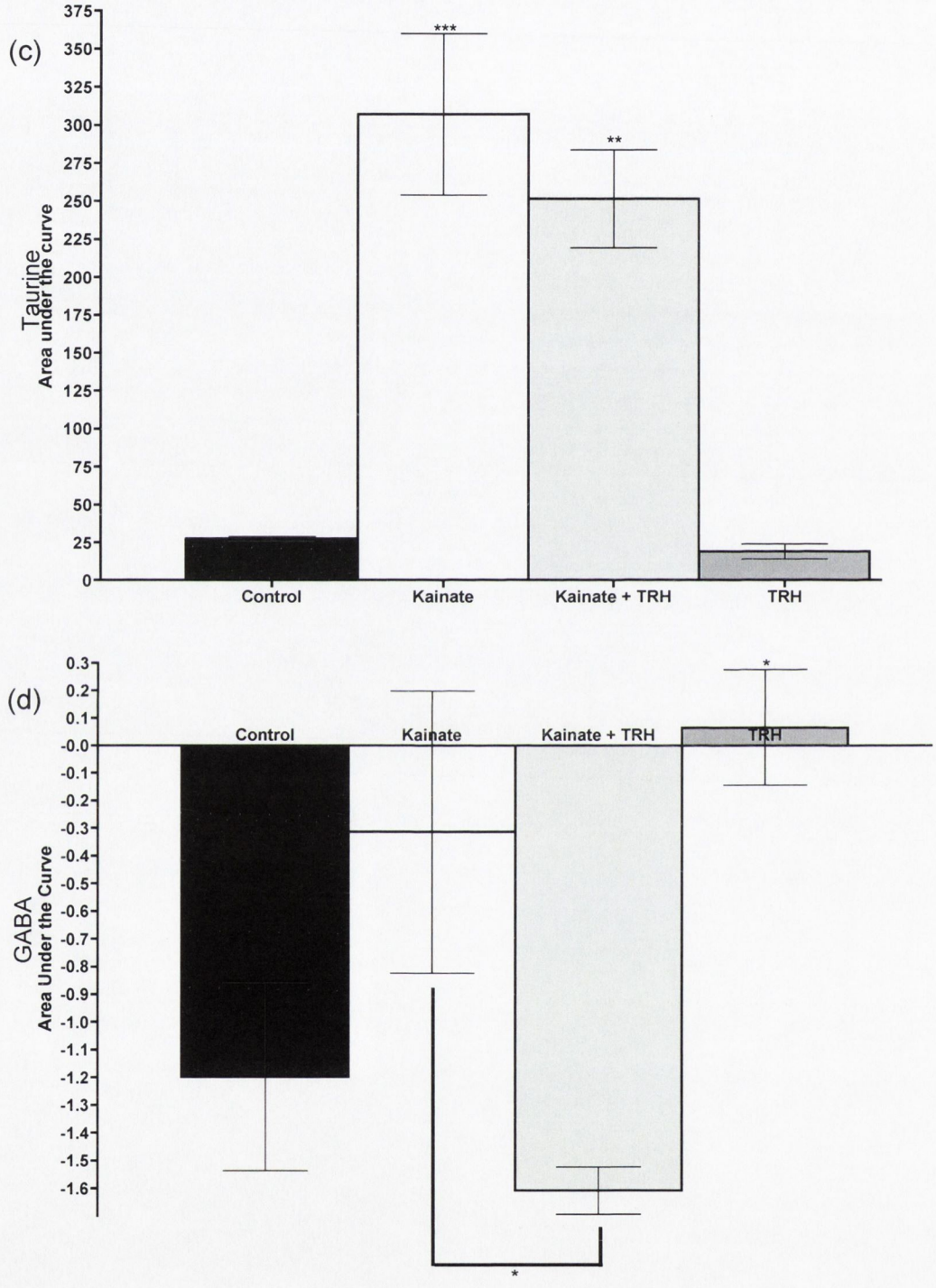

kainate=■) for the release of (a) aspartate, (b) glutamate, (c) taurine and (d) GABA were compared. Data represent mean values ± S.E.M. (n ranged from 5–9 samples). Analysis was performed by two-way ANOVA with Bonferroni's post-test, with *=P<0.05 and ***=P<0.001 significant difference compared to control, except where indicated.

kainate challenged group ($P<0.05$), and the TRH group had a net overall release of glutamate following anaesthesia.

6.3.1.2 *In vivo* monitoring of amine release during kainate challenge with TRH treatment

The release of dopamine and its metabolites DOPAC and HVA in addition to the serotonin metabolite 5HIAA were investigated following potassium challenge and following kainate challenge (Figure 6.9). Animals that underwent treatment with kainate released significantly more dopamine than control animals in the 20 min following kainate treatment ($P<0.01$), however these animals also released significantly more dopamine than the kainate with TRH and the TRH-only groups during potassium stimulation ($P<0.001$). The animals that were subjected to TRH injection prior to kainate treatment also released significantly more dopamine than controls in the 20 min following kainate treatment ($P<0.05$) and the release was not significantly different from the other groups during potassium stimulation. Animals that were injected with TRH but did not undergo kainate challenge released DOPAC at the same levels as control animals following anaesthesia, but release was significantly greater than that released by animals challenged with kainate in ($P<0.001$ and $P<0.01$, in the two fractions collected following kainate treatment and $P<0.01$ and $P<0.05$, in the two fractions collected following kainate stimulation in animals that were injected with TRH). This same trend was also present for HVA release with animals injected with TRH in the absence of kainate releasing significantly greater HVA than animals treated with kainate in the 40 minutes following the kainate challenge (animals treated with kainate alone; $P<0.01$, animals injected with TRH prior to kainate; $P<0.01$ and $P<0.05$). The release of 5HIAA was also different between the TRH treated animals and those that were challenged with kainate in the 20 min following kainate stimulation ($P<0.05$).

The basal and kainate-stimulated levels of amine release were compared in Figure 6.10. In kainate-treated groups dopamine release was significantly greater than the basal, pre-kainate infusion levels and significantly greater than the control and TRH-treated levels ($P<0.001$). Injection of TRH prior to the kainate challenge had no effect on the increased dopamine release, which was

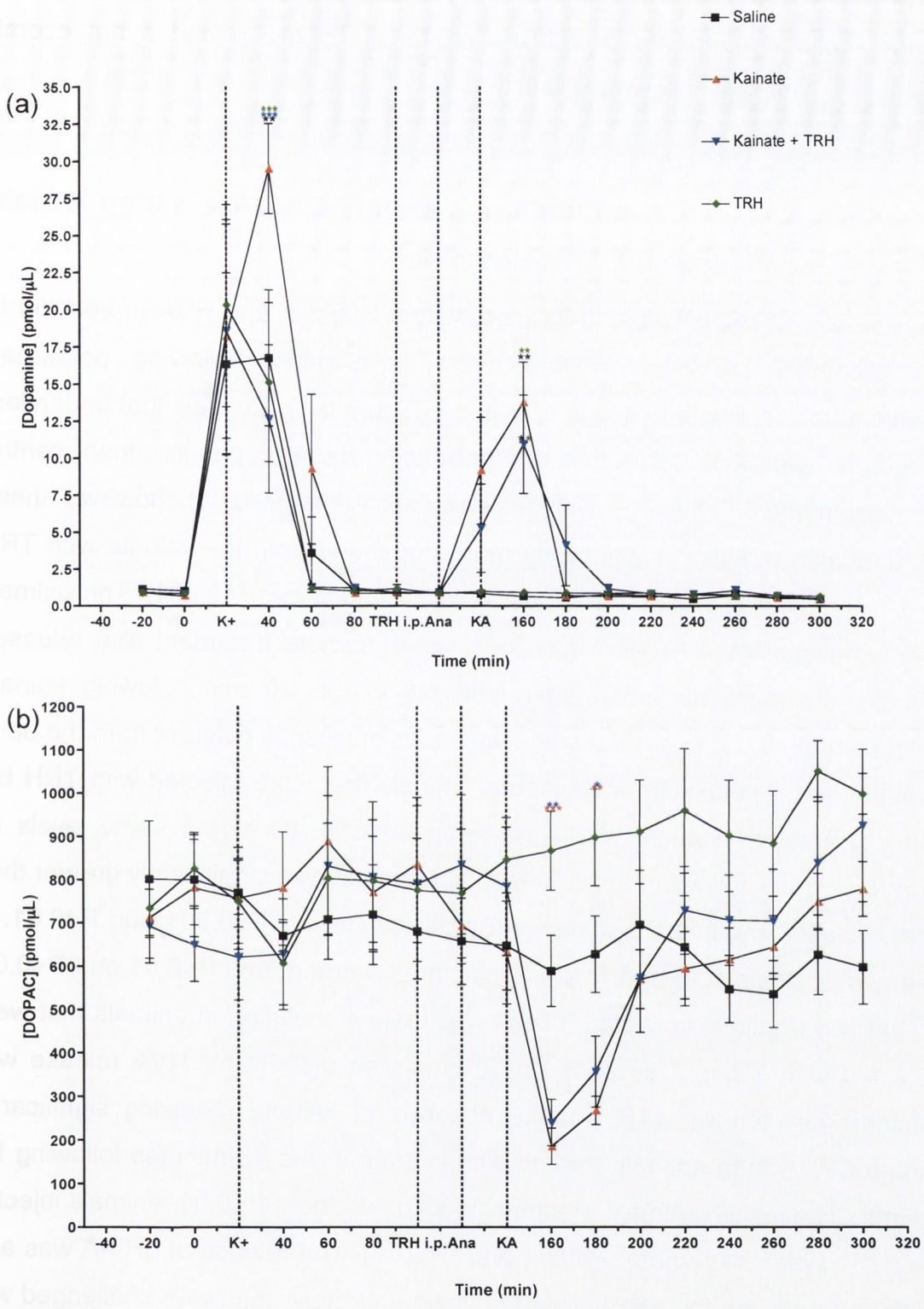

Figure 6.9 The release of amines from the striatum in response to kainate challenge with TRH

Microdialyses fractions were collected at 20 min intervals from control, saline injected rats (■), rats injected with TRH (●), animals that underwent microdialysis with kainate (▲) and rats that were injected with TRH and underwent microdialysis with kainate (▼). The amino acid content of these fractions were analysed by derivatisation followed by HPLC separation.

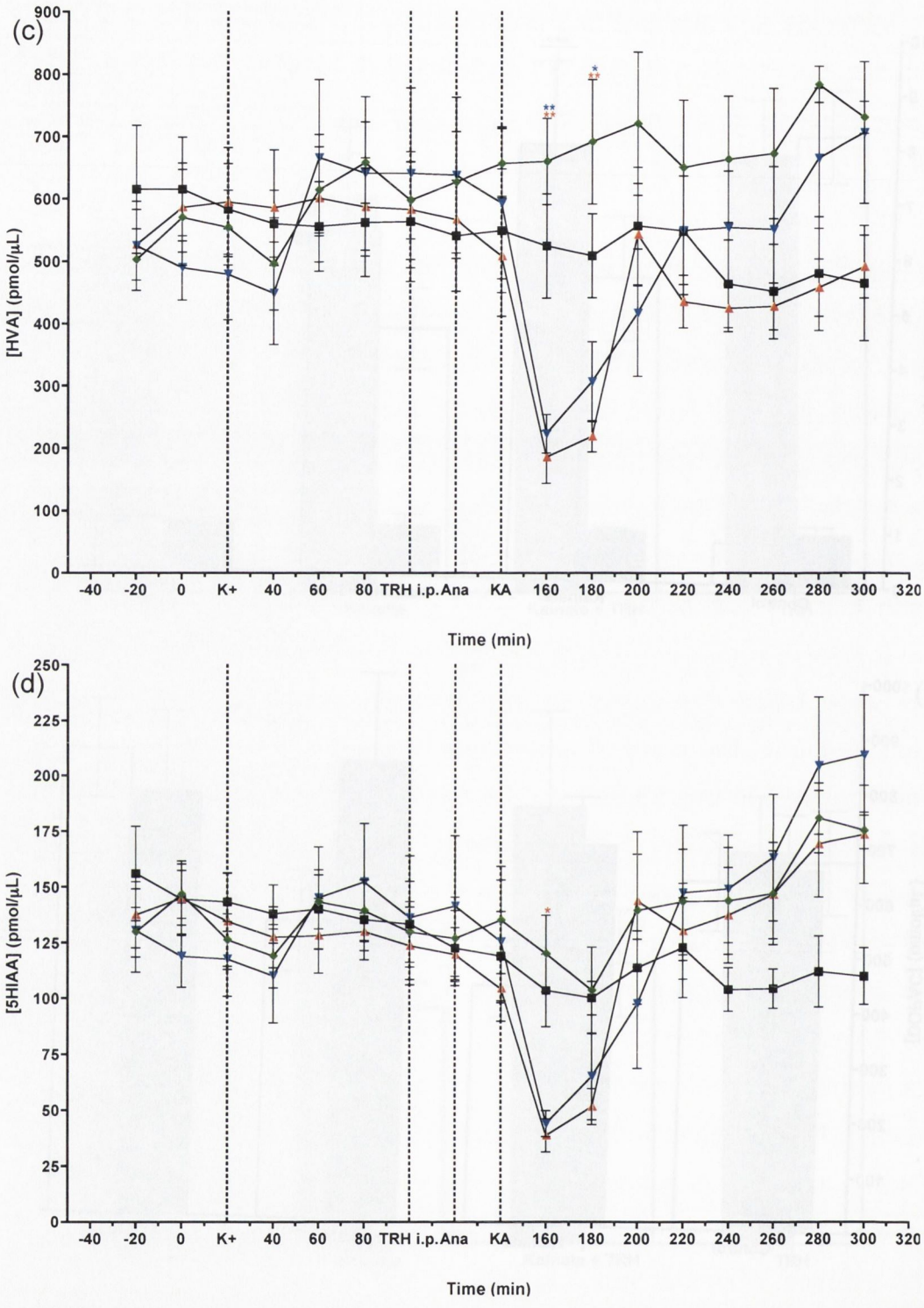

Data represent mean ± S.E.M. (n=6), with (a) dopamine release, (b) DOPAC release, (c) HVA release and (d) 5HIAA release. Analysis was performed by two-way ANOVA with Bonferroni's post-test and significant differences are indicated by *=P<0.05, **=P<0.01 and ***=P<0.001 and are colour-coded with reference to the group compared with.

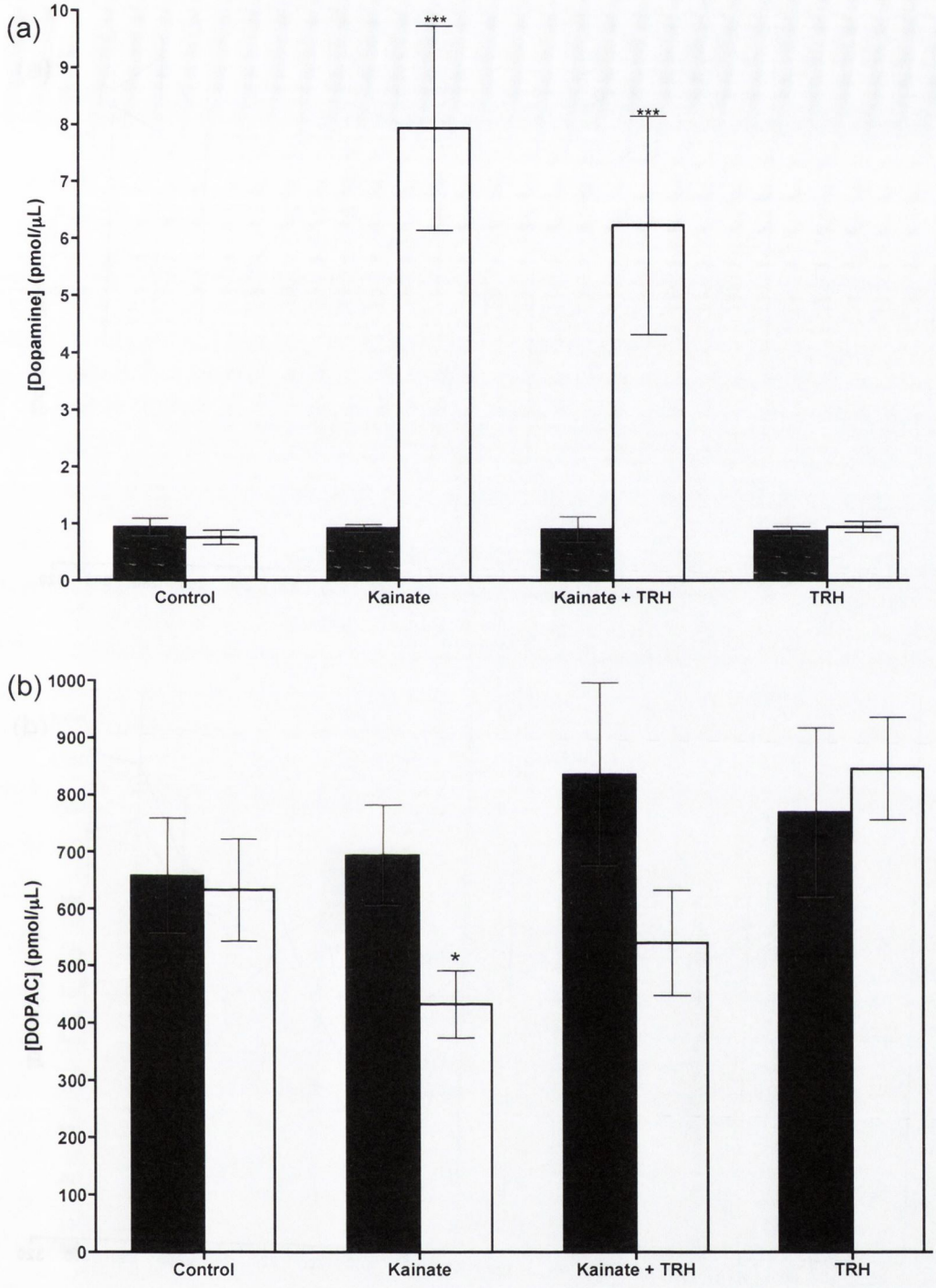
(a)
[Dopamine] (pmol/µL)
10
9
8
7
6
5
4
3
2
1
0
***
***
Control
Kainate
Kainate + TRH
TRH
(b)
[DOPAC] (pmol/µL)
1000
900
800
700
600
500
400
300
200
100
0
*
Control
Kainate
Kainate + TRH
TRH

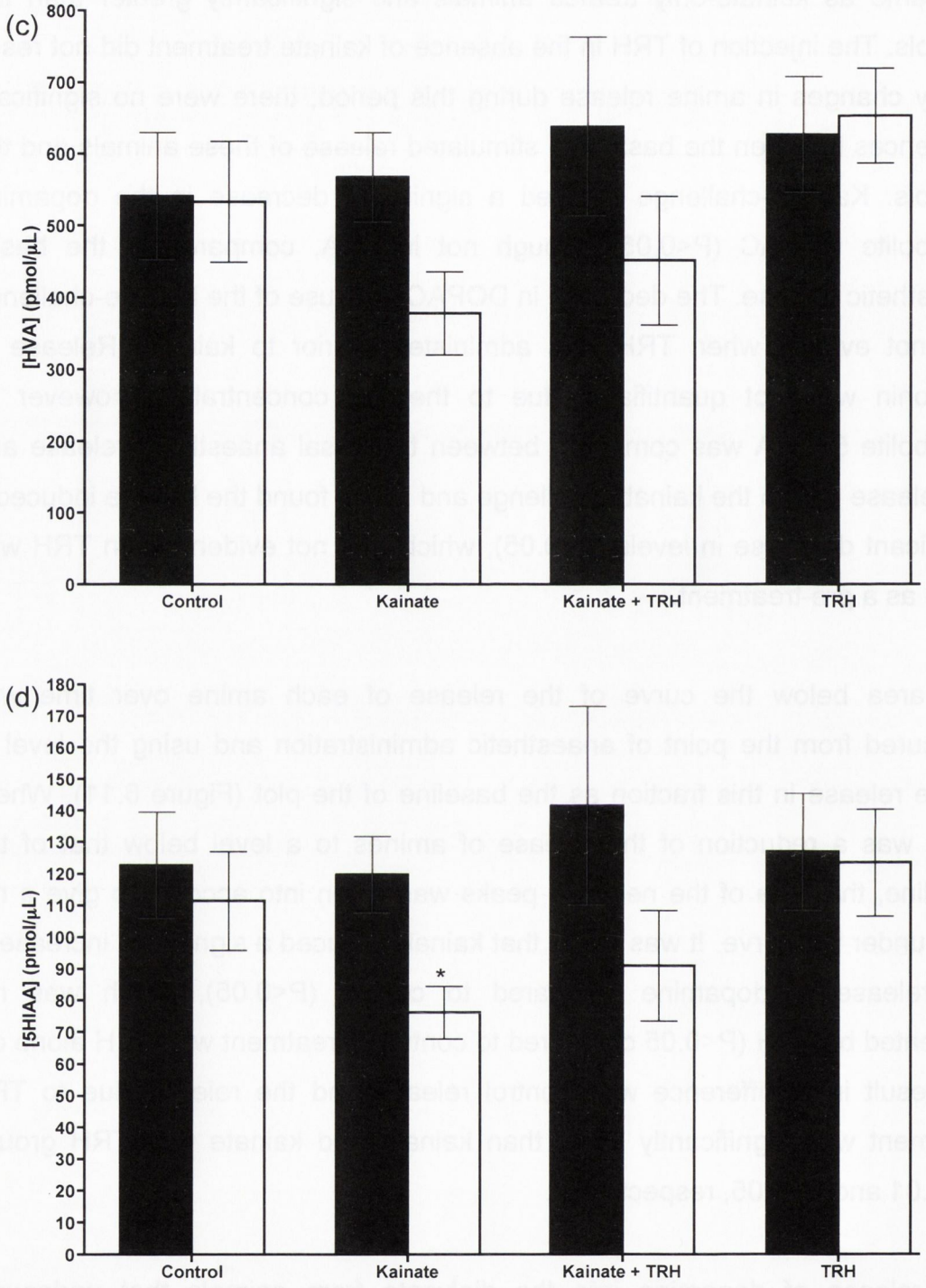

Figure 6.10 Comparison of the basal and stimulated release of amines from the striatum following kainate challenge

The release of (a) dopamine (b) DOPAC, (c) HVA and (d) HIAA from the striatum of during the basal period (■; during anesthetic administration) was compared with the stimulated release (□) by two-way ANOVA with Bonferroni's post-test. Data represent mean values ± S.E.M. (n=6) with *=P<0.05 and ***=P<0.001 compared to basal release.

the same as kainate-only treated animals and significantly greater than the controls. The injection of TRH in the absence of kainate treatment did not result in any changes in amine release during this period; there were no significant differences between the basal and stimulated release of these animals and the controls. Kainate-challenge induced a significant decrease in the dopamine metabolite DOPAC ($P<0.05$), though not in HVA, compared to the basal, anaesthetic release. The decrease in DOPAC because of the kainate-challenge was not evident when TRH was administered prior to kainate. Release of serotonin was not quantifiable due to the low concentration, however its metabolite 5-HIAA was compared between the basal anaesthetic release and the release due to the kainate-challenge and it was found the kainate induced a significant decrease in levels ($P<0.05$), which was not evident when TRH was given as a pre-treatment.

The area below the curve of the release of each amine over time was measured from the point of anaesthetic administration and using the level of amine release in this fraction as the baseline of the plot (Figure 6.11). Where there was a reduction of the release of amines to a level below that of the baseline, the area of the negative peaks was taken into account to give a net area under the curve. It was found that kainate induced a significant increase in the release of dopamine compared to control ($P<0.05$), which was not prevented by TRH ($P<0.05$ compared to control). Treatment with TRH alone did not result in a difference with control release and the release due to TRH treatment was significantly lower than kainate and kainate with TRH groups ($P<0.01$ and $P<0.05$, respectively).

The release of dopamine into the dialysate from animals that underwent treatment with TRH was compared between the fractions collected directly before TRH was injected, when TRH was administered and the fraction collected directly after, during which animals were anaesthetised (each fraction was collected over 20 min). The level of dopamine found was compared between the fractions by one-way ANOVA analysis with Bonferroni's post-test and no significant difference was found (Figure 6.12).

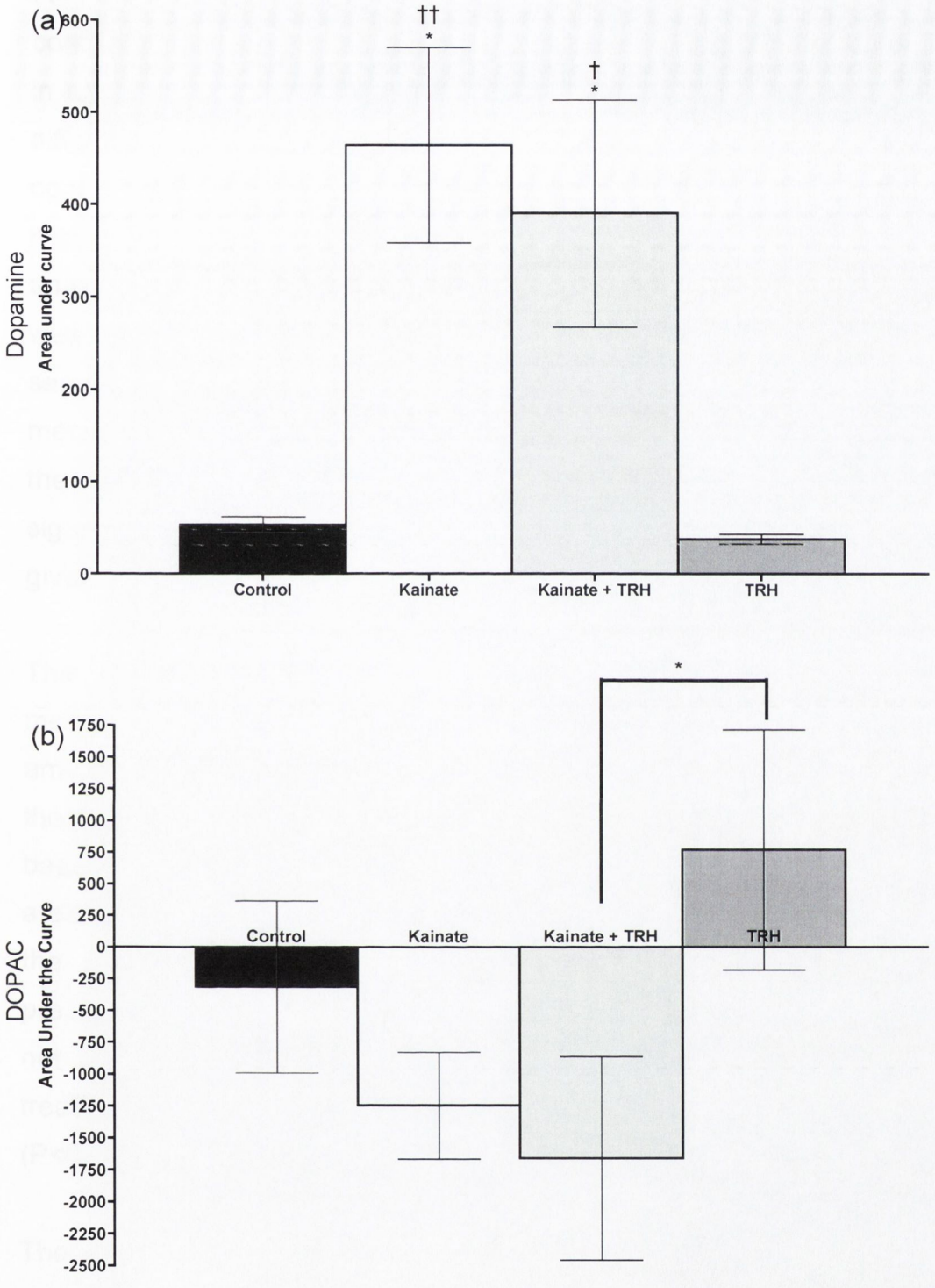

Figure 6.11 Analysis of the area under the curve of amine release during kainate challenge with TRH

The area under the curve of amine release from 120 min in Figure 6.9, using the release level of each amino acid in the fraction collected during anaesthesia as the baseline. Peaks due to the decline of amine release were used to calculate the net area. The areas due to each treatment (control=■, kainate treated animals in the absence of TRH=□, kainate- treated

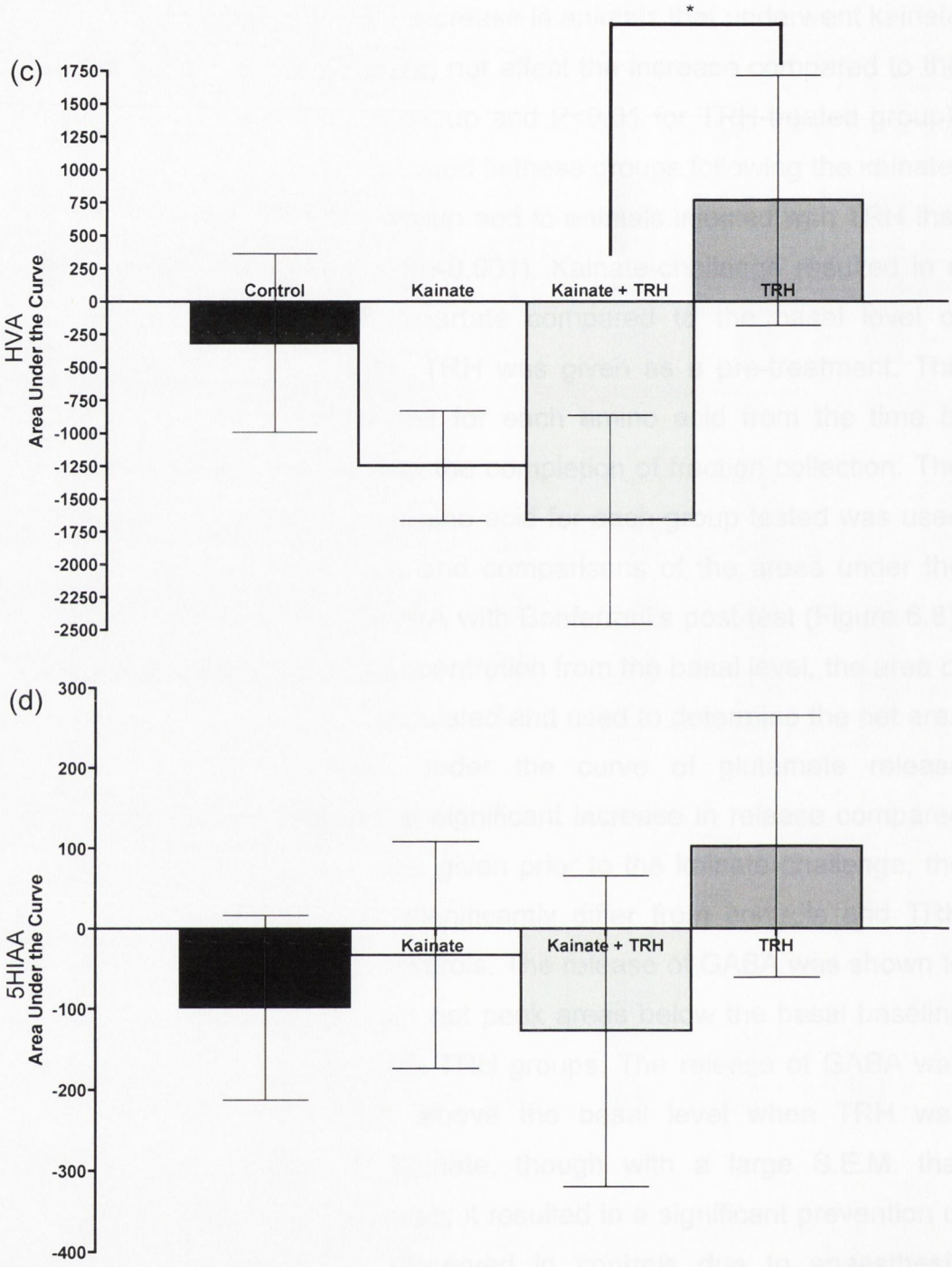

animals that were injected with TRH= and animals injected with TRH in the absence of kainate=) for the release of (a) dopamine, (b) DOPAC, (c) HVA and (d) 5-HIAA were compared. Data represent mean values ± S.E.M. (n ranged from 5–9 samples). Analysis was performed by two-way ANOVA with Bonferroni's post-test, with *=P<0.05 and significant difference compared to control, except where indicated and †=P<0.05 and ††=P<0.01 compared to the group treated with TRH alone.

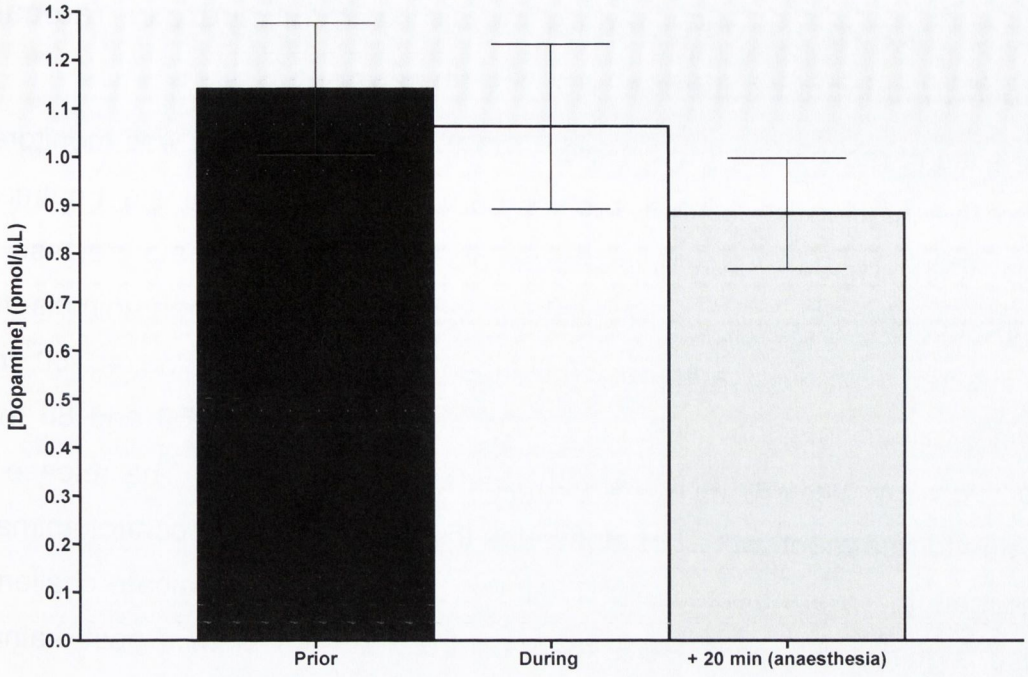

Figure 6.12 The effect of TRH on dopamine release

The release of dopamine from the striatum into fractions collected in the 20 min before TRH administration, the 20 min during which TRH was injected intraperitonially and in the fraction collected directly after, during which animals were anaesthetised. Data represent mean values ± S.E.M. (n=12), comparison was made by one-way ANOVA analysis with Bonferroni's post-test and no significant difference was found.

6.3.1.3 *In vivo* monitoring of the release of hydroxy radicals following kainate challenge with TRH treatment

The release of reactive oxygen species (ROS) from the striatum was monitored prior to the infusion of kainate and for 160 min following kainate treatment (Figure 6.13). Though kainate challenge did not result in greater release of ROS than control animals, the release was significantly more than animals that were injected with TRH and not challenged with kainate in the 40–80 min following kainate infusion ($P<0.05$, <0.001 and <0.05 for 40, 60 and 80 min, respectively, by two-way ANOVA with Bonferroni's post-test). The release of ROS due to treatment with TRH alone was the same as that of control animals, but animals that were treated with TRH and then underwent kainate challenge release significantly more ROS than controls at 40–80 min post kainate treatment and again 140 min after kainate was administered ($P<0.001$, <0.05, <0.001 and <0.05, respectively) and significantly more than animals treated with TRH alone for an extended period (40–140 min post kainate challenge; $P<0.001$). The release of ROS by the TRH with kainate treated group was significantly greater than animals challenged with kainate in the absence of TRH treatment 80 min post-kainate ($P<0.05$). There were no significant differences between the groups during or following the administration of TRH and saline, with increases arising only following the kainate challenge.

The basal level of ROS release, prior to the kainate challenge was compared with the release due to kainate stimulation by two-way ANOVA with Bonferroni's post-test [Figure 6.14 (a)]. Animals treated with TRH prior to kainate challenge were shown to have significantly increased release of ROS due to kainate stimulation compared to the basal level of release ($P<0.01$), all other treatment groups had no significant difference between the basal and stimulated level of release. Figure 6.14 (b) compared the basal and stimulated release between the groups, again there was no significant difference between control, TRH-only and kainate-only animals, however animals given TRH prior to kainate challenge had significantly greater release of ROS than each of the other groups ($P<0.001$ compared to control and TRH groups and $P<0.01$ compared to kainate group).

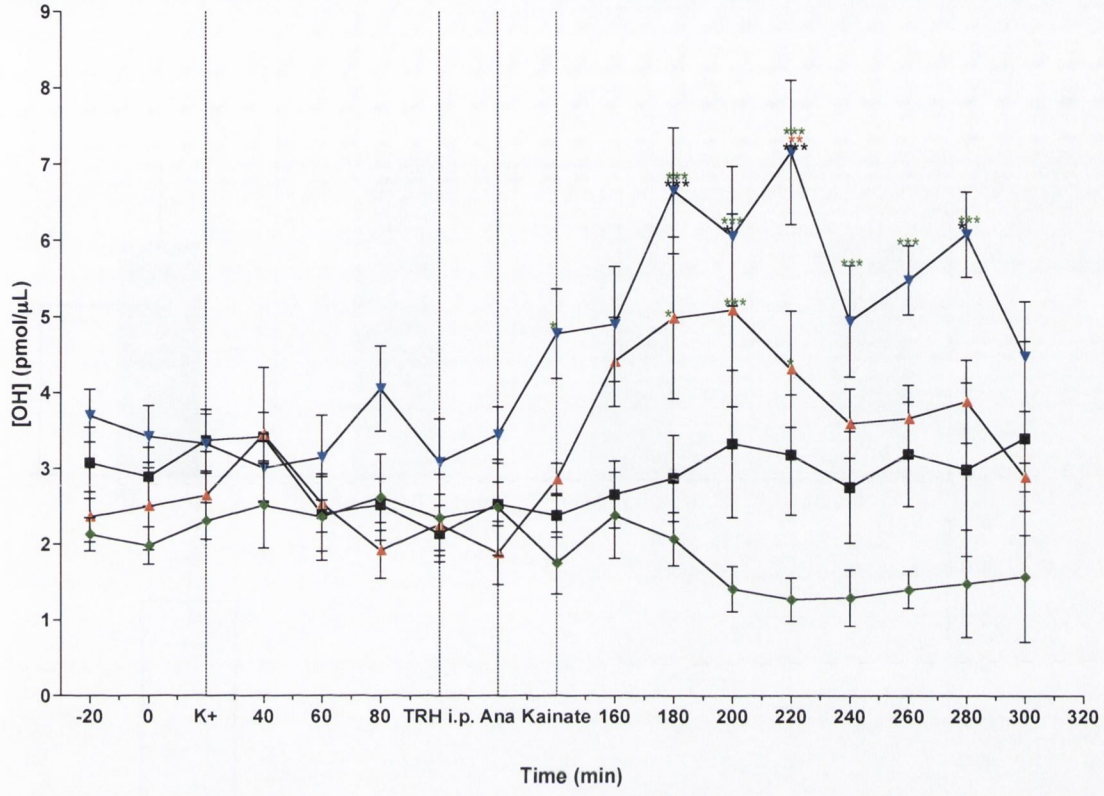

Figure 6.13 The release of reactive oxygen species from the striatum during kainate challenge with TRH

Microdialyses fractions were collected at 20 min intervals from control, saline injected rats (■), rats injected with TRH (●), animals that were injected with saline and underwent microdialysis with kainate (▲) and rats that were injected with TRH and underwent microdialysis with kainate (▼). The reactive oxygen species (ROS) content of these fractions were analysed by reaction with terephthalate (TA) followed by HPLC separation. Data represent mean values ± S.E.M. (n=5–8) and comparison was made by two-way ANOVA with Bonferroni's post-test. *=P<0.05, **=P<0.01 and ***=P<0.001 and are colour-coded in reference to the group compared with.

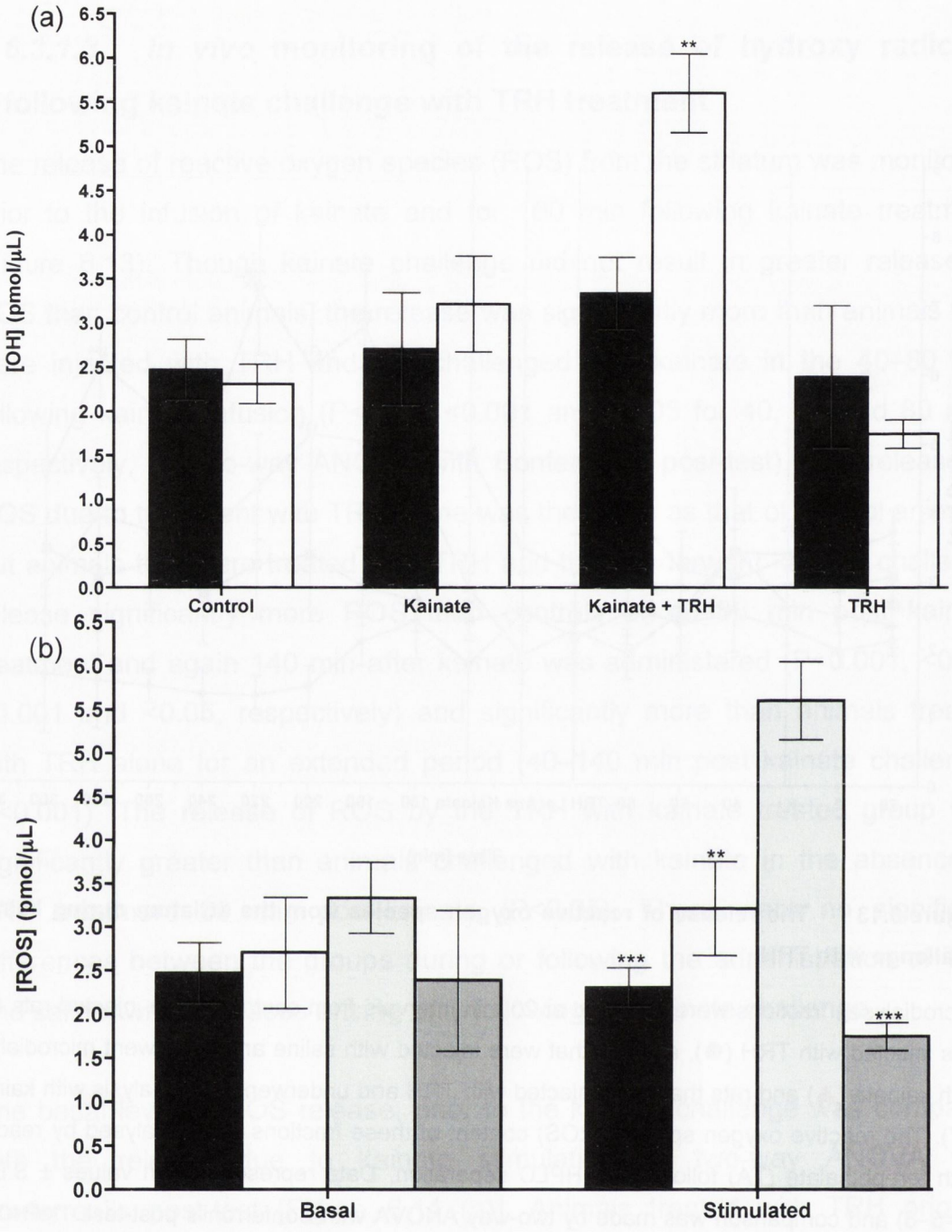

Figure 6.14 Comparison of the basal and kainate-stimulated release of reactive oxygen species from the striatum

The release of reactive oxygen species (ROS) from the striatum during the basal period (■; during anesthetic administration) was compared with the stimulated release (□) by two-way ANOVA with Bonferroni's post-test. Data represent mean values ± S.E.M. (n values range from 5–8) with **=P<0.01 compared to basal release. (b) The basal release and the kainate-stimulated release of ROS were compared between the control (■), kainate (□), TRH with kainate (■) and TRH only (■) groups, with **=P<0.01 and ***=P<0.001 compared to the release from animals subjected to treatment with both TRH and kainate.

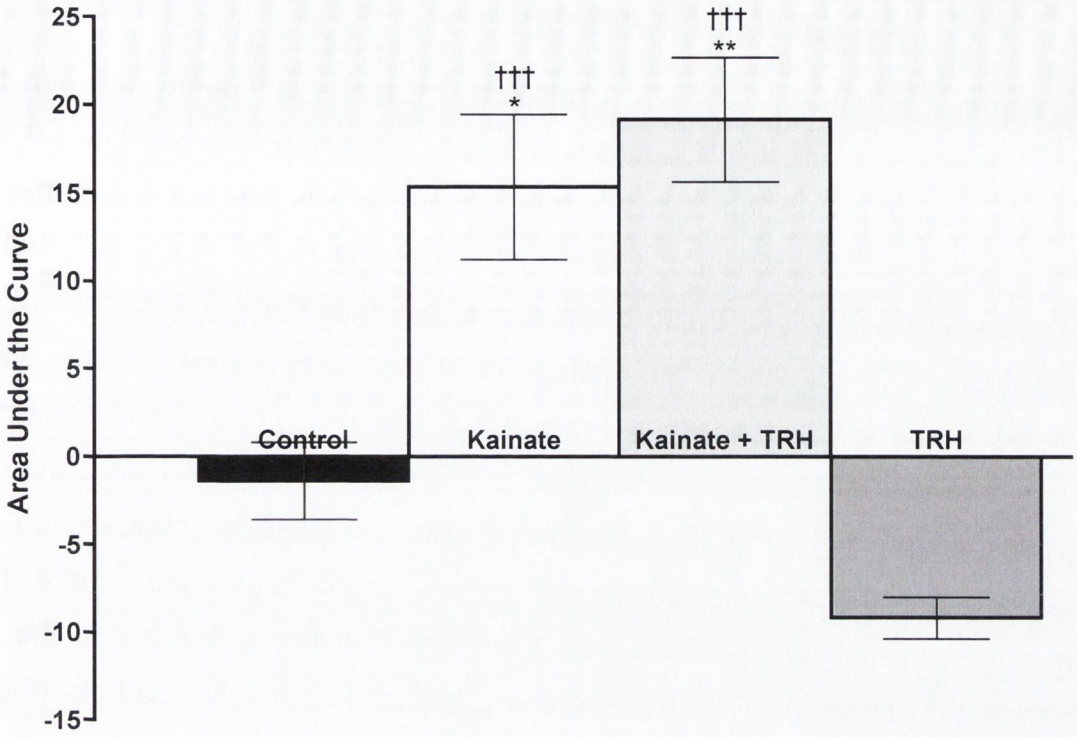

Figure 6.15 Comparison of the release of reactive oxygen species due to kainate and TRH

The area under the curve of the release of reactive oxygen species (ROS) measured in Figure 6.13 was determined using the level of release in the fraction collected during anaesthetic administration as the baseline of the curve and the start point. Where there was a decrease in the ROS relative to the baseline, the area of the negative peak was used to calculated the net area. The treatment groups were compared by one-way ANOVA with Bonferroni's post-test. Data represent mean ± S.E.M. (n range from 5–8), with *=$P<0.05$ and **=$P<0.01$ compared to the control group and †††=$P<0.001$ compared to the group treated with TRH alone.

6.3.2 *Social Recognition studies*

The time spent interacting with a novel juvenile was compared between the initial pairing and the reintroduction 24 h later (Figure 6.16 and Figure 6.17). The time spent interacting on the second encounter was significantly shorter on the second day for the control, kainate with TRH and TRH only groups ($P<0.05$ by two-way ANOVA with Bonferroni's post-test; Figure 6.16a). Only the animals challenged with kainate in the absence of TRH did not reduce the time spent interacting on the second day. Comparison was also made of the interaction time between the groups and it was found that on the initial encounter all groups spent the same time interacting with the juvenile, however on the second day the kainate challenged group spent significantly more time investigating the juvenile compared to the control group, animals in the two groups that received TRH treatment did not differ from the controls (Figure 6.16b). In Figure 6.17 the percent decrease in time spent interacting with the juvenile between the two days was compared by one-way ANOVA with Bonferroni's post-test between the groups and it was found that the kainate challenged group reduced the interaction time between the 2 trials significantly less than each of the other groups ($P<0.05$). The time-decrease did not differ between the control, kainate with TRH or TRH groups.

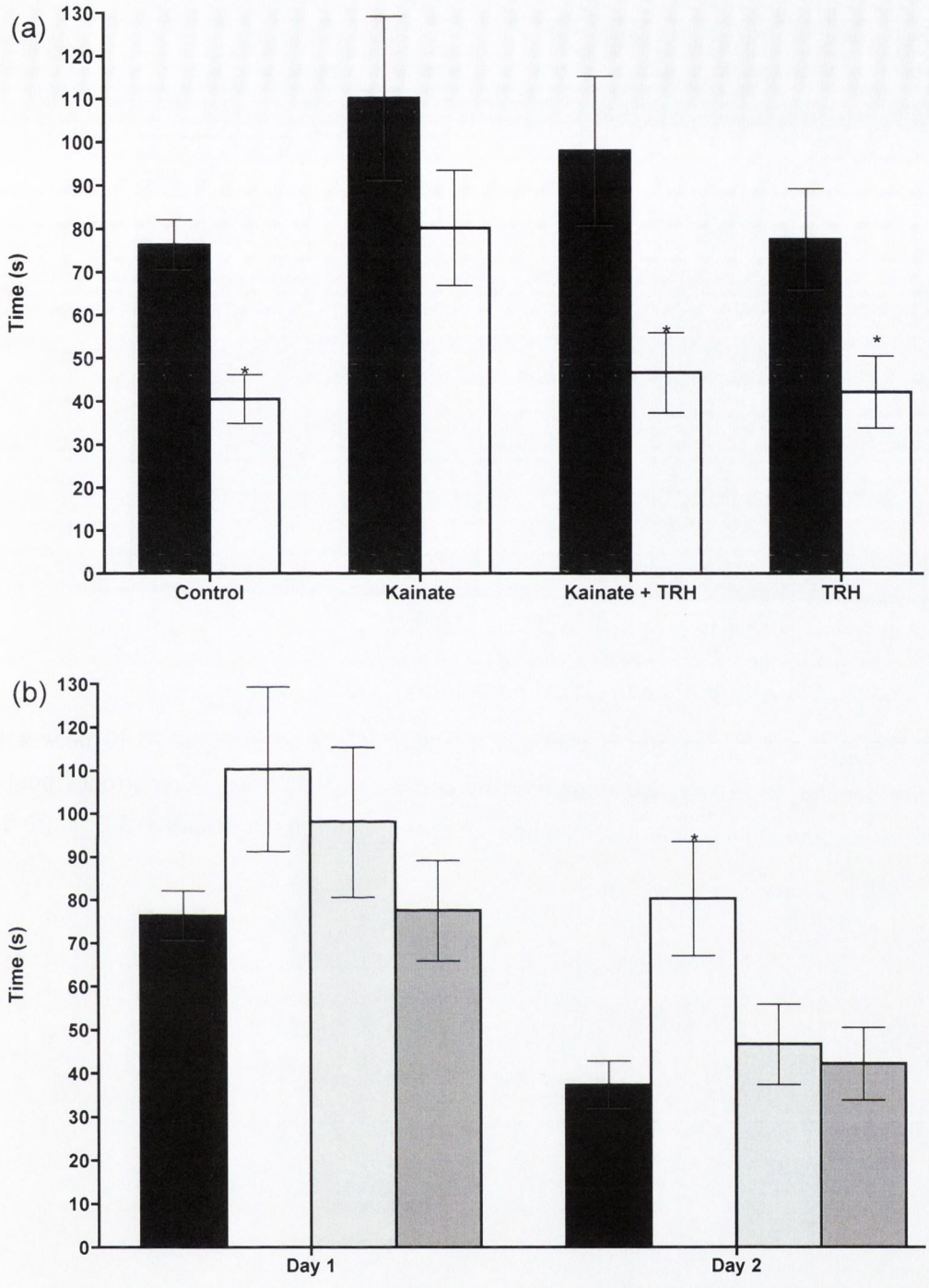

Figure 6.16 Social recognition test

The time spent interacting with a novel juvenile rat introduced to the animals undergoing study was monitored on two consecutive days as a model of short term working memory. (a) The time spent interacting with the juvenile on the first introduction (■) was compared with the time spent on the second encounter 24 h later (□) by two-way ANOVA with Bonferroni's post-test, *=$P<0.05$. (b) The amount of time spent interacting on initial and following encounter was compared between treatment groups (■=control, □=kainate, ▒=kainate with TRH and ■=TRH). Data represent mean values ± S.E.M. (n=6 and 7).

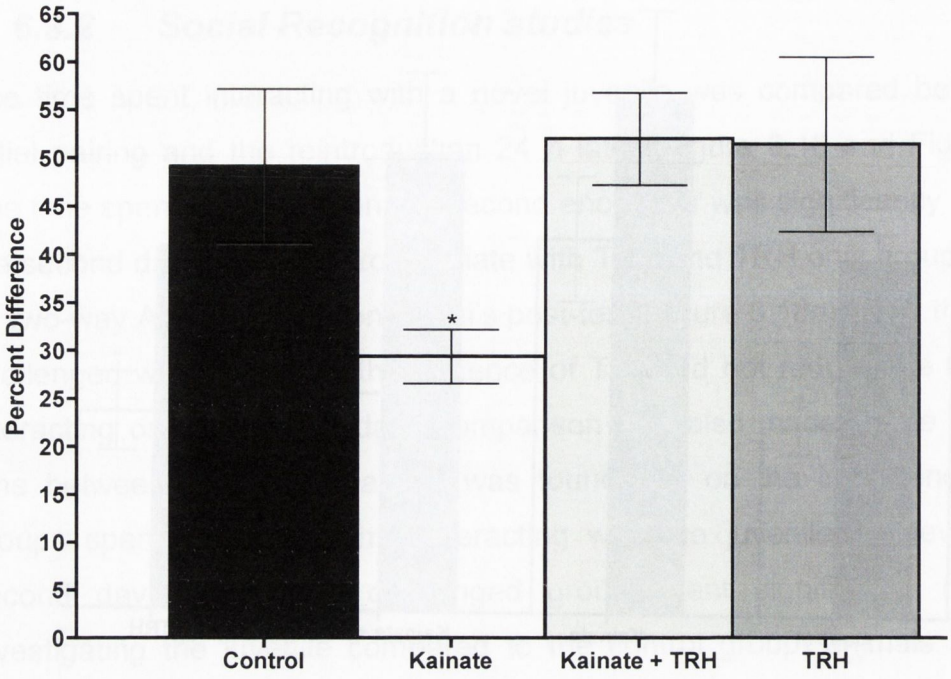

Figure 6.17 Time difference in social recognition test

The percent decrease in the time spent investigating presented in Figure 6.16 between the initial and second encounter was compared by one-way ANOVA with Bonferroni's post-test, with *=P<0.05 compared to the other groups. Data represent mean values ± S.E.M. (n=6 and 7).

6.3.3 Water-maze studies with kainate and TRH

6.3.3.1 Escape latency

The time taken for each group to find the submerged platform, escape latency, was monitored by EthoVision image analysing system from Noldus Information Technology (Wageningen, Holland). Each animal within the group was given five trials per day and the mean times of each animal were used to calculate the mean escape time for each treatment group ± S.E.M. The escape latencies are plotted in Figure 6.18 and it was found by two-way ANOVA analysis that the kainate-treated group took significantly more time to locate the platform on days 1 ($P<0.05$), 5($P<0.01$), 6 ($P<0.05$) and 7 ($P<0.01$) compared to controls. When TRH treatment was administered in conjunction with kainate there was significantly greater escape latency on day 1 only ($P<0.01$). Comparison of the time taken to escape over the course of the seven days was compared between the groups by one-way ANOVA with Bonferroni's post-test and it was found that the time taken by animals in the kainate group took significantly more time than the controls ($P<0.01$), though those that had also undergone TRH treatment were not different to the control group. Comparison of the improvement in the time taken to escape from day to day showed that each treatment group improved from day 1 to day 7 ($P<0.001$), with animals treated with kainate showing significant improvement between days 4 to 5 ($P<0.05$) and between days 5 to 6 ($P<0.001$). Animals that underwent treatment with TRH and kainate improved significantly between days 1 to 2 and 2 to 3 ($P<0.001$), days 4 to 5 ($P<0.05$) and days 6 to 7 ($P<0.01$).

6.3.3.2 Distance swam

The total distance swam by each group in the effort to locate the platform was measured in Figure 6.19 and compared between the groups by two-way ANOVA with Bonferroni's post-test. It was found that animals subjected to kainate swam a significantly greater distance in the pool than the controls on days 5 and 7 ($P<0.01$ on day 5 and $P<0.05$ on day 7). When TRH was

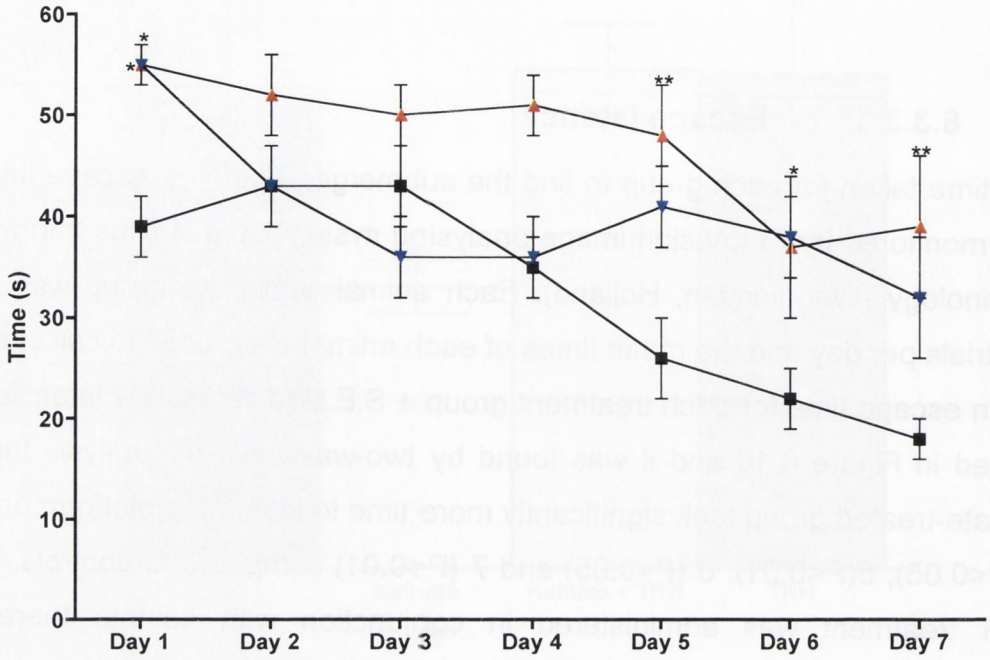

Figure 6.18 Escape latency of animals in the Morris water-maze study

The time taken for animals injected with saline (■), kainate (▲) or kainate with TRH (▼) to find a submerged platform when given 5 trials a day for 7 days. Data represent the mean values ± S.E.M. (n=9–11), with analysis performed by two-way ANOVA with Bonferroni's post-test. *=P<0.05 and **=P<0.01 in comparison to control, saline treated group.

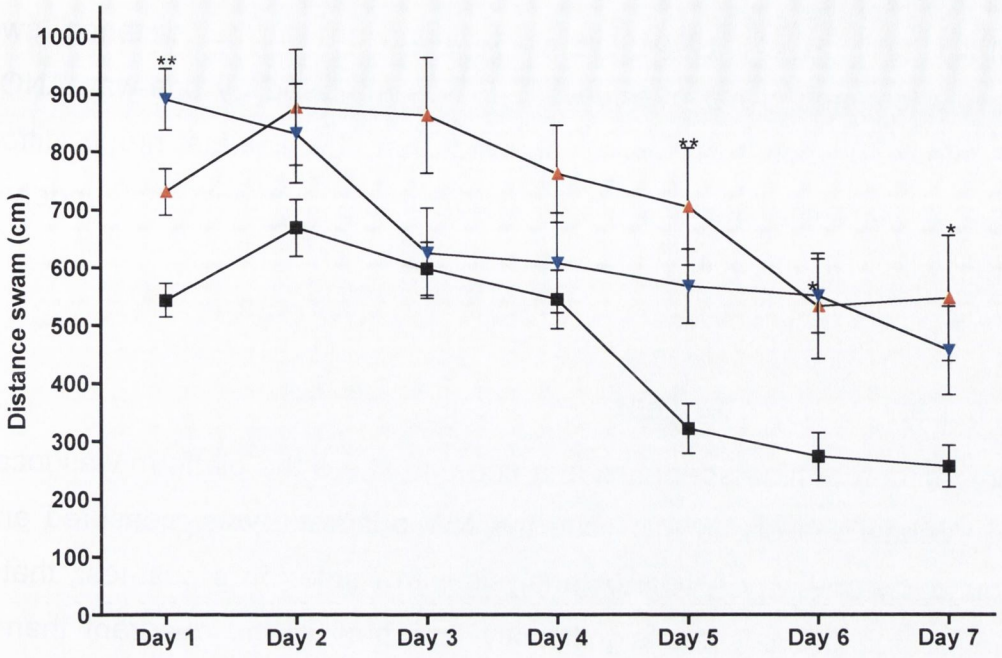

Figure 6.19 The distance swam by animals in the Morris water-maze study

The distance swam by animals injected with saline (■), kainate (▲) or kainate with TRH (▼) in the attempt to find a submerged platform when given 5 trials a day for 7 days was calulated. Data represent the mean values ± S.E.M. (n=9–11), with analysis performed by two-way ANOVA with Bonferroni's post-test. *=P<0.05 and **=P<0.01 in comparison to control, saline treated group.

administered with kainate the animals swam more than controls on days 1 and 6 ($P<0.01$ and <0.05, respectively). Comparison of the distance swum collectively for each group over days 1–7 was analysed by one-way ANOVA with Bonferroni's post-test, which showed that the kainate group differed significantly compared to controls ($P<0.05$), though animals that underwent treatment with TRH in addition to kainate did not differ.

6.3.3.3 Probe Test

The percentage of time spent inside a corridor where the platform was located (called Wishaw's error), in this case the NW quadrant, was measured and it was found, by one-way ANONVA analysis with Bonferroni's post-test, that the kainate treated group spent significantly less time in the quadrant than the control group ($P<0.05$), with no significant difference between the control and TRH with kainate group (Figure 6.20).

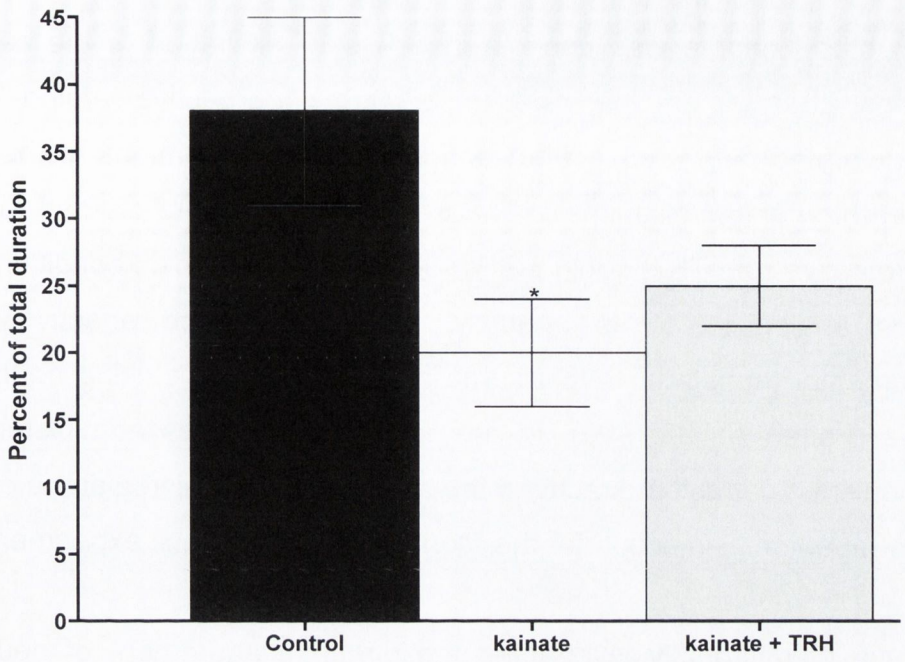

Figure 6.20 Morris water-maze probe-test

The mean percentage of time spent by the animals in the quadrant of the pool in which the submerged platform was located was measured for each group (control, kainate and kainate with TRH). Data represent the mean ± S.E.M. (n=9–11) with analysis performed by one-way ANOVA with Bonferroni's post-test. *=$P<0.05$ compared to control.

6.4 Discussion

In this study kainate was used to induce over excitation of the neurons with resulting changes in the release of both neuroactive amino acids and catecholamine neurotransmitters and subsequent alterations in the behaviour and learning ability of animals. The effects of TRH were studied to determine the protective role TRH could confer during the excitotoxic condition. TRH and various analogues of its structure have been used effectively in many experimental models of CNS trauma and have shown striking neuroprotective effects (Faden et al. 1999). In this study kainate was administered by two mechanisms; perfusion directly to the striatum during microdialysis experiments and intraperitonial injection for the Morris water-maze task experiments.

The use of microdialysis enabled the direct measurement of neurochemical changes in the brain due to the kainate-challenge. Glutamate in the dialysate was measured prior to kainate perfusion, during anaesthesia, and compared to the glutamate released over the period during kainate administration and directly after, however, glutamate release was very variable over this period, perhaps as a result of anaesthesia, resulting in no measurable increase in glutamate due to kainate stimulation. However, an alternative analysis, using the basal level of glutamate that perfused during anaesthesia as a baseline to calculate the area under the plot from anaesthesia to the end, showed that kainate significantly increased glutamate release, whilst treatment with TRH prior to kainate administration resulted in release comparable with controls (Figure 6.8). The inconsistencies in glutamate levels from each animal in the study make glutamate determination unreliable, however taurine, the release of which is known to occur following conditions causing excitotoxicity (Wallin et al. 1999) was significantly increased due to kainate (Figure 6.7 and Figure 6.8). Taurine has been reported to function in nerve transmission, modulation of neurotransmitter release, anti-oxidation, calcium homeostasis and as an anticonvulsant (Della Corte et al. 1999). This increased release of taurine is due to intracellular calcium release, as when receptors involved in calcium release are blocked, taurine release is prevented (Wallin et al. 1999). The kainate-induced increase in taurine release may function endogenously as a

neuroprotectant. The presence of TRH, injected intraperitonially prior to the kainate-challenge, gave rise to the same increase in taurine release, thus the potential protective effects of TRH, may not function through taurine, but may occur as a parallel process.

The measurement of aspartate also resulted in large deviations, again most likely due to the anaesthetic, thus making it difficult to determine the effect of kainate or any possible effects of TRH, though comparison of the level of aspartate release during the period of anaesthetic administration with the kainate-stimulated release showed a significant increase. The release due to the treatment with TRH prior to the kainate-challenge, showed no significant difference, as errors were large, probably due to the anaesthetic, thus making the release levels difficult to interpret. Despite the high variability of measurements, it was evident that the level of GABA decreased from the time of anaesthesia onwards. As previously mentioned, GABA is the primary inhibitory neurotransmitter of the CNS and functions in inhibiting the activity of signal-receiving neurons (Mihic and Harris 1997). Anaesthesia is known to inhibit its release (Westphalen et al. 2007), evidenced by the decline in release and the negative area measured. Interestingly, when TRH was administered in the absence of kainate, the release of GABA did not decline as much as controls, perhaps as protection against unconsciousness (Figure 6.8). TRH has previously been shown to decrease sleep time and increase wake time in various models (Metcalf and Dettmar 1981; Nillni and Sevarino 1999) and to increase GABA release (Deng et al. 2006). Thus, TRH may prevent the chloral hydrate induced reduction of GABA, which may be disguised in the presence of the over-excitatory kainate, evidenced by release at the same level of controls.

Anaesthesia caused a large induction of acetylcholine release and thus it was not possible to evaluate the effects of kainate or TRH (results not shown), it is possible that the effects of TRH are mediated through noradrenaline, as a TRH-analogue (RX 77368) enhances potassium-stimulated release of noradrenaline from ventral spinal cord slices from the rat (Fone et al. 1991), however in these studies, it was not possible to analyse noradrenaline release from the striatum due to the interference of the anaesthetic.

Activation of kainate receptors is known to stimulate the release of dopamine in the striatum (Ghersi et al. 2003). Kainate induced perturbation of the dopamine-signalling pathway was evidenced by the kainate-stimulated release of dopamine, however this was not prevented by TRH (Figure 6.10). TRH has been described as a potent releaser of dopamine (Jaworska-Feil et al. 2001) and is known to co-localise with dopamine and has been shown to modulate the central actions of dopamine (Bennett et al. 1989). However, administration of TRH in this study did not result in any immediate increase in levels in the perfusate, however anaesthesia, given shortly after TRH, may have disguised the longer-term changes in its release (Figure 6.12). The kainate challenge also resulted in decreased release of the dopamine metabolite DOPAC directly after application of kainate, indicating that dopamine signalling had diminished resulting in the decreased level of its products. TRH treatment prior to kainate, however, resulted in no change between the basal and kainate-stimulated level of DOPAC release indicating that it had perhaps conferred some degree of protection against altered dopamine signalling. Serotonin release was not measured in these studies, though its metabolite 5-HIAA was measured and it was demonstrated that though kainate induced a loss, there was no depletion detected when TRH was used as a pre-treatment. It has been previously shown that intrathecal administration of the TRH-analogue mentioned above (RX 77368) resulted in elevated levels of serotonin and 5-HIAA in the ventral portion of the spinal cord of rats (Fone et al. 1989). This was thought be due to the synthesis of serotonin as the increase took days to manifest, though TRH in this study, operating as a homeostatic regulator, may simply maintain serotonin levels and protect against depleted secretion, hence the maintenance of its metabolite levels.

The ability of TRH to antagonise a major factor of kainate induced secondary injury, free radical production, was explored, but was found not to reduce the kainate-induced production of highly reactive oxygen species (Figure 6.14).

Overall, the effectiveness of TRH as a homeostatic regulator or inducer of neurotransmission was not clearly obvious in these studies, though further analysis of the effects of kainate and of TRH on the release of neuroactive

amines and amino acids on the days following kainate-challenge may reveal more substantive results. Anaesthesia caused significant interference with detection and may have disguised altered signalling and thus a modification of the microdialysis procedure may be necessitated. The results from the behavioural effects following inducement of excitotoxicity with kainate were more definite, with findings that indicate TRH significantly improved the behavioural outcome. Rats have a tendency to spend more time exploring novel objects and subjects rather than the familiar, with recognition memory relying on the ability to discriminate the familiarity of things that were previously encountered (Gaskin et al. 2003). As mentioned, this is a form of olfactory memory, which is dependent on the integrity of the neuropeptide systems of oxytocin and vasopressin (Bielsky and Young 2004). The hippocampus, which has a major role in memory and learning, is involved in processing and retrieval of the memory and as such the social discrimination task is a test of hippocampal function.

Utilising this novelty-preference paradigm of rats, the social recognition experiment relied on rats to explore, or interact, with a novel juvenile rat, with which no previous encounter had occurred. The time spent nosing, pawing, sniffing or grooming the juvenile initially by control rats decreased upon the second encounter due to the functioning of the short-term working memory. The initial, novel, encounter was processed and the information was retrieved upon the second encounter, resulting in recognition of the familiar and thus less interest. Kainate, however, prevented the establishment of this memory, and animals that underwent kainate-challenge thus did not decrease time spent interacting with the juvenile on the second encounter, consistent with hipppocampal impairment (Figure 6.16). When animals were pre-treated with TRH prior to kainate, they displayed the ability to process and recall the memory of the initial encounter resulting in a decreased interaction time on the second trial. This demonstrates the protection of the signalling system of the olfactory bulb and hippocampal integrity conferred by TRH.

The cognitive performance by kainate-injected rats was also significantly improved by TRH in the water-maze spatial learning task. Using the Morris

water-maze as an assessment, TRH-treated rats showed reduced latencies to find the submerged platform, decreased path length and greater swim time near the platform, thus TRH improved kainate-induced memory and learning deficits (Figure 6.18–Figure 6.20). Findings in the water-maze study demonstrate that animals treated with TRH following kainate administration performed significantly better than kainate only treated animals indicating diminished damage to the spatial learning ability, thus decreased damage to the hippocampus. The ability of TRH to enhance cognitive function has been previously reported (Olson et al. 1995; Faden et al. 1999) and the improved performance in cognitive tasks probably results from the neuroprotective effect of TRH on cells in regions exposed to excitotoxicity. This ameliorating effect on spatial memory impairment in rats by TRH has also been demonstrated using a structural analogue of TRH, JTP-4819, improved the performance of rats with middle cerebral artery occlusion, hippocampal lesions and scopolamine-induced amnesia in the water-maze task (Shinoda et al. 1996; Toide et al. 1997; Miyazaki et al. 1998).

The *in vivo* use of kainate described in this chapter was applied in order to investigate the protective capability of TRH. Kainate was shown to induce changes in the dopaminergic and seratonergic systems, cause the efflux of taurine and an increase in the production of reactive oxygen species. These biochemical changes were manifested by behavioural alterations, with loss of recognition and spatial memory. The protective effect of TRH on the neurochemical events was difficult to establish, however, there was a significant improvement in the performance of the animals due to TRH, confirming its role as a neuroprotectant.

CHAPTER 7

GENERAL DISCUSSION

7.1 The clinical potential of Thyrotropin-releasing hormone

The pathogenesis of brain damage in response to several acute insults and in some chronic neurodegenerative diseases is thought to arise, in part, from excitotoxic neuronal damage due to excessive or prolonged activation of the excitatory amino acid receptors. This study investigated the effectiveness of thyrotropin-releasing hormone (TRH) in protecting against such over-activation and in the cellular mechanisms leading to neuronal death.

7.2 The inhibition of Thyrotropin-releasing hormone Degrading enzyme

As TRH is rapidly degraded, primarily due to the highly TRH-specific enzyme TRH-degrading enzyme (TRH-DE) (Wilk 1986; Charli et al. 1988; O'Cuinn et al. 1990; Bauer et al. 1997a), inhibition of this enzyme as a drug-target should lead to increased levels of TRH within the CNS. Investigations of some analogues of the TRH structure (pyroglutamate–histidine–prolineamide; Glp-His-ProNH_2) for inhibitory potency against this enzyme were described in Chapter 3. Two lead structures in TRH-DE inhibition had previously been identified, in which the histidine residue of TRH was substituted with asparagine, yielding pyroglutamyl–asparaginyl–prolylNH_2 (Glp-Asn-ProNH_2), and by replacement of the amide group with 7-amino 4-methyl coumarin (AMC), to give Glp-Asn-Pro–AMC (Kelly et al. 2002).

In the studies described in Chapter 3, further modifications to these lead structures were investigated for inhibition potential. The eleven TRH-analogues were screened initially. Of the analogues described, one, Glp-Asn(*N*-Benzyl)-ProNH_2, was found to be degraded by TRH-DE. Owing to the nature of the coupled enzyme assay and the possibility that one of the degradation products of the compound might inhibit the coupling enzyme (dipeptidyl peptidase IV), the inhibitory potency of Glp-Asn(*N*-Benzyl)-ProNH_2 was determined using a discontinuous assay, as described by Kelly *et al.* (1999). The other analogues

studied resisted TRH-DE degradation and were thus assayed using the continuous, coupled enzyme method. The compounds studied were synthesised by Kelly *et al.* (Kelly et al. 2000; Kelly et al. 2005; Scalabrino et al. 2007) or were custom synthesised by American Peptide Company. Because of expense and time constraints, there was only a limited supply of each compound available. Thus, although approximate K_i values of each of the compounds were determined, unavailability of the compounds precluded more detailed studies.

These studies indicate that the proline residue at the third position of TRH provides an important interaction with TRH-DE, substitution with alanine resulted in much poorer inhibition, though modification of proline with methyl and benzyl alcohols were tolerated, implying that aromatic interactions may be important between proline and the active site. Though the substitution of the histidine residue of TRH with asparagine resulted in potent inhibition, modification to the asparagine side chain with benzyl or phenyl groups resulted in poorer inhibition, with addition of the benzyl moiety causing degradation of the compound. This suggests that the asparagine residue provides a key stabilising interaction with the enzyme. The most potent inhibition resulted from extension of the peptide from the carboxy terminus with the hydrophobic amino acids tyrosine and tryptophan.

It was found that extension of the carboxy terminus of the Glp–Asn–Pro–AMC lead structure to yield Glp–Asn–Pro–tyrosyl–tryotophan-AMC gave a potent TRH-DE inhibitor. Further extension of this compound to Glp-Asn-Pro–tyrosyl–tryotophan–tryptophan-AMC resulted in the most potent inhibition achieved thus far. Sufficient amounts of these compounds were synthesised for the kinetic properties to be elucidated in detail. They were both found to be competitive inhibitors of TRH-DE, with K_i values of 0.038±0.007 and 0.0013±0.0001 μM, respectively (Kelly et al., 2005). These *C*-terminal extensions can increase the interactions with the enzyme, resulting in an increased inhibitory potency, possibly through interaction with a hydrophobic pocket at the active site (Kelly et al. 2005). In agreement with these conclusions, subsequent work has shown that the replacement of the L-amino acids of the extended molecule, to form

Glp-Asn-Pro–D–tyrosyl–D–tryptophanNH_2 and Glp-Asn-Pro–D–tyrosyl–D–tryptophanAMC, yielded effective inhibitors (Scalabrino et al. 2007).

7.3 *In vitro* models of neurotoxicity

In order to investigate the potential protection conferred by TRH, *in vitro* models of brain damage and events occurring during neurodegeneration were established using both rat hippocampal slices and the human cell line SH-SY5Y cells, as described in Chapters 4 and 5. In the slice-superfusion system it is possible to study neurodegenerative processes over a short period of time, in such a way that glial–neuronal interactions remain intact (see O' Byrne *et al.,* 1997), whereas using the neuroblastoma SH-SY5Y cell line enabled extended time periods to be used for induction of cell-death and measurement of cellular events. Kainate, an exogenous glutamate analogue, was used to induce cell death in both the hippocampal slice and cell models. Kainate operates as an excitotoxin because it binds to the kainate and AMPA sub-types of glutamate receptors, causing increased glutamate release and hyper-activation of the neurone (Gras et al. 2006). The over-activation of the glutamate receptors results in an influx of calcium into the cell and oxidative stress results due to activation of calcium-dependent enzymes, such as NADPH oxidase, cytosolic phospholipase A2, nitric oxide synthase (NOS) and xanthine oxidase, resulting in production of reactive oxygen species and nitrogen species (ROS/NOS), all factors that ultimately lead to cell degeneration (Doble 1999).

Kainate was shown to induce cell death in both models. Although apoptosis was initiated, demonstrated by caspase activation, there was also loss of membrane integrity as a result of necrosis. Determination of the levels of neuroactive amino acids following slice superfusion and incubation with kainate showed that there was a loss of the glutamine content from the slice. The levels of the excitatory amino acids aspartate and glutamate were also decreased, as were the inhibitory amino acid GABA, and taurine. The released glutamine is probably glial in origin. Glutamine is formed from glutamate in the glutamate–glutamine cycle, whereby released glutamate is taken up by glial cells,

astrocytes in particular, and converted to glutamine by glutamine synthase, which is then released to be taken up by nerve terminals for conversion back to glutamate (see, for example Bröer and Brookes 2001). The release of glutamine from astrocytes appears to be mediated by several different transporters (Deitmer et al. 2003) and is stimulated by extracellular glutamate (Deitmer et al. 2003) and nitric oxide (Segieth et al. 1995; Watts et al. 2005), though, apparently, not directly by kainate (Albrecht 1989; Haas and Erdo 1991). Excess glutamate can also be toxic to glial cells including astrocytes (Haas and Erdo 1991) and it has been demonstrated that AMPA/kainate receptor activation triggers excitotoxic cell death in glial cells (Belachew and Gallo 2004), and astrocytes and microglia express the AMPA/kainate receptor (Noda et al. 2000; Verkhratsky and Steinhauser 2000; Schroder et al. 2002) and therefore may be directly or indirectly involved in the excitotoxic cascade (Belachew and Gallo 2004). The loss of glutamine from the hippocampal superfused slices and the high concentration released from incubated slices may therefore arise from the death of glial cells. Glial cell death was demonstrated to occur due to kainate in the hippocampal slice model, with substantial loss of the glial-cell specific enzyme glutamine synthase. These results suggest that extension of the cultured cell model to include mixed neuronal–glial cell co-cultures would be valuable for investigating the intracellular interactions during kainate-induced cell death.

The origin of the released glutamate remains to be determined. Kainate has been shown to evoke release of glutamate and aspartate from neurones (Ferkany et al. 1982), but extracellular glutamate can also cause release of glutamate from astrocytes (see, for example Xu et al. 2007) and it appears that the major portion of kainate induced glutamate release may come from glial cells (Krespan et al. 1982). The kainate-evoked and transporter-mediated release of GABA and taurine from astrocytes has also been reported (Gallo et al. 1991; Wallin et al. 1999). Further studies on the effects of the sodium channel blocker tetrodotoxin and a non-NMDA receptor antagonist 6,7-dinitroquinoxaline-2,3-dione (see Bianchi et al. 1998; Ballini et al. 2008; van der Zeyden et al. 2008) would help to determine the sites of release.

Kainate also stimulated the loss of biogenic amines from superfused slices. Dopamine levels were depleted to less than a third of controls and levels of the dopamine metabolites DOPAC and HVA doubled. The levels of serotonin and its metabolite 5-hydroxyindoleacetic acid were also reduced. In this study noradrenaline was not affected by kainate, though kainate has previously been demonstrated to indirectly inhibit noradrenaline release through adenosine-mediated inhibition (Kugelgen and Starke 1995).

The neurotoxin 1-methyl-4-phenylpyridinium (MPP^+) was also used to induce cell death. MPP^+ inhibits complex I of the mitochondrial electron transport chain, resulting in ATP-depletion and, consequently increased cytoplasmic calcium levels and reactive oxygen species (ROS), resulting in cell death (for review see Tipton and Singer, 1993). MPP^+ was shown to cause a loss of cellular redox activity following its incubation on cells and cells died by necrosis, demonstrated by the loss of LDH and to a lesser extent by apoptosis, as caspase activity was also evident. In order to fully consider all mechanisms of cell death, staurosporine, a toxin that operated as purely an instigator of apoptosis was also used in cell culture studies and resulted in significant caspase activation.

7.4 *In vitro* attenuation of neurotoxicity by TRH

Having established suitable models of neuronal toxicity in these systems, the neuroprotective effects of TRH were investigated and it was found that it protected against kainate-induced cell death by apoptosis and necrosis in both the hippocampal slice and cell culture model, in a dose- and time-dependent manner. TRH caused a significant depletion in the level of noradrenaline from the hippocampal slice, this TRH-evoked release has been previously reported (Heal et al. 1987; Fone et al. 1991) and it is thought that the noradrenergic system may be most sensitive to TRH (Itoh et al. 1994b). Sodium channel blockers can prevent TRH-induced release of noradrenaline (Fone et al. 1991), and TRH has previously been shown to modulate neuronal sodium channels (Lopez-Barneo et al. 1990). Noradrenaline is found in the CA1, CA3 and the

dentate gyrus areas of the hippocampus and its release is controlled by negative feedback modulation (Milusheva et al. 1994) and in the CA3 area, noradrenaline has been shown to inhibit excitatory synaptic transmission (Sershen et al. 1997). As mentioned kainate inhibits noradrenaline release, and therefore the loss of noradrenaline from the hippocampal slice when TRH was present with kainate may therefore have been a TRH-evoked inhibitory response to the excess excitatory action of kainate operating through modulation of sodium channels.

TRH has been shown to modulate the dopaminergic system (Bennett et al. 1989), possibly as a D_1 dopamine receptor agonist, since a D_1 receptor antagonist (SCH23390) has been shown to block the effects of TRH on dopamine (McCreary and Handley 1999). TRH treatment with kainate was found to protect against the kainate-induced loss of dopamine from the hippocampal slice system and prevented increase in the levels of the dopamine metabolites DOPAC and HVA found in the kainate-treated slices. It is thought that the effects of TRH and serotonin signalling may be complementary as both operate by inhibition of TASK1 potassium channels (Richerson 2004) and in this study TRH was found to prevent kainate induced loss of serotonin and its metabolite 5HIAA from the slice system. TRH was found to protect against glial cell death as the loss of glutamine from the slices, most likely of glial origin, and the depletion of glutamine synthase activity in the slices due to kainate was attenuated by TRH. This protection may be mediated by TRH receptor activation as astrocytes have been demonstrated to express TRH receptors (Fernandez-Agullo 2001), this indicates that some of the neurotrophic actions of TRH upon the central nervous system are mediated by glial cells. TRH also afforded protection against kainate-stimulated loss of aspartate, glutamate and taurine, although it had no effect on the loss of GABA, in the hippocampal slice system (Figure 4.13). TRH is known to facilitate the release of GABA and is thought to regulate the function of GABA in the hippocampus (Kachidian et al. 1991; Heuer et al. 2000; Deng et al. 2006). Since GABA functions to inhibit the activity of signal receiving neurons (Mihic and Harris 1997), it is possible that TRH induced GABA release from the slice to compensate for the kainate-induced over-excitation of neurones. Protection by TRH against potassium-

induced depletion of glutamate and aspartate in slices has been previously described (Nie et al. 2005). These actions of TRH may involve calcium regulation. TRH can cause an increase in free calcium ions but also prevents excessive cellular influx of calcium, activation of the TRH receptors causes an increase in intracellular calcium levels through activation of the $G\alpha_{q/11}$ signalling pathway (Schledermann et al. 2001; Smith et al. 2001), whereas it has also been shown to prevent glutamate-stimulated increases in intracellular calcium (Koenig et al. 1996; Faden et al. 2004). Thus the protective effects demonstrated in both of the *in vitro* models may be due to the role of TRH as a homeostatic regulator of intracellular calcium levels, maintaining a balance against the over-excitation by kainate and oxidative stress induced by MPP^+. TRH also protected against staurosporine induced cell death in the cell culture model. Staurosporine is a general inhibitor of protein kinases (Chae et al. 2000) and, as shown in Figure 5.1, the overlapping event in the toxicity induced by kainate, MPP^+ and staurosporine may centre on either the activation or inhibition of protein kinases.

Activation of protein kinases has been found to be protective against neurone depolarization (Lin et al. 1997), yet over-activation of protein-kinase activity has been found to induce neurodegenerative changes and is toxic in a calcium independent process (Mattson 1991). Pizzi *et al.* (1999) found that the effect of TRH appeared to depend on protein kinase C activation. The neuroprotective effects observed in these studies may, thus, be mediated by homeostatic regulation of protein kinase activity within the cell, serving to activate in the presence of staurosporine, while preventing over activity, through calcium regulation, in the presence of kainate and MPP^+. Excess intracellular calcium levels, due to kainate or MPP^+, activate calmodulin-dependent protein kinases (CaM-K) (Song et al. 2008), whereas staurosporine is an inhibitor of CaM-K. Cam-K is central in regulating neuronal processes, with both increases and decreases in its activity having been reported to cause neuronal damage (Waxham et al. 1996). Further studies should be carried out to measure intracellular calcium levels following exposure to these toxins

in the presence and absence of TRH and to assay protein kinase, CaM-K activity in particular, to measure activity levels in response to TRH.

7.5 *In vivo* attenuation of neurotoxicity by TRH

Following the demonstration of neuroprotection by TRH in the *in vitro* models, the effects of TRH in protecting against kainate toxicity were investigated *in vivo* (Chapter 6). Two types of study were used. Both involved tests of the memory and learning ability of animals following kainate administration. Kainate has also frequently been used *in vivo* as an experimental tool to mimic human temporal lobe epilepsy. Neuronal injury results from excitotoxicity, with damage occurring most notably the CA3 region of hippocampus (Liu et al. 1996; Sharma and Kaur 2005).

In the microdialysis studies, described in Section 6.2.1, kainate was applied directly to the striatum of rats through the probe and TRH was applied peripherally. Because of the traumatic nature of kainate application and the over-excitability this would induce, it was applied under anaesthetic. This resulted significant variation in the levels of amino acids and amines detected in the perfusate collected, nevertheless, analysis showed that kainate caused a significant elevation of extracellular aspartate levels, and that TRH treatment protected against this (Figure 6.7). Anaesthesia caused an induction of acetylcholine release, preventing its determination, and the low levels of serotonin prevented its analysis. TRH did not prevent the kainate-induced release of dopamine, although it did attenuate the decreases in the release of the dopamine metabolite 3,4-dihydroxyphenylacetic acid and the serotonin metabolite 5-hydroxyindole acetic acid that were observed to result from the kainate infusion.

Since a major factor in excitotoxicity is the production of free radicals (Naarala et al. 1993; Beal 1996; Doble 1999), the levels of reactive oxygen species resulting from microdialysis infusion of kainate were measured. However, TRH was found to have no significant effect on the kainate-induced increase in ROS production. At the behavioural level, measured two and three days after kainate

infusion, TRH significantly improved the performance in a social recognition test compared to the memory-impaired animals that underwent kainate challenge in the absence of TRH (Figure 6.18). The injection of kainate intraperitonially was used to induce hippocampal damage in the second *in vivo* study utilising the spatial learning ability of rats in the Morris water-maze task, described in Section 6.2.3. TRH administration was also shown to result in improved performance, with decreased swim distance and increased escape latency, compared to the animals treated with kainate alone.

TRH has a short half-life *in vivo*, in the order of 4–6 min in plasma when injected intravenously in rats and humans (Morley 1979; Moss and Bundgaard 1990). This is primarily due to its rapid degradation by TRH-DE (Bauer et al. 1981; O'Cuinn et al. 1990). TRH also poorly penetrates the blood–brain barrier due to its very low lipophilicity (Metcalf et al. 1981). These factors should limit the neuroprotective capability of TRH *in vivo*, particularly in the learning paradigms described herein, where social recognition testing occurred two and three days following TRH administration and the Morris water-maze test continued for five days following TRH-therapy. This neuroprotection may be due to the concentration of TRH used in these studies, at 10 mg/kg, in excess of physiological TRH levels. It is also possible that some of the protective effects of TRH are actually mediated by its cleavage products. In fact, histidylproline diketopiperazine (cyclo(His-Pro), CHP), arising from the cyclised TRH cleavage product histidyl-prolineamide, has activity in the brain (Prasad et al. 1995; Prakash et al. 2002; Colson and Gershengorn 2006) and several analogues of CHP have demonstrated neuroprotection in *in vitro* and *in vivo* studies (Prakash et al. 2002; Faden et al. 2003a; Faden et al. 2005). It is, perhaps, more likely that the protective effects are mediated by longer-lasting biochemical changes caused by TRH itself. Further studies would be necessary to determine the concentrations and half-life of TRH in the brain after i.p. injection. CHP and histidyl-prolineamide levels should also be measured and the identification of, and the changes in, expression of possibly protective components, such as antiapoptotic members of the Bcl-2 family, that TRH treatment may cause.

7.6 Further Studies

The mechanisms by which TRH operates to confer neuroprotection are not yet fully elucidated. Further work will be necessary to understand how the protective actions reported here occur. In particular, alterations of intracellular signalling processes and pro- and anti-apoptotic protein expression and distribution following TRH administration should be studied. This should reveal whether there is a common mechanism that underlies the protection against kainate, MPP^+ and staurosporine, which operate through different mechanisms. The results of such studies should be of value for the further development of analogues of TRH that targeted towards mimicking these molecular events.

The microdialysis experiments could provide valuable detail on the release and alteration of neuronal signalling events and establishment of the effect of TRH on kainate toxicity would provide a mechanism to determine and compare the protective ability of novel TRH analogues following toxic insult. In the *in vivo* experiments described using microdialysis, the release of amino acids and amines from the day in which kainate was perfused onto the striatum was analysed, dialysis fractions were also collected on the days following kainate-challenge, coinciding with the social recognition tasks. Such data may also reveal the longer-term effects of kainate toxicity on neuronal degeneration and TRH-altered signalling following kainate induced cell necrosis and apoptosis and after possible neurotransmitter receptor desensitisation or up-regulation occurs. Analysis of these fractions may also demonstrate signalling during the learning and recall events measured in the social recognition test. Although substantial changes in neuroactive amino acids or amines during the social learning task may occur, they may not be identifiable as the interaction occurred over 5 min but fractions were collected over 20 min in order to obtain sufficient perfusate for analysis. This may result in a dilution of any short-term alterations in the detected substances. Preliminary work has been initiated to investigate the potential of a novel TRH-analogue, which suggest that, unlike TRH, it does reduce free radical production by kainate (not shown, because of the low sample numbers involved), this may lead to more clinically relevant discoveries and further development of potential drug compounds.

Bibliography

Airaksinen, M.S., Alanen, S., Szabat, E., Visser, T.J. and Panula, P. (1992) Multiple neurotransmitters in the tuberomammillary nucleus: comparison of rat, mouse, and guinea pig. *J. Comp. Neurol.* **323**, 103-116.

Albrecht J. (1989) L-glutamate stimulates the efflux of newly taken up glutamine from astroglia but not from synaptosomes of the rat. *Neuropharmacology* **28,** 885-887.

Alonso, A.D.C., Grundke-Iqbal, I. and Iqbal, K. (1996) Alzheimer's disease hyperphosphorylated tau sequesters normal tau into tangles of filaments and disassembles microtubules. *Nat. Med.* **2**, 783-787.

Angulo, E., Noe, V., Casado, V., Mallol, J., Gomez-Isla, T., Lluis, C., Ferrer, I., Ciudad, C. J. and Franco, R. (2004) Up-regulation of the Kv3.4 potassium channel subunit in early stages of Alzheimer's disease. *J. Neurochem.* **91**, 547-557.

Ao, Y., Go, V.L., Toy, N., Li, T., Wang, Y., Song, M.K., Reeve, J.R., Liu, Y. and Yang, H. (2006) Brainstem thyrotropin-releasing hormone regulates food intake through vagal-dependent cholinergic stimulation of ghrelin secretion. *Endocrinology* **147**, 6004-6010.

Aoki, Y., Masuda, T., Iigo, M. and Yanagisawa, T. (2007) Molecular cloning of prepro-thyrotropin-releasing hormone cDNA from medaka (Oryzias latipes). *Gen. Comp. Endocrin.* **150**, 364-370.

Appenzeller O. and Oribe E. (1997) *The Autonomic Nervous System: An Introduction to Basic and Clinical Concepts (Chapter 6: The enteric nervous system, page 318),* 5th Edition, p 910. Elsevier Science Inc, New York.

Arvidsson, U., Cullheim, S., Ulfhake, B., Luppi, P. H., Kitahama, K., Jouvet, M. and Hokfelt, T. (1994) Quantitative and qualitative aspects on the distribution of 5-HT and its coexistence with substance P and TRH in cat ventral medullary neurons. *J. Chem. Neuroanat.* **7**, 3-12.

Ashworth, R., Yu, R., Nelson, E.J., Dermer, S. and Gershengorn, M.C. (1995) Visualization of the Thyrotropin-Releasing Hormone Receptor and Its Ligand During Endocytosis and Recycling. *Proc. Natl. Acad. Sci.* **92**, 512-516.

Ballard, T.M., Hunter, A.J., Bennett, G.W. (1996) Effect of a thyrotrophin-releasing hormone analogue, RX77368, on AMPA-induced septal-hippocampal lesioned rats in an operant delayed non-matching to position test. *Psychopharmacology* **127**, 265-275.

Ballini C., Della Corte L., Pazzagli M., Colivicchi M. A., Pepeu G., Tipton K. F. and Giovannini M. G. (2008) Extracellular levels of brain aspartate, glutamate and GABA during an inhibitory avoidance response in the rat. *Journal of Neurochemistry* **106,** 1035-1043.

Bauer, K., Nowak, P. and Kleinkauf, H. (1981) Specificity of a serum peptidase hydrolyzing thyroliberin at pyroglutamyl-histidine bone. *Eur. J. Biochem.* **118**, 173-176.

Bauer, K., Carmeliet, P., Schulz, M., Baes, M. and Denef, C. (1990) Regulation and cellular localization of the membrane-bound thyrotropin-releasing hormone-degrading enzyme in primary cultures of neuronal, glial and adenohypophyseal cells. *Endocrinology* **127**, 1224-1233.

Bauer, K. (1994) Purification and characterization of the thyrotropin-releasing-hormone-degrading ectoenzyme. *Eur. J. Biochem.* **224**, 387-396.

Bauer K., Heuer H., Iffländer F., Peters A., Schmitmeier S., Schomburg L., Turwitt S. and Wilkens M. (1997) Inactivation of thyrotropin-releasing hormone (TRH) by a TRH-specific ectoenzyme, in *Cell-surface peptidases in health and disease.* (Kenny A.J. and Boustead C.M., eds), pp 239–248. Scientific Publishers Limited, Oxford, UK.

Beal, M.F. (1996) Mitochondria, free radicals, and neurodegeneration. *Current Opinion in Neurobiology* **6**, 661-666.

Behrmann, D.L., Bresnahan, J.C. and Beattie, M.S. (1993) A comparison of YM-14673, U-50488H, and nalmefene after spinal cord injury in the rat. *Exp. Neurol.* **119**, 258-267.

Belachew S. and Gallo V. (2004) Synaptic and extrasynaptic neurotransmitter receptors in glial precursors' quest for identity. *Glia* **48,** 185-196.

Ben-Ari, Y. (1985) Limbic seizure and brain damage produced by kainic acid: mechanisms and relevance to human temporal lobe epilepsy. *Neuroscience* **14**, 375-403.

Bennett, G.W., Marsden, C.A., Fone, K.C., Johnson, J.V. and Heal, D.J. (1989) TRH-catecholamine interactions in brain and spinal cord. *Ann. N.Y. Acad. Sci.* **553**, 106-120.

Bianchi L., Colivicchi M. A., Bolam J. P. and Della Corte L. (1998) The release of amino acids from rat neostriatum and substantia nigra in vivo: a dual microdialysis probe analysis. *Neuroscience* **87,** 171-180.

Bianchi, L., Della Corte, L. and Tipton, K.F. (1999) Simultaneous determination of basal and evoked output levels of aspartate, glutamate, taurine and 4-aminobutyric acid during microdialysis and from superfused brain slices. *J. Chromatogr. B. Biomed. Sci. Appl.* **723**, 47-59.

Bidaud, I., Lory, P., Nicolas, P., Bulant, M. and Ladram, A. (2002) Characterization and functional expression of cDNAs encoding thyrotropin-releasing hormone receptor from Xenopus laevis. Identification of a novel subtype of thyrotropin-releasing hormone receptor. *Eur. J. Biochem.* **269**, 4566-4576.

Bielsky I. F. and Young L. J. (2004) Oxytocin, vasopressin, and social recognition in mammals. *Peptides* **25,** 1565-1574.

Blanchard, L. and Barden, N. (1986) Ontogeny of receptors for thyrotropin-releasing hormone in the rat brain. *Dev. Brain Res.* **24**, 85-88.

Bogdanov, M., Brown, R.H., Matson, W., Smart, R., Hayden, D., O'Donnell, H., Flint Beal, M. and Cudkowicz, M. (2000) Increased oxidative damage to DNA in ALS patients. *Free Radic. Biol. Med.* **29**, 652-658.

Bohacek, R.S., McMartin, C. and Guida, W.C. (1996) The art and practice of structure-based drug design: A molecular modeling perspective. *Med. Res. Rev.* **16**, 3-50.

Boillee, S., Vande Velde, C. and Cleveland, D.W. (2006) ALS: a disease of motor neurons and their nonneuronal neighbors. *Neuron* **52**, 39-59.

Boler, J., Enzmann, F., Folkers, K., Bowers, C.Y. and Schally, A.V. (1969) The identity of chemical and hormonal properties of the thyrotropin releasing hormone and pyroglutamyl-histidyl-proline amide. *Biochem. Biophys. Res. Commun.* **37**, 705-710.

Boschi, G., Desiles, M., Reny, V., Rips, R. and Wrigglesworth, S. (1983a) Antinociceptive properties of thyrotropin releasing hormone in mice: comparison with morphine. *Br. J. Pharmacol.* **79**, 85-92.

Boschi, G., Nomoto, T. and Rips, R. (1983b) Thyrotropin releasing hormone-induced hyperthermia in mice: possible involvement of adrenal and pituitary glands. *Br. J. Pharmacol.* **80**, 229-233.

Bowers, C.Y., Schally, A.V., Hawley, W.D., Gual, C. and Parlow, A. (1968) Effect of thyrotropin-releasing factor in man. *J. Clin. Endocrinol. Metab.* **28**, 978-982.

Broberger, C. and McCormick, D.A. (2005) Excitatory Effects of Thyrotropin-Releasing Hormone in the Thalamus. *J. Neurosci.* **25**, 1664-1673.

Broer S. and Brookes N. (2001) Transfer of glutamine between astrocytes and neurons. *J. Neurochem.* **77,** 705-719.

Brooks, B.R. (1989) A summary of the current position of TRH in ALS therapy. *Ann. N.Y. Acad. Sci.* **553**, 431-461.

Brown, R.H., (1997) Amyotrophic lateral sclerosis. Insights from genetics. *Arch. Neurol.*, **54**, 1246-1250.

Brownlees, J., Williams, C.H., Brennan, G.P. and Halton, D.W. (1992) Purification and immunochemical studies of dipeptidyl peptidase IV from bovine kidney. *Biol. Chem. Hoppe-Seyler* **373**, 911-914.

Brownstein, M.J., Utiger, R.D., Palkovits, M. and Kizer, J.S. (1975) Effect of Hypothalamic Deafferentation on Thyrotropin-Releasing Hormone Levels in Rat Brain. *Proc. Natl. Acad. Sci. USA* **72**, 4177-4179.

Bulant, M., Delfour, A., Vaudry, H. and Nicolas, P. (1988) Processing of thyrotropin-releasing hormone prohormone (pro-TRH) generates pro-TRH-connecting peptides. Identification and characterization of prepro-TRH-(160-169) and prepro-TRH-(178-199) in the rat nervous system. *J. Biol. Chem.* **263**, 17189-17196.

Burgus, R., Dunn, T.F., Desiderio, D.M., Ward, D.N., Vale, W., Guillemin, R., Felix, A.M., Gillessen, D. and Studer, R.O. (1970) Biological activity of synthetic polypeptide derivatives related to the structure of hypothalamic TRF. *Endocrinology* **86**, 573-582.

Callahan, A.M., Frye, M.A., Marangell, L.B., George, M.S., Ketter, T.A., L'Herrou, T. and Post, R.M. (1997) Comparative antidepressant effects of intravenous and intrathecal thyrotropin-releasing hormone: Confounding effects of tolerance and implications for therapeutics. *Biol. Psychiatry* **41**, 264-272.

Carroll, R.C., Beattie, E.C., Von Zastrow, M. and Malenka, R.C. (2001) Role of ampa receptor endocytosis in synaptic plasticity. *Nat. Rev. Neurosci.* **2**, 315-324.

Chae H. J., Kang J. S., Byun J. O., Han K. S., Kim D. U., Oh S. M., Kim H. M., Chae S. W. and Kim H. R. (2000) Molecular mechanism of staurosporine-induced apoptosis in osteoblasts. *Pharmacol Res* **42,** 373-381.

Charli, J.-L., Cruz, C., Vargas, M.-A. and Joseph-Bravo, P. (1988) The narrow specificity pyroglutamate amino peptidase degrading TRH in rat brain is an ectoenzyme. *Neurochem. Intl.* **13**, 237-242.

Chavez-Gutierrez, L., Matta-Camacho, E., Osuna, J., Horjales, E., Joseph-Bravo, P., Maigret, B. and Charli, J.-L. (2006) Homology modeling and site directed mutagenesis of pyroglutamyl peptidase II. Insights into omega versus aminopeptidase specificity in the M1 family. *J. Biol. Chem.* **281**, 18581-18590.

Choi, D.W. (1988) Glutamate neurotoxicity and diseases of the nervous system. *Neuron* **1**, 623-634.

Chung, S.Y. and Han, S.H. (2003) Melatonin attenuates kainic acid-induced hippocampal neurodegeneration and oxidative stress through microglial inhibition. *J. Pineal Res.* **34**, 95-102.

Clark, G.D. and Rothman, S.M. (1987) Blockade of excitatory amino acid receptors protects anoxic hippocampal slices. *Neuroscience* **21**, 665-671.

Collu, R., Tang, J., Castagne, J., Lagace, G., Masson, N., Huot, C., Deal, C., Delvin, E., Faccenda, E., Eidne, K.A. and Van Vliet, G. (1997) A Novel Mechanism for Isolated Central Hypothyroidism: Inactivating Mutations in the Thyrotropin-Releasing Hormone Receptor Gene. *J. Clin. Endocrinol. Metab.* **82**, 1561-1565.

Colson, A.O. and Gershengorn, M.C. (2006) Thyrotropin-Releasing Hormone Analogs. *Mini Rev. Med. Chem.* **6**, 221-226.

Cook, L.B. and Hinkle, P.M. (2004) Fate of Internalized Thyrotropin-Releasing Hormone Receptors Monitored with a Timer Fusion Protein. *Endocrinology* **145**, 3095-3100.

Croissandeau, G., Pagesy, P., Grouselle, D., Le Dafniet, M., Peillon, F. and Li, J.Y. (1992) Immunoreactive thyroliberin (TRH) precursor forms in human hypothalamus and anterior pituitary tissues. *FEBS Lett.* **298**, 191-194.

Cruz, C., Charli, J.L., Vargas, M.A. and Joseph-Bravo, P. (1991) Neuronal localization of pyroglutamate aminopeptidase II in primary cultures of fetal mouse brain. *J. Neurochem.* **56**, 1594-1601.

Czekay, G. and Bauer, K. (1993) Identification of the thyrotropin-releasing-hormone-degrading ectoenzyme as a metallopeptidase. *Biochem. J.* **290**, 921-926.

De Leonibus, E., Verheij, M.M., Mele, A. and Cools, A. (2006) Distinct kinds of novelty processing differentially increase extracellular dopamine in different brain regions. *Eur. J. Neurosci.* **23**, 1332-1340.

Deitmer J. W., Broer A. and Broer S. (2003) Glutamine efflux from astrocytes is mediated by multiple pathways. *J. Neurochem.* **87,** 127-135.

Del Rio, P., Montiel, T., Chagoya, V. and Massieu, L. (2007) Exacerbation of excitotoxic neuronal death induced during mitochondrial inhibition *in vivo*: Relation to energy imbalance or ATP depletion? *Neuroscience* **146**, 1561-1570.

Della Corte L, Huxtable R.J, Sgaragli G and K.F. T. (1999) Taurine 4, Taurine and excitable tissue, in *Advances in experimental medicine and biology*. Vol. 483, Kluwer Academic/Plenum Publishers, Dordrecht, The Netherlands.

Deng, P.-Y., Porter, J. E., Shin, H.-S. and Lei, S. (2006) Thyrotropin-releasing hormone increases GABA release in rat hippocampus. *J. Physiol.* **577**, 497-511.

Deshpande, S.B. and Warnick, J.E. (1994) Analogs of thyrotropin-releasing hormone in potentiating the spinal monosynaptic reflex *in vitro*. *Eur. J. Pharmacol.* **271**, 439-444.

Dhami, G.K. and Ferguson, S.S.G. (2006) Regulation of metabotropic glutamate receptor signaling, desensitization and endocytosis. *Pharmacol. Ther.* **111**, 260-271.

D'Hooge, R. and De Deyn, P.P. (2001) Applications of the Morris water maze in the study of learning and memory. *Brain Res. Rev.* **36**, 60-90.

Doble, A. (1995) Excitatory amino acid receptors and neurodegeneration. *Therapie.* **50**, 319-337.

Doble, A. (1999) The role of excitotoxicity in neurodegenerative disease: implications for therapy. *Pharmacol. Ther.* **81**, 163-221.

Dworakowska, B. and Dolowy, K. (2000) Ion channels-related diseases. *Acta Biochim. Pol.* **47**, 685-703.

Dykens, J.A., Stern, A. and Trenkner, E. (1987) Mechanism of kainate toxicity to cerebellar neurons in vitro is analogous to reperfusion tissue injury. *J. Neurochem.* **49**, 1222-1228.

Engelmann, M., Wotjak, C.T. and Landgraf, R. (1995) Social discrimination procedure: An alternative method to investigate juvenile recognition abilities in rats. *Physiol. Behav.* **58**, 315-321.

Ewbank, D.C. (1999) Deaths attributable to Alzheimer's disease in the United States. *Am. J. Public Health* **89**, 90-92.

Fadeel, B., Orrenius, S. and Zhivotovsky, B. (1999) Apoptosis in Human Disease: A New Skin for the Old Ceremony? *Biochem. Biophys. Res. Commun.* **266**, 699-717.

Faden, A.I., Vink, R. and McIntosh, T.K. (1989) Thyrotropin-releasing hormone and central nervous system trauma. *Ann. N.Y. Acad. Sci.* **553**, 380-384.

Faden, A.I., Fox, G.B., Fan, L., Araldi, G.L., Qiao, L., Wang, S. and Kozikowski, A.P. (1999) Novel TRH analog improves motor and cognitive recovery after traumatic brain injury in rodents. *Am. J. Physiol.* **277**, R1196-1204.

Faden, A.I., Knoblach, S.M., Cernak, I., Fan, L., Vink, R., Araldi, G.L., Fricke, S.T., Roth, B.L. and Kozikowski, A.P. (2003) Novel diketopiperazine enhances motor and cognitive recovery after traumatic brain injury in rats and shows neuroprotection in vitro and in vivo. *J. Cereb. Blood Flow Metab.* **23**, 342-354.

Faden A. I., Knoblach S. M., Movsesyan V. A. and Cernak I. (2004) Novel small peptides with neuroprotective and nootropic properties. *J. Alzheimers Dis.* **6,** S93-97.

Faden, A.I., Movsesyan, V.A., Knoblach, S.M., Ahmed, F. and Cernak, I. (2005) Neuroprotective effects of novel small peptides *in vitro* and after brain injury. *Neuropharmacology* **49**, 410-424.

Feig, S. and Lipton, P. (1990) *N*-methyl-D-aspartate receptor activation and Ca^{2+} account for poor pyramidal cell structure in hippocampal slices. *J. Neurochem.* **55**, 473-483.

Ferkany, J.W., Zaczek, R. and Coyle, J.T. (1982) Kainic acid stimulates excitatory amino acid neurotransmitter release at presynaptic receptors. *Nature* **298**, 757-759.

Fern, R. and Moller, T. (2000) Rapid Ischemic Cell Death in Immature Oligodendrocytes: A Fatal Glutamate Release Feedback Loop. *J. Neurosci.* **20**, 34-42.

Fernandez-Agullo, T. (2001) Thyrotropin-releasing hormone and its receptor in glia. *Glia* **33**, 267-276.

Fone K.C.F., Johnson J.V., Marsden C.A. and Bennett G.W. (1989) Comparative behavioural and biochemical effects of repeated intrathecal administration of thyrotrophin-releasing hormone (TRH) or two analogues of TRH in adult rats. *Neuropharmacology* **28,** 867-875.

Fone K.C.F., Johnson J.V., Putland A.P. and Bennett G W. (1991) Ventral Horn Neuropeptides Modulate the Release of Noradrenaline from Tissue Slices of Rat Brainstem and Ventral Thoracic Spinal Cord. *J. Neurochem.* **57,** 845-851.

Freinbichler, W., Bianchi, L., Colivicchi, M.A., Ballini, C., Tipton, K.F., Linert, W. and Della Corte, L. (2008a) The detection of hydroxyl radicals *in vivo*. *J. Inorg. Biochem.* **102**, 1329-1333.

Freinbichler, W., Colivicchi, M.A., Fattori, M., Ballini, C., Tipton, K.F., Linert, W. and Della Corte, L. (2008b) Validation of a robust and sensitive method for detecting hydroxyl radical formation together with evoked neurotransmitter release in brain microdialysis. *J. Neurochem.* **105**, 738-749.

Friedman, T.C. and Wilk, S. (1985) The effect of inhibitors of prolyl endopeptidase and pyroglutamyl peptide hydrolase on TRH degradation in rat serum. *Biochem. Biophys. Res. Commun.* **132**, 787-794.

Friedman, T.C. and Wilk, S. (1986) Delineation of a particulate thyrotropin-releasing hormone-degrading enzyme in rat brain by the use of specific inhibitors of prolyl endopeptidase and pyroglutamyl peptide hydrolase. *J. Neurochem.* **46**, 1231-1239.

Friedman, T.C., Loh, Y.P., Cawley, N.X., Birch, N.P., Huang, S.S., Jackson, I.M. and Nillni, E.A. (1995a) Processing of prothyrotropin-releasing hormone (Pro-TRH) by bovine intermediate lobe secretory vesicle membrane PC1 and PC2 enzymes. *Endocrinology* **136**, 4462-4472.

Friedman, T.C., Yanovski, J.A., Jayasvasti, V., Yanovski, S.Z., Koenig, R.J. and Wilk, S. (1995b) Pyroglutamyl peptidase-II ("thyroliberinase") activity in human

serum: influence of weight and thyroid status. *J. Clin. Endocrinol. Metab.* **80**, 1086-1089.

Funk, D., Post, R.M. and Pert, A. (1997) Role of central dopaminergic and 5-hydroxytryptaminergic projections in the behavioral responses elicited by thyrotropin-releasing hormone in rats. *Psychopharmacology* **133**, 356-362.

Fuse, Y., Polk, D.H., Lam, R.W. and Fisher, D.A. (1990) Distribution of thyrotropin-releasing hormone (TRH) and precursor peptide (TRH-Gly) in adult rat tissues. *Endocrinology* **127**, 2501-2505.

Gallo V., Patrizio M. and Levi G. (1991) GABA release triggered by the activation of neuron-like non-NMDA receptors in cultured type 2 astrocytes is carrier-mediated. *Glia* **4,** 245-255.

Garthwaite, G. and Garthwaite, J. (1985) Sites of D-[^{3}H]aspartate accumulation in mouse cerebellar slices. *Brain Res.* **343**, 129-136.

Gary, K.A., Sevarino, K.A., Yarbrough, G.G., Prange, A.J., Jr. and Winokur, A. (2003) The Thyrotropin-Releasing Hormone (TRH) Hypothesis of Homeostatic Regulation: Implications for TRH-Based Therapeutics. *J. Pharmacol. Exp. Ther.* **305**, 410-416.

Gaskin S., Tremblay A. and Mumby D. G. (2003) Retrograde and anterograde object recognition in rats with hippocampal lesions. *Hippocampus* **13,** 962-969.

Ghersi C., Bonfanti A., Manzari B., Feligioni M., Raiteri M. and Pittaluga A. (2003) Pharmacological heterogeneity of release-regulating presynaptic AMPA/kainate receptors in the rat brain: study with receptor antagonists. *Neurochemistry International* **42,** 283-292.

Gibb, W.R. and Lees, A.J. (1991) Anatomy, pigmentation, ventral and dorsal subpopulations of the substantia nigra, and differential cell death in Parkinson's disease. *J. Neurol. Neurosurg. Psychiatry* **54**, 388–396.

Giovannini, M.G., Casamenti, F., Nistri, A., Paoli, F. and Pepeu, G. (1991) Effect of thyrotropin releasing hormone (TRH) on acetylcholine release from different brain areas investigated by microdialysis. *Br. J. Pharmacol.* **102**, 363-368.

Glenner G.G. (1988) Alzheimer's disease: Its proteins and genes. *Cell* **52**, 307-308.

Gras, G., Porcheray, F., Samah, B. and Leone, C. (2006) The glutamate-glutamine cycle as an inducible, protective face of macrophage activation. *J. Leukoc. Biol.* **80**, 1067-1075.

Griffiths, E.C. (1985) Thyrotrophin releasing hormone: endocrine and central effects. *Psychoneuroendocrinology* **10**, 225-235.

Griffiths, E.C., Kelly, J.A., Ashcroft, A., Ward, D.J. and Robson, B. (1989) Comparative metabolism and conformation of TRH and its analogues. *Ann. N.Y. Acad. Sci.* **553**, 217-231.

Ha, B.K., Vicini, S., Rogers, R.C., Bresnahan, J.C., Burry, R.W. and Beattie, M.S. (2002) Kainate-induced excitotoxicity is dependent upon extracellular potassium concentrations that regulate the activity of AMPA/KA type glutamate receptors. *J. Neurochem.* **83**, 934-945.

Haas J. and Erdo S.L. (1991) Quisqualate-induced excitotoxic death of glial cells: Transient vulnerability of cultured astrocytes. *Glia* **4,** 111-114.

Häberle, J., Görg, B., Toutain, A., Rutsch, F., Benoist, J.-F., Gelot, A., Suc, A.-L., Koch, H., Schliess, F. and Häussinger, D. (2006) Inborn error of amino acid synthesis: Human glutamine synthetase deficiency. *J. Inherit. Metab. Dis.* **29**, 352-358.

Harder, S., Dammann, O., Buck, F., Zwiers, H., Lederis, K., Richter, D. and Bruhn, T.O. (2001a) Cloning of two thyrotropin-releasing hormone receptor subtypes from a lower vertebrate (Catostomus commersoni): functional expression, gene structure, and evolution. *Gen. Comp. Endocrinol.* **124**, 236-245.

Harder, S., Lu, X., Wang, W., Buck, F., Gershengorn, M.C. and Bruhn, T.O. (2001b) Regulator of G protein signaling 4 suppresses basal and thyrotropin releasing-hormone (TRH)-stimulated signaling by two mouse TRH receptors, TRH-R(1) and TRH-R(2). *Endocrinology* **142**, 1188-1194.

Harkin, A., Shanahan, E., Kelly, J.P. and Connor, T.J. (2003) Methylenendioxyamphetamine produces serotonin nerve terminal loss and diminished behavioural and neurochemical responses to the antidepressant fluoxetine. *Eur. J. Neurosci.* **18,** 1021-1027.

Heal D.J., Stoodley N., Elliott J.M., Marsden C.A., Bennett G.W. and Youdim M.B.H. (1987) Behavioural and biochemical evidence for the release of noradrenaline in mouse brain by TRH and some of its biologically stable analogues. *Neuropharmacology* **26,** 313-322.

Hermann, D., Heinz, A. and Mann, K. (2002) Dysregulation of the hypothalamic-pituitary-thyroid axis in alcoholism. *Addiction* **97**, 1369-1381.

Heuer, H., Schafer, M.K., O'Donnell, D., Walker, P. and Bauer, K. (2000) Expression of thyrotropin-releasing hormone receptor 2 (TRH-R2) in the central nervous system of rats. *J. Comp. Neurol.* **428**, 319-336.

Hinkle, P.M. (1989) Pituitary TRH receptors. *Ann. N.Y. Acad. Sci.* **553**, 176-187.

Hokfelt, T., Fuxe, K., Johansson, O., Jeffcoate, S. and White, N. (1975) Distribution of thyrotropin-releasing hormone (TRH) in the central nervous system as revealed with immunohistochemistry. *Eur. J. Pharmacol.* **34**, 389-392.

Hokfelt, T., Tsuruo, Y., Ulfhake, B., Cullheim, S., Arvidsson, U., Foster, G.A., Schultzberg, M., Schalling, M., Arborelius, L., Freedman, J. and Post, C. (1989) Distribution of TRH-like immunoreactivity with special reference to coexistence with other neuroactive compounds. *Ann. N.Y. Acad. Sci.* **553**, 76-105.

Horita, A., Carino, M.A. and Lai, H. (1986) Pharmacology of thyrotropin-releasing hormone. *Ann. Rev. Pharmacol. Toxicol.* **26**, 311-332.

Horita, A., Carino, M.A., Zabawska, J. and Lai, H. (1989) TRH analog MK-771 reverses neurochemical and learning deficits in medial septal-lesioned rats. *Peptides* **10**, 121-124.

Horita, A. (1998) An update on the CNS actions of TRH and its analogs. *Life Sci.* **62**, 1443-1448.

Hrabovszky, E., Halasz, J., Meelis, W., Kruk, M. R., Liposits, Z. and Haller, J. (2005a) Neurochemical characterization of hypothalamic neurons involved in attack behavior: glutamatergic dominance and co-expression of thyrotropin-releasing hormone in a subset of glutamatergic neurons. *Neuroscience* **133**, 657-666.

Hrabovszky, E., Wittmann, G., Turi, G. F., Liposits, Z. and Fekete, C. (2005b) Hypophysiotropic Thyrotropin-Releasing Hormone and Corticotropin-Releasing Hormone Neurons of the Rat Contain Vesicular Glutamate Transporter-2. *Endocrinology* **146**, 341-347.

Hsieh, K.P. and Martin, T.F. (1992) Thyrotropin-releasing hormone and gonadotropin-releasing hormone receptors activate phospholipase C by coupling to the guanosine triphosphate-binding proteins Gq and G11. *Mol. Endocrinol.* **6**, 1673-1681.

Ikeda, K., Iwasaki, Y. and Kinoshita, M. (1998) JTP-2942, a novel thyrotropin-releasing hormone analogue, protects against spinal motor neuron degeneration in the wobbler mouse. *Neurosci. Lett.* **250**, 9-12.

Itadani, H., Nakamura, T., Itoh, J., Iwaasa, H., Kanatani, A., Borkowski, J., IHARA, M. and Ohta, M. (1998) Cloning and characterization of a new subtype of thyrotropin-releasing hormone receptors. *Biochem. Biophys. Res. Commun.* **250**, 68-71.

Itoh, Y., Ogasawara, T., Yamazaki, A., Ukai, Y., Miura, A. and Kimura, K. (1994a) Enhancement of noradrenaline release from rat frontal cortex by thyrotropin releasing hormone and its analog, (3R,6R)-6-methyl-5-oxo-3-thiomorpholinylcarbonyl-L-histidyl-L-prolinami de, as studied by intracerebral microdialysis. *J. Pharmacol. Exp. Ther.* **268**, 255-261.

Itoh Y., Ogasawara T., Mushiroi T., yamazaki A., Ukai Y. and Kimura K. (1994b) Effect of NS-3, a thyrotropin-releasing hormone analog, on in vivo acetylcholine release in rat brain: regional differences and its sites of action. *J. Pharmacol. Exp. Ther.* **271,** 884-890.

Jackson, I.M. (1978) Phylogenetic Distribution and Function of the Hypophysiotropic Hormones of the Hypothalamus. *Amer. Zool.* **18**, 385-400.

Jackson, I.M.D. (1986) Phylogenetic Distribution and Significance of the Hypothalamic Releasing Hormones. *Amer. Zool.* **26**, 927-937.

Jackson, I.M. (1989) Controversies in TRH biosynthesis and strategies towards the identification of a TRH precursor. *Ann. N.Y. Acad. Sci.* 553, 7-13.

Jaworska-Feil, L., Kajta, M., Budziszewska, B., Leskiewicz, M. and Lason, W. (2001) Protective effects of TRH and its stable analogue, RGH-2202, on kainate-induced seizures and neurotoxicity in rodents. *Epilepsy Res.* **43**, 67-73.

Jiang, J.K., Thomas, C.J., Neumann, S., Lu, X., Rice, K.C. and Gershengorn, M.C. (2005) 1-(Phenyl)isoquinoline carboxamides: a novel class of subtype selective inhibitors of thyrotropin-releasing hormone (TRH) receptors. *Bioorg. Med. Chem. Lett.* **15**, 733-736.

Judge, S.I.V., Smith, P.J., Stewart, P.E. and Bever, C.T. Jr., (2007) Potassium Channel Blockers and Openers as CNS Neurologic Therapeutic Agents. *Recent Patents CNS Drug Discov.* **2**, 200-228.

Kachidian, P., Poulat, P., Marlier, L. and Privat, A. (1991) Immunohistochemical evidence for the coexistence of substance P, thyrotropin-releasing hormone, GABA, methionine-enkephalin, and leucin-enkephalin in the serotonergic neurons of the caudal raphe nuclei: a dual labeling in the rat. *J. Neurosci. Res.* **30**, 521-530.

Kalivas, P.W., Stanley, D. and Prange, A.J., Jr. (1987) Interaction between thyrotropin-releasing hormone and the mesolimbic dopamine system. *Neuropharmacology* **26**, 33-38.

Katsumata, T., Katayama, Y., Ootori, T., Muramatsu, H., Nishiyama, Y., Nakamura, H., Seta, T. and Terashi, A. (2001) Effect of long-term administration of JTP-2942, a novel thyrotropin-releasing hormone analogue, on neurological outcome, local cerebral blood flow and glucose utilization in a rat focal cerebral ischemia. *Brain Res.* **901**, 62-70.

Kelly, J.A., Slator, G.R., Tipton, K.F., Williams, C.H. and Bauer, K. (1999) Development of a continuous, fluorometric coupled enzyme assay for

thyrotropin-releasing hormone-degrading ectoenzyme. *Anal. Biochem.* **274**, 195-202.

Kelly, J.A., Slator, G.R., Tipton, K.F., Williams, C.H. and Bauer, K. (2000) Kinetic Investigation of the Specificity of Porcine Brain Thyrotropin-releasing Hormone-degrading Ectoenzyme for Thyrotropin-releasing Hormone-like Peptides. *J. Biol. Chem.* **275**, 16746-16751.

Kelly, J.A., Slator, G.R. and O'Boyle, K.M. (2002) Pharmacologically distinct binding sites in rat brain for [^{3}H]thyrotropin-releasing hormone (TRH) and [^{3}H][3-methyl-histidine2]TRH. *Biochem. Pharmacol.* **63**, 2197-2206.

Kelly, J.A., Scalabrino, G.A., Slator, G.R., Cullen, A.A., Gilmer, J.F., Lloyd, D.G., Bennett, G.W., Bauer, K., Tipton, K.F. and Williams, C.H. (2005) Structure-activity studies with high-affinity inhibitors of pyroglutamyl-peptidase II. *Biochem. J.* **389**, 569-576.

Kiley, S.C., Parker, P.J., Fabbro, D. and Jaken, S. (1991) Differential regulation of protein kinase C isozymes by thyrotropin- releasing hormone in GH4C1 cells. *J. Biol. Chem.* **266**, 23761-23768.

Kinoshita, K., Watanabe, Y., Yamamura, M. and Matsuoka, Y. (1998a) TRH receptor agonists ameliorate 3-acetylpyridine-induced ataxia through NMDA receptors in rats. *Eur. J. Pharmacol.* **343**, 129-133.

Kinoshita, K., Yamamura, M., Sugihara, J., Suzuki, M. and Matsuoka, Y. (1998b) Taltirelin hydrate (TA-0910): an orally active thyrotropinreleasing hormone mimetic agent with multiple actions. *CNS Drug Rev.* **4**, 25-41.

Klaus, S., Heringlake, M. and Bahlmann, L. (2004) Bench-to-bedside review: microdialysis in intensive care medicine. *Crit. Care* **8**, 363-368.

Knoblach, S.M. and Kubek, M.J. (1994) Thyrotropin-releasing hormone release is enhanced in hippocampal slices after electroconvulsive shock. *J. Neurochem.* **62**, 119-125.

Knutsen, H., Dolva, L.O., Skrede, S., Bjorklund, R. and Morland, J. (1989) Thyrotropin-releasing Hormone Antagonism of Ethanol Inebriation. *Alcohol. Clin. Exp. Res.* **13**, 365-370.

Koenig, M.L., Yourick, D.L. and Meyerhoff, J.L. (1996) Thyrotropin-releasing hormone (TRH) attenuates glutamate-stimulated increases in calcium in primary neuronal cultures. *Brain Res.* **730**, 143-149.

Koenig, M.L., Sgarlat, C.M., Yourick, D.L., Long, J.B. and Meyerhoff, J.L. (2001) *In vitro* neuroprotection against glutamate-induced toxicity by pGlu-Glu-Pro-NH_2 (EEP). *Peptides* **22**, 2091-2097.

Kolk, S.M., Kramer, B.M.R., Cornelisse, L.N., Scheenen, W.J., Jenks, B.G. and Roubos, E.W. (2002) Multiple control and dynamic response of the Xenopus melanotrope cell. *Comp. Biochem. Physio.l B Biochem. Mo.l Bio.l* **132**, 257-268.

Kollegger, H., McBean, G. and Tipton, K. (1991) The inhibition of glutamine synthetase in rat corpus striatum in vitro by methionine sulfoximine increases the neurotoxic effects of kainate and *N*-methyl-D-aspartate. *Neurosci. Lett.* **130**, 95-98.

Kramer R.H., Kaczmarek L.K. and Levitan E.S. (1991) Neuropeptide inhibition of voltage-gated calcium channels mediated by mobilization of intracellular calcium. *Neuron* **6**, 557-563.

Krespan, B., Berl, S. and Nicklas, W.J. (1982) Alteration in neuronal-glial metabolism of glutamate by the neurotoxin kainic acid. *J. Neurochem.* **38**, 509-518.

Krieger, D.T. (1983) Brain Peptides: What, Where, and Why? *Science* **222**, 975-985.

Kruchkova, Y., Ben-Dror, I., Herschkovitz, A., David, M., Yayon, A. and Vardimon, L. (2001) Basic fibroblast growth factor: a potential inhibitor of glutamine synthetase expression in injured neural tissue. *J. Neurochem.* **77**, 1641-1649.

Kubek, M.J., Low, W.C., Sattin, A., Morzorati, S.L., Meyerhoff, J.L. and Larsen, S.H. (1989) Role of TRH in seizure modulation. *Ann. N.Y. Acad. Sci.* **553**, 286-303.

Kubek, M.J. and Garg, B.P. (2002) Thyrotropin-releasing hormone in the treatment of intractable epilepsy. *Pediatr. Neurol.* **26**, 9-17.

Kugelgen I. and Starke K. (1995) Kainate receptors are involved in the glutamate-induced indirect, purinergic inhibition of [3H]-noradrenaline release in rabbit brain cortex. *Naunyn-Schmiedeberg's Archives of Pharmacology* **353,** 46-54.

Lechan, R.M., Molitch, M.E. and Jackson, I.M. (1983) Distribution of immunoreactive human growth hormone-like material and thyrotropin-releasing hormone in the rat central nervous system: evidence for their coexistence in the same neurons. *Endocrinology* **112**, 877-884.

Lechan, R.M., Wu, P., Jackson, I.M., Wolf, H., Cooperman, S., Mandel, G. and Goodman, R.H. (1986) Thyrotropin-releasing hormone precursor: characterization in rat brain. *Science* **231**, 159-161.

Lechan, R.M. and Segerson, T.P. (1989) Pro-TRH gene expression and precursor peptides in rat brain. Observations by hybridization analysis and immunocytochemistry. *Ann. N.Y. Acad. Sci.* **553**, 29-59.

Lechan, R.M. and Kakucska, I. (1992) Feedback regulation of thyrotropin-releasing hormone gene expression by thyroid hormone in the hypothalamic paraventricular nucleus. *Ciba Found Symp.* **168**, 144-164.

Lechan, R.M., Fekete, C. (2006) The TRH neuron: a hypothalamic integrator of energy metabolism. *Prog. Brain Res.* **153**, 209-235.

Lei, Q., Talley, E.M. and Bayliss, D.A. (2001) Receptor-mediated inhibition of G protein-coupled inwardly rectifying potassium channels involves $G_{\alpha q}$ family subunits, phospholipase C, and a readily diffusible messenger. *J. Biol. Chem.* **276**, 16720-16730.

Leong, D.A., Frawley, L.S. and Neill, J.D. (1983) Neuroendocrine control of prolactin secretion. *Ann. Rev. Physiol.* **45**, 109-127.

Lin, J. and Wilk, S. (1998) Quantitation and regulation of pyroglutamyl peptidase II messenger RNA levels in rat tissues and GH3 cells. *Neuroendocrinology* **67**, 197-208.

Lin W.W., Wang C.W. and Chuang D.M. (1997) Effects of depolarization and NMDA antagonists on the role survival of cerebellar granule cells: a pivotal role for protein kinase C isoforms. *J. Neurochem.* **68,** 2577-2586.

Liu, H.M., Lei, D.L. and Yang, D.L. (1996) Kainate-induced brain lesion: similar local and remote histopathological and molecular changes as in ischemic brain infarct. *J. Neuropathol. Exp. Neurol.* **55**, 787-794.

Lopez-Barneo J., Castellano A. and Toledo-Aral J. (1990) Thyrotropin-releasing-hormone (TRH) and its physiological metabolite TRH-OH inhibit Na^+ channel activity in mammalian septal neurons. *Proc. Natl. Acad. Sci. USA* **87,** 8150-8154.

Lotharius, J. & O'Malley, K.L. (2000) The Parkinsonism-inducing Drug 1-Methyl-4-phenylpyridinium Triggers Intracellular Dopamine Oxidation. A NOVEL MECHANISM OF TOXICITY. *J. Biol. Chem.* **275**, 38581-38588.

Lu, X., Bidaud, I., Ladram, A. and Gershengorn, M.C. (2003) Pharmacological Studies of Thyrotropin-Releasing Hormone (TRH) Receptors from Xenopus laevis: Is xTRHR3 a TRH Receptor? *Endocrinology* **144**, 1842-1846.

Luo, L., Yano, N., Mao, Q., Jackson, I.M.D. and Stopa, E.G. (2002) Thyrotropin releasing hormone (TRH) in the hippocampus of Alzheimer patients. *J. Alzheimer's Dis.* **4**, 97-103.

Luo L. and Stopa E.G. (2004) Thyrotropin releasing hormone inhibits tau phosphorylation by dual signaling pathways in hippocampal neurons. *J Alzheimers Dis.* **6,** 527-536.

Luo, L. and Yano, N. (2005) Thyrotropin releasing hormone (TRH) affects gene expression in pancreatic beta-cells. *Endocr. Res.* **31**, 185-198.

Macek, T.A., Schaffhauser, H. and Conn, P.J. (1998) Protein Kinase C and A3 Adenosine Receptor Activation Inhibit Presynaptic Metabotropic Glutamate Receptor (mGluR) Function and Uncouple mGluRs from GTP-Binding Proteins. *J. Neurosci.* **18**, 6138-6146.

Mantyh, P.W. and Hunt, S.P. (1984) Evidence for cholecystokinin-like immunoreactive neurons in the rat medulla oblongata which project to the spinal cord. *Brain Res.* **291**, 49-54.

Marangell, L.B., George, M.S., Callahan, A.M., Ketter, T.A., Pazzaglia, P.J., L'Herrou, T.A., Leverich, G.S. and Post, R.M. (1997) Effects of intrathecal thyrotropin-releasing hormone (protirelin) in refractory depressed patients. *Arch. Gen. Psychiatry* **54**, 214-222.

Mariani, E., Polidori, M.C., Cherubini, A. and Mecocci, P. (2005) Oxidative stress in brain aging, neurodegenerative and vascular diseases: An overview. *J. Chromatogr. B* **827**, 65-75.

Mason, G., Garbutt, J. and Prange, A.J. (1995) Thyrotropin-releasing hormone: focus on basic neurobiology, Raven Press, New York.

Mattson M.P. (1991) Evidence for the involvement of protein kinase C in neurodegenerative changes in cultured human cortical neurons. *Experimental Neurology* **112,** 95-103.

McBean, G.J. (1990) Intrastriatal injection of DL-alpha-aminoadipate reduces kainate toxicity in vitro. *Neuroscience* **34**, 225-234.

McBean, G. J., Doorty, K. B., Tipton, K. F. and Kollegger, H. (1995) Alteration in the glial cell metabolism of glutamate by kainate and *N*-methyl-D-aspartate. *Toxicon.* **33**, 569-576.

McClure, W.R. (1969) A kinetic analysis of coupled enzyme assays. *Biochemistry* **8**, 2782-2786.

McCreary, A.C. and Handley, S.L. (1999) The thyrotrophin-releasing hormone analogue MK771 induces tic-like behaviours: the effects of dopamine D1 and D2 receptor antagonists. *Eur. J. Pharmacol.* **369**, 1-9.

McCulloch, J. and Dewar, D. (2001) A radical approach to stroke therapy. *Proc. Natl. Acad. Sci. USA* **98**, 10989-10991.

Meldrum, B.S. and Garthwaite, J. (1990) Excitatory amino acid neurotoxicity and neurodegenerative disease. *Trends Pharmacol. Sci.* **11**, 379-387.

Meldrum, B.S. (2002) Implications for neuroprotective treatments. *Prog. Brain Res.* **135**, 487-495.

Mellow, A.M., Sunderland, T., Cohen, R.M., Lawlor, B.A., Hill, J.L., Newhouse, P.A., Cohen, M.R. and Murphy, D.L. (1989) Acute effects of high-dose thyrotropin releasing hormone infusions in Alzheimer's disease. *Psychopharmacology-(Berl)*. **98**, 403-407.

Merchenthaler, I. (1991) Co-localization of enkephalin and TRH in perifornical neurons of the rat hypothalamus that project to the lateral septum. *Brain Res.* **544**, 177-180.

Metcalf, G. and Myers, R.D. (1975) Proceedings: Investigations concerning TRH-induced hypothermia in cats. *Br. J. Pharmacol.* **55**, 273-274.

Metcalf G., Dettmar P. W., Lynn A. G., Brewster D. and Havler M. E. (1981) Thyrotropin-releasing hormone (TRH) analogues show enhanced CNS selectivity because of increased biological stability. *Regul Pept* **2,** 277-284.

Metcalf, G. and Dettmar, P.W. (1981) Is thyrotropin releasing hormone an endogenous ergotropic substance in the brain? *Lancet* **1**, 586-589.

Mihic, S.J. and Harris, R.A. (1997) GABA and the GABAA receptor. *Alcohol Health Res. World* **21**, 127-131.

Milusheva E., Baranyi M., Zelles T. and Vizi M. E. S. (1994) Release of Acetylcholine and Noradrenaline from the Cholinergic and Adrenergic Afferents in Rat Hippocampal CA1, CA3 and Dentate Gyrus Regions. *Eur. J. Neurosci.* **6,** 187-192.

Miranda, P., Giraldez, T., De La Pena, P., Manso, D.G., Alonso-Ron, C., Gomez-Varela, D., Dominguez, P. and Barros, F. (2005) Specificity of TRH receptor coupling to G-proteins for regulation of ERG K^+ channels in GH3 rat anterior pituitary cells. *J. Physiol.* **566**, 717-736.

Miyamoto, M. and Nagawa, Y. (1977) Mesolimbic involvement in the locomotor stimulant action of thyrotropin-releasing hormone (TRH) in rats. *Eur. J. Pharmacol.* **44**, 143-152.

Miyamoto, M., Hirai, K., Toshiro, H. and Akinobu, N. (1994) Effects of a sustained release formulation of thyrotropin-releasing hormone on behavioral abnormalities in senescence-accelerated mice. *Eur. J. Pharmacol.* **271**, 357-366.

Miyazaki A., Toide K., Sasaki Y., Ichitani Y. and Iwasaki T. (1998) Effect of a prolyl endopeptidase inhibitor, JTP-4819, on radial maze performance in hippocampal-lesioned rats. *Pharmacol Biochem Behav* **59,** 361-368.

Montoliu, C., Humet, M., Canales, J.-J., Burda, J., Planells-Cases, R., Sanchez-Baeza, F., Carbonell, T., Perez-Paya, E., Messeguer, A., Ferrer-Montiel, A. and Felipo, V. (2002) Prevention of *in Vivo* Excitotoxicity by a Family of Trialkylglycines, a Novel Class of Neuroprotectants. *J. Pharmacol. Exp. Ther.* **301**, 29-36.

Morley J. E. (1979) Extrahypothalamic thyrotropin releasing hormone (TRH) -- its distribution and its functions. *Life Sci* **25,** 1539-1550.

Morris, R. (1984) Developments of a water-maze procedure for studying spatial learning in the rat. *J. Neurosci. Methods* **11**, 47-60.

Morzorati, S. and Kubek, M.J. (1993) Septal TRH in alcohol-naive P and NP rats and following alcohol challenge. *Brain Res. Bull.* **31**, 301-304.

Moss J. and Bundgaard H. (1990) Kinetics and pattern of degradation of thyrotropin-releasing hormone (TRH) in human plasma. *Pharm Res* **7,** 751-755.

Naarala, J., Nykvist, P., Tuomala, M. and Savolainen, K. (1993) Excitatory amino acid-induced slow biphasic responses of free intracellular calcium in human neuroblastoma cells. *FEBS Lett.* **330**, 222-226.

Nakayama, T., Hashimoto, T. and Nagai, Y. (1996) Involvement of glutamate and gamma-aminobutyric acid (GABA)-ergic systems in thyrotropin-releasing hormone-induced rat cerebellar cGMP formation. *Eur. J. Pharmacol.* **316**, 157-164.

Nemeroff, C.B., Kalivas, P.W., Golden, R.N. and Prange, A.J., Jr. (1984) Behavioral effects of hypothalamic hypophysiotropic hormones, neurotensin, substance P and other neuropeptides. *Pharmacol. Ther.* **24**, 1-56.

Nguyen, V., Zharikova, A.D. and Prokai, L. (2007) Evidence for interplay between thyrotropin-releasing hormone (TRH) and its structural analogue pGlu-Glu-Pro-NH2 ([Glu2]TRH) in the brain: An *in vivo* microdialysis study. *Neuroscience Letters* **415**, 64-67.

Nicklas, W.J., Krespan, B. and Berl, S. (1980) Effect of kainate on ATP levels and glutamate metabolism in cerebellar slices. *Eur. J. Pharmacol.* **62**, 209-213.

Nicklas, W.J., Vyas, I. and Heikkila, R.E. (1985) Inhibition of NADH-linked oxidation in brain mitochondria by 1-methyl-4-phenyl-pyridine, a metabolite of the neurotoxin, 1-methyl-4-phenyl-1,2,5,6-tetrahydropyridine. *Life Sci.* **36**, 2503-2508.

Nicoll, R.A., Alger, B.E., Jahr, C.E. and Morley, J.S. (1980) Peptides as Putative Excitatory Neurotransmitters: Carnosine, Enkephalin, Substance P and TRH [and Discussion]. *Proc. R. Soc. Lon.d B Biol. Sci.* **210**, 133-149.

Nie, Y., Schoepp, D.D., Klaunig, J.E., Yard, M., Lahiri, D.K. and Kubek, M.J. (2005) Thyrotropin-releasing hormone (protirelin) inhibits potassium-stimulated glutamate and aspartate release from hippocampal slices in vitro. *Brain Res.* **1054**, 45-54.

Nillni, E.A., Friedman, T.C., Todd, R.B., Birch, N.P., Loh, Y.P. and Jackson, I.M. (1995) Pro-thyrotropin-releasing hormone processing by recombinant PC1. *J. Neurochem.* **65**, 2462-2472.

Nillni, E.A., Luo, L.G., Jackson, I.M. and McMillan, P. (1996) Identification of the thyrotropin-releasing hormone precursor, its processing products, and its coexpression with convertase 1 in primary cultures of hypothalamic neurons: anatomic distribution of PC1 and PC2. *Endocrinology* **137**, 5651-5661.

Nillni, E.A. and Sevarino, K.A. (1999) The Biology of pro-Thyrotropin-Releasing Hormone-Derived Peptides. *Endocr. Rev.* **20**, 599-648.

Nillni, E.A., Xie, W., Mulcahy, L., Sanchez, V.C. and Wetsel, W.C. (2002) Deficiencies in Pro-thyrotropin-releasing Hormone Processing and Abnormalities in Thermoregulation in Cpefat/fatMice. *J. Biol. Chem.* **277**, 48587-48595.

Nilsson, K.O., Wide, L. and Hokfelt, B. (1975) The effect of apomorphine on basal and TRH stimulated release of thyrotrophin and prolactin in man. *Acta Endocrinol. (Copenh.)* **80**, 220-229.

Nistri, A. (1990) Mechanism of action of protirelin tartrate (TRH-T) on spinal motor neurons. *Ann. Ital. Med. Int.* **5**, 245-248.

Nistri, A., Fisher, N.D. and Gurnell, M. (1990) Block by the neuropeptide TRH of an apparently novel K^+ conductance of rat motoneurones. *Neurosci. Lett.* **120**, 25-30.

Noda, M., Nakanishi, H., Nabekura, J. and Akaike, N. (2000) AMPA-kainate subtypes of glutamate receptor in rat cerebral microglia. *J. Neurosci.* **20**, 251-258.

Obrenovitch, T.P., Urenjak, J., Zilkha, E. and Jay, T.M. (2000) Excitotoxicity in neurological disorders -- the glutamate paradox. *Intl. J. Dev. Neurosci.* **18**, 281-287.

O'Byrne, M., Tipton, K., McBean, G. and Kollegger, H. (1997) Assessment of neurotoxicity and "neuroprotection". *J. Neural Transm. Suppl.* **50**, 153-164.

O'Cuinn, G., O'Connor, B. and Elmore, M. (1990) Degradation of thyrotropin-releasing hormone and luteinising hormone-releasing hormone by enzymes of brain tissue. *J. Neurochem.* **54**, 1-13.

O'Dowd, B.F., Lee, D.K., Huang, W., Nguyen, T., Cheng, R., Liu, Y., Wang, B., Gershengorn, M.C. and George, S.R. (2000) TRH-R2 exhibits similar binding and acute signaling but distinct regulation and anatomic distribution compared with TRH-R1. *Mol. Endocrinol.* **14**, 183-193.

Ogasawara, T., Itoh, Y., Tamura, M., Ukai, Y., Yoshikuni, Y. and Kimura, K. (1996) NS-3, a TRH-Analog, Reverses Memory Disruption by Stimulating Cholinergic and Noradrenergic Systems. *Pharmacol. Biochem. Behav.* **53**, 391-399.

Ogata, A., Nagashima, K., Yasui, K., Matsuura, T. and Tashiro, K. (1998) Sustained release dosage of thyrotropin-releasing hormone improves

experimental Japanese encephalitis virus-induced parkinsonism in rats. *J. Neurol. Sci.* **159**, 135-139.

Ogata, T., Nakamura, Y., Shibata T, Kataoka K. (1992) Release of Excitatory Amino Acids from Cultured Hippocampal Astrocytes Induced by a Hypoxic-Hypoglycemic Stimulation. *J. Neurochem.* **58**, 1957-1959.

Okada, M. (1991) Effects of a new thyrotropin releasing hormone analogue, YM-14673, on the *in vivo* release of acetylcholine as measured by intracerebral dialysis in rats. *J. Neurochem.* **56**, 1544-1547.

O'Leary, R.M. and O'Connor, B. (1995) A study of a synaptosomal thyrotropin releasing hormone-inactivating pyroglutamate aminopeptidase from bovine brain. *Int. J. Biochem. Cell Biol.* **27**, 881-890.

Olson G. L., Cheung H. C., Chiang E., Madison V. S., Sepinwall J., Vincent G. P., Winokur A. and Gary K. A. (1995) Peptide mimetics of thyrotropin-releasing hormone based on a cyclohexane framework: design, synthesis, and cognition-enhancing properties. *J. Med. Chem.* **38,** 2866-2879.

O'Neill C.M., Ball S.G. and Vaughan P.F. (1994) Effects of ischaemic conditions on uptake of glutamate, aspartate, and noradrenaline by cell lines derived from the human nervous system. *J. Neurochem.* **63**, 603-611.

Papadopoulos, T., Heuer, H. and Bauer, K. (2000) Analysis of the thyrotropin-releasing hormone-degrading ectoenzyme by site-directed mutagenesis of cysteine residues Cys68 is involved in disulfide-linked dimerization. *Eur. J. Biochem.* **267**, 2617-2623.

Papadopoulos, T., Kelly, J.A. and Bauer, K. (2001) Mutational Analysis of the Thyrotropin-Releasing Hormone-Degrading Ectoenzyme. Similarities and Differences with Other Members of the M1 Family of Aminopeptidases and Thermolysin. *Biochemistry* **40**, 9347-9355.

Paxinos, G. and Watson, C. (2004) The Rat Brain in Stereotaxic Coordinates, Academic Press, New York.

Pekary, A.E., Meyerhoff, J.L. and Sattin, A. (2000) Electroconvulsive seizures modulate levels of thyrotropin releasing hormone and related peptides in rat hypothalamus, cingulate and lateral cerebellum. *Brain Res.* **884**, 174-183.

Pekary, A.E., Sattin, A., Meyerhoff, J.L. and Chilingar, M. (2004) Valproate modulates TRH receptor, TRH and TRH-like peptide levels in rat brain. *Peptides* **25**, 647-658.

Perlman, J.H., Colson, A.O., Wang, W., Bence, K., Osman, R. and Gershengorn, M.C. (1997) Interactions between conserved residues in transmembrane helices 1, 2, and 7 of the thyrotropin-releasing hormone receptor. *J. Biol. Chem.* **272**, 11937-11942.

Pizzi, M., Boroni, F., Benarese, M., Moraitis, C., Memo, M. and Spano, P. (1999) Neuroprotective effect of thyrotropin-releasing hormone against excitatory amino acid-induced cell death in hippocampal slices. *Eur. J. Pharmacol.* **370**, 133-137.

Pocock, J.M., Murphie, H.M. and Nicholls, D.G. (1988) Kainic acid inhibits the synaptosomal plasma membrane glutamate carrier and allows glutamate leakage from the cytoplasm but does not affect glutamate exocytosis. *J. Neurochem.* **50**, 745-751.

Poulat, P., Marlier, L., Rajaofetra, N. and Privat, A. (1992a) 5-Hydroxytryptamine, substance P and thyrotropin-releasing hormone synapses in the intermediolateral cell column of the rat thoracic spinal cord. *Neurosci. Lett.* **136**, 19-22.

Poulat, P., Sandillon, F., Marlier, L., Rajaofetra, N., Oliver, C. and Privat, A. (1992b) Distribution of thyrotropin-releasing hormone in the rat spinal cord with special reference to sympathetic nuclei: a light- and electron-microscopic immunocytochemical study. *J. Neurocytol.* **21**, 157-170.

Prakash K. R., Tang Y., Kozikowski A. P., Flippen-Anderson J. L., Knoblach S. M. and Faden A. I. (2002) Synthesis and biological activity of novel neuroprotective diketopiperazines. *Bioorg Med Chem* **10,** 3043-3048.

Prasad C., Mizuma H., Brock J. W., Porter J. R., Svec F. and Hilton C. (1995) A paradoxical elevation of brain cyclo(His-Pro) levels in hyperphagic obese Zucker rats. *Brain Research* **699,** 149-153.

Prediger, R.D., Da Cunha, C. and Takahashi, R.N. (2005) Antagonistic interaction between adenosine A2A and dopamine D2 receptors modulates the social recognition memory in reserpine-treated rats. *Behav. Pharmacol.* **16**, 209-218.

Prokai-Tatrai, K., Nguyen, V., Zharikova, A.D., Braddy, A.C., Stevens, S.M. and Prokai, L. (2003) Prodrugs to enhance central nervous system effects of the TRH-like peptide pGlu-Glu-Pro-NH_2. *Bioorg. Med. Chem. Lett.* **13**, 1011-1014.

Rabeler, R., Mittag, J., Geffers, L., Ruther, U., Leitges, M., Parlow, A.F., Visser, T.J. and Bauer, K. (2004) Generation of Thyrotropin-Releasing Hormone Receptor 1-Deficient Mice as an Animal Model of Central Hypothyroidism. *Mol. Endocrinol.* **18**, 1450-1460.

Rakovska, A., Giovannini, M. G., Della Corte, L., Kalfin, R., Bianchi, L. and Pepeu, G. (1998) Neurotensin modulation of acetylcholine and gaba release from the rat hippocampus: an *in vivo* microdialysis study. *Neurochem. Intl.* **33**, 335-340.

Raley, K. M. and Lipton, P. (1990) NMDA receptor activation accelerates ischemic energy depletion in the hippocampal slice and the demonstration of a threshold for ischemic damage to protein synthesis. *Neurosci. Lett.* **110**, 118-123.

Rezvani, A.H., Garbutt, J.C., Shimoda, K., Garges, P.L., Janowsky, D.S. and Mason, G.A. (1992) Attenuation of Alcohol Preference in Alcohol-Preferring Rats by a Novel TRH Analogue, TA-0910. *Alcohol. Clin. Exp. Res.* **16**, 326-330.

Richerson, G.B. (2004) Serotonergic neurons as carbon dioxide sensors that maintain ph homeostasis. *Nat. Rev. Neurosci.* **5**, 449-461.

Rinaman, L. and Miselis, R.R. (1990) Thyrotropin-releasing hormone-immunoreactive nerve terminals synapse on the dendrites of gastric vagal motoneurons in the rat. *J. Comp. Neurol.* **294**, 235-251.

Rothman, S.M., Thurston, J.H., Hauhart, R.E., Clark, G.D. and Solomon, J. S. (1987) Ketamine protects hippocampal neurons from anoxia *in vitro*. *Neuroscience* **21**, 673-678.

Sattin, A., Hill, T.G., Meyerhoff, J.L., Norton, J.A. and Kubek, M.J. (1987) The prolonged increase in thyrotropin-releasing hormone in rat limbic forebrain regions following electroconvulsive shock. *Regul. Pept.* **19**, 13-22.

Sattin, A. (1999) The role of TRH and related peptides in the mechanism of action of ECT. *J. Ect.* **15**, 76-92.

Sattin, A., Senanayake, S.S. and Pekary, A.E. (2002) Lithium modulates expression of TRH receptors and TRH-related peptides in rat brain. *Neuroscience* **115**, 263-273.

Sattin, A., Pekary, A.E., Lloyd, R.L., Paulson, M., Meyerhoff, J.A., Hinkle, P.M. and Faull, K. (2003) TRH and Related Peptides. *Ann. NY Acad. Sci.* **1003**, 458-460.

Sawin, C. T., Bacharach, P. and Lance, V. (1981) Thyrotropin-releasing hormone and thyrotropin in the control of thyroid function in the turtle, Chrysemys picta. *Gen. Compar. Endocrin.* **45**, 7-11.

Scalabrino, G.A., Hogan, N., O'Boyle, K.M., Slator, G.R., Gregg, D.J., Fitchett, C.M., Draper, S.M., Bennett, G.W., Hinkle, P.M., Bauer, K., Williams, C.H., Tipton, K.F. and Kelly, J.A. (2007) Discovery of a dual action first-in-class peptide that mimics and enhances CNS-mediated actions of thyrotropin-releasing hormone. *Neuropharmacology* **52**, 1472-1481.

Scanlon, M.F. and Toft, A.D. (2000) Regulation of thyrotropin secretion. In *Werner and Ingbar's the Thyroid: A Fundamental and Clinical Text* (Braverman, L. and Utiger, R. ed.s) pp 234-254, Lippincott, Williams and Wilkins, New York.

Schally, A.V., Redding, T.W., Bowers, C.Y. and Barrett, J.F. (1969) Isolation and Properties of Porcine Thyrotropin-releasing Hormone. *J. Biol. Chem.* **244**, 4077-4088.

Schauder, B., Schomburg, L., Kohrle, J. and Bauer, K. (1994) Cloning of a cDNA encoding an ectoenzyme that degrades thyrotropin-releasing hormone. *Proc. Natl. Acad. Sci. USA* **91**, 9534-9538.

Schledermann, W., Wulfsen, I., Schwarz, J.R. and Bauer, C.K. (2001) Modulation of rat erg1, erg2, erg3 and HERG K^+ currents by thyrotropin-releasing hormone in anterior pituitary cells via the native signal cascade. *J. Physiol.* **532**, 143-163.

Schnier J. B., Nishi K., Goodrich D.W. and Bradbury E.M. (1996) G1 arrest and down-regulation of cyclin E/cyclin-dependent kinase 2 by the protein kinase inhibitor staurosporine are dependent on the retinoblastoma protein in the bladder carcinoma cell line 5637. *Proc. Natl. Acad. Sci. USA* **93,** 5941-5946.

Schoepp, D.D., Tizzano, J.P., Wright, R.A. and Fix, A.S. (1995) Reversible and Irreversible Neuronal Injury Induced by Intrahippocampal Infusion of the mGluR Agonist 1S,3R-ACPD in the Rat. *Neurodegeneration* **4**, 71-80.

Schroder W., Seifert G., Huttmann K., Hinterkeuser S. and Steinhauser C. (2002) AMPA Receptor-Mediated Modulation of Inward Rectifier K^+ Channels in Astrocytes of Mouse Hippocampus. *Molecular and Cellular Neuroscience* **19,** 447-458.

Schuhler, S., Warner, A., Finney, N., Bennett, G.W., Ebling, F.J. and Brameld, J.M. (2007) Thyrotrophin-releasing hormone decreases feeding and increases body temperature, activity and oxygen consumption in Siberian hamsters. *J. Neuroendocrinol.* **19**, 239-249.

Segieth J., Getting S.J., Biggs C.S. and Whitton P.S. (1995) Nitric oxide regulates excitatory amino acid release in a biphasic manner in freely moving rats. *Neurosci. Lett.* **200,** 101-104.

Selkoe D.J. (2001) Alzheimer's disease results from the cerebral accumulation and cytotoxicity of amyloid \beta-protein. *J. Alz. Dis.* **3**, 75-80.

Sershen H., Balla A., Lajtha A. and Vizi E. S. (1997) Characterization of nicotinic receptors involved in the release of noradrenaline from the hippocampus. *Neuroscience* **77,** 121-130.

Seyfried, C.A., Adam, G. and Greve, T. (1986) An automated direct-injection HPLC-method for the electrochemical/fluorimetric quantitation of monoamines and related compounds optimized for the screening of large numbers of animals. *Biomed. Chromatogr.* **1,** 78-88.

Sharif, N.A. (1989) Quantitative autoradiography of TRH receptors in discrete brain regions of different mammalian species. *Ann. N.Y. Acad. Sci.* **553**, 147-175.

Sharif, N.A., To, Z.P. and Whiting, R.L. (1991) Analogs of thyrotropin-releasing hormone (TRH): Receptor affinities in brains, spinal cords, and pituitaries of different species. *Neurochem. Res.* **16**, 95-103.

Sharma S. and Kaur G. (2005) Neuroprotective potential of dietary restriction against kainate-induced excitotoxicity in adult male Wistar rats. *Brain Res. Bull.* **67,** 482-491.

Shinoda M., Matsuo A. and Toide K. (1996) Pharmacological studies of a novel prolyl endopeptidase inhibitor, JTP-4819, in rats with middle cerebral artery occlusion. *Eur J Pharmacol* **305,** 31-38.

Shytle, R.D., Borlongan, C.V. and Sanberg, P.R. (1995) Nicotine blocks kainic acid-induced wet dog shakes in rats. *Neuropsychopharmacology* **13**, 261-264.

Simonian, N.A., Getz, R.L., Leveque, J.C., Konradi, C. and Coyle, J.T. (1996) Kainate induces apoptosis in neurons. *Neuroscience* **74**, 675-683.

Skaper, S.D., Floreani, M., Ceccon, M., Facci, L. and Giusti, P. (1999) Excitotoxicity, Oxidative Stress, and the Neuroprotective Potential of Melatonin. *Ann. NY Acad. Sci.* **890**, 107-118.

Smith J., Yu R. and Hinkle P. M. (2001) Activation of MAPK by TRH requires clathrin-dependent endocytosis and PKC but not receptor interaction with beta-arrestin or receptor endocytosis. *Mol. Endocrinol.* **15**, 1539-1548.

Song, T., Hatano, N., Kambe, T., Miyamoto, Y., Ihara, H., Yamamoto, H., Sugimoto, K., Kume, K., Yamaguchi, F., Tokuda, M. and Watanabe, Y. (2008) Nitric oxide-mediated modulation of calcium/calmodulin-dependent protein kinase II. *Biochem. J.* **412**, 223-231.

Squires, A.S., Peddle, R., Milway, S.J. and Harley, C.W. (2006) Cytotoxic lesions of the hippocampus do not impair social recognition memory in socially housed rats. *Neurobiol. Learn Mem.* **85**, 95-101.

Stanton, T.L., Bechman, A.L. and Winokur, A. (1981) Thyrotropin-releasing hormone effects in the central nervous system: dependence on arousal state. *Science* **214**, 678-681.

Steward, C.A., Horan, T. L., Schuhler, S., Bennett, G.W. and Ebling, F.J. (2003) Central administration of thyrotropin releasing hormone (TRH) and related peptides inhibits feeding behavior in the Siberian hamster. *Neuroreport* **14**, 687-691.

Storey, E., Hyman, B.T., Jenkins, B., Brouillet, E., Miller, J.M., Rosen, B.R. and Beal, M.F. (1992) 1-Methyl-4-phenylpyridinium produces excitotoxic lesions in rat striatum as a result of impairment of oxidative metabolism. *J. Neurochem.* **58**, 1975-1978.

Straub, R.E., Frech, G.C., Joho, R.H. and Gershengorn, M.C. (1990) Expression cloning of a cDNA encoding the mouse pituitary thyrotropin-releasing hormone receptor. *Proc. Natl. Acad. Sci. USA* **87**, 9514-9518.

Sugenoya, J., Kihara, M., Ogawa, T., Takahashi, A., Mitsuma, T. and Yamashita, Y. (1988) Effects of thyrotropin releasing hormone on human sudomotor and cutaneous vasomotor activities. *Eur. J. Appl. Physiol.* **57**, 632-638.

Sugimoto K., Kume K., Yamaguchi F., Tokuda M. and Watanabe Y. (2008) Nitric oxide-mediated modulation of calcium/calmodulin-dependent protein kinase II. *Biochem. J.* **412,** 223-231.

Sullivan, P.G. (2005) Interventions with neuroprotective agents: Novel targets and opportunities. *Epilepsy Behav.* **7**, 12-17.

Sun, Y., Lu, X. and Gershengorn, M.C. (2003) Thyrotropin-releasing hormone receptors -- similarities and differences. *J. Mol. Endocrinol.* **30**, 87-97.

Syntichaki, P. and Tavernarakis, N. (2003) The biochemistry of neuronal necrosis: rogue biology? *Nat. Rev. Neurosci.* **4**, 672-684.

Szuba, M.P., Amsterdam, J.D., Fernando, A.T., 3RD, Gary, K.A., Whybrow, P.C. and Winokur, A. (2005) Rapid antidepressant response after nocturnal TRH administration in patients with bipolar type I and bipolar type II major depression. *J. Clin. Psychopharmacol.* **25**, 325-330.

Talley, E.M., LEI, Q., Sirois, J.E. and Bayliss, D.A. (2000) TASK-1, a Two-Pore Domain K^+ Channel, Is Modulated by Multiple Neurotransmitters in Motoneurons. *Neuron* **25**, 399-410.

Tanabe, M., Tokuda, Y., Takasu, K., Ono, K., Honda, M. and Ono, H. (2007) The synthetic TRH analogue taltirelin exerts modality-specific antinociceptive effects via distinct descending monoaminergic systems. *Br. J. Pharmacol.* **150**, 403-414.

Tanaka, K., Ogawa, N., Asanuma, M. and Kondo, Y. (1997) Thyrotropin releasing hormone prevents abnormalities of cortical acetylcholine and monoamines in mice following head injury. *Regul. Pept.* **70**, 173-178.

Tetich M., Kutner A., Leskiewicz M., Budziszewska B. and Lason W. (2004) Neuroprotective effects of (24R)-1,24-dihydroxycholecalciferol in human neuroblastoma SH-SY5Y cell line. *J. Steroid Biochem. Mol. Biol* **89-90**, 365-370.

Tipton K.F. and Singer T.P. (1993) Advances in our understanding of the mechanisms of the neurotoxicity of MPTP and related compounds. *J. Neurochem.* **61,** 1191-1206.

Togari, A., Ichinose, H., Kojima, K., Hirata, Y. and Nagatsu, T. (1988) Centrally mediated activation of tyrosine hydroxylation in rat adrenals by thyrotropin-releasing hormone. *Biochem. Pharmacol.* **37**, 1637-1639.

Toide, K., Shinoda, M., Takase, M., Iwata, K. and Yoshida, H. (1993) Effects of a novel thyrotropin-releasing hormone analogue, JTP-2942, on extracellular acetylcholine and choline levels in the rat frontal cortex and hippocampus. *Eur. J. Pharmacol.* **233**, 21-28.

Toide K., Shinoda M., Fujiwara T. and Iwamoto Y. (1997) Effect of a novel prolyl endopeptidase inhibitor, JTP-4819, on spatial memory and central cholinergic neurons in aged rats. *Pharmacol. Biochem. Behav.* **56,** 427-434.

Urayama, A., Yamada, S., Deguchi, Y., Kimura, R., Maeda, Y. and Kobayashi, T. (1999) Brain receptor binding characteristics and pharmacokinetics of JTP-2942, a novel thyrotropin-releasing hormone (TRH) analogue. *Life Sci.* **65**, 2407-2415.

Urayama, A., Yamada, S., Kimura, R., Zhang, J. and Watanabe, Y. (2002) Neuroprotective effect and brain receptor binding of taltirelin, a novel thyrotropin-releasing hormone (TRH) analogue, in transient forebrain ischemia of C57BL/6J mice. *Life Sci.* **72**, 601-607.

Van der Zeyden M., Oldenziel W.H., Rea K., Cremers T.I. and Westerink B.H. (2008) Microdialysis of GABA and glutamate: Analysis, interpretation and comparison with microsensors. *Pharmacology Biochemistry and Behavior* **90,** 135-147.

Vargas, M.A., Cisneros, M., Herrera, J., Joseph-Bravo, P. and Charli, J.L. (1992) Regional distribution of pyroglutamyl peptidase II in rabbit brain, spinal cord, and organs. *Peptides* **13**, 255-260.

Verkhratsky A. and Steinhauser C. (2000) Ion channels in glial cells. *Brain Research Reviews* **32,** 380-412.

Veronesi, M.C., Yard, M., Jackson, J., Lahiri, D.K. and Kubek, M.J. (2007a) An analog of thyrotropin-releasing hormone (TRH) is neuroprotective against glutamate-induced toxicity in fetal rat hippocampal neurons *in vitro*. *Brain Res.* **1128**, 79-85.

Veronesi M.C., Kubek D.J. and Kubek M.J. (2007b) Intranasal delivery of a thyrotropin-releasing hormone analog attenuates seizures in the amygdala-kindled rat. *Epilepsia* **48**, 2280-2286.

Virgili, M., Migani, P., Contestabile, A. and Barnabei, O. (1992) Protection from kainic acid neuropathological syndrome by NMDA receptor antagonists: effect

of MK-801 and CGP 39551 on neurotransmitter and glial markers. *Neuropharmacology* **31**, 469-474.

Volbracht, C., Van Beek, J., Zhu, C., Blomgren, K. and Leist, M. (2006) Neuroprotective properties of memantine in different *in vitro* and *in vivo* models of excitotoxicity. *Eur. J. Neurosci.* **23**, 2611-2622.

Vornov, J. and Coyle, J. (1991) Glutamate neurotoxicity and the inhibition of protein synthesis in the hippocampal slice. *J. Neurochem.* **56**, 996-1006.

Wallin, C., Weber, S.G. and Sandberg, M. (1999) Glutathione Efflux Induced by NMDA and Kainate: Implications in Neurotoxicity? *J. Neurochem.* **73**, 1566-1572.

Walsh, D.M., Tseng, B.P., Rydel, R.E., Podlisny, M.B. and Selkoe, D.J. (2000) The Oligomerization of Amyloid β-Protein Begins Intracellularly in Cells Derived from Human Brain. *Biochemistry* **39**, 10831-10839.

Wang, G., Zeng, J., Ren, R. and Chen, S. (2008) Potassium channels in the basal ganglia: promising new targets for the treatment of Parkinson's disease. *Front. Biosci.* **13**, 3685-3698.

Wang, Q., Yu, S., Simonyi, A., Sun, G. and Sun, A. (2005) Kainic acid-mediated excitotoxicity as a model for neurodegeneration. *Mol. Neurobiol.* **31**, 3-16.

Waters, M.F., Minassian, N.A., Stevanin, G., Figueroa, K.P., Bannister, J.P.A., Nolte, D., Mock, A.F., Evidente, V.G.H., Fee, D.B., Muller, U., Durr, A., Brice, A., Papazian, D.M. and Pulst, S.M. (2006) Mutations in voltage-gated potassium channel KCNC3 cause degenerative and developmental central nervous system phenotypes. *Nat. Genet.* **38**, 447-451.

Watts J., Fowler L., Whitton P.S. and Pearce B. (2005) Release of arginine, glutamate and glutamine in the hippocampus of freely moving rats: Involvement of nitric oxide. *Brain Res. Bull.* **65,** 521-528.

Waxham M.N., Grotta J.C., Silva A.J., Roger S. and Jaroslaw A. (1996) Ischemia-Induced Neuronal Damage: A Role for Calcium/Calmodulin-Dependent Protein Kinase II. *J. Cereb. Blood Flow Metab.* **16**, 1-6.

Weil M., Jacobson M. D., Coles H. S., Davies T. J., Gardner R. L., Raff K. D. and Raff M. C. (1996) Constitutive expression of the machinery for programmed cell death. *J. Cell Biol.* **133**, 1053-1059.

Westphalen R. I., Krivitski M., Amarosa A., Guy N. and Hemmings H. C., Jr. (2007) Reduced inhibition of cortical glutamate and GABA release by halothane in mice lacking the K+ channel, TREK-1. *Br. J. Pharmacol.* **152,** 939-945.

Wilk, S. (1986) Neuropeptide-specific peptidases: does brain contain a specific TRH-degrading enzyme? *Life Sci.* **39**, 1487-1492.

Williams, S., Vachon, P. and Lacaille, J.C. (1993) Monosynaptic GABA-mediated inhibitory postsynaptic potentials in CA1 pyramidal cells of hyperexcitable hippocampal slices from kainic acid-treated rats. *Neuroscience* **52**, 541-554.

Winokur, A. and Utiger, R.D. (1974) Thyrotropin-releasing hormone: regional distribution in rat brain. *Science* **185**, 265-267.

Winokur, A., Amsterdam, J.D., Mihailovic, V. and Caroff, S.N. (1982) Improvement in ratings of tension after TRH administration in healthy women. *Psychoneuroendocrinology* **7**, 239-244.

Wittmann, G., Lechan, R.M., Liposits, Z. and Fekete, C. (2005) Glutamatergic innervation of corticotropin-releasing hormone- and thyrotropin-releasing hormone-synthesizing neurons in the hypothalamic paraventricular nucleus of the rat. *Brain Res.* **1039**, 53-62.

Xu J., Peng H., Kang N., Zhao Z., Lin J. H. C., Stanton P. K. and Kang J. (2007) Glutamate-induced Exocytosis of Glutamate from Astrocytes. *J. Biol. Chem.* **282,** 24185-24197.

Yamada, M., Radovick, S., Wondisford, F.E., Nakayama, Y., Weintraub, B.D. and Wilber, J.F. (1990) Cloning and structure of human genomic DNA and hypothalamic cDNA encoding human prepro thyrotropin-releasing hormone. *Mol. Endocrinol.* **4**, 551-556.

Yamada, M., Saga, Y., Shibusawa, N., Hirato, J., Murakami, M., Iwasaki, T., Hashimoto, K., Satoh, T., Wakabayashi, K., Taketo, M.M. and Mori, M. (1997)

Tertiary hypothyroidism and hyperglycemia in mice with targeted disruption of the thyrotropin-releasing hormone gene. *Proc. Natl. Acad. Sci. USA* **94**, 10862-10867.

Yamamura, M., Kinoshita, K., Nakagawa, H. and Ishida, R. (1991) Pharmacological study of TA-0910, a new thyrotropin-releasing hormone (TRH) analog (II): Involvement of the DA system in the locomotor stimulating action of TA-0910. *Jpn. J. Pharmacol.* **55**, 57-68.

Yarbrough, G.G. (1976) TRH potentiates excitatory actions of acetylcholine on cerebral cortical neurones. *Nature* **263**, 523-524.

Yarbrough, G.G. (1983) Minireview. Thyrotropin releasing hormone and CNS cholinergic neurons. *Life Sci.* **33**, 111-118.

Yarbrough, G.G. (2003) Fundamental molecular mechanism of the CNS effects of TRH. *Trends Pharmacol. Sci.* 24, 617-618.

Yarbrough, G.G., Kamath, J., Winokur, A. and Prange, A.J., Jr. (2007) Thyrotropin-releasing hormone (TRH) in the neuroaxis: Therapeutic effects reflect physiological functions and molecular actions. *Med. Hypotheses* **69**, 1249-1256.

Yonemori, F., Yamaguchi, T., Nakayama, H., Narita, K., Hojo, S. and Tamura, A. (2000) Effect of JTP-2942, a Novel Thyrotropin-Releasing Hormone Analog, on Motor Deficits After Chronic Focal Cerebral Ischemia in Rats. *J. Cereb. Blood. Flow Metab.* **20**, 74-81.

Zeng, H., Schimpf, B.A., Rohde, A.D., Pavlova, M.N., Gragerov, A. and Bergmann, J.E. (2007) Thyrotropin-Releasing Hormone Receptor 1-Deficient Mice Display Increased Depression and Anxiety-Like Behavior. *Mol. Endocrinol.* **21**, 2795-2804.

Appendix A SOURCES OF CHEMICAL REAGENTS

Product:		Supplier:
Standard laboratory reagents		Sigma-Aldrich Ireland Ltd. Airton road, Tallaght, Dublin 24.
		BDH chemicals BDH Chemicals Ltd., Poole, Dorset, U.K.
Biorad Solution		Alpha Technologies Ltd. The Leinster Technology Centre Blessington Industrial Estate Blessington Co. Wicklow Ireland
Caspase Substrate		Calbiochem (EMD Chemicals Inc.) Merck Biosciences, Ltd. Boulevard Industrial Park Padge Road Beeston, Nottingham NG9 2JR, UK
Custom Peptides		APC (American peptide company) 777 E. Evelyn Ave. Sunnyvale, CA 94086 USA
		PolyPeptide Laboratories GmbH Halchtersche Strasse 49 Wolfenbuettel, D-38304 Germany
Kainic Acid	Through	A.G. Scientific, Inc. Fluorochem Wesley Street Old Glossop Derbyshire SK13 7RY U.K.
Tissue Culture Reagents	Through	Invitrogen Cruinn Diagnostics Ltd., Unit 6, Phase 2, Western Industrial Estate, Dublin 12.
TRH-AMC		Bachem AG Hegenheimer Strasse 5 79576 Weil am Rhein Germany

Appendix B Amino Acid Detection

Amino acids released from hippocampal slices were detected by *o*-phthalaldehyde derivatisation and fluorometric detection following HPLC separation, as described in Section 2.11. Column effluent was monitored with an FL2000 fluorescence detector, though with a different lamp to that used to detect amino acids in Figure 2.6. The amino acid standards presented in Figure B.1 were run on a reverse phase 5 µm Nucleosil C18 column (250 × 4 mm) kept at room temperature was used. The retention times of these standards were used to identify the amino acids released from incubated hippocampal slices in Chapter 4, Figure 4.10 and the standard curve in Figure B.2 was used to calculate the concentration of glutamine released from hippocampal slices into the medium.

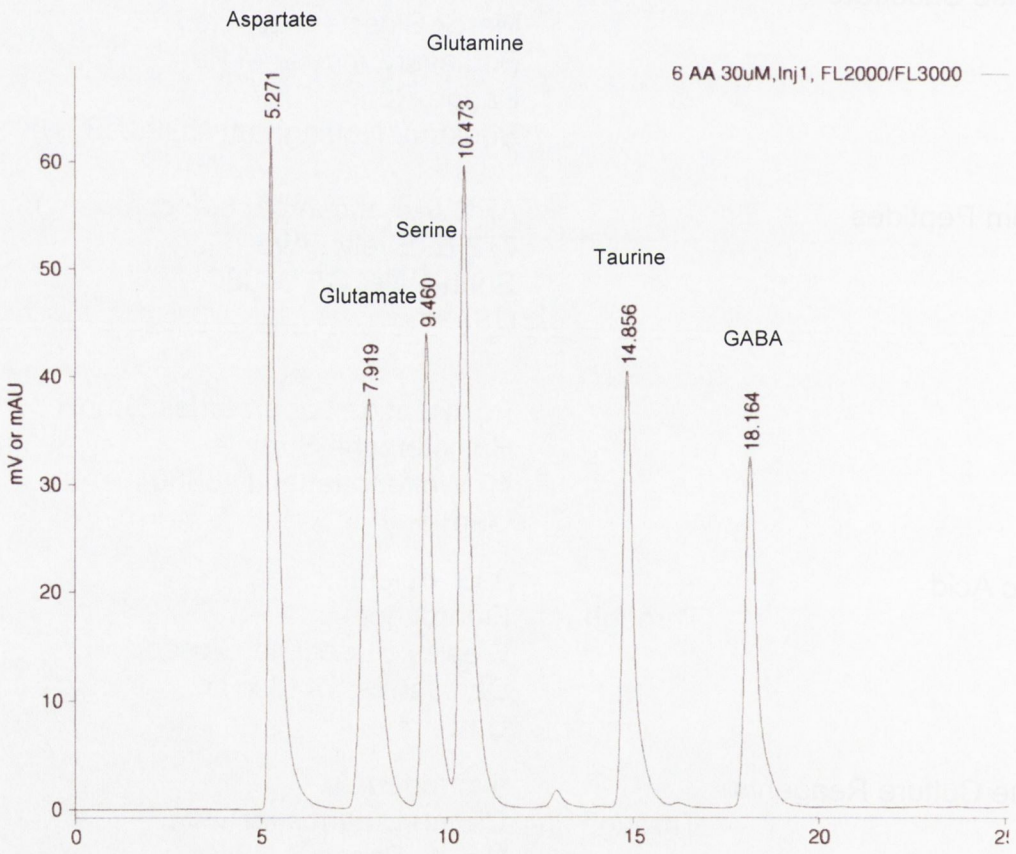

Figure B.1 The elution profile of amino acid standards

A sample trace of the separation of amino acid standards (30 µM) obtained under the conditions outlined in Section 2.7. The separation of aspartate (RT=5.21 min); glutamate (RT= 7.9 min); serine (RT=9.5 min); glutamine (RT = 10.5 min), taurine (RT =14.9 min) and GABA

(RT =18.2 min) over a 25 min elution period. Standards were prepared in 0.05 M HCl at a concentration of 30 µM. Injections of 40 µl were made onto the HPLC column.

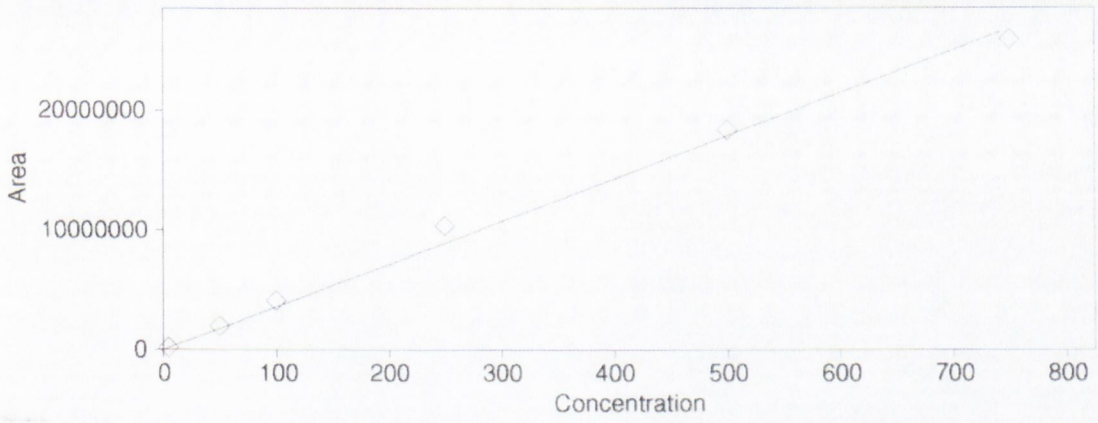

Figure B.2 Standard Curve of Glutamine

Standards of 5–750 µM concentrations of OPA derivatised glutamine were eluted from a C18 reverse phase column with a retention time of ~10.7 minutes. The fluorescence of the amino acid was detected using an FL2000 fluorescence detector and the area of the resulting fluorescence peak was measured and plotted against the corresponding glutamine concentration to produce a standard curve with a correlation coefficient of 0.999.

Biochem. J. (2005) **389**, 569–576 (Printed in Great Britain)

Structure–activity studies with high-affinity inhibitors of pyroglutamyl-peptidase II

Julie A. KELLY*[1], Gaia A. SCALABRINO*, Gillian R. SLATOR*, Aoife A. CULLEN*, John F. GILMER†, David G. LLOYD*, Geoffrey W. BENNETT‡, Karl BAUER§, Keith F. TIPTON* and Carvell H. WILLIAMS*

*Department of Biochemistry, Trinity College Dublin, Dublin 2, Ireland, †Department of Pharmaceutical Chemistry, Trinity College Dublin, Dublin 2, Ireland, ‡School of Physiology and Pharmacology, Queen's Medical Biology Centre, Nottingham NG7 2UH, U.K., and §Max-Planck-Institut für experimentelle Endokrinologie, D-30603 Hannover, Germany

Inhibitors of PPII (pyroglutamyl-peptidase II) (EC 3.4.19.6) have potential applications as investigative and therapeutic agents. The rational design of inhibitors is hindered, however, by the lack of an experimental structure for PPII. Previous studies have demonstrated that replacement of histidine in TRH (thyrotropin-releasing hormone) with asparagine produces a competitive PPII inhibitor (K_i 17.5 μM). To gain further insight into which functional groups are significant for inhibitory activity, we investigated the effects on inhibition of structural modifications to Glp-Asn-ProNH$_2$ (pyroglutamyl-asparaginyl-prolineamide). Synthesis and kinetic analysis of a diverse series of carboxamide and C-terminally extended Glp-Asn-ProNH$_2$ analogues were undertaken. Extensive quantitative structure–activity relationships were generated, which indicated that key functionalities in the basic molecular structure of the inhibitors combine in a unique way to cause PPII inhibition. Data from kinetic and molecular modelling studies suggest that hydrogen bonding between the asparagine side chain and PPII may provide a basis for the inhibitory properties of the asparagine-containing peptides. Prolineamide appeared to be important for interaction with the S_2' subsite, but some modifications were tolerated. Extension of Glp-Asn-ProNH$_2$ with hydrophobic amino acids at the C-terminus led to a novel set of PPII inhibitors active *in vitro* at nanomolar concentrations. Such inhibitors were shown to enhance recovery of TRH released from rat brain slices. Glp-Asn-Pro-Tyr-Trp-Trp-7-amido-4-methylcoumarin displayed a K_i of 1 nM, making it the most potent competitive PPII inhibitor described to date. PPII inhibitors with this level of potency should find application in exploring the biological functions of TRH and PPII, and potentially provide a basis for development of novel therapeutics.

Key words: pyroglutamyl-peptidase II (PPII), pyroglutamyl-peptidase II inhibitor, thyrotropin-releasing hormone (TRH), thyrotropin-releasing hormone-degrading ectoenzyme (TRH-DE), thyrotropin-releasing hormone-degrading ectoenzyme inhibitor.

INTRODUCTION

Enzymic degradation plays an important role in the regulation of biologically active peptides [1]. Extracellularly oriented, membrane-associated peptidases (ectopeptidases), in particular, are strategically located to terminate peptide-mediated cell signalling [2,3]. It is apparent that a relatively small number of ectopeptidases with broad specificities provide a key mechanism for controlling the levels of a large number of peptides [4,5].

PPII (pyroglutamyl-peptidase II) (EC 3.4.19.6), also known as TRH (thyrotropin-releasing hormone)-degrading ectoenzyme, is a highly unusual ectopeptidase in that it appears to display absolute functional specificity for its substrate, TRH [or Glp-His-ProNH$_2$ (pyroglutamyl-histidyl-prolineamide)] [6–9]. Thus PPII catalyses the removal of Glp (pyroglutamic acid) from TRH, but it does not appear to be responsible for the inactivation of other naturally occurring peptides that contain a Glp residue at the N-terminus [7,8,10]. The exclusivity of the relationship between PPII and TRH is emphasized further by the observation that extracellular TRH seems to be degraded only by PPII [7,8,10].

Selective inhibition of ectopeptidases as a means to modulate peptide levels has proved to be useful for investigating the biological functions of many peptidergic systems [11,12]. In addition, inhibitors of a number of such enzymes have found significant medical application. Notable among these are inhibitors of angiotensin-converting enzyme, which are now widely employed to treat hypertension [13]. The actions of TRH in the CNS (central nervous system) are recognized to be potentially beneficial in the treatment of CNS disorders, including CNS trauma, spinocerebellar degeneration, epilepsy, memory loss, and disorders of consciousness and mood [14–24]. It is acknowledged, however, that the rapid inactivation of TRH by PPII critically impedes both research into the functions of TRH within the CNS and its clinical use [17–19]. Thus PPII inhibitors, like those of other ectoenzymes, could have valuable application as both experimental tools and therapeutic agents.

To date, there is no experimental structure for PPII on which to base the rational design of active-site-directed inhibitors. Sequence alignment indicates that PPII is a member of the M1 family of zinc metallopeptidases [25], which includes LTA$_4$H

Abbreviations used: AMC, 7-amino-4-methylcoumarin; APA, aminopeptidase A; APN, aminopeptidase N; Bzl, benzyl; CNS, central nervous system; Dab, α,γ-diaminobutanoic acid; DCC, 1,3-dicyclohexylcarbodi-imide; DCM, dichloromethane; DIPEA, *N,N*-di-isopropylethylamine; DMF, *N,N*-dimethylformamide; DPP-IV, dipeptidyl peptidase IV; eq., equivalent(s); Fmoc, fluoren-9-ylmethoxycarbonyl; Glp, pyroglutamic acid; Glp-Asn-ProNH$_2$, pyroglutamyl-asparaginyl-prolineamide; HBTU, 2-(1*H*-benzotriazole-1-yl)-1,1,3,3-tetramethyluronium hexafluorophosphate; HOBt, *N*-hydroxybenzotriazole; LHRH, luteinizing-hormone-releasing hormone; LTA$_4$H, leukotriene A$_4$ hydrolase; MBHA, 4-methylbenzylhydrylamine; Me, methyl; MOE, Molecular Operating Environment; PDB, Protein Data Bank; PPII, pyroglutamyl-peptidase II; SAR, structure–activity relationship; TFA, trifluoroacetic acid; TRH, thyrotropin-releasing hormone; TRH-AMC, pyroglutamyl-histidyl-prolyl-7-amido-4-methylcoumarin; Trt, trityl; TFA, trifluoroacetic acid.

[1] To whom correspondence should be addressed (email kellyja@tcd.ie).

© 2005 Biochemical Society

(leukotriene A_4 hydrolase) (EC 3.3.2.6), APA (aminopeptidase A) (EC 3.4.11.7) and APN (aminopeptidase N) (EC 3.4.11.2). By analogy with other metalloproteases, a hypothetical model of the active site of PPII has been derived from mutational analysis [26], but this provides insufficient detail for directing inhibitor design. The M1 family displays most sequence conservation in the region of the zinc-binding motif, and a model of the zinc-binding domain of APA has been constructed based on the crystal structure of LTA_4H [27].

Few PPII inhibitors have been identified [8,28]. Until recently, the most potent of these was CPHNA (*N*-[1-carboxy-2-phenylethyl]-*N*-imidazole benzyl histidyl-β-naphthylamide) with a K_i of 8 μM [28,29]. Through a kinetic study of PPII specificity, using a directed peptide library based on the structure of the endogenous ligand, TRH, we previously discovered two novel competitive PPII inhibitors: Glp-Asn-$ProNH_2$ ($K_i = 17.5$ μM) and Glp-Asn-Pro-AMC (where AMC is 7-amido-4-methylcoumarin) ($K_i = 0.97$ μM) [9]. Glp-Asn-Pro-AMC was the most potent PPII inhibitor then identified. Subsequent pilot studies indicated that well-defined central effects of TRH in rat could be enhanced by both intracerebroventricular and intraperitoneal administration of these inhibitors [30]. A recent paper has described the isolation of a PPII inhibitory activity from a marine invertebrate [31]. However, the type of inhibition has not been defined, its molecular structure is not yet known, and it is not certain that inhibition is due to a single chemical entity [31].

Our earlier study [9] showed that Glp-Asn-$ProNH_2$ was the only member of the tripeptide library with the structure Glp-Xaa-$ProNH_2$ to be resistant to hydrolysis and to bind to PPII with greater affinity than TRH. Furthermore, our results indicated that it might be possible to improve inhibitor potency by optimizing binding to what appeared to be a hydrophobic pocket in the area of PPII to which the C-terminus of PPII inhibitors bind, as seen by the lower K_i value for Glp-Asn-Pro-AMC as compared with that of Glp-Asn-$ProNH_2$. Although the hydrolytic activity of PPII appears to be restricted to tripeptides, tripeptide amides and tetrapeptides [9,32–35], the existence of an extended ligand-binding region close to the molecular recognition site for small peptides may also be suggested by the fact that LHRH (luteinizing-hormone-releasing hormone) binds to the enzyme with slightly higher affinity than does TRH [7,35]. TRH and LHRH share the same N-terminal dipeptide sequence, but LHRH is a decapeptide with the primary structure Glp-His-Trp-Ser-Tyr-Gly-Leu-Arg-Pro-$GlyNH_2$ and is not hydrolysed by PPII [7,32,35].

To probe further the binding capacity offered by the region in the vicinity of the S_2' binding site of PPII, we determined quantitative SARs (structure–activity relationships) for a series of structurally diverse carboxamide and C-terminally extended analogues of Glp-Asn-$ProNH_2$ by means of kinetic assays using PPII purified from porcine brain. Significantly, we have found that substantial improvement in potency can be achieved through C-terminal extension of Glp-Asn-$ProNH_2$. This has led to the development of a uniquely effective set of novel, competitive PPII inhibitors that are active at nanomolar levels, the best of which has a K_i value of 1 nM, thus making it the most potent PPII inhibitor to date. Furthermore, we explored the relative importance of particular functional groups within the structure of Glp-Asn-$ProNH_2$ for binding to PPII and inhibiting its activity. A putative binding mode for the inhibitors was also generated using a homology model for PPII based on LTA_4H. Data from these studies provide new insights into the SARs for molecular recognition and inhibition of PPII, as well as critical information for subsequent design of site-directed PPII inhibitors and possible drug development. Moreover, results of the present study show that such inhibitors of PPII enhance the recovery of TRH released from rat brain slices.

EXPERIMENTAL

Materials

All reagents were of analytical grade and were purchased from Sigma–Aldrich Chemical Company (Dublin, Ireland) unless stated otherwise.

Peptide synthesis and analysis

Peptides were synthesized using solution- and/or solid-phase methods and were purified, analysed and judged to be homogeneous by HPLC. HPLC analyses were conducted using a Thermo Separation Products Spectra System HPLC. In each case, products obtained by precipitation with diethyl ether, as described below, were purified using a semi-preparative C_{18} reverse-phase HPLC column (μBondaPak; Waters, Milford, MA, U.S.A.) and a linear gradient of 0–70 % B at a flow rate of 2.5 ml · min^{-1} [solvent A = 0.08 % TFA (trifluoroacetic acid) in water; solvent B = 40 % acetonitrile in 0.08 % TFA]. Peptide purity was confirmed by analytical HPLC analysis as described previously [9] and by MS.

Standard solid-phase Fmoc (fluoren-9-ylmethoxycarbonyl) chemistry was employed using the bubbler system under nitrogen gas [36]. Rink amide MBHA (4-methylbenzylhydrylamine) resin was used for the synthesis of peptide amide sequences, such as Glp-Asn-$AlaNH_2$ and Glp-Asn-$HomoProNH_2$. H-Pro-2-Cl Trt (where Trt is trityl) resin was used for the synthesis of peptides with a C-terminal carboxylic acid. These resins, as well as Fmoc amino acid derivatives and Glp, were purchased from Novabiochem (Merck Biosciences, Poole, Dorset, U.K.). All amino acids were in the L configuration. Tri-functional amino acids were purchased with side-chain-protecting groups as follows: Fmoc-Asp(OtBu)OH, Fmoc-Asn(Trt)OH, Fmoc-Dab(Boc)OH (where OtBu is t-butylester, Dab is α,γ-diaminobutanoic acid and Boc is *N*-α-t-butyloxycarbonyl).

Synthesis of peptide amides was carried out using Rink amide MBHA resin (loading capacity: 0.73 mmol · g^{-1}). This was swollen using DMF (*N*,*N*-dimethylformamide), deprotected with 20 % piperidine in DMF for 30 min and then washed with DMF. Each amino acid [3 eq. (equivalents), i.e. 3-fold excess over the resin-loading capacity] was coupled to the resin with HBTU [2-(1*H*-benzotriazole-1-yl)-1,1,3,3-tetramethyluronium hexafluorophosphate]/HOBt (*N*-hydroxybenzotriazole)/DIPEA (*N*,*N*-di-isopropylethylamine) (3:3:6, eq.) for 1 h. Removal of Fmoc was achieved with 20 % piperidine in DMF. On completion of peptide assembly, the resin was washed with DCM (dichloromethane), followed by methanol, and was allowed to dry overnight. The sequence was cleaved from the resin and was deprotected by stirring the dry resin in a TFA solution (95 %) containing water (2.5 %) and tri-isopropylsilane (2.5 %) (10 ml · g^{-1} dry resin) (by vol.) at room temperature (25 °C) for 2 h. The reaction mixture was filtered under vacuum, and the solvent was evaporated under reduced pressure. The residue was washed with petroleum ether and precipitated with diethyl ether.

Carboxamides of Glp-Asp-$ProNH_2$ were prepared by standard solution synthesis, coupling Glp-Asp-$ProNH_2$ (PolyPeptide Laboratories GmbH, Wolfenbuettel, Germany) to a series of amines: methylamine, dimethylamine, benzylamine, aniline, hydroxylamine and *O*-benzylhydroxylamine. HOBt (1.2 eq.) and DCC (1,3-dicyclohexylcarbodi-imide) (2.0 eq.) were added to a stirring solution of Glp-Asp-$ProNH_2$ (0.15 mmol) in DMF (560 μl, 0.26 M), followed by the required amine (1.2 eq.). The reaction mixture was stirred at room temperature for 24 h. The

© 2005 Biochemical Society

precipitate was filtered and washed with DCM. The solvent was evaporated under reduced pressure, and the residue was washed with petroleum ether and diethyl ether.

Carboxamides of Glp-Asn-Pro (American Peptide Company, Sunnyvale, CA, U.S.A.) were prepared by standard solution-phase coupling to the appropriate amine. All amines were purchased from Sigma–Aldrich, except for 1,3-benzodioxal-5-amine, 3-(trifluoromethyl)aniline, and 6-amino-1,3-dihydroisobenzofuran-1-one, which were supplied by Maybridge (Tintagel, Cornwall, U.K.). To a stirring solution of Glp-Asn-ProOH (0.15 mmol) in DMF (560 μl, 0.26 M), HOBt (1.0 eq.) and DCC (1.0 eq.) were added, followed by the required amine (1.2 eq.). The reaction mixture was stirred at room temperature for 24 h and filtered, and the solvent was evaporated under reduced pressure. The residue was washed successively with small volumes of ethyl acetate, petroleum ether and diethyl ether.

Benzyl and methyl esters of Glp-Asn-Pro were prepared by first synthesizing the tripeptide acid on solid phase using H-Pro-2-Cl Trt resin (loading capacity: 0.7 mmol $\cdot$ g^{-1}). This was swollen using DCM and washed with DMF. Each amino acid (3 eq.) was coupled on to the resin with HBTU/DIPEA (3:6 eq.) at each step. The reaction time for each step was 1 h. Deprotection, cleavage from the resin and precipitation of the product were carried out as described above. To a stirring solution of Glp-Asn-ProOH (0.1 mmol) in DMF (560 μl, 0.5 M), DMAP (4-dimethylaminopyridine) (30 %) and DCC (1.2 eq.) were added, followed by benzyl alcohol (1.2 eq.). The reaction mixture was stirred at room temperature for 16 h. The precipitate was filtered and washed with DCM, and the solvent was evaporated under reduced pressure. The residue was washed with petroleum ether and diethyl ether. The methyl ester was prepared similarly, except that methanol (400 μl) was used as both solvent and reagent.

Glp-Asn-ProNH$_2$, Glp-Asn-Pro-TyrNH$_2$, Glp-Asn-Pro-Trp-Ser-TyrNH$_2$, Glp-Asn-Pro-Trp-TyrNH$_2$, Glp-Asn-Pro-TrpNH$_2$, Glp-Asn-Pro-Tyr-TrpNH$_2$, Glp-Asn-Pro-Tyr-Trp-TrpNH$_2$, Glp-Asn-Pro-AMC Glp-Asn-Pro-Trp-AMC, Glp-Asn-Pro-Trp-Trp-AMC, Glp-Asn-Pro-Tyr-Trp-AMC and Glp-Asn-Pro-Tyr-Trp-Trp-Trp-AMC were custom synthesized either by the American Peptide Company or by PolyPeptide Laboratories GmbH. Glp-βAsn-ProNH$_2$ and Glp-Asn-GlyNH$_2$ were supplied by PolyPeptide Laboratories GmbH. TRH and TRH-AMC were purchased from Sigma–Aldrich and Bachem U.K., St. Helens, U.K. respectively. The homogeneity and identity of each peptide was confirmed by HPLC and mass spectral analysis. All peptides were stored at -20 °C.

Enzyme assays

All enzyme assays were carried out at 37 °C in 20 mM potassium phosphate buffer, pH 7.5. One kat of enzyme activity was defined as that amount of enzyme that catalyses the conversion of 1 mol of substrate per s. As described previously, PPII activity was measured by HPLC and fluorometric assays using enzyme purified from porcine brain [9,37]. The PPII preparation had a protein concentration of 0.8 mg $\cdot$ ml^{-1} and a specific activity of 2.8×10^{-3} μkat $\cdot$ mg^{-1} with TRH-AMC (5 μM) as substrate, while the DPP-IV (dipeptidyl peptidase IV) (EC 3.4.14.5) preparation had a protein concentration of 7.7 mg $\cdot$ ml^{-1} and a specific activity of 0.29 μkat $\cdot$ mg^{-1} with Gly-Pro-AMC (100 μM) as substrate [9]. The final concentration of PPII in the assay was 0.53 μg $\cdot$ ml^{-1}. Compounds were judged to be resistant to hydrolysis by PPII if no Glp was detected in the HPLC assay following the incubation of 1 mM compound for 18 h with PPII (0.08 μg) in a total assay volume of 1 ml. Under these conditions, TRH (1 mM) was completely degraded to yield Glp and His-Pro

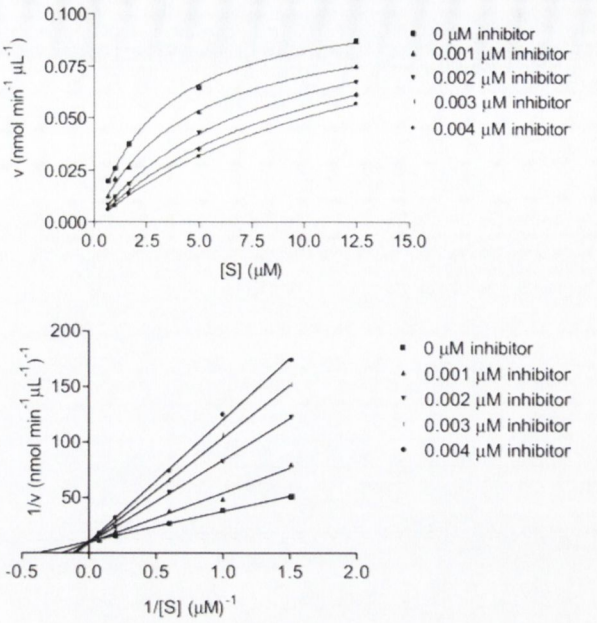

Figure 1 Inhibition of PPII hydrolysis of TRH-AMC by Glp-Asn-Pro-Tyr-Trp-Trp-AMC

Initial rates were determined using the continuous fluorometric assay. Initial rates against substrate concentration for increasing inhibitor concentration were fitted to a rectangular hyperbola (Michaelis–Menten plot) by non-linear regression analysis as shown in the upper graph. All kinetic parameters stated in the text were determined by non-linear regression analysis of data using the computer program Prism (GraphPad Software). Linear regression analysis was used to fit data to a Lineweaver–Burk plot to illustrate the type of inhibition observed. The results shown for Glp-Asn-Pro-Tyr-Trp-Trp-AMC in the lower graph are typical for all compounds with the sequence Glp-Asn-Pro-Xaa, thus far tested. The goodness of fit (r^2) for both non-linear and linear regression analysis plots was > 0.95. All V_{max} values fell within the confidence intervals of the intercept obtained from linear regression analysis, and the slope of a plot of V_{max} versus inhibitor concentration (not shown) was not found to deviate significantly from 0, supporting the interpretation that Glp-Asn-Pro-Tyr-Trp-Trp-AMC is acting as a classical competitive inhibitor of PPII.

diketopiperazine. Kinetic parameters for compounds that were not hydrolysed by PPII were determined using a continuous coupled fluorometric assay, whereas those for PPII substrates were determined using a discontinuous fluorometric assay [9,37]. All the sequences Glp-Asn-Pro-Xaa tested, thus far, behaved as linear competitive inhibitors as indicated by the constancy of V_{max} with changing inhibitor concentration (see [9] and Figure 1). Inhibitory potency of all compounds was therefore calculated by using an appropriate equation i.e. $v_i/v_o = [I]/\{[I] + K_i(1 + [S]/K_m)\}$, where v_i and v_o are the initial rates measured in the presence and absence of inhibitor respectively, K_m is the Michaelis constant, K_i is the inhibitor constant, and [I] and [S] are the inhibitor and substrate concentrations respectively. Initial rates for the hydrolysis of TRH-AMC (5 μM) by PPII were determined in triplicate in the presence and absence of each compound, as described previously [9]. Compounds selected as being of high potency were studied in more detail by non-linear regression analysis of initial-rate data collected in duplicate at five different substrate concentrations and four different concentrations of peptide. The reversibility and time-dependence of inhibition produced by Glp-Asn-Pro-Tyr-Trp-Trp-AMC was examined as described previously [9].

Compounds identified as PPII inhibitors were tested for their ability to inhibit the activity of DPP-IV, the coupling enzyme in the continuous fluorometric assay for PPII. DPP-IV activity was determined directly using a continuous assay employing Gly-Pro-AMC as the substrate, as described previously [9]. None

© 2005 Biochemical Society

of these peptides were found to inhibit DPP-IV activity in this assay, confirming that reduction of AMC production in the continuous coupled assay for PPII was due to inhibition of PPII.

Evaluation of PPII inhibitors in brain slices

Glp-Asn-Pro-AMC and Glp-Asn-Pro-Tyr-Trp-Trp-AMC were tested for their ability to protect endogenous TRH from degradation in hypothalamic slices. Hypothalami were rapidly dissected from male Wistar rats (200–250 g), following decapitation, and slices (300 μm × 300 μm) were cut with a McIlwain tissue chopper. Each incubation contained slices from the hypothalamus of one animal. Slices were initially incubated in a flat-bottomed plastic tube in 0.5 ml Ca^{2+}-free Krebs buffer gassed with 95 % O_2/5 % CO_2 for 10 min in a shaking water bath at 37 °C. In turn, the Ca^{2+}-free buffer was replaced by Krebs buffer containing Ca^{2+} (2.5 mM), and the incubation was continued for a further 10 min. The tubes were then centrifuged at 2000 ***g*** for 10 min. The resulting supernatant was removed and taken to denote 'basal' release. Subsequently, the tissue was incubated at 37 °C for 10 min in buffer containing Ca^{2+} (2.5 mM) and KCl (50 mM), and the supernatant arising from this incubation was taken to represent 'stimulated' release. PPII inhibitor at a final concentration of 0.1 mM or vehicle (1 μl saline or DMSO) was present throughout the last two incubations. Supernatant samples were frozen at − 80 °C until analysis for TRH content by RIA [38].

Modelling of PPII

The lack of availability of a three-dimensional structure for PPII led us to construct a theoretical homology model of its active site in an attempt to gain further insight into the possible binding modes and mechanism of the inhibitors. PPII shares greatest sequence homology with APA and APN, but there is no crystal structure for either of these enzymes. The crystal structure of LTA_4H, however, has been elucidated [39]. This metalloprotease exhibits approx. 30 % overall sequence identity with residues 130–753 in PPII. The HEXXH zinc-binding motif and active site of these two enzymes are highly conserved, with 51 % sequence identity in the region across residues 436–470 of PPII. The crystal structure of human LTA_4H [PDB (Protein Data Bank) code 1HS6; http://www.rcsb.org] [39] was thus used as a template to construct a homology model of human PPII.

The LTA_4H crystal structure 1HS6 was downloaded from the PDB and was read into MOE (Molecular Operating Environment) (Chemical Computing Group), and the sequence was extracted. Subsequently, the 1024-amino-acid sequence for human PPII was read into MOE, and the sequences were aligned using the alignment tools of the homology module. The resulting automated sequence alignment was checked to ensure correct alignment of catalytic core histidine residues within the HEXXH zinc-binding motif, and pre-and post-template non-matched outgap residues were deleted to facilitate construction of a structural model for 624 residues of the PPII query. Co-ordinates were assigned using those residues conserved between both sequences, with 1HS6 serving as a structural template for the procedure. Fine-energy minimization [RMSD (root mean square deviation) 0.0005 Å (1 Å = 0.1 nm)] using the MOE implementation of the AMBER94 force field [40] was utilized for model generation and structure optimization. All zinc-binding residues were constrained during model construction and during the minimization protocol. A total of 300 intermediate models were generated and scored, and the highest scoring final solution (based on packing scores) was utilized in subsequent investigations. Hydrogens were added, assuming a pH of 7.4 and standard amino acid pK_a values. Structures were written out in mol2 format and read into Sybyl 6.91 (Tripos), using the appropriate metal parameters for the treatment of the zinc heteroatom in subsequent modelling.

Table 1 Effects of modifying the amide nitrogen of the asparaginyl side chain and the proline residue in Glp-Asn-ProNH_2 on the interactions with PPII

The ability of each compound to be hydrolysed by PPII was assessed using HPLC. Initial rates were measured in triplicate in the presence (v_i) and absence (v_0) of inhibitor (I) using the continuous fluorometric assay with TRH-AMC (5 μM) as substrate (S). K_i values were calculated from initial rates using the relationship $v_i/v_0 = [I]/\{[I] + K_i(1 + [S]/K_m)\}$. Each value represents the mean ± S.D. [$n = 3$, except when indicated by an asterisk (*), where $n = 11$].

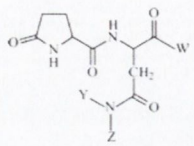

Y	Z	W	K_i (μM)	Hydrolysed
H	H	ProNH_2	16.1 ± 1.6*	−
H	H	HomoProNH_2	19.3 ± 0.8	−
Benzyl	H	ProNH_2	99.6 ± 8.0	+
Hydroxyl	H	ProNH_2	115 ± 11	−
Phenyl	H	ProNH_2	133 ± 20	−
Methyl	H	ProNH_2	103 ± 13	+
Benzyloxy	H	ProNH_2	> 200	−
Methyl	Methyl	ProNH_2	> 200	−
H	H	AlaNH_2	> 200	−
H	H	GlyNH_2	No inhibition	−
H	H	AsnNH_2	No inhibition	−
H	H	TrpNH_2	50 ± 4	−
H	H	ProOH	No inhibition	−

To better understand the SARs observed for the compounds, as well as the determinants of molecular recognition by PPII, computational docking studies were undertaken. Docking was carried out using the FlexX utility as implemented in Sybyl 6.91 [41]. A binding subsite of radius 10 Å from the zinc atom was described, and the zinc atom was explicitly included in the active site consideration. FlexX was run using default settings to obtain up to 100 binding modes for each inhibitor ligand screened, and 300 solutions for the TRH substrate, each ranked by drug score [42]. The top 20 solutions for each ligand were imported, visualized in MOE and common binding modes were identified manually.

Using FlexX with metal parameters assigned for zinc, each of Glp-Asn-ProNH_2, Glp-Asn-Pro-AMC and Glp-Asn-Pro-Tyr-Trp-AMC were docked, resulting in up to 100 ranked poses for each ligand examined. FlexX has previously demonstrated its utility in the simulation of metalloprotease ligand docking [43]. Each set of resultant docked poses was examined to identify conserved binding modes, and a representative of each 'distinct' binding mode was retained. The distinct binding modes identified for each individual ligand were compared with those of every other ligand, and a conserved binding mode for the Glp-Asn-Pro region in all active compounds emerged. A similar docking protocol was employed for the substrate, TRH, in which 300 docked poses were examined, revealing a clear conserved ligand-docked orientation within the model active site.

RESULTS

Effects of modifications to the amide side chain of asparagine and C-terminal proline on binding and inhibition

The results presented in Table 1 show that chemical alterations to the amide nitrogen of the asparagine side chain in

© 2005 Biochemical Society

Glp-Asn-ProNH$_2$ have a significant effect on binding affinity and the susceptibility of the Glp-Xaa peptide bond to hydrolysis. Replacement of one of the amide hydrogen atoms with an aliphatic, aromatic or hydroxy group can be seen to reduce binding affinity considerably. A further decrease in inhibitory potency was caused by dimethylation of the amide nitrogen. Binding was abolished by replacing asparagine with either βAsn or Dab. HPLC analysis revealed that Glp-Asn(*N*-benzyl)-ProNH$_2$ and Glp-Asn(*N*-methyl)-ProNH$_2$ were hydrolysed by PPII, although the rates of hydrolysis for these compounds, as measured by Glp formation, were considerably lower (5.7- and 15.1-fold respectively) than that for TRH, each under essentially saturating conditions. It can be seen from Table 1 that deamidation of the C-terminal proline residue in Glp-Asn-ProNH$_2$ resulted in a loss of inhibition. Elimination of a C-terminal ring through replacing the proline residue with alanine or glycine led to a reduction and loss of inhibition respectively, whereas replacement of the proline residue with tryptophan and expansion of the proline ring did not significantly alter potency.

Kinetic analysis of a series of carboxamide analogues of Glp-Asn-ProNH$_2$

Earlier studies showed that replacement of the C-terminal amino group of Glp-Asn-ProNH$_2$ by AMC resulted in a > 10-fold enhancement of binding affinity to PPII, thus indicating the possible existence of a binding region for hydrophobic moieties in the vicinity of the S_2' subsite on the enzyme. In order to investigate further the enzyme–ligand binding interactions in this region, we synthesized a diverse series of carboxamide analogues of Glp-Asn-ProNH$_2$, containing both unsubstituted and substituted aromatic rings (Table 2). There was no detectable hydrolysis of any of these compounds by PPII, as indicated by absence of Glp formation in the discontinuous HPLC assay. Overall, members of this series did not show wide variations in inhibitory potency, with K_i values generally in the range 1–20 μM (Table 2). Although all of the carboxamides of Glp-Asn-Pro tested exhibited greater affinity for PPII than TRH itself, none had a K_i value less than that of Glp-Asn-Pro-AMC.

Kinetic properties of C-terminally extended analogues of Glp-Asn-ProNH$_2$

The kinetic properties of a set of analogues of Glp-Asn-ProNH$_2$ extended at the C-terminus were analysed to provide information regarding binding capacity and recognition elements distal to the active site. None of the C-terminally extended analogues were PPII substrates. It can be seen from the data presented in Table 3 that C-terminal extension of Glp-Asn-Pro with hydrophobic amino acids resulted in substantial increases in binding affinity. The most potent inhibitor of this set, Glp-Asn-Pro-Tyr-Trp-Trp-AMC, displayed an approx. 500-fold increase in affinity, as measured by its K_i value, compared with Glp-Asn-Pro-AMC (Table 3), which hitherto had been the most potent competitive PPII inhibitor reported. Inhibition by Glp-Asn-Pro-AMC and Glp-Asn-Pro-NH$_2$ was shown previously to be competitive and fully reversible [9]. In the present study, non-linear regression analysis of kinetic data indicated that Glp-Asn-Pro-Tyr-Trp-Trp-AMC and Glp-Asn-Pro-Tyr-Trp-AMC were also classical competitive inhibitors of PPII; data for Glp-Asn-Pro-Tyr-Trp-Trp-AMC are shown in Figure 1. Inhibition by Glp-Asn-Pro-Tyr-Trp-Trp-AMC was found to be fully reversible and not time-dependent.

Effects of PPII inhibitors on the recovery of TRH released from hypothalamic slices

It can be seen from Figure 2 that the recovery of TRH released from rat brain slices under basal and depolarizing conditions

Table 2 Inhibitory effects of compounds in which Glp-Asn-Pro is coupled to an amine or alcohol

HPLC analysis revealed that none of these compounds were PPII substrates. The ability of compounds to inhibit PPII purified from porcine brain was screened using the continuous fluorometric assay with TRH-AMC (5 μM) as substrate. K_i values were calculated from determinations of initial rates in the absence and presence of inhibitor. Results are means ± S.D. ($n = 3$).

Compound	K_i (μM)
Amine	
AMC	0.47 ± 0.05
5-Aminoindan	0.84 ± 0.08
3,5-Dimethoxyaniline	0.85 ± 0.13
4-(Trifluoromethyl)aniline	0.97 ± 0.18
1,3-Benzodioxol-5-amine	1.24 ± 0.07
3-(Trifluoromethoxy)aniline	1.25 ± 0.13
m-Anisidine	1.27 ± 0.06
5-Amino-2-chloropyridine	1.63 ± 0.16
m-Phenetidine	1.67 ± 0.14
6-Amino-3,4-benzocoumarin	1.90 ± 0.40
5-Amino-2-methoxyphenol	2.54 ± 0.00
6-Amino-1,3-dihydroisobenzofuran-1-one	2.78 ± 0.37
Aniline	2.80 ± 0.22
3,4-Dimethoxyaniline	3.18 ± 0.07
4-Phenylbutylamine	3.45 ± 0.58
6-Amino-2-mercaptobenzothiazole	3.62 ± 0.12
2-Phenylethylamine	3.98 ± 0.28
p-Anisidine	4.07 ± 0.02
3-Phenyl-1-propylamine	4.89 ± 0.69
2-Hydroxyaniline	7.42 ± 0.27
4-Amino-*N*-methylphthalamide	8.90 ± 0.56
5,6,7,8-Tetrahydro-1-naphthylamine	10.14 ± 0.00
Methylamine	10.84 ± 1.94
5-Chloro-2-methoxyaniline	10.85 ± 0.03
o-Anisidine	12.63 ± 0.76
Benzylamine	12.81 ± 0.76
2-Aminobenzyl alcohol	21.87 ± 0.62
Dimethylamine	> 200
Piperidine	> 200
Alcohol	
Benzyl alcohol	15.29 ± 0.43
Methyl alcohol	84.16 ± 1.46

Table 3 Inhibition of PPII by C-terminally extended analogues of Glp-Asn-ProNH$_2$

HPLC analysis indicated that all of the compounds were resistant to PPII hydrolysis. K_i values were calculated either from initial rates measured in the absence and presence of inhibitor, using the continuous fluorometric assay with TRH-AMC (5 μM) as substrate, or by non-linear regression analysis of initial-rate data collected in duplicate at five different substrate concentrations and four different concentrations of peptide. Results are means ± S.D. [$n = 3$, except when indicated by an asterisk (*), where $n = 11$, or by a dagger (†), where $n = 4$].

Peptide							
P_1	P_1'	P_2'	P_3'	P_4'	P_5'	P_6'	K_i (μM)
Glp	Asn	Pro	Tyr	Trp	Trp	AMC	0.001 ± 0.000†
Glp	Asn	Pro	Tyr	Trp	AMC		0.038 ± 0.006†
Glp	Asn	Pro	Trp	Trp	AMC		0.072 ± 0.009
Glp	Asn	Pro	Trp	AMC			0.083 ± 0.016
Glp	Asn	Pro	AMC				0.458 ± 0.057*
Glp	Asn	Pro	Tyr	TrpNH$_2$			0.639 ± 0.018
Glp	Asn	Pro	Tyr	Trp	TrpNH$_2$		0.734 ± 0.073
Glp	Asn	Pro	TrpNH$_2$				5.17 ± 0.20
Glp	Asn	Pro	Trp	TyrNH$_2$			5.91 ± 0.85
Glp	Asn	Pro	Trp	Ser	TyrNH$_2$		8.11 ± 0.55
Glp	Asn	Pro	TyrNH$_2$				10.3 ± 0.55
Glp	Asn	ProNH$_2$					16.1 ± 1.6*

© 2005 Biochemical Society

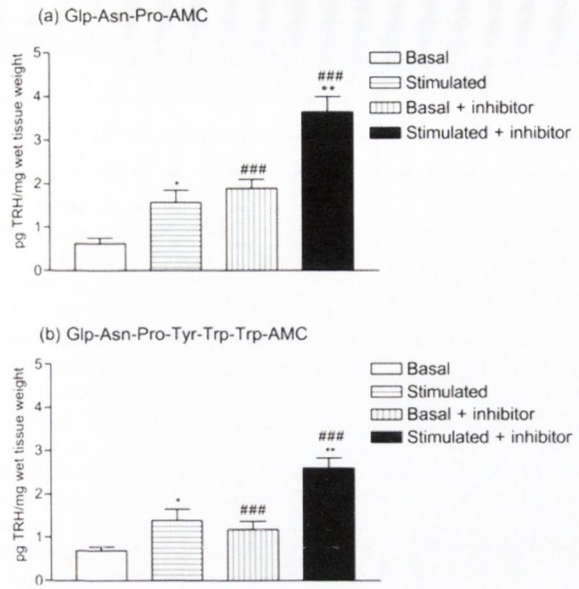

Figure 2 Effects of (a) Glp-Asn-Pro-AMC and (b) Glp-Asn-Pro-Tyr-Trp-Trp-AMC on the release of TRH from rat brain hypothalamic slices

TRH release was measured under basal and depolarizing conditions in the presence of vehicle (saline or DMSO) or (**a**) Glp-Asn-Pro-AMC (0.1 mM in saline) or (**b**) Glp-Asn-Pro-Tyr-Trp-Trp-AMC (0.1 mM in DMSO). Results are means ± S.E.M. ($n = 6$). $^{*}P < 0.05$; $^{**}P < 0.01$ compared with corresponding basal; $^{###}P < 0.001$ compared with corresponding conditions in the absence of inhibitor (Student's t test).

was increased significantly in the presence of Glp-Asn-Pro-AMC or Glp-Asn-Pro-Tyr-Trp-Trp-AMC ($P < 0.001$, $n = 6$; Student's t test).

Model of PPII

Figure 3 illustrates the active site in the homology model of human PPII and highlights the common binding mode observed for the inhibitors (illustrated by Glp-Asn-Pro-NH_2, green) and predicted docked pose for the substrate (TRH, yellow). The orientation of the Glp-Asn-Pro portion for all our docked active species is conserved in this model. In each, asparagine was found to be oriented so as to facilitate direct hydrogen bonding to Glu^{407}. The significance of bound water in molecular design is sometimes underestimated; however, recent work has highlighted the utility of its consideration in mechanistic explanations [44]. When the location of a catalytic water molecule is considered in the homology model of PPII (its location derived from the works of Rozenfeld et al. [27], Thunnissen et al. [39] and Rudberg et al. [45]), a hydrogen-bonding network involving asparagine, water, Glu^{407} and Glu^{441} is predicted. Comparison of the positioning of the inhibitor Glp-Asn-Pro motif within the active site to that of the substrate, TRH, shows that (i) the orientation of the recognition residue, Glp, is conserved and (ii) the pendant His in TRH projects into the region occupied by asparagine in the inhibitors.

DISCUSSION

Our previous observation that replacement of the central histidine in TRH with asparagine produces an analogue that inhibits PPII activity [9] provided a starting point for the present studies. To gain a greater understanding of the structural parameters that influence ligand binding and inhibition, as well as to explore the potential for improving inhibitory potency, we have now investigated the effects of structural modifications to Glp-Asn-ProNH_2 on the kinetics of PPII activity.

The results show that the presence of the amide side chain of asparagine in the P_1' position confers resistance to hydrolysis by PPII and appears to be critical for inhibitory binding interactions. Asparagine can be regarded as an isostere of histidine [46]; its side chain, however, occupies less space and offers different possibilities for the formation of inter- and/or intra-molecular hydrogen bonds than the imidazole ring of histidine. These differences may account for the inhibitory characteristics of P_1' asparagine. Notably, all modifications to the asparagine side chain that were

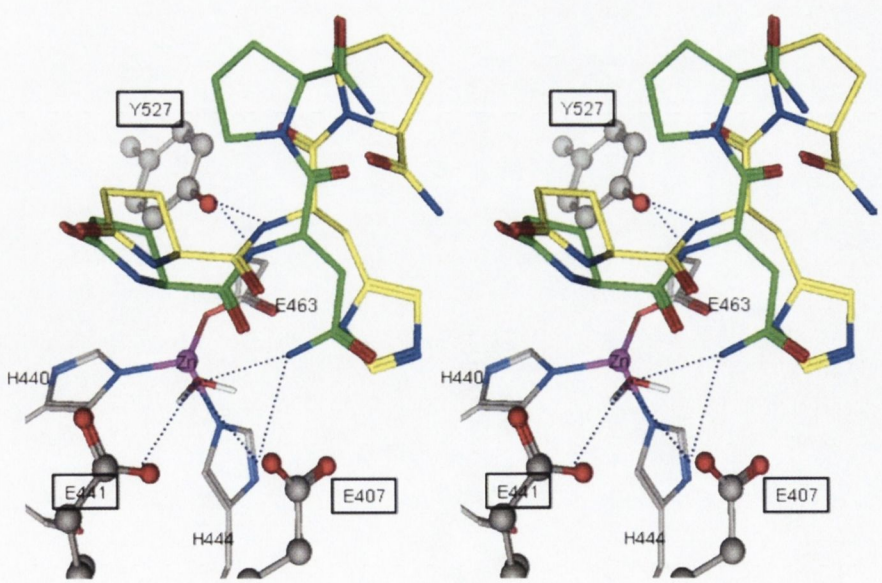

Figure 3 Predicted conserved binding mode for Glp-Asn-Pro inhibitory motif (green), compared with that obtained for TRH (yellow)

The Figure shows the active-site zinc (pink) and key active-site residues of human PPII (labelled in black). Broken lines highlight possible hydrogen-bond interactions that arise in inhibitory peptides that contain a P_1' asparagine residue. Such interactions are not indicated for the substrate, TRH, and suggest a possible mechanism of action for the inhibitor series shown in the present study.

© 2005 Biochemical Society

examined led to marked reduction in inhibitory potency. Thus any change to the amide group of asparagine is deleterious to inhibitory properties. Indeed, all the modifications reduced the capability to form hydrogen bonding, reinforcing the idea that participation in such bonding by the asparagine side chain may be crucial for inhibition. Consistent with this, the model shown in Figure 3 predicts that the asparagine side chain participates in a hydrogen-bonding network, involving Glu^{407} and Glu^{441}, thus appropriating these two residues, which have been shown previously, by site-directed mutagenesis, to be important for the catalytic activity of rat PPII [26]. The amino acid sequences for human and rat PPII display a remarkably high degree of conservation (96 % identical residues), but they differ in length by one amino acid [47]. Thus, when comparing human and rat PPII, it should be noted that residues Glu^{407}, Glu^{441} and Tyr^{527} of human PPII correspond to Glu^{408}, Glu^{442} and Tyr^{528} respectively of rat PPII. The model places the recognition residue (Glp) of both substrate and inhibitor in close proximity and in a similar orientation within the active site of PPII. Binding modes predicted for both TRH and the inhibitors by this model agree with the general model for aminopeptidase activity put forward by Rudberg et al. [45] and includes a predicted interaction of Tyr^{527} with the N of the scissile peptide bond. A key difference between TRH and the inhibitors, however, is the ability of the asparagine-containing peptides to participate in the hydrogen-bonding network noted above.

The C-terminal prolineamide of Glp-Asn-ProNH_2 is important, but not crucial, for binding to the S_2' subsite on PPII. Thus deamidation or replacement of the C-terminal ProNH_2 with amides of glycine, alanine or asparagine causes a loss or substantial reduction of inhibition. The enzyme, nevertheless, does appear to be tolerant to replacement of proline with tryptophan and the expanded (six-membered) ring of homoprolineamide. The complete loss of inhibition observed for Glp-Asn-ProOH mirrors the poor affinity displayed by the TRH analogue Glp-His-ProOH [9]. It seems that this is most likely to be due to the negative charge at the C-terminus being unfavourable. Comparison of K_i values for Glp-Asn-ProNHBzl (where Bzl is benzyl), Glp-Asn-ProOBzl, Glp-Asn-ProNHMe (where Me is methyl) and Glp-Asn-ProOMe indicates aromaticity and/or hydrogen bonding to be important for binding to the enzyme. This is supported by the observation that Glp-Asn-Pro-piperidide and Glp-Asn-Pro-dimethylamide, where the C-terminal groups do not possess such properties, are poor PPII inhibitors. Exploration of this region using Glp-Asn-ProNHY (where Y is a substituted aryl group) reinforced the importance of an aromatic substituent, since all of these compounds showed good inhibitory potency, with a slight preference for oxygen-containing substituents in the meta position. Consistent with this, AMC, which has an oxygen meta to its amino group, was the most favourable C-terminal group of those tested.

The advantage conferred by aromatic substitution at the C-terminus with respect to inhibitory potency was exemplified further by the C-terminal extension of Glp-Asn-ProNH_2 with aromatic amino acids. These elongations can be regarded as probes for additional hydrophobic binding interactions with the target enzyme. The results suggest that such interactions do occur. The most potent inhibitor identified in this set, Glp-Asn-Pro-Tyr-Trp-Trp-AMC, was approx. 16000 and 500 times more potent than Glp-Asn-ProNH_2 and Glp-Asn-Pro-AMC respectively, making it the most potent competitive PPII inhibitor thus far reported.

The increased potency of the extended analogues may simply reflect additional sites of interactions with the PPII molecule. It is possible, though, that they may also affect local conformational changes in the enzyme necessary for catalysis. Members of the MA (E) clan of metalloproteases (zinc metalloproteases in which zinc is ligated to two histidine residues and a glutamate residue, see http://merops.sanger.ac.uk), which includes thermolysin (EC 3.4.24.27), share similar structural and catalytic features with PPII, although the specific details of their catalytic mechanisms may differ [48]. A conformational change on substrate binding, resulting in transition from an open to a closed conformation, has been shown to be necessary for thermolysin to catalyse substrate hydrolysis [49]. If that were also the case for PPII, the effectiveness of the more bulky analogues as inhibitors may result from their preventing this closure. This might also account for the inhibitory activity displayed by LHRH. Modifications to the surface charge of the enzyme [50], as a result of inhibitor binding, may also affect affinity.

The increased recovery of TRH released from brain slices observed in the presence of PPII inhibitors, agrees with the findings of Charli et al. [29] and provides further support for the critical involvement of PPII in the metabolism of neuronally released TRH. Importantly, these results also indicate that the asparagine-containing PPII inhibitors tested are capable of increasing TRH levels in a more physiologically intact environment.

In conclusion, these SAR studies have revealed that, despite PPII having very high substrate specificity for tri- and tetrapeptides, there appears to be an extended binding region contiguous with the active site. The results also demonstrate that it is possible to exploit this in the design of highly potent inhibitors. The SAR for inhibition may be summarized as follows: (i) the N-terminal Glp confers specificity for PPII [10], as well as resistance to hydrolysis by aminopeptidases [1,5]; (ii) the presence of asparagine in position 2 combines resistance to hydrolysis with effective inhibition of the enzyme; (iii) the prolineamide is important for interaction with the S_2' subsite on PPII, but the enzyme appears to be tolerant to a variety of modifications to the C-terminal carboxy function; and (iv) hydrophobic extensions to Glp-Asn-ProNH_2 can produce substantial improvement in inhibitory potency. Notably, the data presented provide critical information for the design of PPII inhibitors, which should be of value as tools for studying the biological functions of TRH and PPII and may provide a basis for the development of new therapeutic agents.

This work was supported by a grant from the Wellcome Trust to J. A. K. G. A. S. and A. A. C. were supported by a grant from the Health Research Board, Ireland. D. G. L. acknowledges the Irish Higher Education Authority's PRTLI (Programme for Research in Third Level Institutions) IITAC (Institute for Information Technology and Advanced Computation) programme for computational infrastructure support.

REFERENCES

1 Griffiths, E. C. and Kelly, J. A. (1979) Mechanisms of inactivation of hypothalamic regulatory hormones. Mol. Cell. Endocrinol. **14**, 3–17
2 Kenny, A. J. and Turner, T. (1987) What are ectoenzymes? In Mammalian Ectoenzymes (Kenny, A.J. and Turner, T., eds.), pp. 1–13, Elsevier Science Publishers, New York
3 O'Cuinn, G., O'Connor, B., Gilmartin, L. and Smyth, M. (1995) Neuropeptide inactivation by peptidases. In Metabolism of Brain Peptides (O'Cuinn, G., ed.), pp. 99–157, CRC Press, Boca Raton
4 Konkoy, C. S. and Davis, T. P. (1996) Ectoenzymes as sites of peptide regulation. Trends Pharmacol. Sci. **17**, 288–294
5 Turner, A. J. (1997) Neuropeptide inactivation in the CNS. In Cell-Surface Peptidases in Health and Disease (Kenny, A. J. and Boustead, C. M., eds.), pp. 275–310, BIOS Scientific Publishers, Oxford
6 Charli, J. L., Cruz, C., Vargas, M. A. and Joseph-Bravo, P. (1988) The narrow specificity pyroglutamate aminopeptidase degrading TRH in rat brain is an ectoenzyme. Neurochem. Int. **13**, 237–242
7 O'Cuinn, G., O'Connor, B. and Elmore, M. (1990) Degradation of thyrotropin-releasing hormone-degrading ectoenzyme and luteinising hormone-releasing hormone by enzymes of brain tissue. J. Neurochem. **54**, 1–13

© 2005 Biochemical Society

8 Bauer, K., Heuer, H., Ifflander, F., Peters, A., Schmitmeier, S., Shomburg, L., Turwitt, S. and Wilkins, M. (1997) Inactivation of thyrotropin-releasing hormone (TRH) by a TRH-specific ectoenzyme. In Cell-Surface Peptidases in Health and Disease (Kenny, A. J. and Boustead, C. M., eds.), pp. 239–248, BIOS Scientific Publishers, Oxford

9 Kelly, J. A., Slator, G. R., Tipton, K. F., Williams, C. H. and Bauer, K. (2000) Kinetic investigation of the specificity of porcine brain thyrotropin-releasing hormone-degrading ectoenzyme for thyrotropin-releasing hormone-like peptides. J. Biol. Chem. **275**, 16746–16751

10 Cummins, P. M. and O'Connor, B. (1998) Pyroglutamyl peptidase: an overview of the three known enzymatic forms. Biochim. Biophys. Acta **1429**, 1–17

11 Beaumont, A., Fournié-Zaluski, M.-C., Noble, F., Maldonado, R. and Roques, B. P. (1997) The chemistry and pharmacology of cell-surface peptidase inhibitors. In Cell-Surface Peptidases in Health and Disease (Kenny, A. J. and Boustead, C. M., eds.), pp. 59–78, BIOS Scientific Publishers, Oxford, U.K.

12 Roques, B. P. (2000) Novel approaches to targeting neuropeptide systems. Trends Pharmacol. Sci. **21**, 475–483

13 Cushman, D. W. and Ondetti, M. A. (1999) Design of angiotensin converting enzyme inhibitors. Nat. Med. **5**, 1110–1112

14 Horita, A., Carino, M. A. and Lai, H. (1986) Pharmacology of thyrotropin-releasing hormone. Annu. Rev. Pharmacol. Toxicol. **26**, 311–332

15 Faden, A. I. and Salzman, S. (1992) Pharmacological strategies in CNS trauma. Trends Pharmacol. Sci. **13**, 29–35

16 Horita, A. (1998) An update on the CNS actions of TRH and its analogs. Life Sci. **62**, 1443–1448

17 Kelly, J. A. (1995) Thyrotropin-releasing hormone: basis and potential for its therapeutic use. Essays Biochem. **30**, 133–149

18 Mason, G., Garbutt, J. and Prange, A. J. (1995) Thyrotropin-releasing hormone: focus on basic neurobiology. In Psychopharmacology: the Fourth Generation of Progress (Bloom, F. E. and Kupfer, D. J., eds.), pp. 495–503, Raven Press, New York

19 Nillni, E. A. and Sevarino, K. A. (1999) The biology of pro-thyrotropin-releasing hormone-derived peptides. Endocr. Rev. **20**, 599–648

20 Vetulani, J. and Nalepa, I. (2000) Antidepressants: past, present and future. Eur. J. Pharmacol. **405**, 351–363

21 Sharma, R. P., Martis, B., Rosen, C., Jonalagadda, J., Nemeroff, C. B. and Bissette, G. (2001) CSF thyrotropin-releasing hormone concentrations differ in patients with schizoaffective disorder from patients with schizophrenia or mood disorders. J. Psychiatr. Res. **35**, 287–291

22 Sattin, A., Senanayake, S. S. and Pekary, A. E. (2002) Lithium modulates expression of TRH receptors and TRH-related peptides in rat brain. Neuroscience **115**, 263–273

23 Kubek, M. J. and Garg, B. P. (2002) Thyrotropin-releasing hormone in the treatment of intractable epilepsy. Pediatr. Neurol. **26**, 9–17

24 Gary, K. A., Sevarino, K. A., Yarbrough, G. G., Prange, Jr, A. J. and Winokur, A. (2003) The thyrotropin-releasing hormone (TRH) hypothesis of homeostatic regulation: implications for TRH-based therapeutics. J. Pharmacol. Exp. Ther. **305**, 410–416

25 Schauder, B., Schomburg, L., Kohrle, J. and Bauer, K. (1994) Cloning of a cDNA encoding an ectoenzyme that degrades thyrotropin-releasing hormone. Proc. Natl. Acad. Sci. U.S.A. **91**, 9534–9538

26 Papadopoulas, T., Kelly, J. A. and Bauer, K. (2001) Mutational analysis of the thyrotropin-releasing hormone-degrading ectoenzyme: similarities and differences with other members of the M1 family of aminopeptidases and thermolysin. Biochemistry **40**, 9347–9355

27 Rozenfeld, R., Iturrioz, X., Maigret, B. and Llorens-Cortes, C. (2002) Contribution of molecular modeling and site-directed mutagenesis to the identification of two structural residues, Arg-220 and Asp-227, in aminopeptidase A. J. Biol. Chem. **277**, 29242–29252

28 Wilk, S. (1989) Inhibitors of TRH-degrading enzymes. Ann. N.Y. Acad. Sci. **553**, 252–264

29 Charli, J.-L., Mendez, M., Vargas, M.-A., Cisneros, M., Assai, M., Joseph-Bravo, P. and Wilk, S. (1989) Pyroglutamyl peptidase II inhibition specifically increases the recovery of TRH released from rat brain slices. Neuropeptides **14**, 191–196

30 Kelly, J. A., Bennett, G. W., Beckett, S., Slator, G. R., Roe, C. H., O'Loinsigh, E. D. and O'Boyle, K. M. (2000) Effects of thyrotropin-releasing hormone-degrading ectoenzyme inhibitors on thyrotropin-releasing hormone actions *in vivo*. Br. J. Pharmacol. **133**, 187P

31 Pascual, I., Gil-Parrado, S., Cisneros, M., Joseph-Bravo, P., Diaz, J., Possani, L. D., Charli, J. L. and Chavez, M. (2004) Purification of a specific inhibitor of pyroglutamyl aminopeptidase II from the marine annelide *Hermodice carunculata*: *in vivo* effects in rodent brain. Int. J. Biochem. Cell Biol. **36**, 138–152

32 Wilk, S. and Wilk, E. K. (1989) Pyroglutamyl peptidase II, a thyrotropin releasing hormone degrading enzyme: purification and substrate specificity studies of the rabbit brain enzyme. Neurochem. Int. **15**, 81–89

33 O'Connor, B. and O'Cuinn, G. (1985) Purification of and kinetic studies on a narrow specificity synaptosomal membrane pyroglutamate aminopeptidase from guinea-pig brain. Eur. J. Biochem. **150**, 47–52

34 Elmore, M. A., Griffiths, E. C., O'Connor, B. and O'Cuinn, G. (1990) Further characterisation of the substrate specificity of a TRH hydrolysing pyroglutamate aminopeptidase from guinea-pig brain. Neuropeptides **15**, 31–36

35 Gallagher, S. P. and O'Connor, B. (1998) Study of a highly specific pyroglutamyl aminopeptidase type-II from the membrane fraction of bovine brain. Int. J. Biochem. Cell Biol. **30**, 115–133

36 Walker, B. (1994) Solid-phase peptide synthesis. In Synthetic Antigens: A Practical Approach (Wisdom, G. B., ed.), pp. 27–81, Oxford University Press, Oxford

37 Kelly, J. A., Slator, G. R., Tipton, K. F., Williams, C. H. and Bauer, K. (1999) Development of a discontinuous, quantitative HPLC assay for thyrotropin-releasing hormone-degrading ectoenzyme. Anal. Biochem. **274**, 195–202

38 Lighton, C., Marsden, C. A. and Bennett, G. W. (1984) The effects of 5,7-dihydroxytryptamine and p-chlorophenylalanine on thyrotropin-releasing hormone in regions of the brain and spinal cord of the rat. Neuropharmacology **23**, 55–60

39 Thunnissen, M. M., Nordlund, P. and Haeggstrom, J. Z. (2001) Crystal structure of human leukotriene A_4 hydrolase, a bifunctional enzyme in inflammation. Nat. Struct. Biol. **8**, 131–135

40 Cornell, W. D., Cieplak, P., Bayly, C. I., Gould, I. R., Merz, Jr, K. M., Ferguson, D. M., Spellmeyer, D. C., Fox, T., Caldwell, J. W. and Kollman, P. A. (1995) A second generation force field for the simulation of proteins, nucleic acids, and organic molecules. J. Am. Chem. Soc. **117**, 5179–5197

41 Rarey, M., Kramer, B., Lengauer, T. and Klebe, G. (1996) A fast flexible docking method using an incremental construction algorithm. J. Mol. Biol. **261**, 470–489

42 Böhm, H.-J. (1994) On the use of LUDI to search the Fine Chemicals Directory for ligands of proteins of known three-dimensional structure. J. Comput. Aided Mol. Des. **8**, 243–256

43 Hu, X., Balaz, S. and Shelver, W. H. (2004) A practical approach to docking of zinc metalloproteinase inhibitors. J. Mol. Graphics Modell. **22**, 293–307

44 Lloyd, D. G., García-Sosa, A. T., Alberts, I. L., Todorov, N. P. and Mancera, R. L. (2004) The effect of tightly bound water molecules on the structural interpretation of ligand-derived pharmacophore models. J. Comput. Aided Mol. Des. **18**, 89–100

45 Rudberg, P. C., Tholander, F., Thunnissen, M. M. and Haeggstrom, J. Z. (2002) Leukotriene A_4 hydrolase/aminopeptidase: glutamate 271 is a catalytic residue with specific roles in two distinct enzyme mechanisms. J. Biol. Chem. **277**, 1398–1404

46 Lowe, D. M., Fersht, A. R., Wilkinson, A. J., Carter, P. and Winter, G. (1985) Probing histidine–substrate interactions in tyrosyl-tRNA synthetase using asparagine and glutamine replacements. Biochemistry **24**, 5106–5109

47 Schomburg, L., Turwitt, S., Prescher, G., Lohmann, D., Horsthemke, B. and Bauer, K. (1999) Human TRH-degrading ectoenzyme: cDNA cloning, functional expression, genomic structure and chromosomal assignment. Eur. J. Biochem. **265**, 415–422

48 Marie-Claire, C., Ruffet, E., Tiraboschi, G. and Fournié-Zaluski, M.-C. (1998) Differences in transition state stabilization between thermolysin (EC 3.4.24.27) and neprilysin (EC 3.4.24.11). FEBS Lett. **438**, 215–219

49 Hausrath, A. C. and Matthews, B. W. (2002) Thermolysin in the absence of substrate has an open conformation. Acta Crystallogr. Sect. D Biol. Crystallogr. **58**, 1002–1007

50 de Kreij, A., van den Burg, B., Venema, G., Vriend, G., Eijsink, V. G. H. and Nielsen, J. E. (2002) The effects of modifying the surface charge on the catalytic activity of a thermolysin-like protease. J. Biol. Chem. **277**, 15432–15438

Received 12 October 2004/2 March 2005; accepted 31 March 2005
Published as BJ Immediate Publication 31 March 2005, DOI 10.1042/BJ20041722

© 2005 Biochemical Society